

**PHOTOCHROMIC
G-PROTEIN COUPLED RECEPTOR
LIGANDS**

Dissertation

zur Erlangung des Doktorgrades der Naturwissenschaften

(Dr. rer. nat.)

an der Fakultät für Chemie und Pharmazie
der Universität Regensburg



vorgelegt von
Daniel Lachmann
aus Kelheim

2019

Der experimentelle Teil der vorliegenden Arbeit wurde in der Zeit von Oktober 2015 bis Dezember 2018 unter der Betreuung von Prof. Dr. Burkhard König am Institut für Organische Chemie der Universität Regensburg durchgeführt.

| | |
|------------------------------------|---------------------------------|
| Diese Arbeit wurde angeleitet von: | Prof. Dr. Burkhard König |
| Promotionsgesuch eingereicht am: | 16.01.2019 |
| Promotionskolloquium am: | 01.03.2019 |
| Prüfungsausschuss | |
| Vorsitzende: | Prof. Dr. Julia Rehbein |
| 1. Gutachter: | Prof. Dr. Burkhard König |
| 2. Gutachter: | Prof. Dr. Joachim Wegener |
| 3. Prüfer: | Prof. Dr. Frank-Michael Matysik |

MEINEN ELTERN & KERSTIN

Table of contents

| | |
|---|-----------|
| Fulgimides in biological applications | 1 |
| 1. Introduction | 1 |
| 2. Fulgimides as photoswitches in biological applications | 5 |
| 3. Conclusion | 10 |
| 4. Literature | 11 |
| 1. Photochromic Dopamine Receptor Ligands based on Dithienylethenes and Fulgides | 15 |
| 1. Introduction | 16 |
| 2. Results and Discussion | 18 |
| 2.1 Synthesis - pharmacophoric headgroups | 18 |
| 2.2 Synthesis - maleimides and cyclopentenones | 19 |
| 2.3 Photophysical properties - arylethenes | 21 |
| 2.4 Synthesis - fulgides and fulgimides | 23 |
| 2.5 Photophysical investigations - fulgimides | 25 |
| 2.6 Biological investigations | 26 |
| 3. Conclusions | 29 |
| 4. Experimental section | 29 |
| 4.1 Synthesis | 30 |
| 4.2 Assays | 58 |
| 5. Literature | 61 |
| 6. Supporting Information | 64 |
| 2. Photochromic Peptidic NPY Y₄-Receptor Ligands | 89 |
| 1. Introduction | 90 |
| 2. Discussion | 91 |
| 2.1 Synthesis | 91 |
| 2.2 Photophysical properties | 93 |
| 2.3 Biological investigations | 97 |
| 3. Conclusion | 99 |
| 4. Experimental Section | 99 |
| 4.1 General Conditions | 99 |
| 4.2 Synthesis procedures | 100 |
| 4.3 Assays | 110 |
| 5. Literature | 112 |
| 6. Supporting information | 114 |
| 6.4 Biological characterization | 119 |

| | |
|---|------------|
| 3. Covalent binding photochromic GPCR-Ligands for single molecule spectroscopy | 129 |
| 1. Introduction | 130 |
| 2. β_2 -Adrenergic receptor | 131 |
| 2.1 Molecular docking studies | 131 |
| 2.2 Synthesis of the photochromic β_2 -AR ligands | 133 |
| 2.3 Photophysical investigations | 136 |
| 2.4 Biological investigations | 137 |
| 2.5 Single molecule spectroscopy | 138 |
| 3. μ -Opioid receptor | 140 |
| 3.1 Docking studies towards the μ OR | 140 |
| 3.2 Synthesis of the azopyrazole based fentanyl derivatives | 142 |
| 3.3 Photophysical investigations | 146 |
| 3.4 Biological investigations | 148 |
| 4. Conclusion and Outlook – β_2 -AR and μ OR | 149 |
| 5. Experimental section | 150 |
| 6. Literature | 185 |
| 7. Supporting information | 188 |
| 4. Appendix | |
| 1. Abbreviations | 206 |
| 2. Danksagung | 208 |
| 3. Curriculum Vitae | 209 |

INTRODUCTION

Fulgimides in biological applications

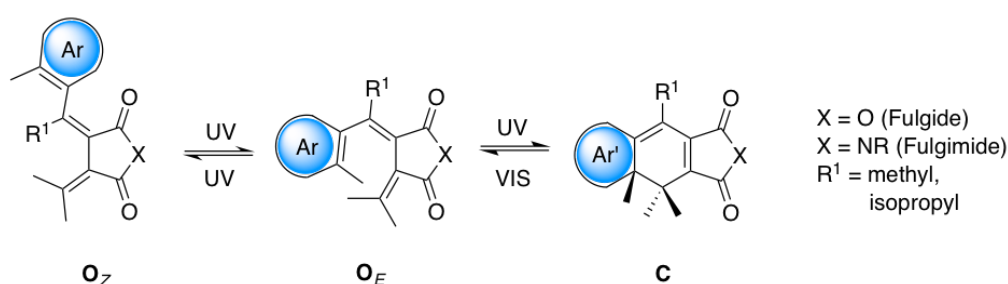
Parts of this chapter have been published as:

D. Lachmann, R. Lahmy, B. König, *Eur. J. Org. Chem*, Minireview

1. Introduction

Within the field of photopharmacology, photoswitches have drawn increasing attention over the past years. Adjacent to photocaging¹, which is an irreversible process, the common reversible photoswitches, which are used in biological applications are mainly azobenzenes and diarylethenes (DTEs).^{2,3} In addition, molecules like spiropyranes⁴, hemithioindigos⁵, donor-acceptor Stenhouse adducts (DASAs)⁶ and fulgides^{7,8} were also used for the reversible modulation of biological targets by light. Photoresponsive molecules can be divided into two groups: the thermally bistable switches (T-type, e.g. azobenzenes, hemithioindigos) and the thermally stable ones (P-type, e.g. diarylethenes, fulgides). Fulgimides are the imide derivatives of fulgides and were mainly used in optical data storage⁹, molecular computing¹⁰ and photomechanical materials.¹¹ However, beyond applications in material science, fulgimides are also well suited for biological applications.^{7,12,13} Their stability in conditions typical for biological assays was proven by Lees *et al.* with the development of highly polar indolyl fulgimides, which switch reversibly in sodium phosphate buffer.¹⁴

Fulgimides show excellent photochemical properties: High photostationary states (PSS) and reversible toggling between both photoisomers without degradation. In general, the photochromism occurs between the colourless *O*-isomers and the coloured *C*-isomer in a conrotatory electrocyclicization. The *O*-isomer shows *E/Z* isomerization depending on the substitution pattern of the 1,3,5-hexatrien-system. The thermal stability reveals from the substitution of the methylene hydrogen atoms by methyl groups.¹⁵ Introducing a more sterically demanding group (e.g. isopropyl) at position R¹ limits the isomerization to the *O_E*/*C*-isomerization (**Scheme 1**).¹⁶



Scheme 1. Photoisomerization of fulgides/fulgimides with UV or visible light. When R¹ is replaced by an isopropyl group, the switching is confined to the *O_E*- and *C*-isomer interconversion.

Table 1 summarizes the mainly used heteroaromatics for the fulgide and fulgimide synthesis resulting in different photochromic properties. The most extensive research was done on thiophenyl-, furyl- and indolyl fulgides and fulgimides.

Table 1. Characteristic wavelengths and photostationary states of fulgides and fulgimides comprising different heteroaromatic moieties.

| Fulgide/fulgimide | λ_{\max} [nm] | λ_{\max} [nm] | PSS ^[a] | QY ^[b] |
|---|----------------------------|-----------------------|--------------------|--------------------|
| Heteroaromatic moiety | (O _{EZ} -isomers) | (C-isomer) | | O _E → C |
| Furane ^{16,12} | 333-364 | 472-519 | 96-98% | 0.18 |
| Thiophene ^{16,17,18} | 272-339 | 514-532 | 51-92% | 0.13 |
| Pyrrole ¹⁹ | 364-389 | 584-642 | 30-60% | 0.20 |
| Benzofurane ^{20,21,22,23} | 330-387 | 488-511 | 43% | 0.17 |
| Benzothiophene ^{7,24,25} | 307-328 | 473-567 | 45-70% | 0.39 |
| Indole ^{7,13,26} | 360-481 | 543-606 | 19-86% | 0.045 |

[a] Amount of closed isomer at the best fitting irradiation wavelength. [b] R¹ position is replaced by a methyl group; X = O, see **Scheme 1**; solvent toluene, irradiation wavelength 366 nm except for the indole derivative, 405 nm was used.

Electron rich heteroaromatic moieties^{27,28,29} or a dicyanomethylene modified anhydride²⁶ as part of the fulgimide structure cause a bathochromic shift of the absorption spectrum, which is beneficial for biological applications as longer wavelengths can be used to initiate the isomerization (**Figure 1**). Indolyl fulgimides, for example, can be photoisomerized by blue and green light. Furthermore, their photostationary states are much higher due to a better separation of the absorption bands of the O- and C-isomer. **Figure 1** depicts exemplarily the bathochromic shift of the absorption spectra of indolyl fulgide **2** (right) in comparison to the benzothiophenyl fulgide **1** (left).

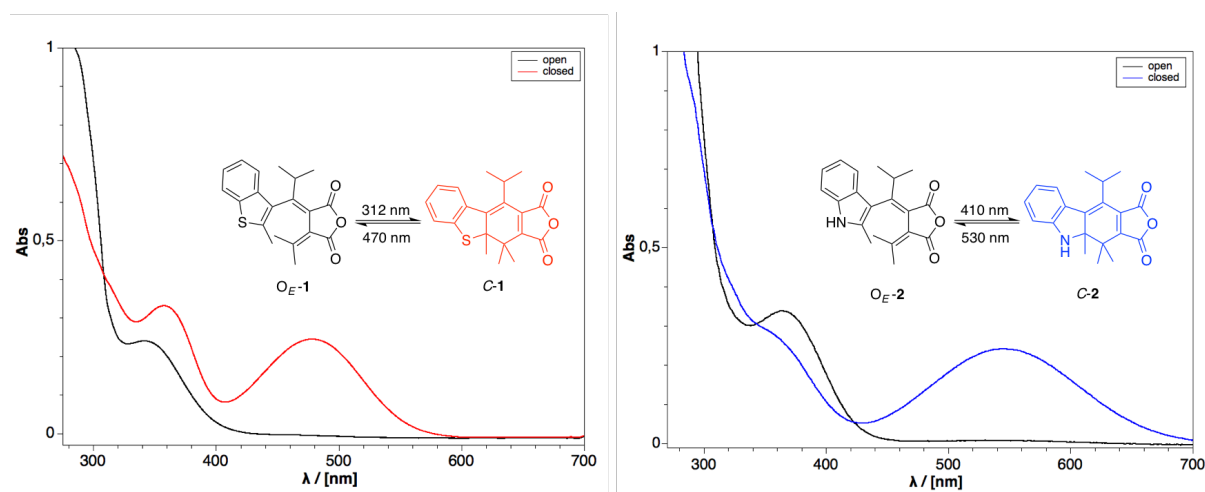


Figure 1. Comparison of the UV/VIS spectra ($c = 10^{-4}$ M in DMSO) of the benzothiophene fulgide **1** (left) and the indolyl fulgide **2** (right). The spectrum of the indolyl fulgide **2** exhibits a bathochromic shift compared to the benzothiophene derivative **1**.

Upon isomerization, the change in electronic properties and flexibility is accompanied by a change in geometry. Whereas the *C*-isomer is almost planar, the *O_E* isomer is twisted and sterically more demanding (**Figure 2**).

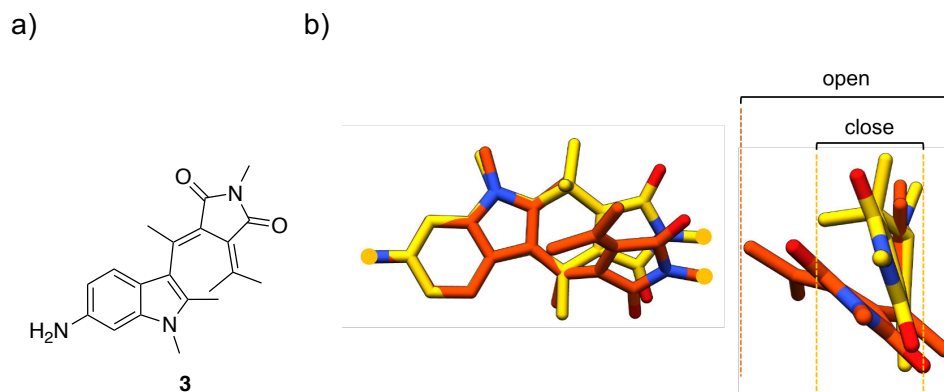


Figure 2. Topology and flexibility of indolyl fulgimide **3**. A) Structure of the fulgimide **3**. b) Left: sterically more demanding *O_E*-isomer superimposed to the more planar *C*-isomer; Right: change in lateral steric demand, frontview. The geometry of the structures was optimized using Gaussian09 at the B3LYP/6-31G(d) level.³⁰

Table 2 summarizes the photochemical parameters, essential for biological applications of photoswitches in general. Fulgimides are very promising candidates as the most photophysical criteria are perfectly fulfilled.

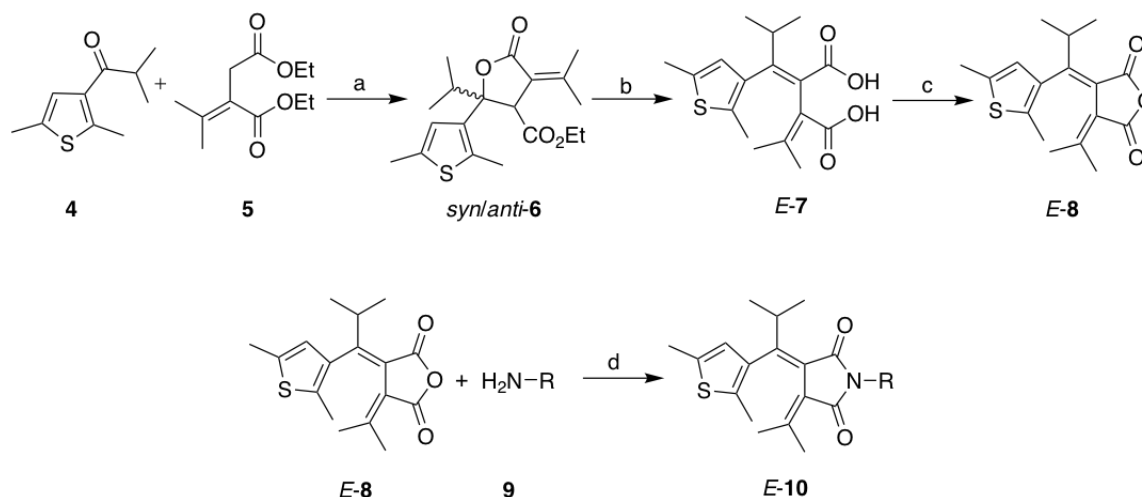
Table 2. Photophysical properties of different photoswitches: Azobenzenes^{31,32}, hemithioindigos^{5,33}, spiropyrans³⁴⁻³⁷, DASAs^{6,38,39}, diarylethenes^{32,40-42}, fulgimides^{7,36,26}.

| Property | Azobenzenes | Hemithioindigos | Spiropyrans | DASAs | Diarylethenes | Fulgimides |
|---|--------------------------------|--------------------------------|-----------------------------|-----------------------------|-----------------------------|-----------------------------|
| Thermal stability (thermal half-life) ^[a] | – (days) | – (hours) | – (hours) | – (minutes) | + | + |
| Fatigue resistance (aqueous solution) ^[b] | + | + | + | – | + ^[e] | + |
| λ_{\max} (<i>O</i> -isomer/ <i>E</i> -isomer) ^[c] | 310-440 nm | 480-514 nm | 320-380 nm | 450-700 nm | 230-300 nm | 270-481 nm |
| λ_{\max} (<i>C</i> -isomer/ <i>Z</i> -isomer) ^[c] | 420-900 nm | 400-415 nm | 440-660 nm | UV | 530-980 nm | 470-825 nm |
| Switching effect | conformation, dipole moment | conformation, dipole moment | conformation, polarity | geometry, polarity | rigidity, electronics | rigidity, electronics |
| Mechanism | <i>E/Z</i> | <i>Z/E</i> | cyclization/ring opening | cyclization/ring opening | cyclization/ring opening | cyclization/ring opening |

[a] + \rightarrow thermally stable, – \rightarrow thermally non-stable. [b] + \rightarrow toggling between the isomers without degradation in aqueous solution, – \rightarrow no reversible switching in aqueous solution. [c] Range of irradiation wavelength to obtain the *O* \rightarrow *C/E* \rightarrow *Z* or the *C* \rightarrow *O/Z* \rightarrow *E* photoisomer. [d] Very strong depending on the substitution pattern.

The key step of the fulgide synthesis, the Stobbe condensation, affords a mixture of the *syn*- and *anti*-lactone isomers or *E/Z* halfesters depending on the heteroaromatic moiety that is

installed.^{7,16} The ratio depends mainly on the sterically demand of the acyl residue. In addition, the heteroaromatic moiety also influences the reaction process whereby a strongly electron-donating system lowers the reactivity.^{43,44} **Scheme 2** shows the synthesis of the thiophene fulgimide *E-10* based on a general fulgide and fulgimide procedure.⁷



Scheme 2. Synthesis of the thiophene fulgimide *E-10*: (a) Stobbe condensation of **4** and **5** forming a mixture of lactones syn/anti-**6**. (b) Saponification of **6** forming the diacid *E-7*. (c) Anhydride formation of *E-7* (d) Imide formation of fulgide *E-8* and amine **9**.⁷

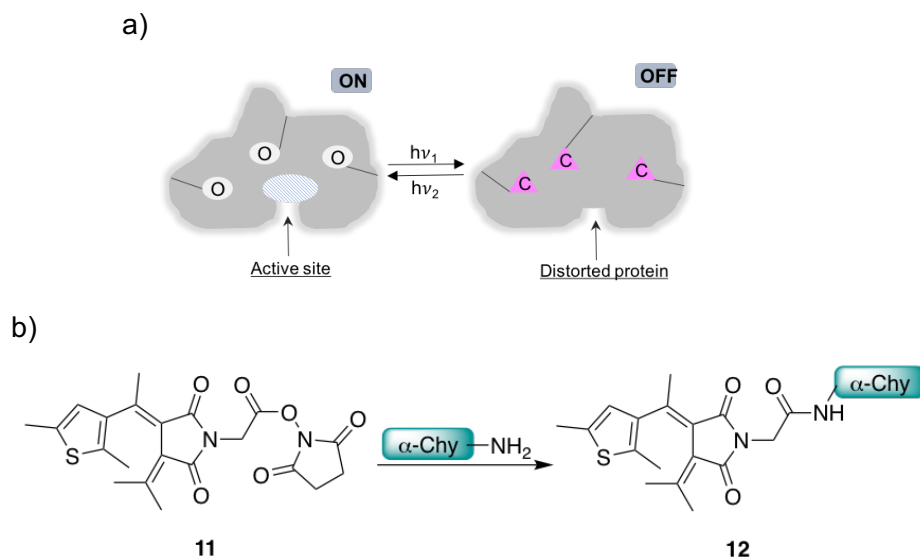
Nevertheless, in the last years slightly improvements of the synthesis were achieved.^{17,45,46} Furthermore, Kiji *et al.* reported a Pd-catalyzed carbonylation synthesis yielding fulgides and the corresponding fulgenic acids of substituted 1,4-butyne diols. This method is suitable for the synthesis of sterically demanding fulgides, but does not work for the synthesis of fulgides with strongly electron-donating aryl groups e.g. indolyl fulgimide **16**.^{44,47}

The aim of this microreview is to summarize the biological applications of fulgimides over the last 30 years. The first reports focused on the modification of an enzyme or protein whereas recent publications discuss modifications of ligands that binds to a receptor or protein.

2. Fulgimides as photoswitches in biological applications

The first incorporation of fulgides in biological structures was reported by Bäuerle *et al.*⁴⁸ The carbohydrate-binding protein Concanavalin A (ConA) was chemically modified into a thiophenefulgide to control the binding of a D-mannopyranoside by light. The thiophene fulgide was functionalized by a *N*-hydroxysuccinimide (NHS) ester, which was supposed to react with lysine residues of the ConA (**Scheme 3**). The photoregulated association of 4-nitrophenyl- α -D-mannopyranoside towards the fulgide in its open and closed isomeric state, respectively, was investigated by the determination of association constants. The highest difference was achieved when 9 fulgides were connected to the protein.

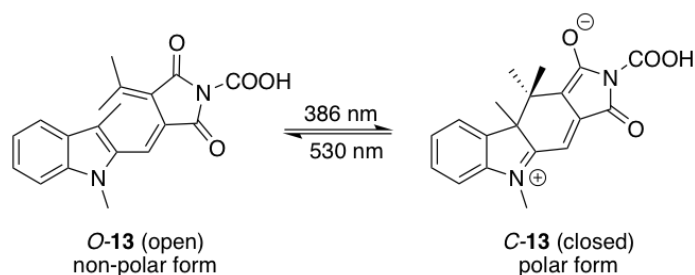
Further studies on an esterification reaction, catalyzed by the enzyme α -Chymotrypsin followed the same strategy for a photoresponsive modification of proteins. Structural changes of the protein were observed, but only moderate differences upon the interconversion of the two photoisomers.



Scheme 3. a) Schematic representation of the photostimulated “on” – “off” activities of an enzyme by covalent modification of a protein with fulgides (O = open, C = closed). b) Reaction of lysine residues of α -Chymotrypsin with the NHS ester derivatized fulgimide **11**.

A possible explanation for those slight differences is the marginal conformational perturbation of the protein backbone upon photoisomerization. As the fulgide-modified α -Chymotrypsin system did not work in aqueous solution, a bioimprinted version of the fulgide-modified α -Chymotrypsin was used to record the esterification rates of *N*-acetyl-L-phenylalanine and ethanol in cyclohexane. Online switching experiments, which showed an increase or decrease of the esterification rate, were done successfully. Finally, they could show that the bioimprinted protein revealed enhanced biocatalytic activity in an organic solvent but the switching efficiency remained moderate.

A polarity dependent indolyl fulgimide that switches fluorescence in living cells was developed (**Scheme 4**) by the group of Rentzepis.⁴⁹ The fulgimide **13** only exhibited strong fluorescence in its polar, ring closed isomer, while the non-polar, open form showed no fluorescence.

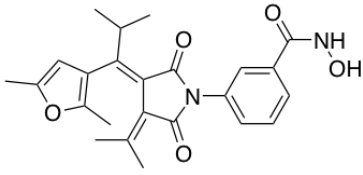


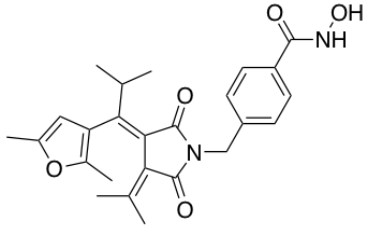
Scheme 4. Structure of the open and closed isomer of indolyl fulgimide **13**. The closed isomer emits at 630 nm after excitation at 550 nm.

Ultrafast time resolved spectroscopy for the transformation of the polar (closed isomer) to the non-polar (open isomer) form was measured to record kinetics and intermediate spectra. The obtained data suggested, that the reversible switching between the two states is rather in the picosecond time scale compared to the far slower diffusion controlled rates of most chemical and biological reactions. The indolyl fulgimide **13** could be used as an intracellular chemical/molecular sensor to investigate local changes in living cells, such as pH and viscosity. The cell experiments showed that the fulgimide **13** enters the living cell and associates with internal membranous organelles, especially with mitochondria. Seven performed cycles showed the stability of fulgimide **13** within the living cell.

In more recent publications, fulgimides are often used to overcome specific limitations of the photochemical properties of diarylethenes. Some cyclopentene-dithienylethenes derivatives showed degradation after a few isomerizations and dithienylmaleimides do not switch reversibly in aqueous buffer solutions.⁷ Fulgimides typically show high fatigue resistance and high PSS, dependent on the heteroaromatic moiety and substitution of the 1,3,5-hexatrien-system.

Photoresponsive histone deacetylase (HDAC) inhibitors, based on thermally stable diarylethenes and fulgimides were developed.¹² The enzyme plays a role in cancer formation and catalyzes the deacetylation of lysine residues from acetylated lysine residues. First approaches were conducted on dithienylethenes (DTEs) and dithienylmaleimides, which were functionalized by hydroxamic acids binding to zinc dependent HDACs. As the photochemical properties of the cyclopentene-DTEs and the dithienylmaleimides showed drastic limitations, the photochromic scaffold was replaced by a fulgimide. The fulgimide derivatives **14** and **15**, containing the hydroxamic acids, showed excellent properties exhibiting high photostationary states and good fatigue resistance (**Scheme 5**).

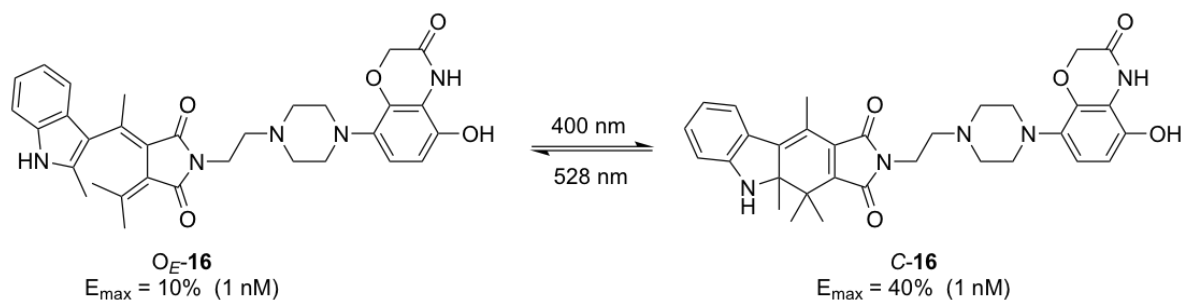
| Compd. | IC ₅₀ <i>h</i> HDAC6 | | |
|--------|------------------------------------|---|-----------|
| O-14 | 1.8 ± 0.5 |  | 14 |
| C-14 | 6.1 ± 1.7 | | |
| O-15 | 0.047 ± 0.032 | | |
| C-15 | 0.075 ± 0.047 | | |

| | |
|--|-----------|
|  | 15 |
|--|-----------|

Scheme 5. Structures of the furylfulgimide based HDAC inhibitors **14** and **15** (right). Exemplary IC₅₀ values of compound **14** and **15** at the *h*HDAC6.

The IC₅₀ values of the respective isomers of fulgimides **14** and **15** were determined and for the *h*HDAC6 inhibition, a 3-fold difference between the photoisomers of compound **14** could be obtained. In order to explain the *in vitro* activity of the photochromic inhibitors, docking on different classes of HDACs was performed. While the docking studies rationalized the potency well, no explanation for the lack of selectivity between the open and closed photoisomers could be derived.

First investigations on fulgides, embedded into dopaminergic G protein-coupled receptor ligands (GPCRs) were performed by König and coworkers.⁷ Fulgides, dithienylethens and dithienylmaleimides were incorporated in highly potent and selective dopamine D_{2S} receptor ligands, for instance 1,4-disubstituted aromatic- and hydroxybenzoxazinone piperazines. The obtained photochromic ligands are biochemical tools and are useful for the investigation of the receptor's function or dynamics. Different fulgimides were synthesized comprising benzothiophene, thiophene and indole heteroaromatic moieties resulting in different photochromic properties. Particularly, the indolyl fulgimides showed a red shift in the absorption spectra, high PSS and could be reversibly switched several times in aqueous buffer. The biological investigation was targeted towards the activation of the dopamine D_{2S} receptor and revealed good agonistic activity observed for the G-protein mediated signaling and weak arrestin recruitment. Compounds with isomer-specific activities were subjected to a IP-One accumulation assay. At a concentration of 1 nM a cyclopentene-DTE derivative showed 11-fold difference between the open and closed state and the fulgimide **16** was discovered as an alternative photoswitch with an inverse activation profile exhibiting four-fold difference between the O_E-**16** and the C-**16** state (**Scheme 6**).



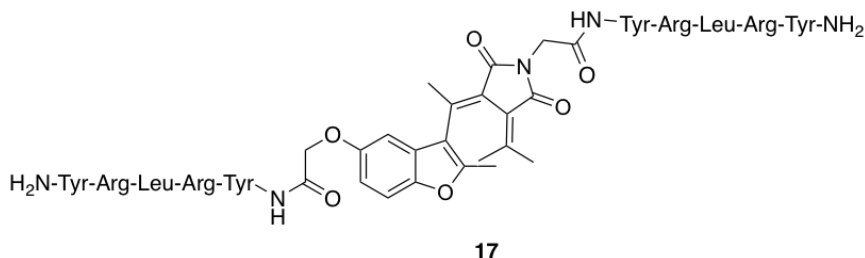
Scheme 6. The hydroxybenzoxazinone piperazine substituted fulgimide **16** was reversibly switched with light of 400 nm and 528 nm. The E_{max} values were determined in comparison to the reference quinpirole at a concentration of 1 nM.

As fulgimide **16** fulfilled most of the requirements for an application in biological systems, it represents a promising tool for the regulation of the pharmacologically important dopamine D_{2S} receptor.

Simeth *et al.* attempted to improve dithienylmaleimide based photocontrolable inhibitors for sirtuins by introducing *N*-alkylated indolyl fulgimides.¹³ As the dithienylmaleimides were not photoisomerizable in aqueous solution, indolyl fulgimides with improved photochromic properties were used. In addition, a bathochromic shift in the absorption profile caused by the indolyl moiety is beneficial for potential applications in biological systems. Different substitution patterns of the heteroaromatic moiety affected the synthesis yields and the photochemical properties. Again, the Stobbe condensation was the limiting reaction step. For steric reasons, also the fulgimide formation occurred with low yields below 10%. The synthesized fulgimide-derivatives are addressable with purple (400 nm) and orange (590 nm) light and showed fluorescence when irradiated with light of 400 nm. The fulgimides could be toggled between their open and closed state several times without significant loss of responsiveness. Three human sirtuin isoforms (hSirt1-3) were treated with two different fulgimide derivatives in a fluorescence-based ZMAL assay. The closed isomer was generated during the assay applying a 96-well plate LED irradiation setup. All compounds inhibited hSirt3. One derivative showed an IC_{50} value of 19.9 μM in its open isomer and 1.5-fold lower inhibition in its closed state. In summary, the photochromic properties could be improved as desired, but compared to the previously reported maleimides partially at the expense of inhibitory activity and isomer specificity.

Recently, photoresponsive dimeric peptides were developed to further investigate the G protein-coupled neuropeptide Y Y_4 receptor (NPY Y_4 receptor).²² The NPY Y_4 receptor is targeted by pancreatic polypeptide, a homologue of NPY. Selective Y_4R agonists were suggested as potential therapeutics for the treatment of obesity. Highly potent dimeric peptidic

Y_4R agonists, constituted by two pentapeptide moieties connected through an aliphatic linker, represent an interesting class of Y_4R ligands. Based on this compound class, photoresponsive Y_4R ligands, containing an azobenzene, azopyrazole, diethienylethene or a fulgimide chromophore as linker were synthesized to explore structural requirements of such Y_4R agonists on Y_4R binding (**Scheme 7**).



Scheme 7. The structure of the benzofuryl fulgimide based dimeric peptidic NPY Y_4 receptor ligand (**17**) is shown.

The synthesized Y_4R ligands, containing a non-aliphatic rigid photochromic linker, showed an efficient and reversible switching in aqueous buffer and exhibited high Y_4R affinity. This demonstrated that the replacement of the highly flexible aliphatic linker by a considerably less flexible photochromic linker was well tolerated with respect to Y_4R binding. Differences in Y_4R affinity and activity between the individual photoisomers, varying in spatial orientation and flexibility, were marginal suggesting that the linking element in the dimeric ligands is less important for the adaptation of high-affinity binding modes at the receptor.

3. Conclusion

The photochemical properties of indolyl-, thiophene- and furane- fulgides are well-suited for applications in the photomodulation of biological properties. Their photochemical reversibility, stability and absorption wavelength range is in many cases superior to azobenzenes or diethenylethenes. However, the number of applications of fulgides and fulgimides is still small and one reason for this is their challenging synthesis. The success of the Stobbe condensation and the fulgimide formation depend on the amine that is used and partially on the substitution pattern of the hexatrien system. More predictable and more general synthetic routes to functionalized fulgides and fulgimides are clearly in demand to provide this interesting class of photochromic molecules for broader applications in life science.

4. Literature

- 1 P. Klán, T. Šolomek, C. G. Bochet, A. Blanc, R. Givens, M. Rubina, V. Popik, A. Kostikov, J. Wirz, *Chem. Rev.* **2013**, *113*, 119
- 2 W. C. Lin, M. C. Tsai, R. Rajappa, R. H. Kramer, *J. Am. Chem. Soc.* **2018**, *140*, 7445.
- 3 B. Reisinger, N. Kuzmanovic, P. Löffler, R. Merkl, B. König, R. Sterner, *Angew. Chem. Int. Ed.*, **2014**, *126*, 606.
- 4 T. Hirakura, Y. Nomura, Y. Aoyama, K. Akiyoshi, *Biomacromolecules* **2004**, *5*, 1804.
- 5 S. Kitzig, M. Thilemann, T. Cordes, K. Rück-Braun, *ChemPhysChem* **2016**, *17*, 1252.
- 6 M. M. Lerch, W. Szymanski, B. L. Feringa, *Chem. Soc. Rev.* **2018**, *47*, 1910.
- 7 D. Lachmann, C. Studte, B. Männel, H. Harald, P. Gmeiner, B. König, *Chem. Eur. J.* **2017**, *23*, 13423.
- 8 I. Willner, M. Lion-Dagan, S. Rubin, J. Wonner, F. Effenberger, P. Bäuerle, *Photochem. Photobiol.* **2004**, *5*, 169.
- 9 M. Seibold, M. Handschuh, H. Port, H. C. Wolf, *J. Luminescence* **1997**, *72-74*, 454.
- 10 P. Remon, M. Bälter, S. Li, J. Andreasson, U. Pischel, *J. Am. Chem. Soc.* **2011**, *133*, 20742.
- 11 T. Kim, L. Zhu, R.O. Al-Kaysi, Ch. J. Bardeen, *Chem. Phys. Chem.*, **2014** *15*, 400.
- 12 D. Wutz, D. Gluhacevic, A. Chakrabarti, K. Schmidtkunz, D. Robaa, F. Erdmann, C. Romier, W. Sippl, M. Jung, B. König, *Org. Biomol. Chem.* **2017**, *15*, 4882.
- 13 N. A. Simeth, L.-M. Altmann, N. Wössner, E. Bauer, M. Jung, B. König, *J. Org. Chem.* **2018**, *83*, 7919.
- 14 X. Chen, N.I. Islamova, P.S. Garcia, J.A. DiGirolamo, E.J. Lees, *J. Org. Chem.* **2009**, *74*, 6777.
- 15 J.P. Darcy, G.H. Heller, P.J. Strydom, J. Whittall, *J. Chem. Soc., P. Trans. 1* **1981**, 202.
- 16 Strübe F., Siewertsen R., Sönnichsen D.R., Renth T., Temps F., Mattay F., *Eur. J. Org. Chem.*, **2011**, *10*, 1947.
- 17 B. Otto, K. Rück-Braun, *Eur. J. Org. Chem.* **2003**, *13*, 2409
- 18 K. Ulrich, H. Port, H. C. Wolf, J. Wonner, F. Effenberger, H.-D. Ilge, *Chem. Phys.* **1991**, *2*, 311
- 19 S. A. Harris, H. G. Heller, S. N. Oliver, *J. Chem. Soc. Perkin Trans 1*, **1991**, 3259
- 20 V. P. Rybalkin, N. I. Makarova, S. Yu. Pluzhnikova, L. L. Popova, A. V. Metelitsa, V. A. Bren, V. I. Minkin, *Russ. Chem. Bull., Int. Ed.* **2014**, *63*, 1780
- 21 F. Strübe, S. Rath, J. Mattay, *Eur. J. Org. Chem.* **2011**, *24*, 4645
- 22 D. Lachmann, A. Konieczny, M. Keller, B. König, *Org. Biomol. Chem.* **2019**, submitted
- 23 R. Siewertsen, F. Strübe, J. Mattay, F. Renth, F. Temps, *Phys. Chem. Phys.* **2011**, *13*, 3800

- 24 S. I. Luyksaar, V. A. Migulin, B. V. Nabatov, M. M. Krayushkin, *Russ. Chem. Bull., Int. Ed.* **2010**, *59*, 446
- 25 M. Kose, E. Orhan, *J. Photochem. Photobiol. A* **2006**, *177*, 170
- 26 A. Liang, A. S. Dvornikov, P. M. Rentzepis, *J. Mater. Chem.* **2003**, *13*, 286.
- 27 Y. Yokoyama, T. Sagisaka, Y. Mizuno, Y. Yokoyama, *Chem. Lett.* **1996**, 587–588.
- 28 L. Yu, Y. Ming, W. Zhao, M. Fan, *J. Photochem. Photobiol. A* **1992**, *68*, 309–317.
- 29 Y. Yokoyama, T. Tanaka, T. Yamane, Y. Kurita, *Chem. Lett.* **1991**, *7*, 1125–1128.
- 30 M. J., G. W. Trucks, H. B. Schlegel, G. E. Scuseria, M. A. Robb, J. R. Cheeseman, G. Scalmani, V. Barone, B. Mennucci, G. A. Petersson, H. Nakatsuji, M. Caricato, X. Li, H. P. Hratchian, A. F. Izmaylov, J. Bloino, G. Zheng, J. L. Sonnenberg, M. Hada, M. Ehara, K. Toyota, R. Fukuda, J. Hasegawa, M. Ishida, T. Nakajima, Y. Honda, O. Kitao, H. Nakai, T. Vreven, J. A. Montgomery, Jr., J. E. Peralta, F. Ogliaro, M. Bearpark, J. J. Heyd, E. Brothers, K. N. Kudin, V. N. Staroverov, R. Kobayashi, J. Normand, K. Raghavachari, A. Rendell, J. C. Burant, S. S. Iyengar, J. Tomasi, M. Cossi, N. Rega, J. M. Millam, M. Klene, J. E. Knox, J. B. Cross, V. Bakken, C. Adamo, J. Jaramillo, R. Gomperts, R. E. Stratmann, O. Yazyev, A. J. Austin, R. Cammi, C. Pomelli, J. W. Ochterski, R. L. Martin, K. Morokuma, V. G. Zakrzewski, G. A. Voth, P. Salvador, J. J. Dannenberg, S. Dapprich, A. D. Daniels, J. Farkas; Foresman, J. V. B.; Ortiz, J. Cioslowski, and D. J. Fox. 2009. 'Gaussian 09, revision B.01', *Gaussian, Inc.: Wallingford, CT*.
- 31 K. Hüll, J. Morstein, D. Trauner, *Chem. Rev.* **2018**, *118*, 10710
- 32 D. Bléger, S. Hecht, *Angew. Chem. Int. Ed.* **2015**, *54*, 11338
- 33 W. Szymanski, J. M. Bierle, H. A. V. Kistemaker, W. A. Velema, B. L. Feringa, *Chem. Rev.* **2013**, *113*, 6114
- 34 R. Klajn, *Chem. Soc. Rev.* **2014**, *43*, 148
- 35 M. Hammarson, J. R. Nilson, S. Li, T. Beke-Somfai, J. Andréasson, *J. Phys. Chem. B* **2013**, *117*, 13561
- 36 V. I. Minkin, in *Molecular Switches*, Wiley-VCH Verlag GmbH & Co. KGaA, **2011**, pp. 37-80.
- 37 T. Halbritter, C. Kaiser, J. Wachtveitl, A. Heckel, *J. Org. Chem.* **2017**, *82*, 8040
- 38 J. R. Hemmer, S. O. Poelma, N. Treat, Z. A. Page, N. D. Dolinski, Y. J. Diaz, W. Tomlinson, K. D. Clark, J. P. Hooper, C. Hawker, J. R. de Alaniz, *J. Am. Chem. Soc.* **2016**, *138*, 13960
- 39 J. D. Harris, M. J. Moran, I. Aprahamian, *PNAS* **2018**, *115*, 9414
- 40 M. Irie, *Chem. Rev.* **2000**, *100*, 1685
- 41 S. Kobatake, M. Irie, *Ann. Rep. Prog. Chem. Sect. C.* **2003**, *99*, 277
- 42 K. Matsuda, M. Irie, *Photochem. Photobiol. C.* **2004**, *5*, 169

- 43 J. Kiji, H. Kitamura, Y. Yokoyama, S. Kubota, Y. Kurita, *Bull. Chem. Soc. Jpn.* **1995**, 68, 616.
- 44 S. Uchida, Y. Yokoyama, J. Kiji, T. Okano, H. Kitamura, *Bull. Chem. Soc. Jpn.* **1995**, 68, 2961.
- 45 C. J. Thomas, M. A. Wolak, R. R. Birge, W. J. Lees, *J. Org. Chem.* **2001**, 66, 1914
- 46 K. K. Krawczyk, D. Madej, J. K. Maurin, Z. Czarnocki, *C. R. Chimie* **2012**, 15, 384
- 47 J. Kiji, T. Okano, H. Kitamura, Y. Yokoyama, S. Kubota, Y. Kurita, *Bull. Chem. Soc. Jpn.* **1995**, 68, 616.
- 48 I. Willner, S. Rubin, J. Wonner, F. Effenberger, P. Bäuerle, *J. Am. Chem. Soc.* **1992**, 114, 3151
- 49 I. Willner, M. Lion-Dagan, S. Rubin, J. Wonner, F. Effenberger, P. Bäuerle, *Photochem. Photobiol.* **1994**, 59, 491

CHAPTER 1

1. Photochromic Dopamine Receptor Ligands based on Dithienylethenes and Fulgides

This chapter has been published as:

D. Lachmann, C. Studte, B. Männel, H. Hübner, P. Gmeiner, B. König, *Chem. Eur. J.* **2017**, *23*, 13423.

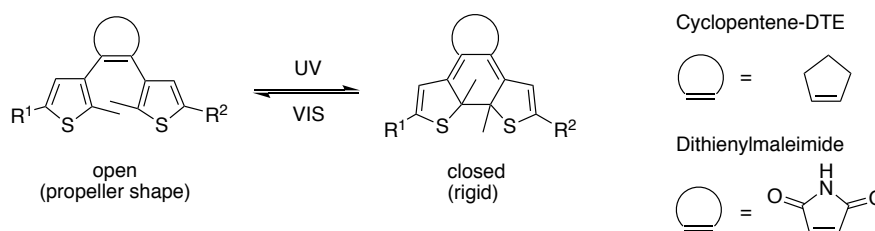
DL synthesized compounds **25**, **32**, **34**, **36**, **37** – **52** and performed the corresponding photochemical measurements and wrote the manuscript. CS synthesized compounds **21** – **24** and **26** – **31** and performed the corresponding photochemical measurements. BM synthesized compounds **2** – **17**. HH did the biological investigations. BK supervised the project and is corresponding author.

1. Introduction

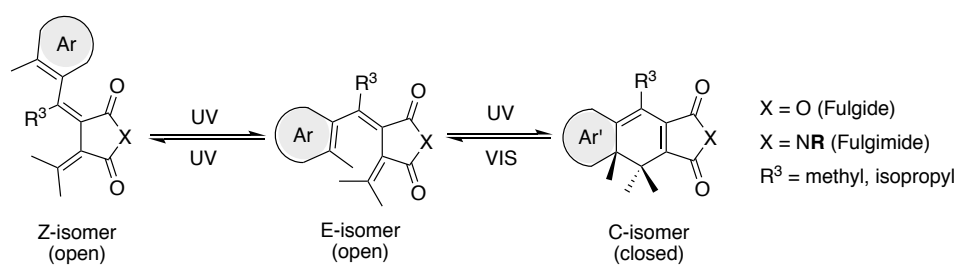
G-protein coupled receptors (GPCRs) are a vibrant field of research because their dysfunction is linked to numerous diseases like central nervous system (CNS) disorders, cancer or inflammatory diseases.^{1a-c} Therefore, more than 30% of the approved drugs target the GPCR family. Focusing on the dopamine receptors several CNS disorders like schizophrenia, drug addiction, Parkinson's and Huntington's disease are linked to their dysfunction.² Privileged structures targeting the dopamine D₂-like receptors are derivatives of 1,4-disubstituted aromatic piperazines (1,4-DAPs), hydroxybenzoxazinone substituted piperazines as well as conformationally restricted dopamine analogs involving aminoindanes. The synthesis of D₂, D₃ and D₄ receptor agonists and antagonists with individual subtype selectivity or functional selectivity (biased signaling) has received considerable attention, in recent years.^{3a-f} Although a better understanding of the mechanism of GPCR-promoted drug action was achieved, there is still a need to develop selective molecular tools to obtain more insight into the dynamics or receptors function.

Photopharmacology can address this issue in a non-invasive way with high spatial and temporal precision. The importance of this concept is revealed by the increasing number of photochromic enzyme inhibitors,^{4a-f} photochromic ligands for receptors and ion channels,^{5a-e} photoswitchable antibiotics,^{6a-b} photo-switches, which are applicable *in vivo* using visible-light,^{7a-c} and recently even photochromic ligands, which change their intrinsic activity.⁸ Recently, photochromic azobenzol based opioids^{5c} and dopamine receptor ligands, embedded in a phenethyl-propyl-hydroxytetraline (PPHT) structure, were developed by Trauner *et al.*⁹ Azobenzenes as well as dithienylethenes (DTEs) and fulgides convert light-induced between two isomers, which differ for the azobenzenes in geometry and dipole moment and for the DTEs in conformational flexibility and electronic properties.¹⁰ Both classes of switches show a high fatigue resistance, but only the open and closed form of the DTEs and fulgides are thermally stable, which makes them interesting candidates for photopharmaceuticals.^{11a-b} Especially fulgides are very interesting for biological applications, because they show high fatigue resistance and are mostly water soluble and switchable in aqueous buffer solutions (**Scheme 1**).^{12a-b}

a)



b)



Scheme 1. a) Switching principle of dithienylethene based switches. b) Photochromic fulgides/fulgimides, depicted in three forms after irradiation with UV light.

Two major strategies are commonly applied to introduce a photoswitchable moiety into a bioactive compound: the chromophore can either be embedded into the structure of a pharmacophore or attached to one or two pharmacophores via a suitable linker.^{10,13} In each case, it is desirable that the light induced switching between the two isomers results in a distinct difference in affinity or intrinsic activity. This would allow the photocontrol of biological functions and offer the possibility to investigate drug targets like GPCRs very precisely.

We envisioned that a formal exchange of a structural appendage of known dopamine ligands by a photoswitchable unit would lead to potent photochromic dopaminergic ligands (**Figure 1**). Herein, we discuss the synthesis, photophysical characterization and biological evaluation of photochromic dopamine receptor ligands based on dithienylethene- and fulgide-type scaffolds.

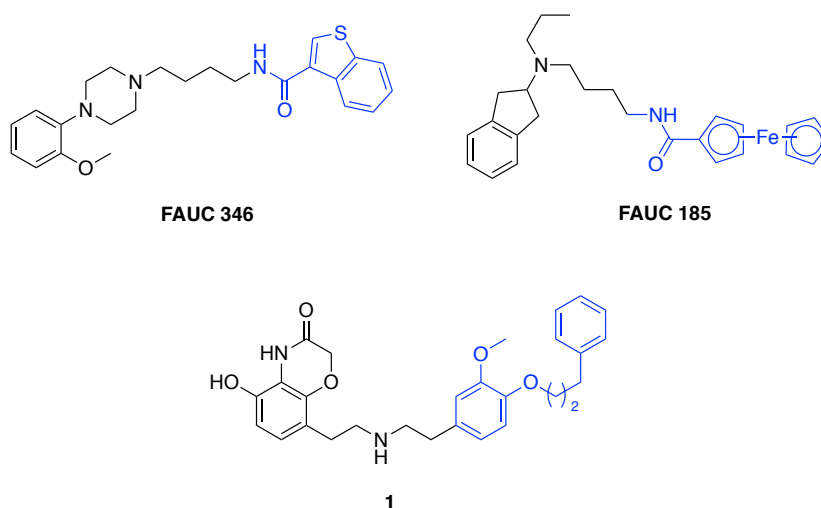


Figure 1. Structures of known dopamine ligands: 1,4-DAP **FAUC 346**¹⁴, aminoindane **FAUC 185**¹⁵ and benzoxazinone derivative¹⁶ **1**, where the blue coloured moieties are replaced by a photochromic diarylmaleimide, dithienylethene or fulgide.

2. Results and Discussion

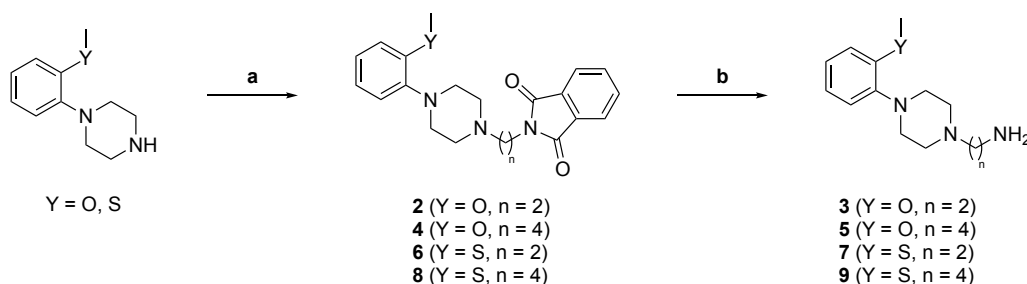
Due to their thermal stability, we investigated DTEs first. Within this classes two kind of photoswitches were used to synthesize photoresponsive dopamine ligands: 1) the cyclopentene based switches and 2) the diarylmaleic anhydrides. Both types of DTEs have been successfully applied in photopharmacology.^[21] Furthermore, the isomerization wavelength for the chromophores can be bathochromically shifted, reducing cell damage otherwise caused by high energy light.^{11a} The photoswitches differ in their attachment mode to the pharmacological headgroups. Introducing two different sterically demanding photochromic groups to the pharmacological headgroups allows us to investigate the importance of the size of the heterocyclic appendage for the affinity and subtype selectivity.

2.1 Synthesis - pharmacophoric headgroups

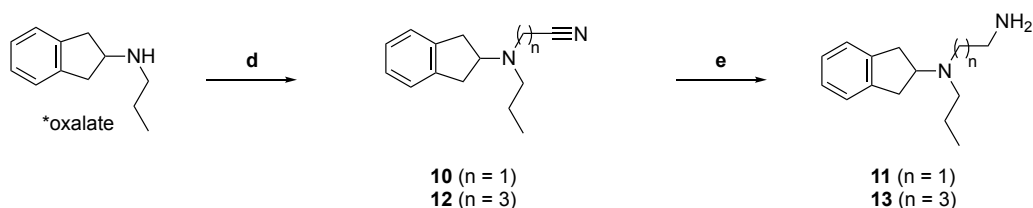
Privileged structures for aminergic GPCR ligands are 1,4-DAPs **3**, **5**, **7** and **9**, aminoindanes **11** and **13** and the benzoxazinon piperazine **17**. A coupling reaction between the pharmacophoric head groups and the photoswitches gave the target structures. The 2-methoxy- and 2-methylthiophenylpiperazine building blocks were synthesized as described in literature.¹⁷ Commercially available 1-(2-methoxyphenyl)- and 1-(2-(methylthio)phenyl)-piperazine were alkylated with *N*-(4-bromobutyl)- or *N*-(2-bromoethyl)phthalimide to give intermediates **2**, **4**, **6** and **8** in good yields. Hydrazinolyses of the respective phthalimides yielded building blocks **3**, **5**, **7**, and **9**. The same protocol was used to obtain hydroxybenzoxazinone substituted piperazine **17**. The synthesis of precursor **14** is described in the supporting information (SI1). Alkylation of **14** with *N*-(2-bromoethyl)phthalimide gave compound **15**. Subsequent hydrazinolysis and acid mediated cleavage of the benzyl protecting groups yielded compound **17**. Building blocks **11** and **13** were readily accessible following a two-step literature procedure.¹⁸

2-Propylaminoindane oxalate was reacted with 4-bromobutyronitrile, respectively 2-bromoacetonitrile to afford compounds **10** and **12**. Reduction of the nitrile group by LiAlH₄ yielded compounds **11** and **13** (Scheme 2).

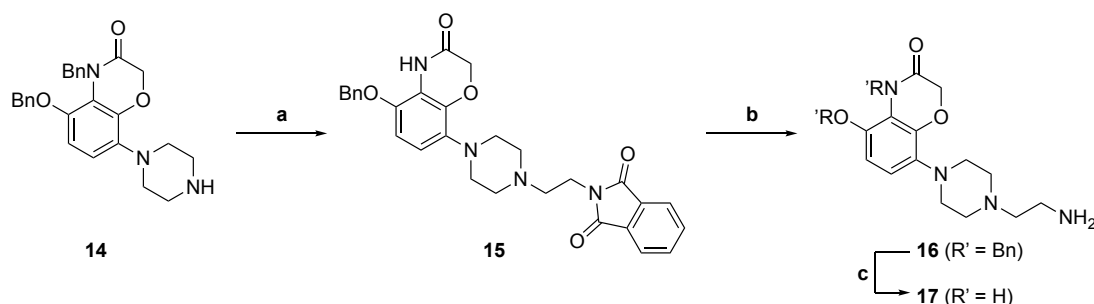
Headgroups A:



Headgroups B:



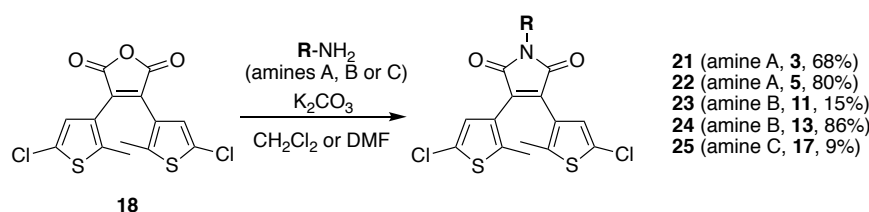
Headgroup C:



Scheme 2. Synthesis of pharmacophore building blocks, headgroups A, B and C. Reagents and conditions: (a) *N*-(4-bromobutyl)- or *N*-(2-bromo-ethyl)phthalimid, K_2CO_3 , KI, MeCN, 75 °C, 5–16 h, 75–90%. (b) Hydrazine hydrate, EtOH, 75 °C, 2 h, then 2 M HCl, EtOH, 75 °C, 2 h, 60–85%. (c) MsOH, toluene, 100°C, 2 h, 89%. (d) 4-bromobutyronitrile or 2-bromoacetonitrile, K_2CO_3 , KI, MeCN, 75 °C, 16 h 88%. (e) LiAlH_4 , Et_2O , 0 °C \rightarrow r.t., 1 h, 71–90%.

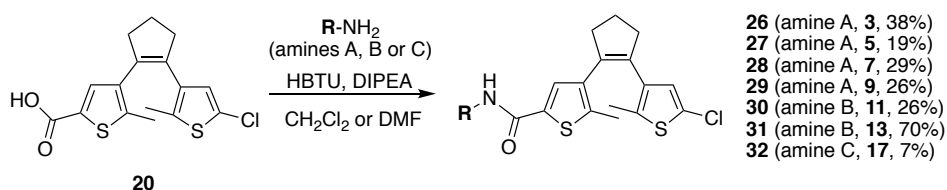
2.2 Synthesis - maleimides and cyclopentenes

The DTE and diarylmaleic based pharmacophores, containing the 1,4-DAP, were used with two different spacer lengths. Depending on the DTEs, two different strategies were applied to combine photoswitch **18** with headgroups **3**, **5**, **11**, **13**, **17** and cyclopentene-DTE **20** with the pharmacophores **3**, **5**, **7**, **9**, **11**, **13** and **17**. In case of the diarylmaleic anhydride **18**, the coupling was performed with the core of the DTE, while the cyclopentene based DTE **20** was coupled with one of the thiophene moieties. Diarylmaleimide **18** was easily accessible according to literature as well as the precursor **19**, which was then carboxylated on only one thiophene moiety to obtain **20**.^{19,20a-b} The syntheses of the diarylmaleic anhydride based photochromic ligands **21–25** were performed under slightly basic conditions using potassium carbonate as base and are outlined in **Scheme 3**.



Scheme 3. Syntheses of the diarylmaleimide based photochromic ligands **21 – 25**.

Standard peptide coupling conditions using HBTU and *N,N*-diisopropylethylamine were applied to synthesize the photochromic ligands **26 - 32** (Scheme 4).



Scheme 4. Syntheses of the cyclopentene-DTE based photochromic ligands **26 - 32**.

Following these two synthetic strategies, we were able to readily obtain various photochromic ligands in just one step. A stock solution for the biological testing was prepared with dimethyl sulfoxide as solvent. Dilutions thereof were used to study the photophysical properties. Even though it is reported that diarylmaleimides cannot be reversibly toggled between their two photoisomers in polar solvents due to a twisted intramolecular charge transfer (TICT), we observed a reversible photoisomerization in dimethyl sulfoxide for all photochromic ligands based on diarylmaleimides.^{21a-c}

2.3 Photophysical properties - arylethenes

The photophysical properties of the photochromic dopamine receptor ligands **21-25** and **26-32** were investigated by absorption spectroscopy. Therefore, the dissolved compounds were irradiated with UV-light (312 or 400 nm) which resulted in a color change of the solution accompanied with new absorption maxima, characteristic for each of the photochromic ligands. The resulting isosbestic points indicate a clean two-component switching. In addition, the PSS was determined by HPLC measurements. All photophysical properties of the compounds **21-25** and **26-32** are summarized in **Table 1**.

Table 1. UV-Vis data of the open and closed form of the synthesized ligands **21-25** and **26-32** (50 or 100 μ M in DMSO) after irradiation with $\lambda = 312$ or 410 nm.

| Entry | Compd. | λ_{max} (open) [nm] | λ_{max} (closed) [nm] | λ_{iso} [nm] | PSS ^[a] |
|-------|--------|---------------------------------------|---|--------------------------------|--------------------|
| 1 | 21 | 260, 378 | 355, 493 | 300, 376, 413 | 46% |
| 2 | 22 | 261, 390 | 356, 509 | 305, 377, 413 | 38% |
| 3 | 23 | 264, 360 | 355, 500 | 301, 379, 413 | 49% |
| 4 | 24 | 263, 391 | 354, 504 | 300, 376, 411 | 52% |
| 5 | 25 | 261, 385 | 354, 500 | 300, 380, 412 | 72% |
| 6 | 26 | 259 | 491 | 295 | 83% |
| 7 | 27 | 270 | 490 | 293 | 73% |
| 8 | 28 | 262 | 491 | 292 | 72% |
| 9 | 29 | 259 | 489 | 291 | 77% |
| 10 | 30 | 262 | 494 | 292 | 71% |
| 11 | 31 | 264 | 490 | 291 | 76% |
| 12 | 32 | 263 | 503 | 300 | 61% |

[a] Determined by HPLC measurements.

Entries 1-5 represent the photophysical characterization of the diarylmaleimide based photochromic ligands **21**, **22**, **23**, **24** and **25**, whereas entries 6-12 summarize the cyclopentene based photochromic ligands **26-32**. A slightly bathochromic shift is observed for the new arising absorption maxima corresponding to the closed photoisomers of the diarylmaleimides **21-25**, which is characteristic for this class of DTEs.^{11a} To our surprise, the photoconversion of the diarylmaleimides **21**, **22**, **23** and **24** (excluded **25**) is not as efficient as for the cyclopentene ligands **26-32**. Compared to a recently reported PSS of 94% for a diarylmaleimide photoswitch, with a free maleimide core and a phenyl substitution pattern on the thiophene moieties,^{4a} the substitution on the nitrogen atom of the maleimide core with the pharmacophores dramatically decreases the efficacy of the photoisomerization. In contrast, the cyclopentenones **26-32** exhibit

sufficiently high photoconversions shown by PSS ranging from 61-83%. Surprisingly, the cycle performance exhibits a better fatigue resistance for the maleimide-based switches **21-25**. **Figure 2** exemplary shows the UV-Vis absorption spectra and the cycle performance for the diarylmaleimide based ligand **23** and for the cyclopentene based ligand **30**.

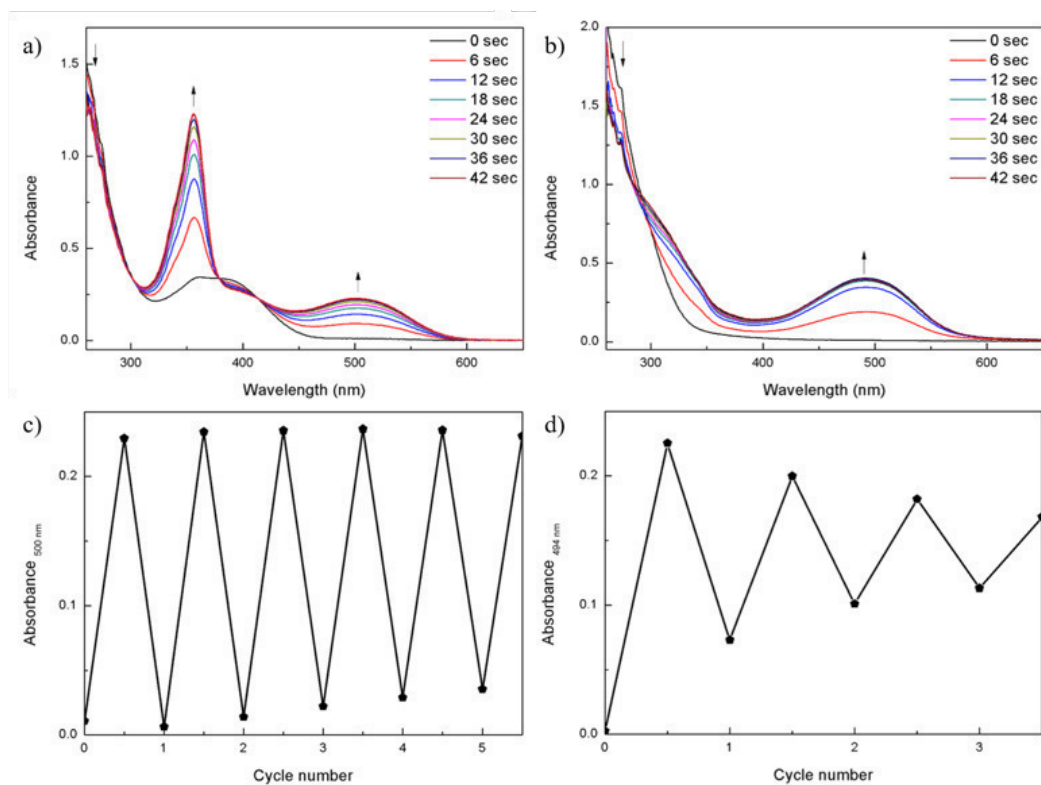
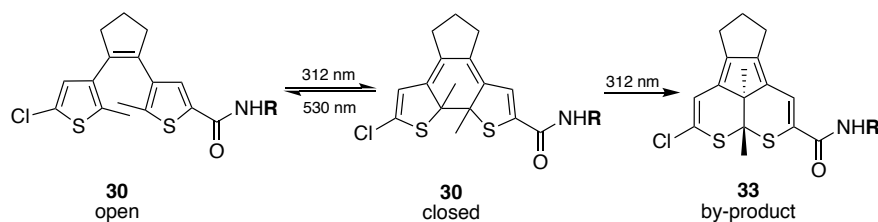


Figure 2. Comparison of the photochromic properties of diarylmaleimide based ligand **23** (a, c) ($100\ \mu\text{M}$ in DMSO) with the cyclopentene based ligand **30** (b, d) ($100\ \mu\text{M}$ in DMSO); a) and b) represent the UV-Vis absorption spectra upon continuous irradiation with light of $\lambda = 312\ \text{nm}$ (Herolab, 6 W), respectively; c) and d) represent the cycle performance using $\lambda = 312\ \text{nm}$ (Herolab, 6 W) for the ring closing and $\lambda = 530\ \text{nm}$ (green LED, 2.5 W) for the ring opening reaction, respectively: a) UV-Vis absorption spectra of ligand **23**; b) UV-Vis absorption spectra of ligand **30**; arrows indicate the characteristic changes in the absorption spectra; c) repetitive switching cycles at 500 nm of ligand **23**; d) repetitive switching cycles at 494 nm of ligand **30**.

The arrows indicate the characteristic changes in the spectra upon continuous irradiation with light of $\lambda = 312\ \text{nm}$ (Herolab, 6 W), accompanied by a characteristic color change of the samples. The cycle performance showed that ligand **23** is stable over at least six switching cycles, whereas a fast degradation of cyclopentene **30** was observed.

Further investigations by continuous irradiation with UV light ($\lambda = 312\ \text{nm}$) revealed the formation of an irreversible by-product **33** (Scheme 5). The phenomenon of this annulated isomer has been reported previously, but the mechanism of the by-product formation, which is related to the substitution pattern of the DTEs is not yet fully understood.^{22a-c}

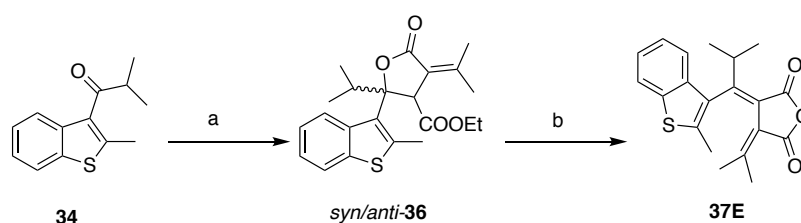


Scheme 5. Formation of the irreversible by-product **33** of the ligand **30** (R = **11**) upon continuous UV irradiation.

The photoisomerization can be monitored by UV-Vis absorption spectroscopy and is depicted in **Figure SI2a-c**. By irradiating the dissolved compound **30** with $\lambda = 312$ nm (Herolab, 6 W) one new maximum is arising at 494 nm, which is decreasing upon further UV irradiation. A new absorption maximum is observed, hypsochromically shifted to 360 nm, which is attributed to the irreversible occurring by-product **33**. The HPLC traces in **Figure SI2d** show that upon reaching the PSS, approximately 55% of the by-product has already been formed and its formation is completed after 192 sec. Similar to the results by Hecht *et al.*^{22a} we could confirm the structure of **33** with 2D-NMR spectroscopy experiments (see **SI3**, **Scheme SI3-1** and **SI3-2**).

2.4 Synthesis - fulgides and fulgimides

In a second series of dopamine receptor ligands, fulgides were synthesized, promising reversible switching in aqueous solution^{12a-b} and good fatigue resistance. The synthesis of the benzothiophene fulgide **37** was performed according to the experimental protocol of Stobbe *et al.* and Mattay *et al.*^{23a-b} The challenging step, the Stobbe condensation, was accomplished by enolization of isopropylidenesuccinate and subsequent reaction with **34**. This reaction results in a mixture of *syn/anti* lactones **36** whereby the *syn*-isomer **36** is the favoured one due to the isopropylgroup of **34**. The diacids were obtained after an elimination reaction and subsequent saponification by aqueous potassium hydroxide solution. For the anhydride formation, the crude diacids were treated with acetyl chloride to form the fulgide **37E** (**Scheme 6**).



Scheme 6. Benzothiophene fulgide **37** synthesis according Stobbe *et al.*; Reagents and conditions: (a) Isopropylidenesuccinate, LDA, THF, -78 °C \rightarrow r.t., 48 h, 16%. b) Step 1: KOH, EtOH, H₂O, 70 °C, 24 h; Step 2: AcCl, CH₂Cl₂, 40 °C, 20 h, 87%.

2.5 Photophysical investigations - fulgimides

Applications of photoswitches in biological assays require their solubility in aqueous buffer. Hence, the photoisomerization of the fulgimides **45**, **50** and **52** were carried out in polar solvents to obtain UV/Vis absorption spectra. **Table 2** summarizes the photostationary states (PSS), isosbestic points as well as the absorption maxima of **43** and **45**, determined in DMSO. The method for the PSS determination by HPLC is exemplarily shown for compound **48** in the **SI4**. The indolyl fulgimides **45**, **50** and **52** were also measured in a 10% DMSO – tris-buffer solution (pH = 7.4) (**Table 2**, Entry 3,7 and 9), whereby a hypsochromic shift of 18 nm of the absorption maximum in the visible light range was observed.

Table 2. Photochemical properties of fulgimides **43-52**.

| Entry | Compd. | λ_{\max} (open) | λ_{\max} (closed) | λ_{iso} | PSS ^[a] | PSS ^[b] |
|-------|--------------------------|-------------------------|---------------------------|------------------------|--------------------|--------------------|
| | | [nm] | [nm] | [nm] | O→C (Z:E:C) | C→O (Z:E) |
| 1 | 43 ^[c] | 307 | 473 | 290, 342, 347 | 0:30:70 | - |
| 2 | 45 ^[c] | 360 | 543 | 310, 344, 420 | 0:20:80 | - |
| 3 | 45 ^[d] | 356 | 525 | 305, 337, 417 | 0:19:81 | - |
| 4 | 46 ^[c] | 272 | 532 | 360 | 0:16:84 | - |
| 5 | 48 ^[c] | 328 | 486 | 315, 357 | 19:36:45 | 19:81 |
| 6 | 50 ^[c] | 370 | 564 | 306, 436 | 6:16:78 | 6:94 |
| 7 | 50 ^[d] | 370 | 325, 546 | 475 | 4:18:78 | 4:96 |
| 8 | 52 ^[c] | 363 | 563 | 302, 325, 430 | 4:12:84 | 4:96 |
| 9 | 52 ^[d] | 279, 366 | 300, 545 | 300, 320, 409 | 4:10:86 | 4:96 |

[a] Closing of the open E-isomers with UV light, PSS determined by HPLC measurements. [b] Opening of the closed mixture with visible light, PSS determined by HPLC measurements. [c] Solvent: DMSO. [d] Solvent: Tris-buffer + 10% DMSO.

The UV/Vis absorption spectra changes are exemplarily shown for compound **45** in **Figure 3** upon irradiation with 410 nm light in periods of 2 sec. New absorption bands arise at 543 nm and 330 nm, the band at 360 nm decreases and belongs to the open isomer. The opening of the closed photoisomers was accomplished by irradiation with light of 505 or 530 nm (1-2 min) for **43**, **45**, **46**, **48**, **50** and **52**.

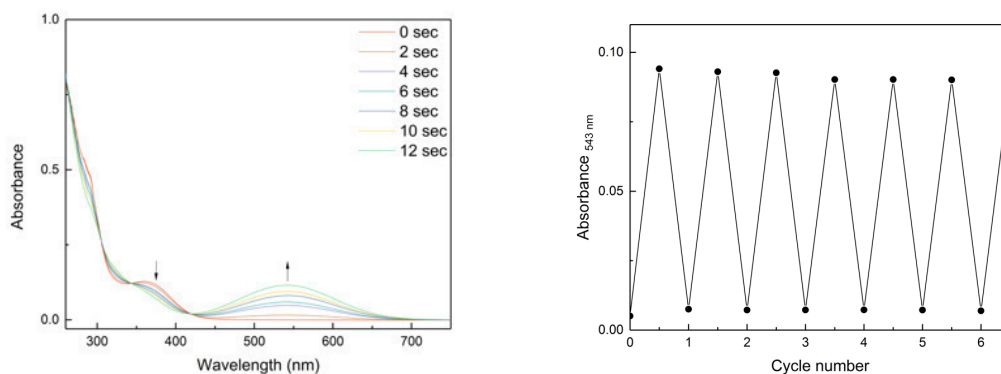


Figure 3. Left) the photochromic properties of a solution of **45** (50 μM in DMSO). The slightly yellow open form turned purple after 12 sec irradiation with 410 nm. The absorption spectra showed a new absorption band at 543 nm. Right) Repetitive switching of **45** is depicted on the right side.

The cycle performances of compounds **43**, **45**, **46**, **48**, **50** and **52** were studied by alternating irradiation at the appropriate wavelengths (**43** \rightarrow 312_{close} nm, 505_{open} nm; **45** \rightarrow 400_{close} nm, 530_{open} nm; **46**, **48** \rightarrow 365_{close} nm, 530_{open} nm; **50**, **52** \rightarrow 400_{close} nm, 530_{open} nm). The compounds showed good fatigue resistance and only little degradation was observed. Exemplarily, the cycle performance of compound **45** is depicted in **Figure 3**.

2.6 Biological investigations

The biological investigation of all test compounds was targeted towards their ability to activate the dopamine D_{2S} receptor. Our studies were directed to the identification of compound pairs exhibiting different activation profiles for the open and the closed photostationary state. Therefore, we applied screening assays for G-protein mediated signaling and arrestin recruitment at a fixed concentration (10 μM). The G-protein pathway was investigated utilizing the IP-One[®] assay (Cisbio) with HEK 293T cells transiently co-expressing D_{2S} and the hybrid G-protein G α qi5HA while β -arrestin-2 recruitment was determined applying the PathHunter[®] assay (DiscoverX). All activation data are summarized in **Table 3**, **SI5** and **SI6** in comparison to the reference ligand quinpirole. In the arrestin assay, the cyclopentene DTEs **26-30**, **32**, the diarylmaleimides **21-23**, **25** and the fulgimides **43**, **45**, **46**, **48**, **50** and **52** showed E_{max} values less than 15%. Only DTE **31** and the maleimide **24** both bearing the indanylamine moiety and a 4-atom spacer between the pharmacophoric headgroup and the photochromic entity (13) showed E_{max} values of 70% (**31**-open), 76% (**31**-closed), 33% (**24**-open), and 37% (**24**-closed), respectively.

Additional measurement of arrestin recruitment for those compounds at 100 nM revealed E_{max} values less than 10% and no differences in the activation pattern of the open and closed conformation. Whereas weak arrestin recruitment was observed, the determination of the G-

protein mediated signaling revealed agonist properties with efficacies in the range of 40 to 95% for all test compounds (Figure S15, Table S15-1, S15-2). More detailed measurements at 100 nM and 1 nM showed a dose-dependent range of efficacies allowing a precise evaluation of the open and closed conformations of each photochromic ligand. Within the series of maleimides, the indanylamine **24** showed the highest E_{max} values of 95% for both conformers, which is similar to the rank order of agonist effects derived from the arrestin assay, but without any difference between the open and the closed form. This observation can be confirmed by the results for the cyclopentene DTEs, where **31** (indanylamine with headgroup **13**) showed an E_{max} value of 95% for the open and the closed conformation, respectively.

Clear differences in E_{max} between both photochromic states could be observed for the methyl ether substituted phenylpiperazines **27** and **29** both carrying a 4-carbon spacer and only differing in the heteroatom of the ether group (O for **27**, S for **29**). For **29**, E_{max} values of 77% (10 μM), 80% (100 nM) and 32% (1 nM) have been determined for the open state, while efficacies of 70% (10 μM), 47% (100 nM) and 3% (1 nM) could be measured for the closed form (Table 3, Figure 4). This data indicate a 11-fold more efficient receptor activation by the open conformer compared to the closed derivative at low concentration (1 nM). In contrast, the methoxyphenylpiperazine **27** showed stronger receptor activation profile in the closed state compared to the open derivative, when a 3-fold increase of efficacy was determined for **27**-closed at 100 nM (closed-open: 49%-16% at 100 nM, 15%-11% at 1 nM). A similar selectivity profile could be detected for the indolyl fulgimides **45** and **52**. The methylthiophenylpiperazine **45**-closed showed a 2-fold increase of efficacy at 100 nM compared to the open state, while the benzoxazinone **52**-closed revealed a 4-fold improve of activity at 1 nM (for **45**: closed-open: 45%-25% at 100 nM, 8%-5% at 1 nM, for **52**: closed-open: 47%-48% at 100 nM, 40%-10% at 1 nM).

To learn more about the mechanistic relations of these selective photoswitchable ligands, we investigated the binding affinities of the most promising compounds **27**-open, **27**-closed, **29**-open, **29**-closed, **45**-open, **45**-closed, and **52**-(E)-open, **52**-closed at the dopamine D_{2S} receptor in a competition binding experiment. As all compounds displayed K_i values between 9 and 17 nM (Table S16), the state-selective intrinsic activity appears to be controlled by the individual ability to preferentially stabilize the active state of the receptor rather than by different binding affinities.

Table 3. Functional screening of the most promising photoactive ligands **27**, **29**, **45** and **52** for G-protein mediated activation of the dopamine D_{2S} receptor applying an IP accumulation assay^[a].

| Entry | Compd. | Photoactive state | Emax [% ± SEM] ^[b] | | |
|-------|-------------------|-------------------|-------------------------------|----------|-----------|
| | | | 10 [μM] | 100 [nM] | 1 [nM] |
| 1 | 27 | open | 85 ± 2.6 | 16 ± 9.6 | 11 ± 9.8 |
| 2 | 27 | closed | 67 ± 7.4 | 49 ± 2.0 | 15 ± 0.9 |
| 3 | 29 | open | 77 ± 3.8 | 80 ± 2.8 | 32 ± 4.6 |
| 4 | 29 | closed | 70 ± 6.8 | 47 ± 5.2 | 2.9 ± 3.2 |
| 5 | 45 | open | 68 ± 2.8 | 25 ± 5.3 | 5.6 ± 3.2 |
| 6 | 45 | closed | 62 ± 2.4 | 45 ± 7.8 | 7.7 ± 2.6 |
| 7 | 52 ^[c] | open | 58 ± 6.9 | 48 ± 8.5 | 10 ± 3.8 |
| 8 | 52 ^[c] | closed | 69 ± 6.6 | 47 ± 4.2 | 40 ± 4.6 |

[a] IP accumulation determined by applying the IP-One[®] assay (from Cisbio) with HEK 239T cells co-transfected with the cDNA of the dopamine D_{2S} receptor and that of the hybrid G-protein Gαqi5HA. [b] Emax value ± S.E.M. derived from 4 to 8 individual experiments each done in quadruplicate relative to the maximum effect of quinpirole. [c] The open isomer describes only the E-isomer.

An overall analysis of the data confers that the photoswitches **29** and **52** are most promising biochemical tools for the regulation of the pharmacologically important dopamine D_{2S} receptor. The potency of the more active isomers is comparable to the activation power of the reference dopaminergic agent quinpirole. The compounds require a very low dose of 1nM to exhibit a degree of receptor activation that strongly depends on the photostationary state of the ligand. Hence, the presence of the cyclopentene-DTE based photochromic ligands **29** in the open state induces an 11-fold higher G protein-promoted signaling than the existence of **29**-open in the same concentration. As a complementary pair of photochromic ligands, the fulgimide **52** shows four-fold higher D_{2S} receptor activation in the closed state compared to **52**-open (**Figure 4**).

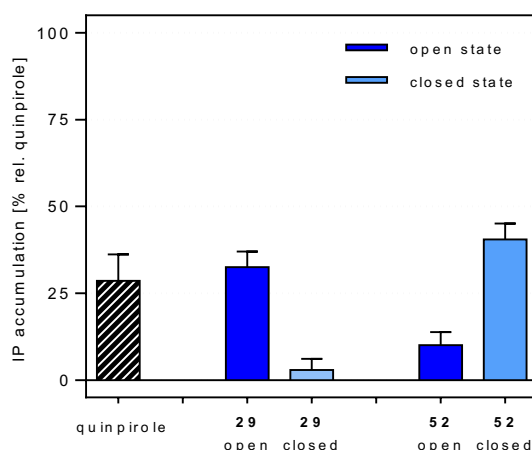


Figure 4. Activation of G-protein mediated receptor signaling determined by an IP accumulation assay using D_{2S} and the G-protein hybrid $G\alpha q5HA$. Accumulation of IP for the most promising photoswitchable ligands **29** and **52** in comparison to the reference quinpirole all determined at 1 nM. The DTE **29** shows an 11-fold improved activity for the open state (dark blue) than the closed state (light blue). In contrary, fulgimide **52** is 4-fold less active in the open conformation than for the closed one. For comparison, receptor activation induced by 1 nM of quinpirole (striped) reveals an efficacy of 28 % (derived from the dose-response curve, **Figure S14**). Bars represent average efficacy [% \pm S.E.M.] derived from 4 to 8 individual experiments each done in quadruplicates.

3. Conclusions

We succeeded in synthesizing DTE and fulgide based photochromic dopamine receptor ligands. The maleimides could not be switched in aqueous solution and the cyclopentene-DTEs had a low fatigue resistance, whereas the fulgimides showed excellent photophysical properties in aqueous solution. At a concentration of 1 nM, the cyclopentene-DTE **29**-open showed a more than 10-fold higher activation of D_{2S} , a pharmacologically important G protein-coupled receptor, than its photochromic congener **29**-closed. Interestingly, the fulgimide-based pair **52**-open/**52**-closed could be discovered as an alternative photoswitch with inverse activation properties exhibiting four-fold higher activity in the closed state. Further studies on the optimization of GPCR-regulating photoswitches and biological investigations including reversible, light-induced control of photochromic ligands when bound to the receptor are in progress.

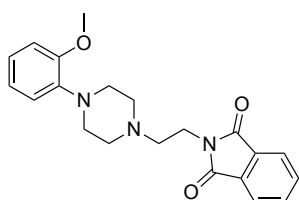
4. Experimental section

Starting materials were purchased from commercial suppliers and used without any further purification. Solvents were used in p.a. quality and dried according to common procedures, if necessary. Dry nitrogen was used as inert gas atmosphere. Thin-layer chromatography (TLC) for reaction monitoring was performed with alumina plates coated with Merck silica gel 60 F₂₅₄ (layer thickness: 0.2 mm) and analyzed under UV-light (254 nm). Flash column chromatography was performed with Sigma Aldrich MN silica gel 60M (0.040-0.063 mm, 230-

400 mesh) as stationary phase or a reversed phase column (KP-C18-HS) on a Biotage Isolera One automated flash purification system with UV-Vis detector. NMR spectra were recorded using a *Bruker Avance 300* (^1H : 300 MHz, ^{13}C : 75 MHz, T = 295 K), *Bruker Avance 360* (^1H : 360 MHz, ^{13}C : 91 MHz, T = 295 K), *Bruker Avance 400* (^1H 400.1: MHz, ^{13}C : 100.6 MHz, T = 300K) or a *Bruker Avance 600* (^1H : 600 MHz, ^{13}C : 151 MHz, T = 295 K) instrument. The spectra are referenced against the NMR solvent and are reported as follows: ^1H : chemical shift δ (ppm), multiplicity, integration, coupling constant (J in Hz). ^{13}C : chemical shift δ (ppm), abbreviations: (+) = primary/tertiary, (-) = secondary, (q) = quaternary carbon. The assignment resulted from DEPT, COSY, HMBC and HSQC experiments. Mass spectra were measured with a Finnigan MAT 95, Finnigan MAT SSS 710 A, ThermoQuest Finnigan TSS 7000 or an Agilent Q-TOF 6540 UHD instrument. Standard hand-held lamps (Herolab, 312 nm, 6 W) and LEDs with 365 nm (3.2 W) 400 nm (2.5 W) were used for visualizing TLC and to perform the ring closure reactions. The ring opening reactions were performed using LEDs with 505 nm (2.5 W) and 530 nm (2.5 W) emission maximum. Absorption spectra were recorded on a Varian Cary 50 Bio UV/Vis spectrophotometer. Preparative HPLC was performed on a Knauer HPLC (column: Luna 10 250 x 21 mm; flow: 3 mL/min, solvent A: H_2O [0.1 Vol% TFA], solvent B: MeCN \rightarrow prep-HPLC-1) and on an *Agilent 1100 Series* (Column: *Phenomenex Luna 10, C18, 100A, 250 x 21.2 mm*, flow 20 mL/min, solvent A: H_2O [0.05 Vol% TFA], solvent B: MeCN \rightarrow prep-HPLC-2). Photostationary states of the final compounds were measured on an Agilent 1290 Series HPLC (Column: Phenomenex Luna C18, 3 μm , 150 x 2.00 mm, 100 \AA ; flow: 0.3 mL/min) and *Agilent 1220 Infinity LC System* (column: *Phenomenex Luna, 3 μ C18(2) 100A, 150 x 2.0 mm, 100 \AA , 40 $^\circ\text{C}$*). All biological investigations were performed in the group of Prof. Dr. P. Gmeiner by Dr. H. Hübner (University of Erlangen-Nürnberg).

4.1 Synthesis

Compound 2: 4-(2-Methoxyphenyl)-1-[2-(*N*-phthalimido)ethyl]piperazine

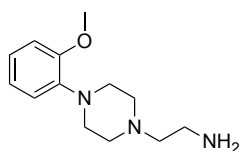


1-(2-Methoxyphenyl)piperazine (673 mg, 3.5 mmol, 1.0 eq) and *N*-(2-bromoethyl)phthalimide (1.07 g, 4.2 mmol, 1.2 eq) were dissolved in MeCN (12 mL). K_2CO_3 (725 mg, 5.2 mmol, 1.5 eq) and a catalytic amount of KI were added and the reaction mixture was stirred under reflux for 5 h. After cooling down to room temperature, the precipitate was filtered off and washed with acetonitrile. The solvent was evaporated and the crude product was purified via column

chromatography (CH₂Cl₂/MeOH, 100:1) to yield **2** (914 mg, 2.5 mmol, 71%) as a colorless solid.

Analytical data as described in literature.¹⁶

Compound 3: 1-(2-Aminoethyl)-4-(2-methoxyphenyl)piperazine

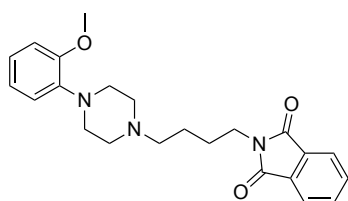


C₁₃H₂₁N₃O, MW = 235.33 g/mol

4-(2-Methoxyphenyl)-1-[2-(*N*-phthalimido)ethyl]piperazine (**2**) (350 mg, 0.96 mmol, 1.0 eq) was dissolved in EtOH (2.0 mL) and 80% hydrazine hydrate solution (90 μL, 1.4 mmol, 1.5 eq) was added. The reaction mixture was stirred under reflux for 2 h, then HCl (2 M, 1.1 mL) was added and stirring was continued under reflux for two hours. After cooling down to room temperature, the precipitate was filtered off. The solvent was evaporated and the residue was dissolved in H₂O. The pH was adjusted to 8 with NaOH (1 M) and the product was extracted with CH₂Cl₂. The combined organic layers were dried over Na₂SO₄ and the solvent was evaporated. The crude product was purified by flash chromatography (CH₂Cl₂/MeOH, 40:1 → 12:1) to yield **3** (178 mg, 0.76 mmol, 73%) as a colorless solid.

Analytical data as described in literature.¹⁶

Compound 4: 4-(2-Methoxyphenyl)-1-[4-(*N*-phthalimido)butyl]piperazine

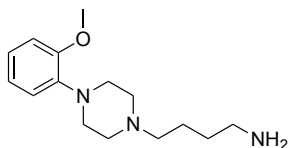


C₂₃H₂₇N₃O₃, MW = 393.49 g/mol

Compound **4** was prepared as described for **2**, using a solution of 1-(2-methoxyphenyl)piperazine (600 mg, 3.1 mmol, 1.0 eq), *N*-(4-bromobutyl)phthalimide (967 mg, 3.4 mmol, 1.1 eq), K₂CO₃ (646 mg, 4.7 mmol, 1.5 eq) and a catalytic amount of KI in MeCN (10 mL), allowing a reaction time of 16h. Purification of the crude product by column chromatography yielded **4** (1.1 g, 2.8 mmol, 88%) as yellow oil.

Analytical data as described in literature.¹⁶

Compound 5: 1-(4-Aminobutyl)-4-(2-methoxyphenyl)piperazine

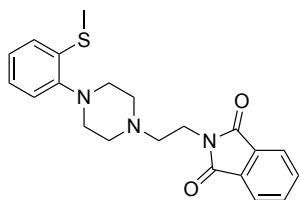


$C_{15}H_{25}N_3O$, MW = 263.39 g/mol

Compound **5** was prepared as described for **3**, using a solution of 4-(2-methoxyphenyl)-1-[4-(*N*-phthalimido)butyl]piperazine (**4**) (260 mg, 0.66 mmol, 1.0 eq), 80% hydrazine hydrate solution (62 μ L, 0.99 mmol, 1.5 eq) in EtOH (1.3 mL) and HCl (2 M, 0.7 mL). Purification of the crude product by flash chromatography yielded **5** (137 mg, 0.52 mmol, 79%) as a light yellow oil.

Analytical data as described in literature.¹⁶

Compound 6: 4-(2-Methylthiophenyl)-1-[2-(*N*-phthalimido)ethyl]piperazine



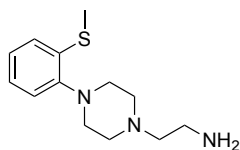
$C_{21}H_{23}N_3O_2S$, MW = 381.49 g/mol

Compound **6** was prepared as described for **2**, using a solution of 1-(2-(methylthio)phenyl)piperazine (650 mg, 3.1 mmol, 1.0 eq), *N*-(2-bromoethyl)phthalimide (871 mg, 3.4 mmol, 1.1 eq), K_2CO_3 (646 mg, 4.7 mmol, 1.5 eq) and a catalytic amount of KI in MeCN (10 mL), allowing a reaction time of 16h. Purification of the crude product by column chromatography yielded **6** (890 mg, 2.3 mmol, 75%) as a yellow solid.

1H -NMR (360 MHz, $CDCl_3$): δ = 2.40 (s, 3H), 2.59 – 2.85 (m, 6H), 2.86 – 3.05 (m, 4H), 3.86 (t, J = 6.6 Hz, 2H), 6.98 – 7.04 (m, 1H), 7.05 – 7.15 (m, 3H), 7.71 (dd, J = 5.4, 3.1 Hz, 2H), 7.85 (dd, J = 5.5, 3.0 Hz, 2H).

^{13}C -NMR (91 MHz, $CDCl_3$): δ = 14.6 (+), 35.5 (-), 51.8 (-), 53.6 (-), 56.0 (-), 119.8 (+), 123.3 (+), 124.4 (+), 125.0 (+), 132.4 (q), 134.0 (+), 135.0 (q), 149.7 (q), 168.5 (q);

ESI-MS: m/z (%) = 381.9 ($M+H^+$)

Compound 7: 1-(2-Aminoethyl)-4-(2-methylthiophenyl)piperazine

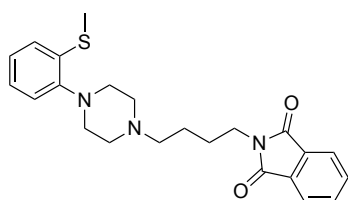
$C_{13}H_{21}N_3S$, MW = 251.39 g/mol

Compound **7** was prepared as described for **3**, using a solution of 4-(2-methylthiophenyl)-1-[2-(*N*-phthalimido)ethyl]piperazine (**6**) (400 mg, 1.0 mmol, 1.0 eq), 80% hydrazine hydrate solution (0.1 mL, 1.6 mmol, 1.6 eq) in EtOH (2.1 mL) and HCl (2 M, 1.2 mL). Purification of the crude product by flash chromatography yielded **7** (233 mg, 0.93 mmol, 82%) as a yellow oil.

1H -NMR (360 MHz, $CDCl_3$): δ = 2.41 (s, 3H), 2.51 (t, J = 6.2 Hz, 2H), 2.65 (m, 4H), 2.84 (t, J = 6.2 Hz, 2H), 3.08 – 2.97 (m, 4H), 7.16 – 7.02 (m, 4H);

^{13}C -NMR (151 MHz, $CDCl_3$): δ = 14.6 (+), 39.1 (-), 51.8 (-), 53.8 (-), 61.4 (-), 119.7 (+), 124.4 (+), 124.5 (+), 125.0 (+), 135.1 (q), 149.7 (q).

ESI-MS: m/z (%) = 251.9 ($M+H^+$)

Compound 8: 4-(2-Methoxyphenyl)-1-[4-(*N*-phthalimido)butyl]piperazine

$C_{23}H_{27}N_3O_2S$, MW = 409.55 g/mol

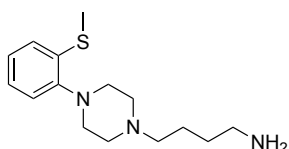
Compound **8** was prepared as described for **4**, using a solution of 1-(2-(methylthio)phenyl)piperazine (650 mg, 3.1 mmol, 1.0 eq), *N*-(4-bromobutyl)phthalimide (967 mg, 3.4 mmol, 1.1 eq), K_2CO_3 (646 mg, 4.7 mmol, 1.5 eq) and a catalytic amount of KI in MeCN (10 mL), allowing, a reaction time of 16 h. Purification of the crude product by column chromatography yielded **8** (1.15 g, 2.8 mmol, 90%) as a yellow solid.

1H -NMR (360 MHz, $CDCl_3$): δ = 1.53 – 1.68 (m, 2H), 1.68 – 1.90 (m, 2H), 2.40 (s, 3H), 2.44 – 2.57 (m, 2H), 2.62 – 2.80 (m, 4H), 2.91 – 3.15 (m, 4H), 3.73 (t, J = 7.0 Hz, 2H), 7.01 – 7.07 (m, 1H), 7.07 – 7.14 (m, 3H), 7.64 – 7.78 (m, 2H), 7.78 – 7.93 (m, 2H).

¹³C-NMR (91 MHz, CDCl₃): δ = 14.6 (+), 24.3 (-), 26.8 (-), 38.0 (-), 51.6 (-), 53.7 (-), 58.2 (-), 119.8 (+), 123.3 (+), 124.4 (+), 124.6 (+), 125.1 (+), 132.3 (q), 134.0 (+), 135.1 (q), 149.6 (q), 168.6 (q).

ESI-MS: m/z (%) = 410.3 (M+H⁺)

Compound 9: 1-(4-Aminobutyl)-4-(2-methylthiophenyl)piperazine



C₁₅H₂₅N₃S, MW = 279.45 g/mol

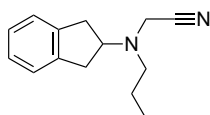
Compound **9** was prepared as described for **3**, using a solution of 4-(2-methoxyphenyl)-1-[4-(*N*-phthalimido)butyl]piperazine (**8**) (400 mg, 0.98 mmol, 1.0 eq), 80% hydrazine hydrate solution (0.1 mL, 1.5 mmol, 1.5 eq) in EtOH (2 mL). Purification of the crude product by flash chromatography yielded **9** (156 mg, 0.56 mmol, 57%) as a yellow oil.

¹H-NMR (360 MHz, CDCl₃): δ = 1.42 – 1.69 (m, 4H), 2.41 (s, 3H), 2.40 – 2.47 (m, 2H), 2.58 – 2.69 (s, 4H), 2.69 – 2.89 (m, 2H), 2.93 – 3.15 (m, 4H), 7.02 – 7.18 (m, 4H).

¹³C-NMR (151 MHz, CDCl₃): δ = 14.6 (+), 24.6 (-), 31.9 (-), 42.2 (-), 51.8 (-), 53.8 (-), 58.7 (-), 119.8 (+), 124.3 (+), 124.5 (+), 125.1 (+), 135.1 (q), 149.7 (q).

ESI-MS: m/z (%) = 280.17 (M+H⁺)

Compound 10: 2-[(*N*-Indan-2-yl)(propyl)amino]acetonitrile



C₁₄H₁₈N₂, MW = 214.31 g/mol

2-Propylaminoindane oxalate (210 mg, 0.82 mmol, 1.0 eq), K₂CO₃ (634 mg, 4.6 mmol, 5.6 eq) and KI (136 mg, 0.82 mmol, 1.0 eq) were suspended in MeCN (5.5 mL) and stirred for 5 min. Chloroacetonitrile (0.13 mL, 2.0 mmol, 2.4 eq) was added dropwise and the mixture was stirred under reflux for 2 h. After cooling down to room temperature, the solvent was removed under reduced pressure. Water was added to the residue and the pH was adjusted to 7 with NaOH (1 M). The product was extracted with CH₂Cl₂. The organic layers were dried over Na₂SO₄ and

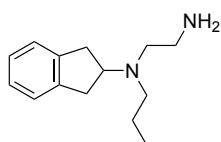
evaporated. Purification of the crude product by flash chromatography (PE/EtOAc, 10:1) yielded **10** (153 mg, 0.71 mmol, 89%) as a yellow oil.

¹H-NMR (600 MHz, CDCl₃): δ = 0.95 (t, *J* = 7.4 Hz, 3H), 1.53 (dq, *J* = 14.7, 7.3 Hz, 2H), 2.56 – 2.67 (m, 2H), 2.88 (dd, *J* = 14.8, 9.2 Hz, 2H), 3.14 (dd, *J* = 14.7, 7.4 Hz, 2H), 3.47 – 3.59 (m, 1H), 3.67 (s, 2H), 7.11 – 7.17 (m, 2H), 7.17 – 7.22 (m, 2H).

¹³C-NMR (151 MHz, CDCl₃): δ = 11.8 (+), 20.6 (-), 37.9 (C1, C3), 40.2 (-), 53.6 (-), 64.3 (+), 115.5 (q), 124.6 (+), 126.8 (+), 141.0 (q).

ESI-MS: *m/z* (%) = 215.0 (M+H⁺)

Compound **11**: 2-[(*N*-Indan-2-yl)(propyl)amino]ethane-1-amine



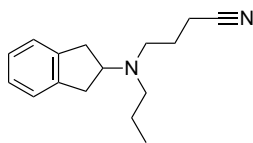
C₁₄H₂₂N₂, MW = 218.34 g/mol

2-[(*N*-Indan-2-yl)(propyl)amino]acetonitrile (**10**) (149 mg, 0.69 mmol, 1.0 eq) was dissolved in Et₂O (7 mL) and cooled to 0°C. LiAlH₄ (0.35 mL, 1.4 mmol, 2.0 eq) was added dropwise and the mixture was stirred at room temperature for 1 h. Saturated NaHCO₃ was added at 0°C. The precipitate was filtered off and the product was extracted with CH₂Cl₂. The organic layers were dried over Mg₂SO₄ and evaporated. Purification of the crude product by flash chromatography (CH₂Cl₂/MeOH, 15:1, 0.1% NH₃) yielded **11** (107 mg, 0.49 mmol, 71%) as a colorless oil.

¹H-NMR (600 MHz, CDCl₃): δ = 0.89 (t, *J* = 7.4 Hz, 3H), 1.46 – 1.56 (m, 2H), 2.47 – 2.56 (m, 2H), 2.60 (t, *J* = 6.1 Hz, 2H), 2.80 (m, 2H), 2.90 (dd, *J* = 15.5, 8.3 Hz, 2H), 3.03 (dd, *J* = 15.5, 7.9 Hz, 2H), 3.74 (p, *J* = 8.1 Hz, 1H), 7.10 – 7.15 (m, 2H), 7.17 (dt, *J* = 7.2, 3.6 Hz, 2H).

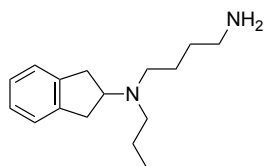
¹³C-NMR (151 MHz, CDCl₃): δ = 12.0 (+), 20.8 (-), 36.4 (-), 40.2 (-), 53.9 (-), 54.0 (-), 63.0 (+), 124.6 (+), 126.4 (+), 142.0 (q).

ESI-MS: *m/z* (%) = 219.0 (M+H⁺)

Compound 12: 4-[(*N*-Indan-2-yl)(propyl)amino]butyronitrile $C_{16}H_{22}N_2$, MW = 242.37 g/mol

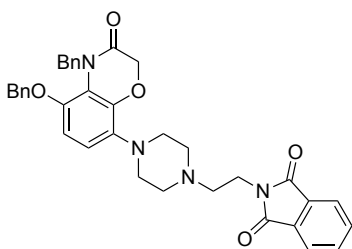
Compound **12** was prepared as described for **10**, using a solution of 2-propylaminoindane oxalate (80 mg, 0.38 mmol, 1.0 eq), K_2CO_3 (294 mg, 2.1 mmol, 5.5 eq), KI (63 mg, 0.38 mmol, 1.0 eq) and 4-bromobutyronitrile (90 μ L, 0.91 mmol, 2.4 eq) in MeCN (2.5 mL). Purification of the crude product by flash chromatography (PE/EtOAc, 9:1) yielded **12** (81 mg, 0.33 mmol, 88%) as a brownish oil.

Analytical data as described in literature.²

Compound 13: 4-[(*N*-Indan-2-yl)(propyl)amino]butane-1-amine $C_{16}H_{26}N_2$, MW = 246.40 g/mol

Compound **13** was prepared as described for **11**, using a solution of 4-[(*N*-indan-2-yl)(propyl)amino]butyronitrile (30 mg, 0.12 mmol, 1.0 eq) and $LiAlH_4$ (75 μ L, 0.30 mmol, 2.5 eq) in Et_2O (0.85 mL). Purification of the crude product by flash chromatography ($CH_2Cl_2/MeOH$ 15:1, 0.1% NH_3) yielded **13** (18 mg, 0.073 mmol, 57%) as a colorless oil.

Analytical data as described in literature.¹⁸

Compound 15: 4-[4-Benzyl-5-(benzyloxy)-2*H*-benzo[*b*][1,4]oxazin-3(4*H*)-one-8-yl]-1-[2-(*N*-phthalimido)ethyl] piperazine $C_{36}H_{34}N_4O_5$, MW = 602.69 g/mol

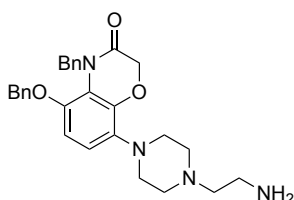
Compound **15** was prepared as described for **2**, using a solution of 4-[4-benzyl-5-(benzyloxy)-2*H*-benzo[*b*][1,4]oxazin-3(4*H*)-one-8-yl]piperazine (**14**) (339 mg, 0.79 mmol, 1.0 eq) and *N*-(2-bromoethyl) phthalimide (220 mg, 0.89 mmol, 1.1 eq), K₂CO₃ (163 g, 1.18 mmol, 1.5 eq) and a catalytic amount of KI in MeCN (8 mL). Purification by flash chromatography (CH₂Cl₂/MeOH 50:1) to yielded **15** (318 mg, 0.53 mmol, 67 %) as a colorless solid.

¹H-NMR (600 MHz, CDCl₃): δ = 2.58 – 2.80 (m, 6H), 2.84 – 3.02 (m, 4H), 3.85 (t, *J* = 6.3 Hz, 2H), 4.56 (s, 2H), 4.90 (s, 2H), 5.38 (s, 2H), 6.50 (d, *J* = 9.0 Hz, 1H), 6.56 (d, *J* = 9.0 Hz, 1H), 7.08 – 7.17 (m, 3H), 7.28 – 7.32 (m, 2H), 7.32 – 7.39 (m, 3H), 7.69 – 7.73 (m, 2H), 7.82 – 7.89 (m, 2H).

¹³C-NMR (91 MHz, CDCl₃): δ = 35.4 (-), 46.8 (-), 51.2 (-), 53.3 (-), 55.9 (-), 68.9 (-), 71.6 (-), 107.8 (+), 114.2 (+), 120.1 (q), 123.3 (+), 123.5 (q), 126.9 (+), 127.0 (+), 127.7 (+), 128.3 (+), 128.3 (+), 128.8 (+), 132.4 (q), 134.0 (+), 134.1 (q), 136.5 (q), 137.4 (q), 142.7 (q), 145.1 (q), 166.7 (q), 168.5 (q).

ESI-MS: *m/z* (%) = 603.2 (M+H⁺)

Compound 16: 1-(2-Aminoethyl)-4-[4-benzyl-5-(benzyloxy)-2*H*-benzo[*b*][1,4]oxazin-3(4*H*)-one-8-yl]piperazine



C₂₈H₃₂N₄O₃, MW = 472.59 g/mol

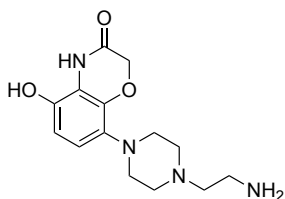
Compound **16** was prepared as described for **3**, using a solution of 4-[4-benzyl-5-(benzyloxy)-2*H*-benzo[*b*][1,4]oxazin-3(4*H*)-one-8-yl]-1-[2-(*N*-phthalimido)ethyl] piperazine (**15**) (310 mg, 0.51 mmol, 1.0 eq) and 80% hydrazine hydrate solution (50 μL, 0.77 mmol, 1.5 eq) in EtOH (5 mL). Purification by flash chromatography (CH₂Cl₂/MeOH 20:1, 0.1% NH₃) yielded **16** (206 mg, 0.44 mmol, 85%) as a colorless solid.

¹H-NMR (600 MHz, D₆-DMSO): δ = 2.51 – 2.60 (m, 6H), 2.81 – 2.95 (m, 6H), 4.60 (s, 2H), 5.02 (s, 2H), 5.29 (s, 2H), 6.63 (d, *J* = 9.1 Hz, 1H), 6.71 (d, *J* = 9.1 Hz, 1H), 7.00 (d, *J* = 7.2 Hz, 2H), 7.15 (t, *J* = 7.3 Hz, 1H), 7.21 (t, *J* = 7.4 Hz, 2H), 7.44 – 7.31 (m, 5H).

¹³C-NMR (91 MHz, D₆-DMSO): δ = 35.8 (-), 45.6 (-), 50.3 (-), 52.6 (-), 54.7 (-), 68.2 (-), 70.7 (-), 107.9 (+), 113.9 (+), 119.5 (q), 126.4 (+), 126.8 (+), 127.7 (+), 127.9 (+), 128.2 (+), 128.5 (+), 135.5 (q), 136.5 (q), 137.4 (q), 142.1 (q), 144.2 (q), 166.3 (q).

ESI-MS: m/z (%) = 473.3 (M+H⁺)

Compound 17: 1-(2-Aminoethyl)-4-(5-Hydroxy-2*H*-benzo[*b*][1,4]oxazin-3(4*H*)-one-8-yl)piper-azine



C₁₄H₂₀N₄O₃, MW = 292.34 g/mol

1-(2-Aminoethyl)-4-[4-benzyl-5-(benzyloxy)-2*H*-benzo[*b*][1,4]oxazin-3(4*H*)-one-8-yl]piperazine (**16**) (120 mg, 0.25 mmol, 1.0 eq) was suspended in toluene (3.6 mL) and methansulfonic acid (0.2 mL, 2.5 mmol, 10 eq) was added. The reaction mixture was stirred under reflux for 3 h. After cooling down to room temperature, the solvent was removed. Purification of the crude product by preparative flash chromatography (CH₂Cl₂/MeOH, 12:1, 0.5% NH₃) yielded **17** (65 mg, 0.22 mmol, 89%) as a colorless solid.

¹H-NMR (600 MHz, D₆-DMSO): δ = 2.55 – 2.71 (m, 4H), 2.81 – 2.93 (m, 4H), 2.93 – 3.06 (m, 2H), 3.10 – 3.24 (m, 2H), 4.48 (s, 2H), 6.44 (s, 2H), 9.78 (s, 1H), 9.48 (s, 1H).

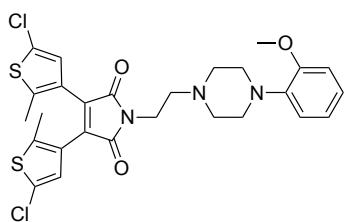
¹³C-NMR (101 MHz, D₆-DMSO): δ = 33.5 (-), 47.9 (-), 51.9 (-), 52.6 (-), 66.9 (-), 108.6 (+), 112.8 (+), 116.7 (q), 131.1 (q), 137.6 (q), 141.7 (q), 164.4 (q).

ESI-MS: m/z (%) = 293.1 (M+H⁺)

General preparation of diarylmaleimide based switches **21-24**:

To a suspension of **18** (61 mg, 0.17 mmol, 1.0 eq) and K₂CO₃ (23 mg, 0.17 mmol, 1.0 eq) in CH₂Cl₂ (1.5 mL) was added an amine of A or B (0.17 mmol, 1.0 eq). After stirring for 0.25 - 3 h at r.t., water (1 mL) was added and the aqueous phase was extracted with CH₂Cl₂ (2 x 4 mL). The combined organic phases were dried over MgSO₄, filtered and the solvent was removed under reduced pressure. The crude product was first purified by automated flash column chromatography and second by preparative HPLC.

Compound 21: 3,4-Bis(5-chloro-2-methylthiophen-3-yl)-1-(2-(4-(2-methoxyphenyl)-piperazin-1-yl)ethyl)-1H-pyrrole-2,5-dione



$C_{27}H_{27}Cl_2N_3O_3S_2$, MW = 576.55 g/mol

Yellow solid: 68% yield; reaction time: 2 h; flash chromatography: $CH_2Cl_2/MeOH$: 0-5% MeOH; preparative HPLC (prep-HPLC-1, gradient A/B: 0-25 min: 80/20, 25-35 min: 5/95; t_R = 19.6 min)

TLC: ($CH_2Cl_2/MeOH$, 10:1) R_f = 0.10

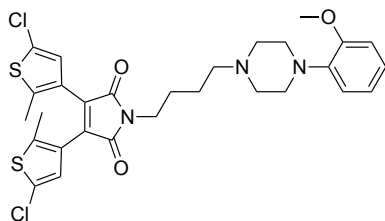
1H -NMR (600 MHz, $CDCl_3$) δ = 1.98 (s, 6H), 3.08-3.20 (m, 2H), 3.30-3.40 (m, 2H), 3.43 (t, 2H, J = 5.7 Hz), 3.46-3.57 (m, 2H), 3.87 (s, 3H), 3.92-4.02 (m, 2H), 4.05 (t, 2H, J = 5.7 Hz), 6.88-6.90 (m, 3H), 6.92-6.98 (m, 2H), 7.07-7.10 (m, 1H).

^{13}C -NMR (151 MHz, $CDCl_3$) δ = 14.8 (+), 32.5 (-), 47.4 (-), 52.3 (-), 55.0 (-), 55.5 (+), 111.4 (+), 119.1 (+), 121.3 (+), 124.9 (+), 125.7 (q), 127.0 (q), 127.3 (+), 133.1 (q), 138.2 (q), 140.9 (q), 152.0 (q), 169.8 (q).

HR-MS (ESI): calcd. for $C_{27}H_{28}Cl_2N_3O_3S_2$ ($M+H^+$), m/z = 576.0944, found 576.0945

UV/Vis (50 μM in DMSO): open isomer: λ_{max} = 261 nm, 390 nm; closed isomer: λ_{max} = 356 nm, 509 nm.

Compound 22: 3,4-Bis(5-chloro-2-methylthiophen-3-yl)-1-(4-(4-(2-methoxyphenyl)-piperazin-1-yl)butyl)-1H-pyrrole-2,5-dione



$C_{29}H_{31}Cl_2N_3O_3S_2$, MW = 604.61 g/mol

Orange solid: 80% yield; reaction time: 0.25 h; flash chromatography: CH₂Cl₂/MeOH: 0-10% MeOH; preparative HPLC (prep-HPLC-1, gradient A/B: 0-25 min: 80/20, 25-35 min 5/95; t_R = 19.2 min)

TLC: (CH₂Cl₂/MeOH, 10:1) R_f = 0.63

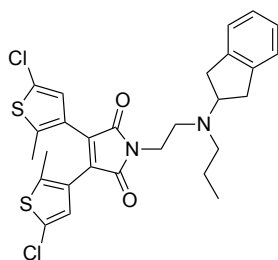
¹H-NMR (600 MHz, CDCl₃) δ = 1.72-1.81 (m, 2H), 1.82-1.91 (m, 2H), 1.94 (s, 6H), 3.09- 3.17 (m, 4H), 3.27 (t, 2H, J = 12.3 Hz), 3.49-3.55 (m, 2H), 3.62- 3.71 (m, 4H), 3.87 (s, 3H), 6.86- 6.89 (m, 1H), 6.90 (s, 2H), 6.92- 6.97 (m, 2H), 7.08 (ddd, J = 8.1, 6.2, 2.8 Hz, 1H);

¹³C-NMR (151 MHz, CDCl₃) δ = 14.9 (+), 20.8 (-), 25.8 (-), 37.2 (-), 47.6 (-), 52.2(-), 55.5 (+), 56.5 (-), 111.4 (+), 119.0 (+), 121.3 (+), 124.7 (+), 125.8 (q), 127.1 (+), 127.2 (q), 132.5 (q), 138.6 (q), 140.5 (q), 152.1 (q), 170.1 (q);

HR-MS (ESI): calcd. for C₂₉H₃₂Cl₂N₃O₃S₂ (M+H⁺), m/z = 604.1257, found 604.1253

UV/Vis (100 μM in DMSO): open isomer: λ_{max} = 260 nm, 378 nm; closed isomer: λ_{max} = 355 nm, 493 nm.

Compound 23: 3,4-Bis(5-chloro-2-methylthiophen-3-yl)-1-(2-((2,3-dihydro-1H-inden-2-yl)-(propyl)amino)ethyl)-1H-pyrrole-2,5-dione



C₂₈H₂₈Cl₂N₂O₂S₂, MW = 559.56 g/mol

Orange solid: 15% yield; reaction time: 3 h; no flash chromatography, preparative HPLC (prep-HPLC-1, solvent A: H₂O [0.05 Vol% TFA], solvent B: MeCN, gradient A/B: 0-30 min: 60/40, 30-40 min 5/95; t_R = 21.6 min)

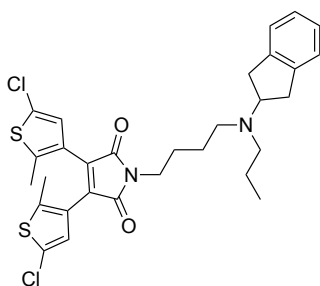
¹H-NMR (300 MHz, D₆-DMSO + D₂O) δ = 0.97 (t, 3H, J = 7.3 Hz), 1.68-1.81 (m, 2H), 1.91 (s, 6H), 3.18-3.26 (m, 4H), 3.30-3.37 (m, 4H), 3.13-3.21 (m, 4H), 3.29- 3.40 (m, 4H), 3.88-4.00 (m, 2H), 4.31-4.44 (m, 1H), 6.99 (s, 2H), 7.19-7.23 (m, 2H), 7.25-7.29 (m, 2H).

¹³C-NMR (151 MHz, D₆-DMSO) δ = 10.9 (+), 14.3 (+), 16.3 (-), 32.6 (-), 34.3 (-), 47.1 (-), 51.9 (-), 62.9 (+), 124.4 (+), 125.0 (q), 126.2 (q), 127.2 (+), 127.6 (+), 132.7 (q), 138.9 (q), 140.2 (q), 169.4 (q);

HR-MS (ESI): calcd. for C₂₈H₂₉Cl₂N₂O₂S₂ (M+H⁺), m/z = 559.1042, found 559.1048

UV/Vis (100 μM in DMSO): open isomer: λ_{max} = 264 nm, 360 nm; closed isomer: λ_{max} = 355 nm, 500 nm.

Compound 24: 3,4-Bis(5-chloro-2-methylthiophen-3-yl)-1-(4-((2,3-dihydro-1H-inden-2-yl)-(propyl)amino)butyl)-1H-pyrrole-2,5-dione



C₃₀H₃₂Cl₂N₂O₂S₂, MW = 587.62 g/mol

Orange solid: 86% yield; reaction time: 3 h; flash chromatography: CH₂Cl₂/MeOH: 0-10% MeOH; preparative HPLC (prep-HPLC-1, gradient A/B: 0-30 min: 60/40, 30-40 min 2/98; t_R = 16.7 min)

TLC: (CH₂Cl₂/MeOH, 10:1) R_f = 0.14

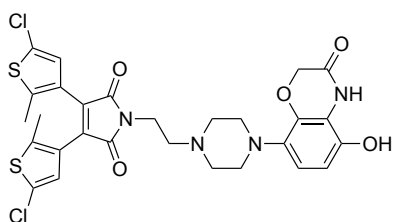
¹H-NMR (400 MHz, D₆-DMSO) δ = 0.92 (t, 3H, J = 7.3 Hz), 1.59-1.83 (m, 6H), 1.91 (s, 6H), 3.03- 3.10 (m, 2H), 3.12-3.19 (m, 2H), 3.24-3.36 (m, 4H), 3.55 (t, 2H, J = 6.7 Hz), 4.13-4.29 (m, 1H), 6.99 (s, 2H), 7.18-7.21 (m, 2H), 7.22-7.26 (m, 2H), 10.32 (bs, 1H).

¹³C-NMR (101 MHz, D₆-DMSO): δ = 10.9 (+), 14.2 (+), 16.5 (-), 20.3 (-), 25.2 (-), 34.3 (-), 37.1 (-), 49.9 (-), 51.9 (-), 62.7 (+), 124.2 (q), 124.3 (q), 124.7 (+), 126.4 (q), 127.1 (+), 127.7 (+), 132.4 (q), 139.1 (q), 139.9 (q), 169.8 (q);

HR-MS (ESI): calcd. for C₃₀H₃₃Cl₂N₂O₂S₂ (M+H⁺), m/z = 587.1355, found 587.1359;

UV/Vis (50 μM in DMSO): open isomer: λ_{max} = 263 nm, 391 nm; closed isomer: λ_{max} = 354 nm, 504 nm.

Compound 25: 3,4-bis(5-chloro-2-methylthiophen-3-yl)-1-(2-(4-(5-hydroxy-3-oxo-3,4-dihydro-2H-benzo[b][1,4]oxazin-8-yl)piperazin-1-yl)ethyl)-1H-pyrrole-2,5-dione



Dithienylmaleimide **18** (50.0 mg, 0.14 mmol, 1 eq) was dissolved in DMF (5 mL). Then K_2CO_3 (19.1 mg, 0.14 mmol, 1eq) and amine **17** (40.5 mg, 0.14 mmol, 1 eq) were added and the mixture was stirred for 24 h at room temperature. Water (5 mL) was added and the aqueous layer was extracted with CH_2Cl_2 (3x 50 mL). The combined organic layers were dried over Na_2SO_4 and the solvent was reduced *in vacuo*. The crude product was first purified by automated flash chromatography ($CH_2Cl_2/MeOH$: 0-10% MeOH) and second purified by preparative HPLC (prep-HPLC-2, gradient A/B: 0-15 min: 30/70, 15-20 min: 2/98, t_R = 8.2 min) to obtain **25** (6.0 mg, 9.5 μ mol, 9%) as a light yellow solid.

TLC: ($CH_2Cl_2/MeOH$, 20:1) R_f = 0.55

1H -NMR (400 MHz, D_6 -DMSO): δ = 1.95 (s, 6H), 2.82-2.96 (m, 2H), 3.22-3.35 (m, 2H), 3.35-3.48 (m, 4H), 3.67-3.73 (m, 2H), 3.40-3.96 (m, 2H), 4.51 (s, 2H), 6.44 (d, J = 8.7 Hz, 1H), 6.50 (d, J = 8.7 Hz, 1H), 6.98 (s, 2H).

^{13}C -NMR (151 MHz, D_6 -DMSO): δ = 14.7 (+), 32.7 (-), 47.6 (-), 51.4 (-), 53.2 (-), 66.8 (-), 108.4 (+), 112.5 (+), 116.8 (q), 125.0 (q), 126.2 (q), 127.6 (+), 131.6 (q), 132.7 (q), 137.5 (q), 140.3 (q), 141.4 (q), 164.3 (q), 169.5 (q).

HR-MS (ESI): calcd. for $C_{28}H_{26}Cl_2N_4O_5S_2$ ($M+H^+$), m/z = 633.0794, found 633.08

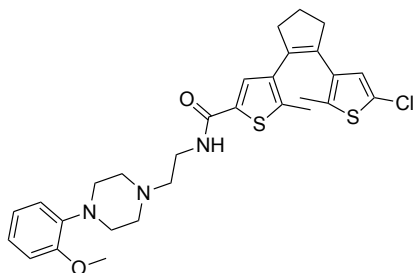
UV/Vis (50 μ M in DMSO): open isomer: λ_{max} = 370 nm, closed isomer: λ_{max} = 564 nm.

General preparation of cyclopentene-DTE based switches 26-31:

To a solution of **20** (44 mg, 0.13 mmol, 1.0 eq) and HBTU (46 mg, 0.12 mmol, 0.95 eq) in CH_2Cl_2 (1 mL) at 0 °C were added DIPEA (45 μ L, 0.26 mmol, 2.0 eq) and a solution of amines A or B (0.13 mmol, 1.0 eq) in CH_2Cl_2 (0.2 mL). The reaction was allowed to come to RT overnight. Water (2 mL) was added and the aqueous phase was extracted with CH_2Cl_2

(3 x 3 mL). The combined organic phases were dried over MgSO_4 , filtered and the solvent was removed under reduced pressure. The crude product at **26** and **27** was first purified by automated flash column chromatography ($\text{CH}_2\text{Cl}_2/\text{MeOH}$: 0-10% MeOH). In general, the cyclopentene-DTEs **26-31** were then purified by preparative HPLC.

Compound 26: 4-(2-(5-Chloro-2-methylthiophen-3-yl)cyclopent-1-en-1-yl)-N-(4-(4-(2-methoxyphenyl)piperazin-1-yl)butyl)-5-methylthiophene-2-carboxamide



$\text{C}_{29}\text{H}_{34}\text{ClN}_3\text{O}_2\text{S}_2$, MW = 555.18 g/mol

Light beige solid: 19% yield; preparative HPLC (prep-HPLC-1, gradient A/B: 0-25 min: 60/40, 25-40 min 5/95; t_R = 17.5 min)

TLC: ($\text{CH}_2\text{Cl}_2/\text{MeOH}$, 10:1) R_f = 0.29

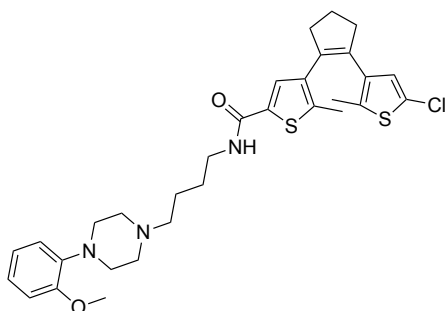
$^1\text{H-NMR}$ (600 MHz, $\text{D}_6\text{-DMSO}$): δ = 1.82 (s, 3H), 1.91 (s, 3H), 1.97-2.03 (m, 2H), 2.71-2.77 (m, 4H), 2.89-2.95 (m, 2H), 3.21- 3.28 (m, 2H), 3.31-3.36 (m, 2H), 3.50-3.54 (m, 2H), 3.56-3.61 (m, 2H), 3.63-3.68 (m, 2H), 3.79 (s, 3H), 6.81 (s, 1H), 6.89-6.92 (m, 1H), 6.94-6.96 (m, 1H), 6.97-6.99 (m, 1H), 7.00-7.04 (m, 1H), 7.51 (s, 1H), 8.62 (t, 1H, J = 5.7 Hz), 9.47 (bs, 1H).

$^{13}\text{C-NMR}$ (151 MHz, $\text{D}_6\text{-DMSO}$): δ = 13.8 (+), 14.2 (+), 22.3 (-), 34.0 (-), 37.8 (-), 38.1 (-), 47.0 (-), 51.5 (-), 54.8 (-), 55.4 (+), 111.9 (+), 118.3 (+), 120.8 (+), 123.5 (q), 123.6 (+), 127.3 (+), 129.3 (+), 133.0 (q), 134.0 (q), 134.1 (q), 134.9 (q), 134.9 (q), 136.1 (q), 139.2 (q), 139.6 (q), 151.8 (q), 161.6 (q).

HR-MS (ESI): calcd. for $\text{C}_{29}\text{H}_{35}\text{ClN}_3\text{O}_2\text{S}_2$ ($\text{M}+\text{H}^+$), m/z = 556.1854, found 556.1857

UV/Vis (50 μM in DMSO): open isomer: λ_{max} = 259 nm; closed isomer: λ_{max} = 323 nm, 491 nm.

Compound 27: 4-(2-(5-Chloro-2-methylthiophen-3-yl)cyclopent-1-en-1-yl)-N-(2-(4-(2-methoxyphenyl)piperazin-1-yl)ethyl)-5-methylthiophene-2-carboxamide



$C_{31}H_{38}ClN_3O_2S_2$, MW = 583.21 g/mol

Light beige solid: 38% yield; after stirring over night + 2 d at r.t.; preparative HPLC (prep-HPLC-1, gradient A/B: 0-25 min: 60/40, 25-40 min 5/95; t_R = 14.5 min)

TLC: ($CH_2Cl_2/MeOH$ 100:1) R_f = 0.42

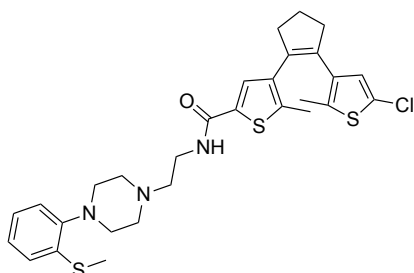
1H -NMR (600 MHz, D_6 -DMSO): δ = 1.49-1.58 (m, 2H), 1.64-1.73 (m, 2H), 1.81 (s, 3H), 1.89 (s, 3H), 1.95-2.04 (m, 2H), 2.68-2.78 (m, 4H), 2.86-2.93 (m, 2H), 3.13- 3.20 (m, 4H), 3.21-3.26 (m, 2H), 3.49-3.56 (m, 4H), 3.78 (s, 3H), 6.81 (s, 1H), 6.88-6.92 (m, 1H), 6.93-6.95 (m, 1H), 6.97-6.99 (m, 1H), 7.00-7.04 (m, 1H), 7.50 (s, 1H), 8.38 (t, 1H, J = 5.7 Hz), 9.37 (bs, 1H).

^{13}C -NMR (151 MHz, D_6 -DMSO): δ = 13.8 (+), 14.1 (+), 20.9 (-), 22.3 (-), 26.3 (-), 37.8 (-), 38.1 (-), 38.4 (-), 47.1 (-), 51.3 (-), 55.3 (-), 55.4 (+), 111.9 (+), 118.3 (+), 120.8 (+), 123.5 (q), 123.6 (+), 127.3 (+), 128.6 (+), 133.0 (q), 133.9 (q), 134.3 (q), 135.0 (q), 135.8 (q), 136.0 (q), 138.9 (q), 139.3 (q), 151.8 (q), 160.9 (q).

HR-MS (ESI): calcd. for $C_{31}H_{39}ClN_3O_2S_2$ ($M+H^+$), m/z = 584.2167, found 584.2169.

UV/Vis (50 μM in DMSO): open isomer: λ_{max} = 270 nm; closed isomer: λ_{max} = 490 nm.

Compound 28: 4-(2-(5-Chloro-2-methylthiophen-3-yl)cyclopent-1-en-1-yl)-5-methyl-N-(2-(4-(2-(methylthio)phenyl)piperazin-1-yl)ethyl)thiophene-2-carboxamide



$C_{29}H_{34}ClN_3OS_3$, MW = 572.24 g/mol

Light beige solid: 29% yield; preparative HPLC (prep-HPLC-1, gradient A/B: 0-35 min: 60/40, 35-40 min 5/95; t_R = 17.8 min)

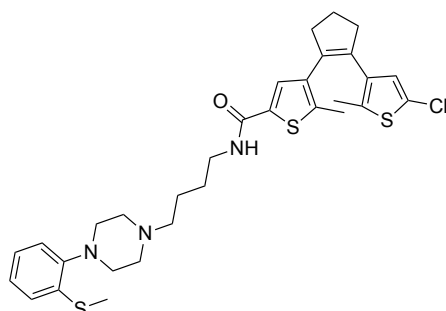
1H -NMR (600 MHz, D_6 -DMSO): δ = 1.83 (s, 3H), 1.92 (s, 3H), 1.99-2.03 (m, 2H), 2.40 (s, 3H), 2.72-2.78 (m, 4H), 2.97-3.05 (m, 2H), 3.16-3.29 (m, 4H), 3.35-3.43 (m, 2H), 3.55-3.62 (m, 2H), 3.65-3.75 (m, 2H), 6.82 (s, 1H), 7.12-7.17 (m, 3H), 7.18-7.20 (m, 1H), 7.53 (s, 1H), 8.63 (bs, 1H), 9.65 (bs, 1H).

^{13}C -NMR (151 MHz, D_6 -DMSO): δ = 13.6 (+), 13.8 (+), 14.2 (+), 22.3 (-), 34.1 (-), 37.9 (-), 38.1 (-), 48.1 (-), 51.9 (-), 55.0 (-), 119.7 (+), 123.7 (q), 124.6 (+), 125.0 (+), 127.3 (+), 129.3 (+), 133.0 (q), 134.1 (q), 134.2 (q), 134.4 (q), 134.9 (q), 136.1 (q), 139.7 (q), 147.1 (q), 157.8 (q), 158.0 (q).

HR-MS (ESI): calcd. for $C_{29}H_{34}ClN_3NaOS_3$ ($M+Na^+$), m/z = 594.1445, found 594.1446

UV/Vis (50 μ M in DMSO): open isomer: λ_{max} = 262 nm; closed isomer: λ_{max} = 491 nm.

Compound 29: 4-(2-(5-Chloro-2-methylthiophen-3-yl)cyclopent-1-en-1-yl)-5-methyl-N-(4-(4-(2-(methylthio)phenyl)piperazin-1-yl)butyl)thiophene-2-carboxamide



$C_{31}H_{38}ClN_3OS_3$, MW = 600.30 g/mol

Light beige solid: 26% yield; preparative HPLC (prep-HPLC-1, gradient A/B: 0-25 min: 60/40, 30-35 min 5/95; t_R = 16.1 min)

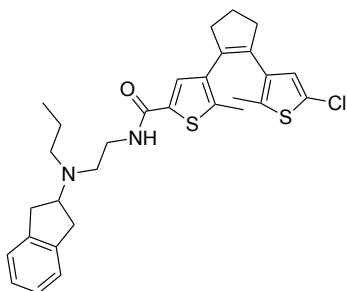
$^1\text{H-NMR}$ (600 MHz, D_6 -DMSO): δ = 1.52-1.60 (m, 2H), 1.67-1.76 (m, 2H), 1.83 (s, 3H), 1.91 (s, 3H), 1.98-2.06 (m, 2H), 2.41 (s, 3H), 2.73-2.79 (m, 4H), 2.96-3.05 (m, 2H), 3.10- 3.18 (m, 2H), 3.20-3.29 (m, 4H), 3.30-3.35 (m, 2H), 3.56-3.62 (m, 2H), 6.84 (s, 1H), 7.13-7.15 (m, 1H), 7.17-7.19 (m, 2H), 7.19-7.22 (m, 1H), 7.53 (s, 1H), 8.41 (t, 1H, J = 5.7 Hz), 9.59 (bs, 1H).

$^{13}\text{C-NMR}$ (151 MHz, D_6 -DMSO): δ = 14.0 (+), 14.3 (+), 14.6 (+), 21.4 (-), 22.8 (-), 26.8 (-), 38.3 (-), 38.6 (-), 38.8 (-), 48.6 (-), 52.1 (-), 55.8 (-), 120.2 (+), 124.1 (q), 125.1 (+), 125.5 (+), 125.7 (+), 127.8 (+), 129.1 (+), 133.5 (q), 134.4 (q), 134.8 (q), 134.9 (q), 135.5 (q), 136.3 (q), 136.4 (q), 139.4 (q), 147.8 (q), 161.4 (q).

HR-MS (ESI): calcd. for $\text{C}_{31}\text{H}_{38}\text{ClN}_3\text{OS}_3$ ($\text{M}+\text{H}^+$), m/z = 600.1943, found 600.1947

UV/Vis (50 μM in DMSO): open isomer: λ_{max} = 259 nm; closed isomer: λ_{max} = 489 nm.

Compound 30: 4-(2-(5-Chloro-2-methylthiophen-3-yl)cyclopent-1-en-1-yl)-N-(2-((2,3-dihydro-1H-inden-2-yl)(propyl)amino)ethyl)-5-methylthiophene-2-carboxamide



$\text{C}_{30}\text{H}_{35}\text{ClN}_2\text{OS}_2$, MW = 539.19 g/mol

Light beige solid: 26% yield; preparative HPLC (prep-HPLC-1, gradient A/B: 0-30 min: 60/40, 30-40 min 5/95; t_R = 17.1 min)

TLC: ($\text{CH}_2\text{Cl}_2/\text{MeOH}$, 100:1) R_f = 0.42

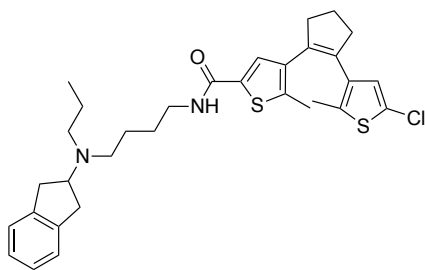
$^1\text{H-NMR}$ (600 MHz, D_6 -DMSO): δ = 0.92 (t, 3H, J = 7.3 Hz), 1.65-1.76 (m, 2H), 1.79 (s, 3H), 1.90 (s, 3H), 1.95-2.04 (m, 2H), 2.69-2.77 (m, 4H), 3.13-3.21 (m, 4H), 3.29- 3.36 (m, 4H), 3.56-3.64 (m, 2H), 4.27-4.36 (m, 1H), 6.81 (s, 1H), 7.19-7.22 (m, 2H), 7.24-7.26 (m, 2H), 7.50 (s, 1H), 8.62-8.69 (m, 1H), 9.89 (bs, 1H).

¹³C-NMR (151 MHz, D₆-DMSO): δ = 11.3 (+), 14.3 (+), 14.7 (+), 16.9 (-), 22.8 (-), 34.7 (-), 34.8 (-), 34.9 (-), 38.3 (-), 38.6 (-), 49.6 (-), 52.7 (-), 63.5 (+), 124.2 (q), 124.9 (+), 127.1 (q), 127.6 (+), 127.7 (+), 129.8 (+), 133.5 (q), 134.6 (q), 135.2 (q), 135.4 (q), 136.6 (q), 139.4 (q), 140.2 (q), 141.1 (q), 162.0 (q).

HR-MS (ESI): calcd. for C₃₀H₃₅ClN₂OS₂ (M+H⁺), m/z = 539.1957; found 539.1960

UV/Vis (100 μM in DMSO): open isomer: λ_{max} = 262 nm; closed isomer: λ_{max} = 494 nm.

Compound 31: 4-(2-(5-Chloro-2-methylthiophen-3-yl)cyclopent-1-en-1-yl)-N-(4-((2,3-dihydro-1H-inden-2-yl)(propyl)amino)butyl)-5-methylthiophene-2-carboxamide



C₃₂H₃₉ClN₂OS₂, MW = 567.25 g/mol

Light beige solid: 70% yield; preparative HPLC (prep-HPLC-1, gradient A/B: 0-30 min: 60/40, 30-40 min 5/95, t_R = 20.2 min).

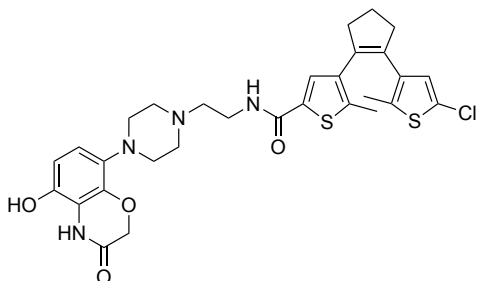
¹H-NMR (600 MHz, D₆-DMSO): δ = 0.91 (t, 3H, J = 7.3 Hz), 1.52-1.59 (m, 2H), 1.63-1.68 (m, 2H), 1.63-1.73 (m, 2H), 1.80 (s, 3H), 1.89 (s, 3H), 1.94-2.07 (m, 2H), 2.69-2.76 (m, 4H), 3.04-3.11 (m, 2H), 3.11-3.18 (m, 4H), 3.22-3.27 (m, 2H), 3.28-3.31 (m, 2H), 4.13-4.25 (m, 1H), 6.81 (s, 1H), 7.19-7.21 (m, 2H), 7.22-7.26 (m, 2H), 7.50 (s, 1H), 8.36 (t, 1H, J = 5.7 Hz), 9.38 (bs, 1H).

¹³C-NMR (151 MHz, D₆-DMSO): δ = 11.4 (+), 14.3 (+), 14.6 (+), 17.3 (-), 21.1 (-), 22.8 (-), 26.7 (-), 34.8 (-), 34.9 (-), 38.3 (-), 38.5 (-), 38.6 (-), 50.9 (-), 52.6 (-), 63.3 (+), 124.1 (q), 124.8 (+), 124.9 (+), 127.7 (+), 127.8 (+), 129.1 (+), 133.5 (q), 134.4 (q), 134.8 (q), 135.4 (q), 136.2 (q), 136.4 (q), 139.4 (q), 139.5 (q), 139.5 (q), 161.5 (q).

HR-MS (calcd. for C₃₂H₄₀ClN₂OS₂ (M+H⁺), m/z = 567.2265, found 567.2279

UV/Vis (50 μM in DMSO): open isomer: λ_{max} = 264 nm; closed isomer: λ_{max} = 490 nm.

Compound 32: 4-(2-(5-chloro-2-methylthiophen-3-yl)cyclopent-1-en-1-yl)-N-(2-(4-(5-hydroxy-3-oxo-3,4-dihydro-2H-benzo[b][1,4]oxazin-8-yl)piperazin-1-yl)ethyl)-5-methylthiophene-2-carboxamide



$C_{30}H_{33}ClN_4O_4S_2$, MW = 613.19 g/mol

Compound **20** (20.0 mg, 0.059 mmol, 1.0 eq) and HBTU (21.3 mg, 0.06 mmol, 1.0 eq) were dissolved in DMF (2 mL). DIPEA (0.02 mL, 0.12 mmol, 2 eq) and a solution of amine **17** (17.3 mg, 0.06 mmol, 1.0 eq) in DMF (0.5 mL) was added. The mixture was stirred at room temperature for 4h. The solvent was evaporated and the crude mixture was first purified by automated flash column chromatography ($CH_2Cl_2/MeOH$: 0-20% MeOH) and second purified by preparative HPLC (prep-HPLC-2, gradient A/B: 0-15 min: 70/30, 15-20 min: 5/95, t_R = 14.1 min) to afford **32** (2.00 mg, 0.003 mmol, 6%) as a light yellow solid.

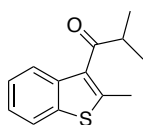
TLC: ($CH_2Cl_2/MeOH$, 20:1) R_f = 0.78

1H -NMR (400 MHz, D_6 -DMSO): δ = 1.83 (s, 3H), 1.92 (s, 3H), 2.01 (qi, J = 7.3 Hz, 2H), 2.75 (q, J = 6.9 Hz, 4H), 2.90 (t, J = 11.4 Hz, 2H), 3.17-3.27 (m, 2H), 3.35-3.41 (m, 4H), 3.54-3.68 (m, 4H), 4.51 (s, 2H), 6.45 (d, J = 8.7 Hz, 1H), 6.50 (d, J = 8.8 Hz, 1H), 6.82 (s, 1H), 7.52 (s, 1H), 8.62 (bs, 1H), 9.62 (bs, 1H), 9.88 (bs, 1H).

^{13}C -NMR (151 MHz, D_6 -DMSO): δ = 13.8 (+), 14.2 (+), 22.3 (-), 34.0 (-), 37.9 (-), 38.2 (-), 47.7 (-), 51.5 (-), 54.9 (-), 66.8 (-), 108.4 (+), 112.5 (+), 116.8 (q), 123.7 (q), 127.3 (+), 129.3 (+), 131.6 (q), 133.0 (q), 134.1 (q), 134.2 (q), 134.9 (q), 136.1 (q), 137.5 (q), 139.6 (q), 141.4 (q), 161.6 (q), 164.3 (q).

HR-MS (ESI): calcd. for $C_{30}H_{33}ClN_4O_4S_2$ ($M+H^+$), m/z = 613.1705, found 613.1708

UV/VIS: (50 μ M in DMSO): open isomer: λ_{max} = 263 nm, closed isomer: λ_{max} = 503 nm.

Compound 34: 2-Methyl-1-(2-methylbenzo[*b*]thiophen-3-yl)propan-1-one

$C_{13}H_{14}OS$, MW = 218.31 g/mol

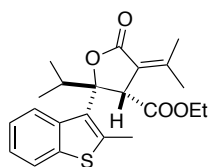
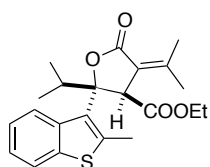
A mixture of 2-methylbenzothiophene (1.1 g, 7.4 mmol, 1.0 eq) and isobutyryl chloride (0.9 mL, 8.2 mmol, 1.1 eq) in dry toluene (40 mL) was cooled to 5 °C under stirring and nitrogen atmosphere. $SnCl_4$ was dissolved in toluene (5 mL) and added dropwise to the reaction mixture. The solution was stirred 2 h at room temperature before it was quenched by adding HCl-solution (2 M, 20 mL). After separation of the organic layer, it was dried over Na_2SO_4 and the solvent was evaporated. The crude product **34** was recrystallized from hexane to obtain a yellow solid (1.1 g, 5.0 mmol, 70%).

TLC: (PE/EtOAc, 20:1) R_f = 0.46

1H -NMR (400 MHz, $CDCl_3$): δ = 1.23 (d, J = 6.8 Hz, 6H), 2.67 (s, 3H), 3.36 (sept, J = 6.8 Hz, 1H), 7.29-7.41 (m, 2H), 7.76 (d, J = 8.0 Hz, 1H), 7.84 (d, J = 8.0 Hz, 1H).

^{13}C -NMR (101 MHz, $CDCl_3$): δ = 15.9 (+), 18.5 (+), 40.6 (+), 121.9 (+), 122.9 (+), 124.3 (+), 125.0 (+), 133.5 (q), 137.9 (q), 138.5 (q), 144.9 (q), 205.0 (q).

HR-MS (ESI): calcd. for $C_{13}H_{14}OS$ ($M+H^+$), m/z = 219.0838, found 219.0839

Compound 36: (anti/syn)-Ethyl 2-isopropyl-2-(2-methylbenzo[*b*]thiophen-3-yl)-5-oxo-4-(propan-2-ylidene)tetrahydrofuran-3-carboxylate

$C_{22}H_{26}O_4S$, MW = 386.50 g/mol

Diisopropylamine (1.17 g, 16.0 mmol, 1.6 eq) was dissolved in tetrahydrofuran and cooled to -78 °C under nitrogen atmosphere. After addition of *n*-butyllithium (0.96 g, 15.0 mmol, 1.5 eq) the mixture was stirred at this temperature for 30 min. Diisopropylidenesuccinate **15** (3.22 g, 15.0 mmol, 1.2 eq) was added and the mixture was stirred at -78 °C for 1h. Then compound

34 (2.20 g, 10.1 mmol, 1.0 eq) was added and the mixture was allowed to warm to room temperature overnight. The reaction mixture was stirred for 24 h at room temperature and then quenched with HCl-solution (2 M, 60 mL). The aqueous layer was extracted with ethyl acetate (3 x 100 mL) and the combined organic layers were dried over Na₂SO₄. The solvent was removed *in vacuo* and the crude product was purified by automated flash column chromatography (CH₂Cl₂/MeCN, gradient 0 - 3% MeCN then 3 - 20%) to obtain the product **36** as a colourless oil of *syn/anti* isomers (622 mg, 16.1 mmol, 16%). To determine the *syn/anti* isomers, the lactone mixture was separated by preparative HPLC. (analytical HPLC: t_R (*anti*-**36**) = 21.76 min, t_R (*syn*-**36**) = 19.89 min, flow rate: 0.3 mL/min, A = H₂O (0.05 Vol% TFA), B = MeCN, gradient: 30-95% B);

anti-**36**:

TLC: (CH₂Cl₂/MeCN, 100:1) R_f = 0.73

¹H-NMR (600 MHz, CDCl₃): δ = 0.73 (d, J = 7.0 Hz, 3H), 1.01 (d, J = 6.4 Hz, 3H), 1.38 (t, J = 7.2 Hz, 3H), 1.66 (s, 3H), 2.28 (s, 3H), 2.66 (s, 3H), 2.94 (sep, J = 6.7 Hz, 1H), 4.23-4.32 (m, 1H), 4.34-4.40 (m, 1H), 4.53 (s, 1H), 7.29 (t, J = 7.3 Hz, 1H), 7.38 (t, J = 7.7 Hz, 1H) 7.72 (d, J = 7.9 Hz, 1H), 8.27 (d, J = 7.3 Hz, 1H).

¹³C-NMR (151 MHz, CDCl₃): δ = 14.2 (+), 17.0 (+), 19.7 (+), 20.6 (+), 24.8 (+), 33.7 (+), 54.5 (+), 61.9 (-), 90.3 (q), 115.1 (q), 119.9 (q), 122.3 (+), 122.7 (+), 123.7 (+), 124.3 (+), 131.6 (q), 138.2 (q), 138.6 (q), 155.1 (q), 168.9 (q), 170.6 (q).

HR-MS (ESI): calcd. for C₂₂H₂₆O₄S (M+H⁺), m/z = 387.1625, found 387.1627

syn-**36**:

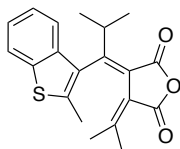
TLC: (CH₂Cl₂/MeCN, 100:1) R_f = 0.77

¹H-NMR (600 MHz, CDCl₃): δ = 0.58 (t, J = 7.1 Hz, 3H), 0.78 (d, J = 6.7 Hz, 3H), 0.97 (d, J = 6.8 Hz, 3H), 1.97 (s, 3H), 2.34 (s, 3H), 2.71 (s, 3H), 2.77 (sep, J = 6.8 Hz, 1H), 3.43-3.54 (m, 2H) 4.42 (s, 1H), 7.20-7.24 (m, 1H), 7.27-7.30 (m, 1H), 7.67 (t, J = 9.1 Hz, 2H).

¹³C-NMR (151 MHz, CDCl₃): δ = 13.3 (+), 16.2 (+), 17.3 (+), 17.5 (+), 20.6 (+), 24.2 (+), 38.3 (+), 56.1 (+), 61.0 (-), 89.4 (q), 121.5 (q), 122.0 (+), 123.3 (+), 123.4 (+), 123.5 (+), 128.6 (q), 137.3 (q), 138.1 (q), 138.6 (q), 152.0 (q), 168.3 (q), 170.0 (q).

HR-MS (ESI): calcd. for C₂₂H₂₆O₄S (M+H⁺), m/z = 387.1625, found 387.1631

Compound E-37: (E)-3-(2-methyl-1-(2-methylbenzo[b]thiophen-3-yl)propylidene)-4-(propan-2-ylidene)dihydrofuran-2,5-dione



$C_{20}H_{20}O_3S$, MW = 340.44 g/mol

Compound **36** (622 mg, 1.61 mmol, 1.0 eq) was dissolved in ethanol (40 mL) and after addition of KOH (4.5 g, 80.5 mmol, 50 eq) and H₂O (10 mL), the mixture was stirred for 20 h at 70 °C. The reaction mixture was poured onto ice and quenched with an aqueous HCl-solution (2 M, 50 mL). The aqueous layer was extracted with ethyl acetate (3 x 60 mL) and the combined organic layers were washed with brine (40 mL) and dried over Na₂SO₄. The organic solvent was removed *in vacuo* to get the crude diacid as a yellow solid (258 mg, 0.72 mmol). The diacid was suspended in dichloromethane (30 mL) and after adding acetyl chloride (380 mg, 4.83 mmol, 3.0 eq) the solution was stirred for 1 day at 40 °C. The mixture was neutralized with saturated NaHCO₃ solution and the aqueous layer was extracted with dichloromethane (2 x 30 mL). The combined organic layers were dried over Na₂SO₄ and the solvent was removed *in vacuo*. Then, the crude product was purified by automated flash column chromatography (cyclohexane/EtOAc, gradient 1-5% EtOAc) to obtain a slightly yellow solid E-**37** (213 mg, 0.65 mmol, 87%).

TLC: (Cyclohexane/EtOAc, 9:1) R_f = 0.71

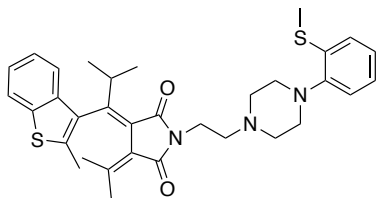
¹H-NMR (400 MHz, CDCl₃): δ = 0.99 (d, *J* = 7.0, 3H), 1.08 (s, 3H), 1.33 (d, *J* = 7.0, 3H), 2.13 (s, 3H), 2.30 (s, 3H), 3.98 (sep, *J* = 7.0 Hz, 1H), 7.27-7.38 (m, 2H), 7.48-7.52 (d, 1H), 7.71-7.75 (m, 1H).

¹³C-NMR (101 MHz, CDCl₃): δ = 15.6 (+), 21.2 (+), 23.1 (+), 23.4 (+), 26.8 (+), 33.7 (+), 120.6 (q), 122.3 (+), 123.0 (+), 124.4 (+), 124.9 (+), 125.1 (q), 132.2 (q), 136.8 (q), 138.5 (q), 157.5 (q), 158.6 (q), 159.4 (q), 162.8 (q), 163.0 (q).

HR-MS (ESI): calcd. for C₂₀H₂₀O₃S (M+H⁺), *m/z* = 341.1133, found 341.1135

UV/Vis (100 μM in DMSO): open isomer: λ_{max} = 342 nm; closed isomer: λ_{max} = 479 nm.

Compound 43: (E)-3-(2-methyl-1-(2-methylbenzo[b]thiophen-3-yl)propylidene)-1-(2-(4-(2-(methylthio)-phenyl)piperazin-1-yl)ethyl)-4-(propan-2-ylidene)pyrrolidine-2,5-dione



$C_{33}H_{39}N_3O_2S$, MW = 573.81 g/mol

The phenyl piperazine derivative **7** (57.8 mg, 0.30 mmol, 1.1 eq) and compound **E-37** (71.0 mg, 0.21 mmol, 1.0 eq) were dissolved in chloroform (30 mL) and heated to 60 °C overnight to form amide acid **42**. After cooling to room temperature, DCC (55.9 mg, 0.27 mmol, 1.3 eq), HOBT (36.6 mg, 0.27 mmol, 1.3 eq) and DIPEA (35.0 mg, 0.27 mmol, 1.3 eq) were added. The mixture was stirred for 3 days and quenched with saturated $NaHCO_3$ (10 mL) solution. The aqueous layer was separated and extracted with ethyl acetate (3 x 20 mL). The combined organic layers were dried over Na_2SO_4 and the solvent was removed under reduced pressure. Purification was done by automated flash column chromatography (PE/EtOAc, gradient 0-12% EtOAc) to yield **43** (93.3 mg, 0.16 mmol, 74%) as a colorless solid.

TLC: (PE/EtOAc, 5:1, 0.1 % NEt_3) R_f = 0.38

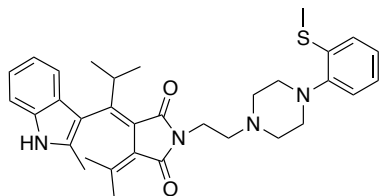
1H -NMR (400 MHz, $CDCl_3$): δ = 0.99 (d, J = 7.0, 3H), 1.05 (s, 3H), 1.32 (d, J = 7.0, 3H), 2.09 (s, 3H), 2.29 (s, 3H), 2.41 (s, 3H), 2.76 (m, 6H), 3.00 (m, 4H), 3.84 (q, J = 6.8 Hz, 2H), 4.17 (sep, J = 7.0 Hz, 1H), 6.97-7.02 (m, 1H), 7.12-7.05 (m, 3H), 7.24-7.34 (m, 2H), 7.54 (d, J = 7.4 Hz, 1H), 7.72 (d, J = 8.2 Hz, 1H).

^{13}C -NMR (101 MHz, $CDCl_3$): δ = 14.6 (+), 15.7 (+), 21.6 (+), 22.0 (+), 23.7 (+), 26.7 (+), 32.6 (+), 34.9 (-), 51.7 (-), 53.6 (-), 55.4 (-), 119.6 (+), 122.1 (+), 123.3 (+), 123.4 (+), 123.9 (+), 124.4 (+), 124.5 (+), 125.0 (+), 128.9 (q), 133.0 (q), 135.1 (q), 136.6 (q), 138.4 (q), 139.3 (q), 144.5 (q), 149.6 (q), 152.7 (q), 168.1 (q), 168.3 (q).

HR-MS (ESI): calcd. for $C_{33}H_{39}N_3O_2S_2$ ($M+H^+$), m/z = 574.2556, found 574.2566

UV/Vis (50 μM in DMSO): open isomer: λ_{max} = 307 nm; closed isomer: λ_{max} = 473 nm.

Compound 45: Synthesis of (3*E*,4*E*)-3-ethylidene-4-(2-methyl-1-(2-methyl-1*H*-indol-3-yl)propylidene)-1-(2-(4-(2-(methylthio)phenyl)piperazin-1-yl)ethyl)-pyrrolidine-2,5-dione



$C_{33}H_{40}N_4O_2S$, MW = 556.76 g/mol

The amide acid **44** was formed of amine **7** (20.0 mg, 0.06 mmol, 1.0 eq) and fulgide **38** (16.3 mg, 0.07 mmol, 1.1 eq) in chloroform (20 mL) at 60 °C overnight. After cooling to room temperature DCC (15.8 mg, 0.08 mmol, 1.3 eq), HOBt (10.3 mg, 0.08 mmol, 1.3 eq) and DIPEA (10.3 mg, 0.08 mmol, 1.3 eq) were added. The mixture was stirred for 4 days at room temperature and quenched with saturated $NaHCO_3$ (8 mL) solution. The aqueous layer was separated and extracted with ethyl acetate (3 x 20 mL). The combined organic layers were dried over Na_2SO_4 and the solvent was evaporated. The crude product was first purified by automated NP flash column chromatography (PE/EtOAc, gradient 0 - 8% EtOAc), and second with RP flash column chromatography ($H_2O/MeCN$, gradient 30 - 95% MeCN) to obtain **45** (8.2 mg, 0.015 mmol, 25%) as a slightly yellow solid.

TLC: (PE/EtOAc, 2:1, 0.1% NEt_3) R_f = 0.47

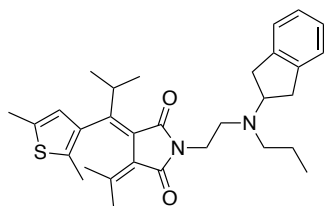
1H -NMR (600 MHz, $CDCl_3$): δ = 0.96 (d, J = 7.0 Hz, 3H), 1.00 (s, 3H), 1.41 (d, J = 7.1 Hz, 3H), 2.09 (s, 3H), 2.12 (s, 3H), 2.41 (s, 3H), 2.65-2.95 (m, 6H), 2.98-3.12 (m, 4H), 3.80-3.94 (m, 2H), 4.32 (sep, J = 7.0 Hz), 7.00-7.05 (m, 1H), 7.07-7.11 (m, 4H), 7.12-7.15 (m, 1H), 7.24-7.26 (m, 1H), 7.28-7.30 (m, 1H), 7.46-7.48 (m, 1H), 8.00 (s, 1H).

^{13}C -NMR (151 MHz, $CDCl_3$): δ = 13.2 (+), 14.5 (+), 21.1 (+), 21.9 (+), 23.8 (+), 26.9 (+), 32.3 (+), 34.8 (-), 35.0 (-), 53.5 (-), 55.3 (-), 110.2 (+), 110.4 (q), 114.2 (q), 119.5 (q), 119.7 (+), 119.8 (q), 120.4 (+), 120.7 (+), 121.2 (q), 121.6 (+), 123.9 (q), 124.4 (+), 124.7 (+), 125.1 (+), 127.5 (q), 132.0 (q), 135.1 (q), 135.5 (q), 168.2 (q), 168.7 (q).

HR-MS (ESI): calcd. for $C_{33}H_{40}N_4O_2S$ ($M+H^+$), m/z = 557.2945, found 557.2946

UV/Vis (50 μM in DMSO): open isomer: λ_{max} = 360 nm; closed isomer: λ_{max} = 543 nm.

Compound 46: (E)-3-(1-(2,5-dimethylthiophen-3-yl)-2-methylpropylidene)-4-(propan-2-ylidene)dihydrofuran-2,5-dione



$C_{31}H_{40}N_2O_2S$, MW = 504.73 g/mol

Fulgide **39** (100 mg, 0.33 mmol, 1.0 eq) and *N*-1-(2,3-dihydro-1*H*-inden-2-yl)-*N*¹-propylethane-1,2-diamine **11** (108 mg, 0.49 mmol, 1.5 eq) were dissolved in chloroform (50 mL) and heated up to 60 °C for 48 h. The solvent was evaporated and the residue was purified by automated NP column chromatography (PE/EtOAc, gradient 0 – 50% EtOAc, 1% NEt₃) and second with RP flash column chromatography (H₂O/MeCN, gradient 30 - 95% MeCN) to obtain **46** (16,1 mg, 0.032 mmol, 10%) as a colourless solid.

TLC: (PE/EtOAc, 9:1, 0.1% NEt₃) R_f = 0.25

¹H-NMR (400 MHz, D₆-DMSO): δ = 0.69 (d, *J* = 7.1 Hz, 3H), 0.80 (t, *J* = 7.3 Hz, 3H), 1.19 (s, 3H), 1.29 (d, *J* = 7.1 Hz, 3H), 1.38 (sx, *J* = 7.3 Hz, 2H), 1.89 (s, 3H), 2.14 (s, 3H), 2.39 (s, 3H), 2.43 (t, *J* = 7.2 Hz, 2H), 2.61-2.73 (m, 4H), 2.93 (dd, *J* = 7.7 Hz, 15.7 Hz, 2H), 3.54-3.62 (m, 2H), 3.67 (qi, *J* = 8.0 Hz, 1H), 4.34 (sep, *J* = 7.0 Hz), 6.71 (s, 1H), 7.05-7.11 (m, 2H), 7.12-7.17 (m, 2H).

¹³C-NMR (151 MHz, D₆-DMSO): δ = 11.7 (+), 13.6 (+), 14.8 (+), 20.2 (+), 21.2 (+), 22.9 (+), 25.4 (+), 29.3 (+), 32.5 (-), 35.6 (-), 35.8 (-), 47.3 (-), 52.7 (-), 61.7 (+), 122.8 (+), 124.3 (+), 124.7 (q), 125.5 (+), 126.2 (+), 129.0 (q), 129.6 (q), 132.4 (q), 135.3 (q), 135.8 (q), 141.5 (q), 147.0 (q), 152.2 (q), 167.5 (q).

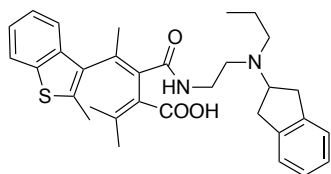
HR-MS (ESI): calcd. for C₃₁H₄₀N₂O₂S (M+H⁺), *m/z* = 505.2883, found 505.2892

UV/Vis (100 μM in DMSO): open isomer: λ_{max} = 272 nm; closed isomer: λ_{max} = 526 nm.

Preparation of amide acids 47 and 49:

The fulgide (1.0 eq) was dissolved in CHCl₃ (10 mL). Than amine **11** (1.5 eq) was added and the mixture was heated up to 70 °C for 4h. The solvent was evaporated and the crude mixture was purified by preparative HPLC (prep-HPLC-2, gradient A/B: 0-15 min: 30/70, 15-20 min: 2/98).

Compound 47: (E)-3-((2-((2,3-dihydro-1H-inden-2-yl)(propyl)amino)ethyl)carbamoyl)-4-(2-methylbenzo-[b]thiophen-3-yl)-2-(propan-2-ylidene)pent-3-enoic acid



$C_{32}H_{38}N_2O_3S$, MW = 530.73 g/mol

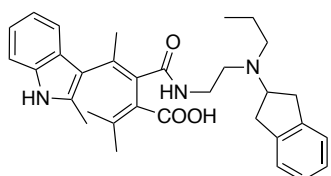
Colourless solid: 18% yield; preparative HPLC: t_R = 7.9 min.

1H -NMR (400 MHz, $CDCl_3$): δ = 0.96-1.07 (m, 3H), 1.75 (s, 6H) 1.78-1.94 (m, 2H), 2.26 (s, 3H), 2.33 (s, 3H), 2.99-3.17 (m, 2H), 3.25-3.46 (m, 6H), 3.65-3.99 (m, 2H), 4.15-4.26 (m, 1H), 7.17-7.26 (m, 6H), 7.49-7.58 (m, 1H), 7.64-7.69 (m, 1H).

^{13}C -NMR (151 MHz, $CDCl_3$): δ = 11.2 (+), 14.4 (+), 17.3 (-), 21.7 (+), 22.2 (+), 24.4 (+), 34.6 (-), 36.1 (-), 51.8 (-), 54.5 (-), 54.7 (-) 64.3 (+), 114.7 (q), 122.0 (+), 122.4 (+), 122.5 (q), 123.8 (+), 123.9 (+), 124.4 (+), 124.5 (+), 124.7 (+), 128.1 (+), 132.8 (q), 135.7 (q), 138.1 (q), 138.2 (q), 138.4 (q), 138.8 (q), 151.2 (q), 169.0 (q), 172.2 (q).

HR-MS (ESI): calcd. for $C_{32}H_{39}N_2O_3S$ ($M+H^+$), m/z = 531.2676, found 531.2676.

Compound 49: (E)-3-((2-((2,3-dihydro-1H-inden-2-yl)(propyl)amino)ethyl)carbamoyl)-4-(2-methyl-1H-indol-3-yl)-2-(propan-2-ylidene)pent-3-enoic acid



$C_{32}H_{39}N_3O_3$, MW = 513.68 g/mol

Yellow solid: 48% yield; preparative HPLC: t_R = 6.9 min.

1H -NMR (400 MHz, D_6 -DMSO): δ = 0.98 (t, J = 7.2 Hz, 3H), 1.66 (s, 3H) 1.69-1.79 (m, 2H), 1.82 (s, 3H), 2.07 (s, 3H), 2.25 (s, 3H), 3.15-3.29 (m, 6H), 3.32-3.43 (m, 2H), 3.50-3.56 (m, 2H), 4.30-4.41 (m, 1H), 6.88 (dt, J = 0.79 Hz, 8.0 Hz, 1H), 6.96 (dt, J = 1.1 Hz, 7.9 Hz, 1H) 7.18-7.25 (m, 4H), 7.26-7.31 (m, 2H).

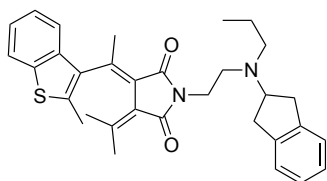
¹³C-NMR (151 MHz, D₆-DMSO): δ = 10.9 (+), 12.2 (+), 16.9 (-), 21.8 (+), 22.1 (+), 23.9 (+), 34.1 (-), 34.3 (-), 34.5 (-), 49.1 (-), 52.7 (-), 63.0 (+), 110.5 (+), 113.5 (q), 115.2 (q), 118.1 (q), 118.5 (+), 118.6 (+), 120.1 (q), 124.4 (+), 126.6 (+), 127.2 (+), 132.2 (q), 135.4 (q), 139.0 (q), 139.4 (q), 139.6 (q), 168.3 (q), 169.5 (q).

HR-MS (ESI): calcd. for C₃₂H₃₉N₃O₃ (M+H⁺), m/z = 514.3064, found 514.3068.

Preparation of fulgimides **48** and **50**:

MSNT (1.2 eq) and Me-imidazole (0.5 eq) were added to a solution of amide acid **47** or **49** (1.0 eq) in CHCl₃ at room temperature. The mixture was stirred for 24 h at 40 °C. The solvent was reduced *in vacuo* and the mixture was purified by automated column chromatography and preparative HPLC (prep-HPLC-2, gradient A/B: 0-15 min: 30/70, 15-20 min 2/98).

Compound 48: (E)-1-(2-((2,3-dihydro-1H-inden-2-yl)(propyl)amino)ethyl)-3-(1-(2-methylbenzo[b]thiophen-3-yl)ethylidene)-4-(propan-2-ylidene)pyrrolidine-2,5-dione



C₃₂H₃₆N₂O₂S, MW = 512.71 g/mol

White solid: 9% yield; column chromatography (PE/EtOAc: 0-50% EtOAc); preparative HPLC: t_R = 10.3 min.

TLC: (PE/EtOAc, 9:1, 0.1% NEt₃) R_f = 0.82

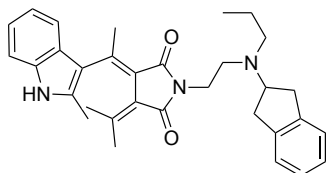
¹H-NMR (400 MHz, CDCl₃): δ = 1.03 (s, 3H), 1.08 (t, J = 7.3 Hz, 3H), 1.49-1.61 (m, 2H), 2.17 (s, 3H), 2.26 (s, 3H), 2.69 (s, 3H), 2.79-2.93 (m, 4H), 3.08 (m, 2H), 3.72-3.81 (m, 3H), 7.09-7.21 (m, 3H), 7.27-7.39 (m, 3H), 7.48 (t, J = 7.8 Hz, 1H), 7.74 (t, J = 7.0 Hz, 1H);

¹³C-NMR (151 MHz, CDCl₃): δ = 11.4 (+), 15.4 (+), 17.6 (-), 22.2 (+), 22.6 (+), 26.2 (+), 31.6 (-), 34.8 (-), 35.2 (-), 53.8 (-), 64.6 (+), 122.3 (+), 122.5 (+), 124.4 (q), 124.8 (+), 124.9 (+), 125.8 (q), 128.0 (+), 135.4 (q), 136.7 (q), 138.0 (q), 138.1 (q), 138.2 (q), 138.7 (q), 153.4 (q), 167.7 (q), 168.3 (q).

HR-MS (ESI): calcd. for C₃₂H₃₇N₂O₂S (M+H⁺), m/z = 513.2570, found 513.2573;

UV/Vis (50 μ M in DMSO): open isomer: λ_{\max} = 328 nm; closed isomer: λ_{\max} = 486 nm.

Compound 50: (E)-1-(2-((2,3-dihydro-1H-inden-2-yl)(propyl)amino)ethyl)-3-(1-(2-methyl-1H-indol-3-yl)ethylidene)-4-(propan-2-ylidene)pyrrolidine-2,5-dione



$C_{32}H_{37}N_3O_2$, MW = 495.67 g/mol

Yellow solid: 14% yield; column chromatography (CH_2Cl_2 , MeOH: 0-10% MeOH); preparative HPLC: t_R = 9.9 min.

TLC: (CH_2Cl_2 /MeOH, 20:1) R_f = 0.62

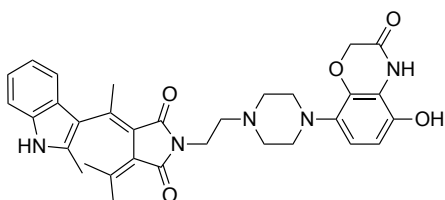
1H -NMR (400 MHz, $CDCl_3$): δ = 0.98 (s, 3H), 1.06 (t, J = 7.3 Hz, 3H), 1.94 (q, J = 7.4 Hz, 2H), 2.18 (s, 6H), 2.79 (s, 3H), 3.28-3.43 (m, 4H), 3.44-3.55 (m, 4H), 4.01-4.10 (m, 2H), 4.15 (qi, J = 8.5 Hz, 1H), 6.88 (m, 1H), 7.09-7.18 (m, 2H), 7.19-7.24 (m, 4H), 7.29 (d, J = 7.9 Hz, 1H), 7.38 (d, J = 7.9 Hz, 1H).

^{13}C -NMR (151 MHz, $CDCl_3$): δ = 11.4 (+), 13.7 (+), 17.6 (-), 22.3 (+), 22.8 (+), 26.3 (+), 31.1 (-), 35.1 (-), 36.6 (-), 46.8 (-), 53.5 (-), 64.5 (+), 110.8 (+), 117.5 (q), 119.8 (+), 120.7 (+), 122.1 (q), 122.3 (+), 123.4 (q), 124.8 (+), 126.3 (q), 127.8 (+), 133.0 (q), 135.6 (q), 137.6 (q), 138.4 (q), 145.5 (q), 150.3 (q), 168.1 (q), 168.5 (q).

HR-MS (ESI): calcd. for $C_{32}H_{38}N_3O_2$ ($M+H^+$), m/z = 496.2959, found 496.2961

UV/Vis (100 μ M in DMSO): open isomer: λ_{\max} = 370 nm; closed isomer: λ_{\max} = 564 nm.

Compound 52: (E)-1-(2-(4-(5-hydroxy-3-oxo-3,4-dihydro-2H-benzo[*b*][1,4]oxazin-8-yl)piperazin-1-yl)ethyl)-3-(1-(2-methyl-1H-indol-3-yl)ethylidene)-4-(propan-2-ylidene)pyrrolidine-2,5-dione



$C_{32}H_{35}N_5O_5$, MW = 569.66 g/mol

Indolyl fulgide **41** (10.0 mg, 0.034 mmol, 1.0 eq) and the benzoxazinon derivative **17** (8.87 mg, 0.041 mmol, 1.2 eq) were dissolved in DMF (4 mL). The mixture was stirred at 60 °C for 4 h and cooled to room temperature. HOBt (4.58 mg, 0.034 mmol, 1.0 eq), HBTU (15.4 mg, 0.041 mmol, 1.2 eq) and DIPEA (4.38 mg, 0.034 mmol, 1.0 eq) were added and the mixture was stirred for 4 h at room temperature. The crude product was first purified by automated flash chromatography (CH₂Cl₂/MeOH: 0-30% MeOH) and second purified by preparative HPLC (prep-HPLC-2, gradient A/B: 0-15 min: 30/70, 15-20 min: 2/98, t_R = 5.2 min) to obtain **52** (2.0 mg, 3.5 μmol, 10%) as a white solid.

TLC: (CH₂Cl₂/MeOH, 20:1) R_f = 0.15

¹H-NMR (600 MHz, D₆-DMSO): δ = 0.87 (s, 3H), 2.13 (s, 3H), 2.17 (s, 3H), 2.75 (s, 3H), 2.84-2.95 (m, 2H), 3.12-3.22 (m, 2H), 3.41-3.51 (m, 4H), 3.68-3.80 (m, 2H), 3.86-4.01 (m, 2H), 4.51 (s, 2H), 6.43-6.47 (m, 1H), 6.50-6.55 (m, 1H), 6.96-7.03 (m, 1H), 7.04-7.09 (m, 1H), 7.29-7.36 (m, 2H).

¹³C-NMR (151 MHz, D₆-DMSO): δ = 12.8 (+), 21.2 (+), 22.0 (+), 25.1 (+), 31.6 (-), 47.2 (-), 51.2 (-), 52.8 (-), 66.4 (-), 103.3 (q), 108.0 (+), 110.6 (+), 112.2 (+), 113.6 (q), 115.6 (q), 116.4 (q), 118.6 (+), 119.1 (+), 120.8 (+), 120.9 (q), 123.2 (q), 125.2 (q), 134.1 (q), 135.1 (q), 137.1 (q), 141.0 (q), 164.0 (q), 167.3 (q), 167.9 (q).

HR-MS (ESI): calcd. for C₃₂H₃₅N₅O₅ (M+H⁺), m/z = 570.2711, found 570.2720

UV/Vis (50 μM in DMSO): open isomer: λ_{max} = 363 nm; closed isomer: λ_{max} = 563 nm.

4.2 Assays

IP accumulation assay

The measurement of D_{2S} receptor stimulated activation of the G-protein mediated pathway was performed applying the IP-One HTRF[®] assay (Cisbio, Codolet, France) according to the manufacturer's protocol. In brief, HEK-293T cells were grown to a confluence of approx. 70% and transiently cotransfected with the cDNAs of the human D_{2S} receptor (in pcDNA3.1) and the hybrid G-protein Gαq_{i5}-HA (Gαq protein with the last five amino acids at the C-terminus replaced by the corresponding sequence of Gα_i; gift from The J. David Gladstone Institutes, San Francisco, CA)^{27,28} applying TransIT-293 Mirus transfection reagent (MoBiTec, Goettingen, Germany). After one day cells were detached from the culture dish with Versene (Life Technologies GmbH, Darmstadt, Germany), seeded into black 384-well plates (10000 cells/well) (Greiner Bio-One, Frickenhausen, Germany) and maintained for 24 h at 37 °C. Test

compounds (final concentration of 10 μ M, 100 nM and 1 nM) were dissolved in stimulation buffer and added to the cells as quadruplicates in a black box under illumination with monochromatic light of a wave length of 625 nm or in the dark according to the photostability of the ligands. Incubation was performed for 2 hrs at 37 °C and subsequently stopped by adding the detection reagents (IP1-d2 conjugate and Anti-IP1cryptate TB conjugate each dissolved in lysis buffer). After waiting for further 1 h at room temperature time resolved fluorescence resonance energy transfer (HTRF) was measured using the Clariostar plate reader (BMG, Ortenberg, Germany) according to the requirements of the company. FRET data were normalized to basal (= 0%) and the maximum effect of quinpirole (= 100%). Average values including standard deviation are the result of three to ten individual experiments each done in quadruplicate and calculated using PRISM 6.0 (GraphPad software, San Diego, CA).

β -Arrestin recruitment assay

D_{2S}R mediated β -arrestin-2 recruitment was determined using the PathHunter[®] assay (DiscoverX, Birmingham, U.K.) as described previously.²⁹ In brief, HEK293 cells stably expressing the enzyme acceptor (EA) tagged β -arrestin-2 fusion protein were transiently transfected with the ProLink tagged D2SR-ARMS2-PK2 construct employing Mirus TransIT-293. One day (24 hrs) after transfection, cells were detached from the culture dish with Versene (Life Technologies, Darmstadt, Germany), seeded into 384-well plates (white plates with transparent bottom, Greiner Bio-One, Frickenhausen, Germany) at a cell number of 5000 cells/well and maintained for further 24 h at 37 °C, 5 % CO₂. Test compounds at a final concentration of 10 μ M, 100 nM and 1 nM were dissolved in PBS and added to the cells as quadruplicates in a black box under illumination with monochromatic light of a wave length of 625 nm or in the dark according to the photostability of the ligands. Incubation with the test compounds was continued for 5 hrs at 37 °C and was stopped by adding the detection mix to every well. After further 1 h at room temperature chemiluminescence was determined using a Clariostar plate reader (BMG, Ortenberg, Germany). Row data were normalized to basal (= 0%) and the maximum effect of quinpirole (= 100%). Average values including standard deviation were derived from four to ten individual experiments each done in quadruplicate and mean values were calculated using PRISM 6.0 (GraphPad software, San Diego, CA).

Dopamine D_{2S} receptor binding

Receptor binding studies were carried out as described previously.³⁰ In brief, competition binding experiments were performed using preparations of membranes from CHO cells stably expressing the human D_{2S}R³¹ and the radioligand [³H]spiperone (specific activity = 81 Ci/mmol, PerkinElmer, Rodgau, Germany) at a final concentration of 0.20 nM. The assays were carried out with a protein concentration of 2 μ g per assay tube, a K_D value of 0.050 nM and a corresponding B_{max} value of 2000 fmol/mg. Test compounds were applied at final

concentrations in the range from 0.01 nM to 10000 nM each done as triplicates. Unspecific binding was determined in the presence of haloperidol (10 μ M), the protein concentration was established by the method of Lowry using bovine serum albumin as standard.³² The resulting competition curves of the binding experiments were analyzed by nonlinear regression using the algorithms in PRISM 6.0 (GraphPad Software, San Diego, CA). For each individual experiment, the data was fitted using a monophasic competition model to provide an IC₅₀ value, which was then transformed into a K_i value according to the equation of Cheng and Prusoff.³³ Mean K_i values \pm SEM were derived from four to six individual experiments.

5. Literature

- 1 a) R. Lappano, M. Maggiolini, *Nat Rev Drug Discov* **2011**, *10*, 47-60; b) N. Packiriswamy, N. Parameswaran, *Genes Immun* **2015**, *16*, 367-77; c) P. Jeffrey Conn, A. Christopoulos, C. W. Lindsley, *Nat Rev Drug Discov* **2009**, *8*, 41-54
- 2 J.-M. Beaulieu, R. R. Gainetdinov, *Pharmacol. Rev.* **2011**, *63*, 182-217
- 3 a) S. Löber, H. Hübner, N. Tschammer, P. Gmeiner, *Trends Pharmacol. Sci.* **2011**, *32*, 148-157; b) D. Möller, R. C. Kling, M. Skultety, K. Leuner, H. Hübner, P. Gmeiner, *J. Med. Chem.* **2014**, *57*, 4861-4875; c) D. Weichert, A. Banerjee, C. Hiller, R. C. Kling, H. Hübner, P. Gmeiner, *J. Med. Chem.* **2015**, *58*, 2703-2717; d) N. Tschammer, J. Elsner, A. Goetz, K. Ehrlich, S. Schuster, M. Ruberg, J. Kühhorn, D. Thompson, J. Whistler, H. Hübner, P. Gmeiner, *J. Med. Chem.* **2011**, *54*, 2477-2491; e) J. Elsner, F. Boeckler, F. W. Heinemann, H. Hübner, P. Gmeiner, *J. Med. Chem.* **2005**, *48*, 5771-5779; f) C. Haubmann, H. Hübner, P. Gmeiner, *Bioorg. Med. Chem. Lett.* **1999**, *9*, 3143-3146; g) P. Rodriguez Loaiza, S. Löber, H. Hübner, P. Gmeiner, *J. Comb. Chem.* **2006**, *8*, 252-261
- 4 a) C. Falencyk, M. Schiedel, B. Karaman, T. Rumpf, N. Kuzmanovic, M. Grötli, W. Sippl, M. Jung, B. König, *Chem. Sci.* **2014**, *5*, 4794-4799; b) D. Vomasta, C. Högner, N. R. Branda, B. König, *Angew. Chem., Int. Ed.* **2008**, *47*, 7644-7647; c) D. Vomasta, A. Innocenti, B. König, C. T. Supuran, *Bioorg. Med. Chem. Lett.* **2009**, *19*, 1283-1286; d) B. Reisinger, N. Kuzmanovic, P. Löffler, R. Merkl, B. König, R. Sterner, *Angew. Chem., Int. Ed.* **2014**, *53*, 595-598; e) J. Broichhagen, I. Jurastow, K. Iwan, W. Kummer, D. Trauner, *Angew. Chem., Int. Ed.* **2014**, *53*, 7657-7660; f) R. Ferreira, J. R. Nilsson, C. Solano, J. Andreasson, M. Groetli, *Sci. Rep.* **2015**, *5*, 9769
- 5 a) J. Broichhagen, A. Damijonaitis, J. Levitz, K. R. Sokol, P. Leippe, D. Konrad, E. Y. Isacoff, D. Trauner, *ACS Cent. Sci.* **2015**, *1*, 383-393; b) T. Fehrentz, C. A. Kuttruff, F. M. E. Huber, M. A. Kienzler, P. Mayer, D. Trauner, *ChemBioChem* **2012**, *13*, 1746-1749, S46/1-S46/28; c) M. Schoenberger, D. Trauner, *Angew. Chem., Int. Ed.* **2014**, *53*, 3264-3267; d) A. Rullo, A. Reiner, A. Reiter, D. Trauner, E. Y. Isacoff, G. A. Woolley, *Chem. Commun. (Cambridge, U. K.)* **2014**, *50*, 14613-14615 e) S. Pittolo, X. Gomez-Santacana, K. Eckelt, X. Rovira, J. Dalton, J. Giraldo, C. Goudet, J.-P. Pin, A. Llobet, A. Llebaria, P. Gorostiza, *Nat. Chem. Biol.* **2014**, *10*, 813-815
- 6 a) W. A. Velema, J. P. van der Berg, M. J. Hansen, W. Szymanski, A. J. M. Driessen, B. L. Feringa, *Nat. Chem.* **2013**, *5*, 924-928; b) W. A. Velema, M. J. Hansen, M. M. Lerch, W. Szymanski, B. L. Feringa, A. J. M. Driessen, *Bioconjug Chem* **2015**, *26*, 2592-2597
- 7 a) M. Dong, A. Babalhavaeji, S. Samanta, A. A. Beharry, G. A. Woolley, *Acc. Chem. Res.* **2015**, *48*, 2662-2670; b) S. Samanta, A. A. Beharry, O. Sadovski, T. M.

- McCormick, A. Babalhavaeji, V. Tropepe, G. A. Woolley, *J. Am. Chem. Soc.* **2013**, *135*, 9777-9784; c) D. Bleger, S. Hecht, *Angew. Chem., Int. Ed.* **2015**, *54*, 11338-11349
- 8 M. I. Bahamonde, J. Taura, S. Paoletta, A. A. Gakh, S. Chakraborty, J. Hernando, V. Fernández-Dueñas, K. A. Jacobson, P. Gorostiza, F. Ciruela, *Bioconjugate Chem.* **2014**, *25*, 1847-1854
- 9 M. Schönberger, *Developing Photoswitchable Ligands for Transmembrane Receptors*, Diss. **2014**, LMU München
- 10 W. A. Velema, W. Szymanski, B. L. Feringa, *J. Am. Chem. Soc.* **2014**, *136*, 2178-2191
- 11 a) M. Irie, *Chem. Rev.* **2000**, *100*, 1685-1716; b) C. Brieke, F. Rohrbach, A. Gottschalk, G. Mayer, A. Heckel, *Angew. Chem., Int. Ed.* **2012**, *51*, 8446-8476
- 12 a) X. Chen, N. I. Islamova, S. P. Gracia, J. A. DiGirolamo, W. J. Lees, *J. Org. Chem.* **2009**, *74*, 6777-6783; b) X. Chen, N. I. Islamova, R. V. Robles, W. J. Lees, *Photochem. Photobiol. Sci.* **2011**, *10*, 1023-1029
- 13 W. Szymański, J. M. Beierle, H. A. V. Kistemaker, W. A. Velema, B. L. Feringa, *Chem. Rev.* **2013**, *113*, 6114-6178
- 14 L. Bettinetti, K. Schlotter, H. Hübner, P. Gmeiner, *J. Med. Chem.* **2002**, *45*, 4594-4597
- 15 K. Schlotter, F. Böckler, H. Hübner, P. Gmeiner, *J. Med. Chem.* **2005**, *48*, 3696-3699
- 16 D. Weichert, M. Stanek, H. Hübner, P. Gmeiner, *Bioorg. Med. Chem.* **2016**, *24*, 2641-2653
- 17 N. Nebel, S. Maschauer, A. L. Bartuschat, S. K. Fehler, H. Hübner, P. Gmeiner, T. Kuwert, M. R. Heinrich, O. Prante, C. Hocke, *Bioorganic & Medicinal Chemistry Letters* **2014**, *24*, 5399-5403
- 18 N. Tschammer, M. Dörfler, H. Hübner, P. Gmeiner, *ACS Chemical Neuroscience* **2009**, *1*, 25-35
- 19 D. Wutz, C. Falenczyk, N. Kuzmanovic, B. König, *RSC Adv.* **2015**, *5*, 18075-18086
- 20 a) A. J. Myles, Z. Zhang, G. Liu, N. R. Branda, *Org. Lett.* **2000**, *18*, 2749-2751; b) Linda N. Lucas, Jaap J. D. d. Jong, Jan H. v. Esch, Richard M. Kellogg, Ben L. Feringa, *Eur. J. Org. Chem.* **2003**, *2003*, 155-166
- 21 a) T. Yamaguchi, M. Irie, *Chem. Lett.* **2004**, *33*, 1398-1399; b) T. Yamaguchi, K. Uchida, M. Irie, *J. Am. Chem. Soc.* **1997**, *119*, 6066-6071; c) M. Irie, K. Sayo, *J. Phys. Chem.* **1992**, *96*, 7671-7674
- 22 a) M. Herder, B. M. Schmidt, L. Grubert, M. Paetzel, J. Schwarz, S. Hecht, *J. Am. Chem. Soc.* **2015**, *137*, 2738-2747; b) J. R. Matis, J. B. Schoenborn, P. Saalfrank, *Phys. Chem. Chem. Phys.* **2015**, *17*, 14088-14095; c) M. Irie, T. Lifka, K. Uchida, S. Kobatake, Y. Shindo, *Chem. Commun.* **1999**, 747-750

-
- 23 a) H. Stobbe, *Ber. Dtsch. Chem. Ges.* **1905**, 38, 3893-3678; b) F. Strübe, R. Siewertsen, F. D. Sönnichsen, F. Renth, F. Temps, J. Mattay, *Eur. J. Org. Chem.* **2011**, 10, 1947-1955
- 24 Dietrich. S., *Synthese und Photochrome Eigenschaften funktionalisierter Indolyfulgimide*, Diss. **2006**, Berlin
- 25 B. Otto, K. Rück-Braun, *Eur. J. Org. Chem.* **2011**, 10, 1947-1955
- 26 S. I. Luyksaar, V. A. Migulin, B. B. Nabatov, M. M. Krayushkin, *Russ. Chem. Bull., Int. Ed* **2010**, 59, 446-451
- 27 A.C. Kruse, A.M. Ring, A. Manglik, J. Hu, K. Hu, K. Eitel, H. Huebner, E. Pardon, C. Valant, P.M. Sexton, A. Christopoulos, C.C. Felder, P. Gmeiner, J. Steyaert, W.I. Weis, K.C. Garcia, J. Wess, and B.K. Kobilka, *Nature* **2013**, 504, 101-106
- 28 B.R. Conklin, Z. Farfel, K.D. Lustig, D. Julius, H.R. Bourne, *Nature* **1993**, 363, 274-276
- 29 D. Möller, R.C. Kling, M. Skultety, K. Leuner, H. Hübner, P. Gmeiner, *J. Med. Chem.* **2014**, 57, 4861-4875
- 30 H. Hübner, C. Haubmann, W. Utz, P. Gmeiner, *J. Med. Chem.* **2000**, 43, 756-762
- 31 G. Hayes, T.J. Biden, L.A. Selbie, J. Shine. *Mol. Endocrinol.* **1992**, 6, 920-926
- 32 O.H. Lowry, N.J. Rosebrough, A.L. Farr, R.J. Randall, *J. Biol. Chem.* **1951**, 193, 265-275
- 33 Y.-C. Cheng, W.H. Prusoff, *Biochem. Pharmacol.* **1973**, 22, 3099-3108
- 34 B. Männel, H. Hübner, D. Möller, P. Gmeiner, *Bioorg. Med. Chem.* **2017**, 25, 5613

6. Supporting Information

SI1: Synthesis of 14

The synthesis of precursor **14** is described by Männel *et al.*³⁴

SI2: UV/VIS absorption spectroscopy of 30/33

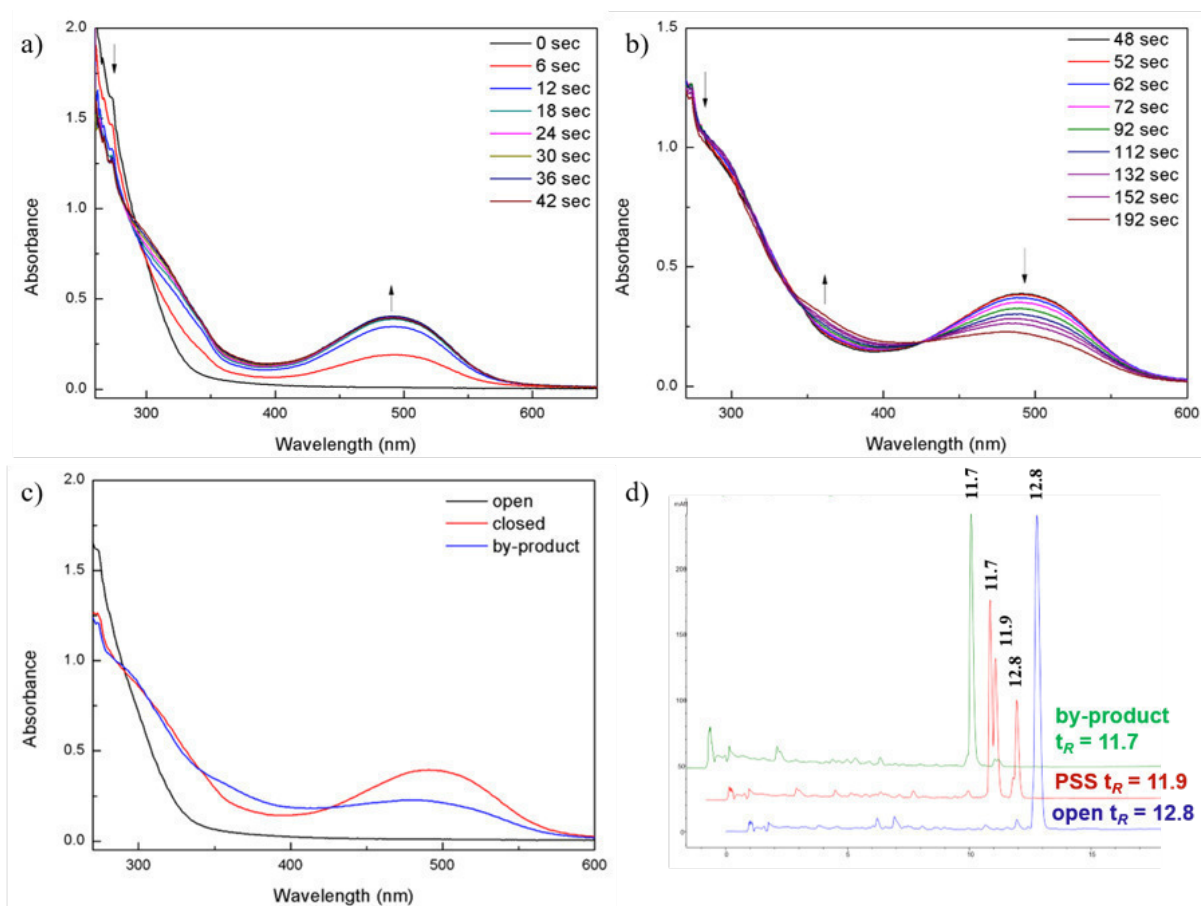
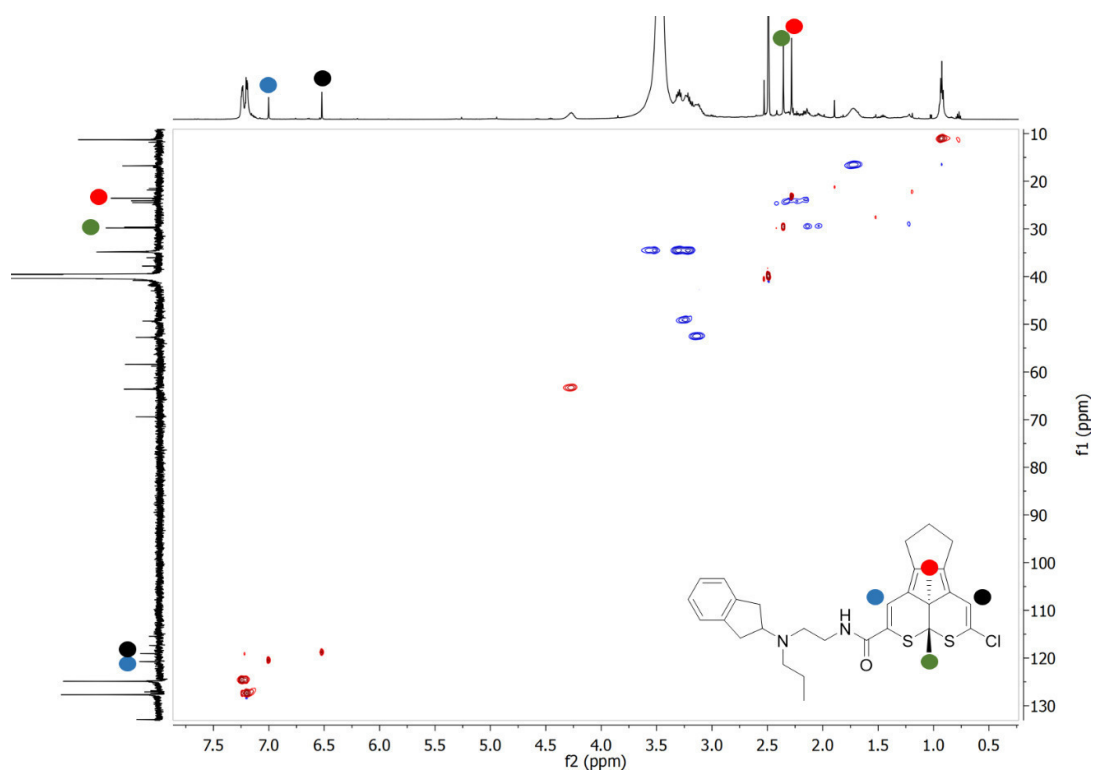
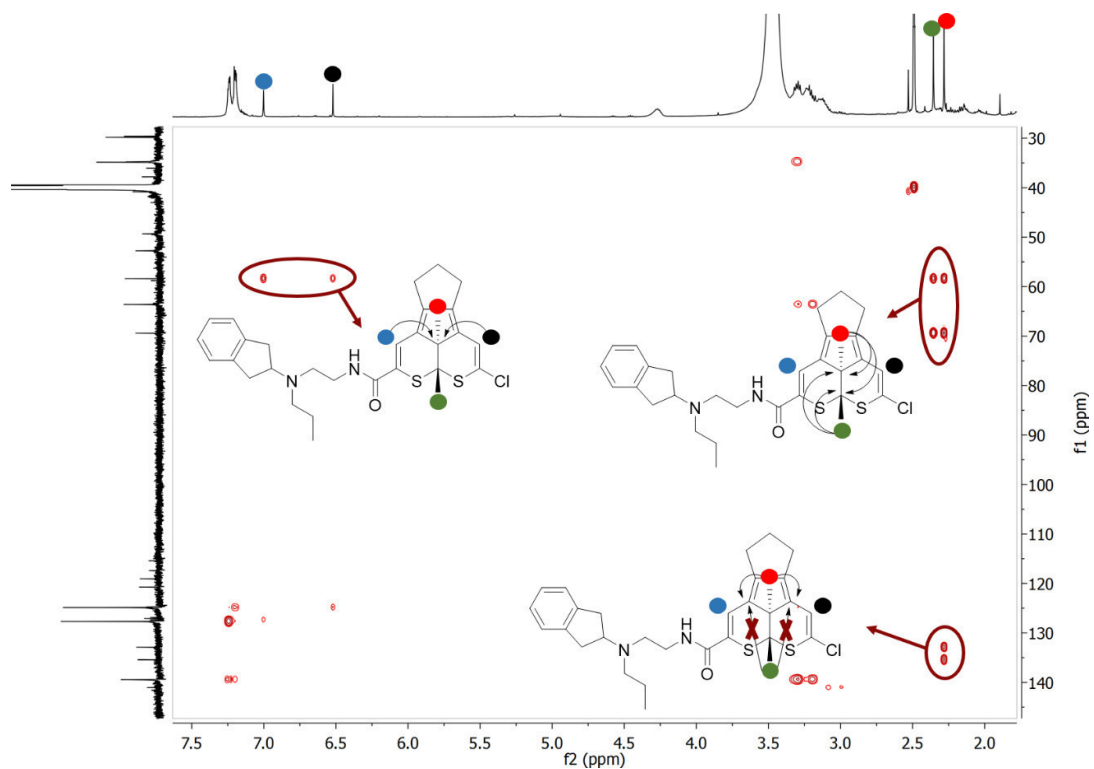


Figure SI2. a) UV-Vis absorption spectra of the ligand **30** (50 μM in DMSO) under irradiation with light of $\lambda = 312$ nm (Herolab, 6 W) until the PSS is reached; b) continuous irradiation causes the decrease at 494 nm and a hypsochromically shifted new maxima is arising at 360 nm; c) combination of the absorbance maxima of the three occurring photoisomers of **30**; d) HPLC traces of the corresponding isomers (blue: open isomer; red: PSS; green: by-product). A new absorption maximum is observed, hypsochromically shifted to 360 nm, which is attributed to the irreversible occurring by-product **33**. The HPLC traces in Figure 3d) show that upon reaching the PSS approximately 55% of the by-product has already been formed and its formation is completed after 192 sec.

SI3: 2D-NMR spectra of compound 33



Scheme SI3-1: HMBC spectroscopy from the by-product 33.



Scheme SI3-2: HSQC spectroscopy from the by-product 33.

SI4: PSS-determination via HPLC

Compound **48**-(E) was irradiated with UV-light of 365 nm for 30 sec. The resulting “closed” mixture contained the Z, E and C isomer of **48** and the ratio was determined by a HPLC measurement (detection at the isosbestic point at 357 nm). After irradiation of the closed mixture of **48** with light of 530 nm for 2 min, a mixture of Z/E isomers as the open form was obtained (**Figure SI4-1**). The same method was applied to determine the PSS of diarylmaaleimide **23** (**Figure SI4-2**).

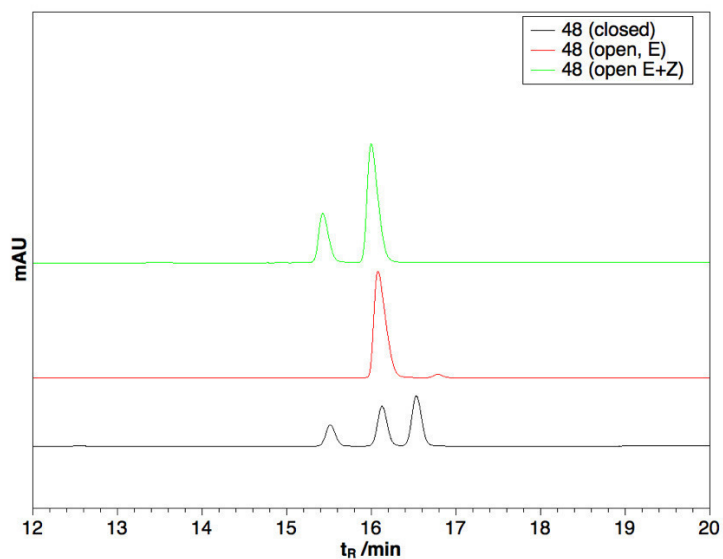


Figure SI4-1. HPLC traces of the E-isomer (open, isolated E-isomer, red), the closed mixture (black) and the open form after irradiating the closed mixture with light of 530 nm for 2 min (green).

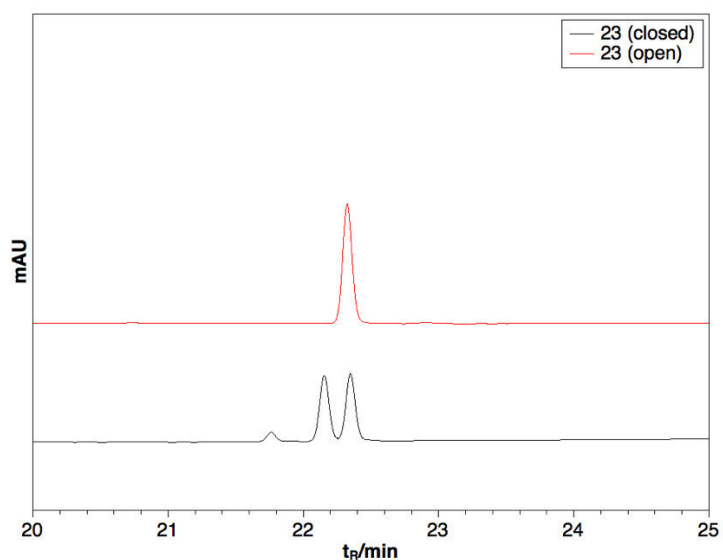


Figure SI4-2. HPLC traces of the open isomer of compound **23** (red) and the closed isomer after irradiation with 312 nm for 42 sec (black).

SI5: Activation data

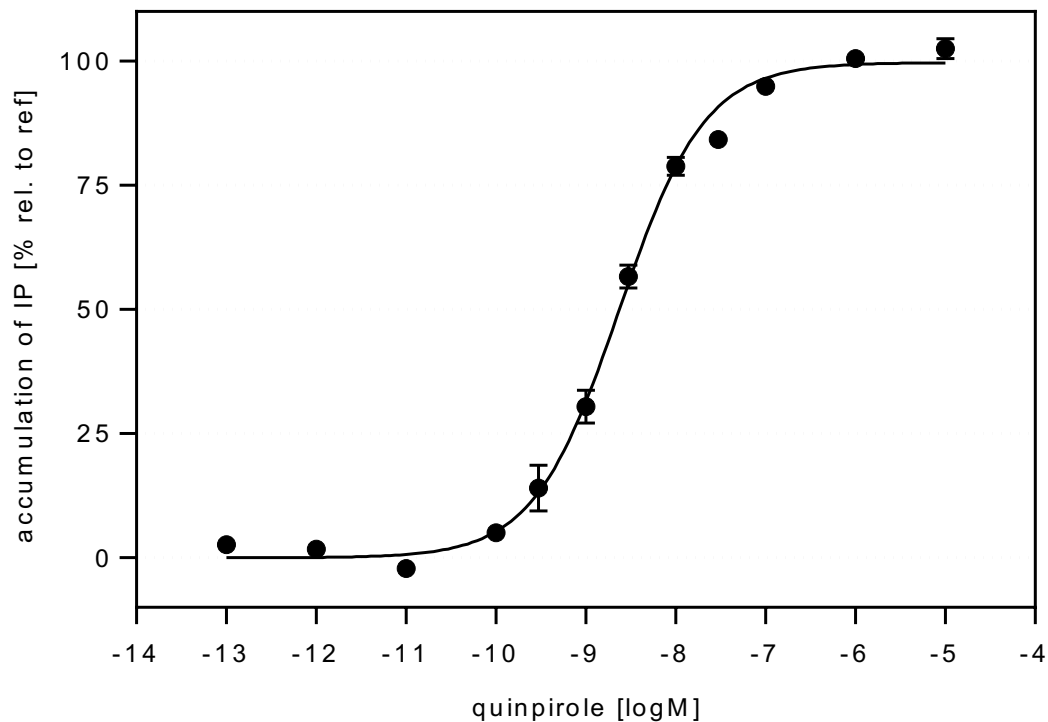


Figure SI5. Dose-response curve for the reference agonist quinpirole at the dopamine D_{2S} receptor determined with the IP-accumulation assay IP-One[®] assay (from Cisbio). For the test HEK 293T cells were transiently co-transfected with the cDNAs of the human D_{2short} receptor isoform and the G-protein hybrid G_{αqi5HA}. The graph displays a mean curve from 19 individual experiments each done in duplicates and indicates an EC₅₀ value of 2.3 nM.

Table SI5-1. Screening of photoactive ligands based on the diaryl maleimides **21-25** and the cyclopentene dithienylethenes **26-32** for functional activity at the dopamine D_{2S} receptor applying an IP accumulation assay and a β-arrestin recruitment assay

| comp. | photo- active state | IP accumulation ^a | | | β-arrestin recruitment ^b | | |
|-----------|---------------------------|---|-----------|-----------|---|-----------|-----------|
| | | E _{max} [% ± SEM] ^c | | | E _{max} [% ± SEM] ^d | | |
| | | 10 μM | 100 nM | 1 nM | 10 μM | 100 nM | 1 nM |
| 21 | open | 84 ± 1.2 | 49 ± 6.4 | 6.6 ± 8.4 | 4.1 ± 0.9 | nd | nd |
| | closed | 81 ± 1.1 | 37 ± 6.0 | 7.0 ± 6.3 | 3.2 ± 1.4 | nd | nd |
| 22 | open | 65 ± 5.8 | 18 ± 3.3 | 10 ± 3.2 | 3.0 ± 0.9 | nd | nd |
| | closed | 69 ± 2.9 | 20 ± 7.1 | 13 ± 5.9 | 3.2 ± 1.6 | nd | nd |
| 23 | open | 53 ± 4.5 | 3.5 ± 4.2 | 5.5 ± 1.8 | -0.7 ± 2.6 | nd | nd |
| | closed | 66 ± 5.8 | 14 ± 4.3 | 9.3 ± 4.9 | 0.8 ± 1.3 | nd | nd |
| 24 | open | 91 ± 3.0 | 73 ± 4.4 | 35 ± 13 | 33 ± 9.1 | 12 ± 1.2 | 2.7 ± 0.8 |
| | closed | 95 ± 1.5 | 68 ± 1.9 | 39 ± 9.6 | 37 ± 10 | 5.0 ± 1.3 | 0.7 ± 0.4 |
| 25 | open | 80 ± 3.7 | 22 ± 6.7 | 14 ± 1.6 | 16 ± 2.4 | 1.5 ± 0.7 | 1.2 ± 0.7 |
| | closed | 63 ± 8.0 | 34 ± 6.1 | 5.1 ± 5.3 | 6.2 ± 1.4 | 2.3 ± 0.8 | 1.0 ± 0.5 |
| 26 | open | 44 ± 3.5 | 43 ± 10 | 31 ± 16 | 2.3 ± 0.7 | nd | nd |
| | closed | 72 ± 3.5 | 41 ± 4.6 | 21 ± 5.7 | 0.7 ± 1.0 | nd | nd |
| 27 | open | 85 ± 2.6 | 16 ± 9.6 | 11 ± 9.8 | 1.9 ± 0.7 | nd | nd |
| | closed | 67 ± 7.4 | 49 ± 2.0 | 15 ± 0.9 | 0.4 ± 0.4 | nd | nd |
| 28 | open | 56 ± 3.3 | 22 ± 1.8 | 11 ± 4.8 | 0.6 ± 0.4 | nd | nd |
| | closed | 69 ± 5.0 | 38 ± 1.3 | 4.8 ± 1.5 | 0.3 ± 0.9 | nd | nd |
| 29 | open | 77 ± 3.8 | 80 ± 2.8 | 32 ± 4.6 | 9.3 ± 4.8 | n.d. | n.d. |
| | closed | 70 ± 6.8 | 47 ± 5.2 | 2.9 ± 3.2 | 3.6 ± 0.8 | n.d. | n.d. |
| 30 | open | 90 ± 2.9 | 60 ± 5.2 | 6.3 ± 4.3 | 15 ± 1.8 | n.d. | n.d. |
| | closed | 86 ± 2.2 | 28 ± 5.9 | 15 ± 7.5 | 14 ± 2.0 | n.d. | n.d. |
| 31 | open | 92 ± 4.8 | 79 ± 4.8 | 24 ± 9.5 | 87 ± 4.9 | 32 ± 3.3 | 3.3 ± 1.0 |
| | closed | 84 ± 3.9 | 80 ± 3.2 | 24 ± 15 | 83 ± 5.4 | 52 ± 3.2 | 10 ± 2.6 |
| 32 | open | 41 ± 5.3 | 52 ± 17 | 27 ± 11 | 2.7 ± 0.9 | n.d. | n.d. |
| | closed | 59 ± 4.5 | 37 ± 14 | 13 ± 5.1 | 4.6 ± 1.9 | n.d. | n.d. |

^a IP accumulation determined by applying the IP-One[®] assay (from Cisbio) with HEK 239T cells co-transfected with the cDNA of the dopamine D_{2S} receptor and that of the hybrid G-protein G_{α_q5HA}. ^b β-arrestin recruitment measured using the PathHunter[®] complementation assay (from DiscoverX) consisting of (EA)-β-arrestin-2-HEK293 cells and the transiently transfected vector D2SR-ARMS2-PK2. ^c E_{max} value ± S.E.M. derived from 3 to 10 individual experiments each done in quadruplicate relative to the maximum effect of quinpirole. ^d E_{max} value ± S.E.M. derived from 4 to 10 individual experiments each done in quadruplicate relative to the maximum effect of the reference ligand quinpirole. n.d. = not determined.

Table S15-2. Screening of the fulgide based photoactive ligands **43**, **45**, **46**, **48,50** and **52** for functional activity at the dopamine D_{2S} receptor applying an IP accumulation assay and a β -arrestin recruitment assay

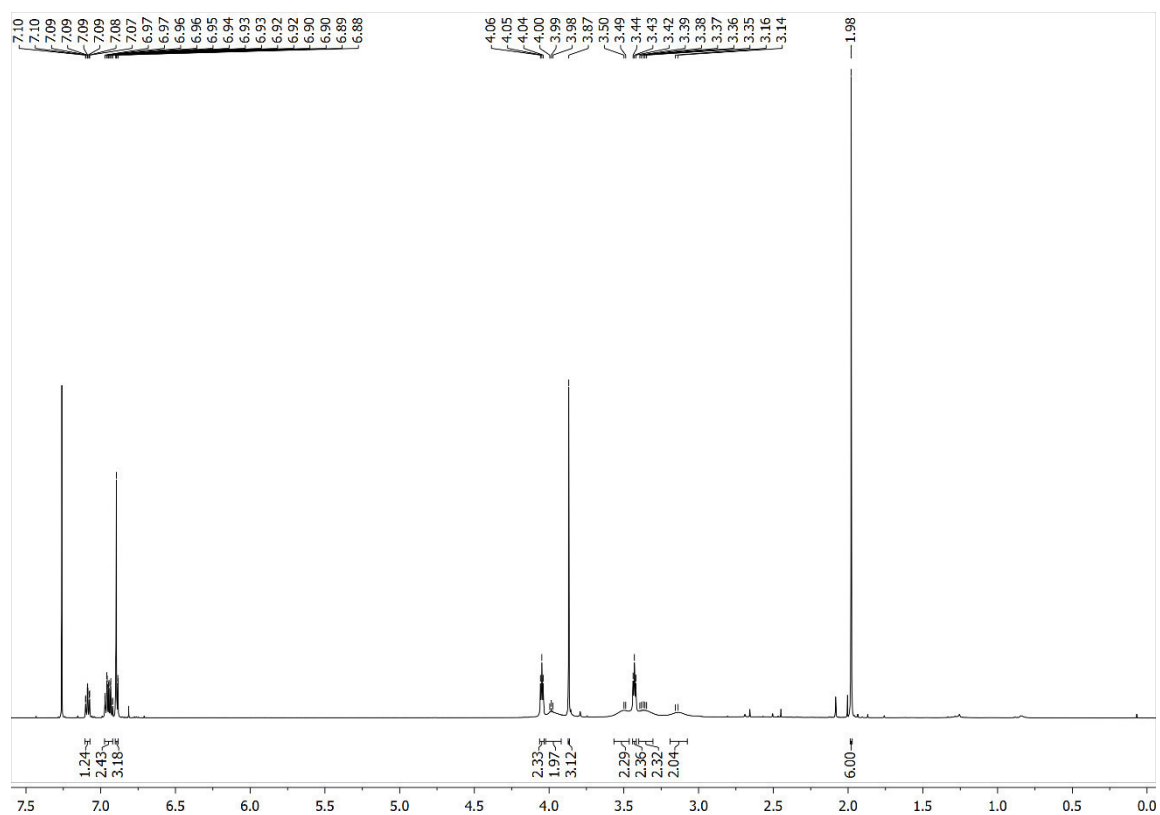
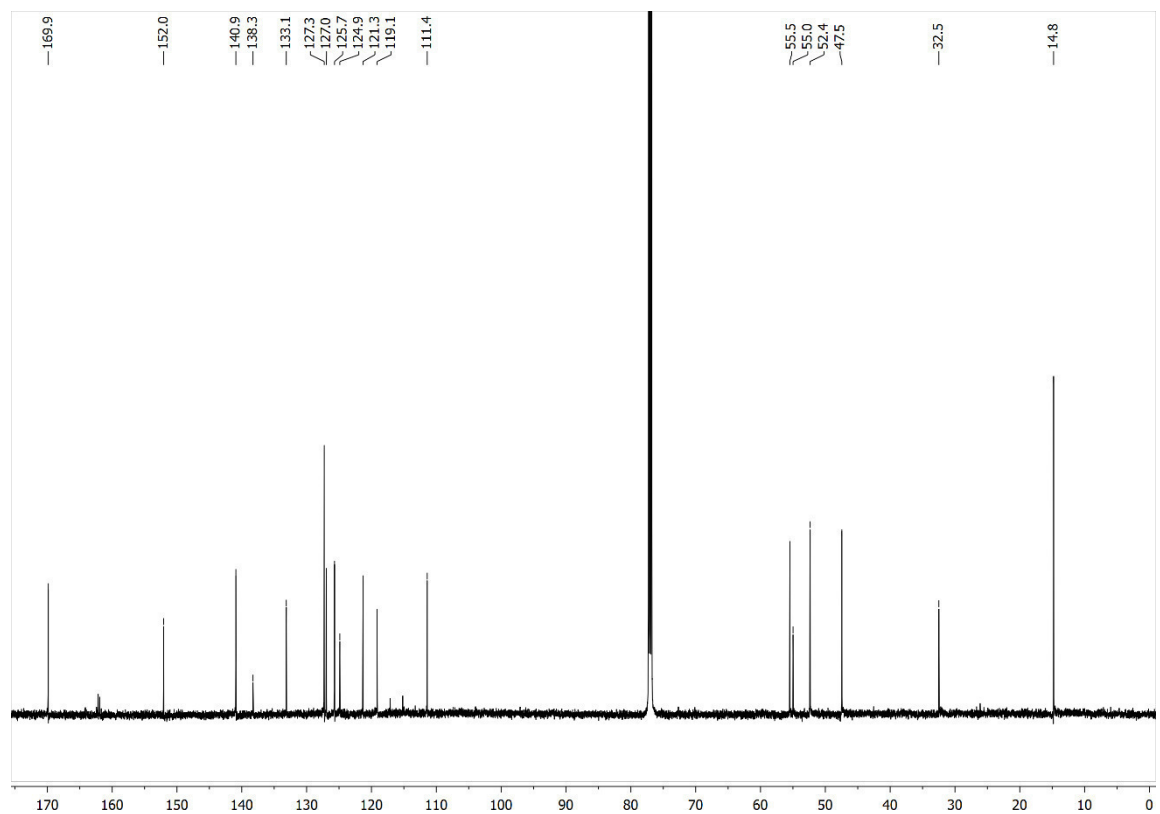
| comp. | photo-active state | IP accumulation ^a | | | β -arrestin recruitment ^b |
|-----------|------------------------------|---|---------------|---------------|---|
| | | E _{max} [% \pm SEM] ^c | | | E _{max} [% \pm SEM] ^d |
| | | 10 μ M | 100 nM | 1 nM | 10 μ M |
| 43 | open | 64 \pm 5.4 | 14 \pm 5.3 | 13 \pm 3.0 | 2.4 \pm 1.6 |
| | closed | 57 \pm 7.3 | 12 \pm 3.4 | 5.7 \pm 3.0 | 5.6 \pm 4.1 |
| 45 | open | 68 \pm 2.8 | 25 \pm 5.3 | 5.6 \pm 3.2 | 2.4 \pm 1.4 |
| | closed | 62 \pm 2.4 | 45 \pm 7.8 | 7.7 \pm 2.6 | -4.1 \pm 1.9 |
| 46 | open | 81 \pm 10 | 52 \pm 2.4 | 6.6 \pm 4.8 | 2.6 \pm 0.9 |
| | closed | 86 \pm 6.2 | 37 \pm 5.5 | 0.6 \pm 0.8 | 6.1 \pm 2.7 |
| 48 | <i>E</i> / open ^e | 92 \pm 3.6 | 39 \pm 1.9 | 6.0 \pm 3.2 | 3.6 \pm 1.4 |
| | <i>Z</i> / open ^f | 64 \pm 7.1 | 12 \pm 5.4 | 1.4 \pm 6.0 | 3.0 \pm 0.8 |
| | closed | 58 \pm 8.6 | 22 \pm 12 | 4.9 \pm 4.5 | 3.5 \pm 1.4 |
| 50 | <i>E</i> / open ^e | 94 \pm 2.9 | 10 \pm 4.7 | 2.1 \pm 4.4 | -2.3 \pm 0.5 |
| | <i>Z</i> / open ^f | 80 \pm 8.7 | 9.8 \pm 7.1 | 0.1 \pm 0.2 | 0.4 \pm 3.9 |
| | closed | 92 \pm 4.3 | 14 \pm 6.1 | 6.1 \pm 3.8 | 8.4 \pm 3.3 |
| 52 | open ^e | 58 \pm 6.9 | 48 \pm 8.5 | 10 \pm 3.8 | 7.2 \pm 1.3 |
| | closed | 69 \pm 6.6 | 47 \pm 4.2 | 40 \pm 4.6 | 5.4 \pm 1.8 |

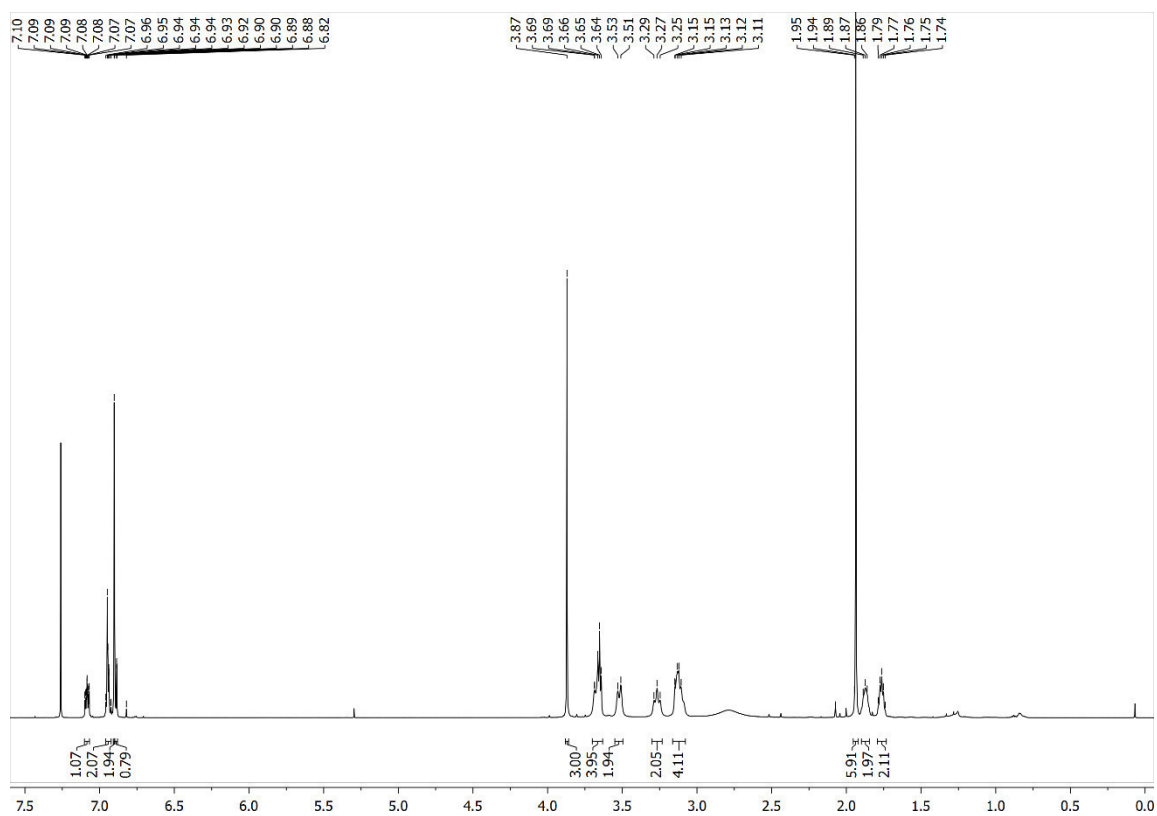
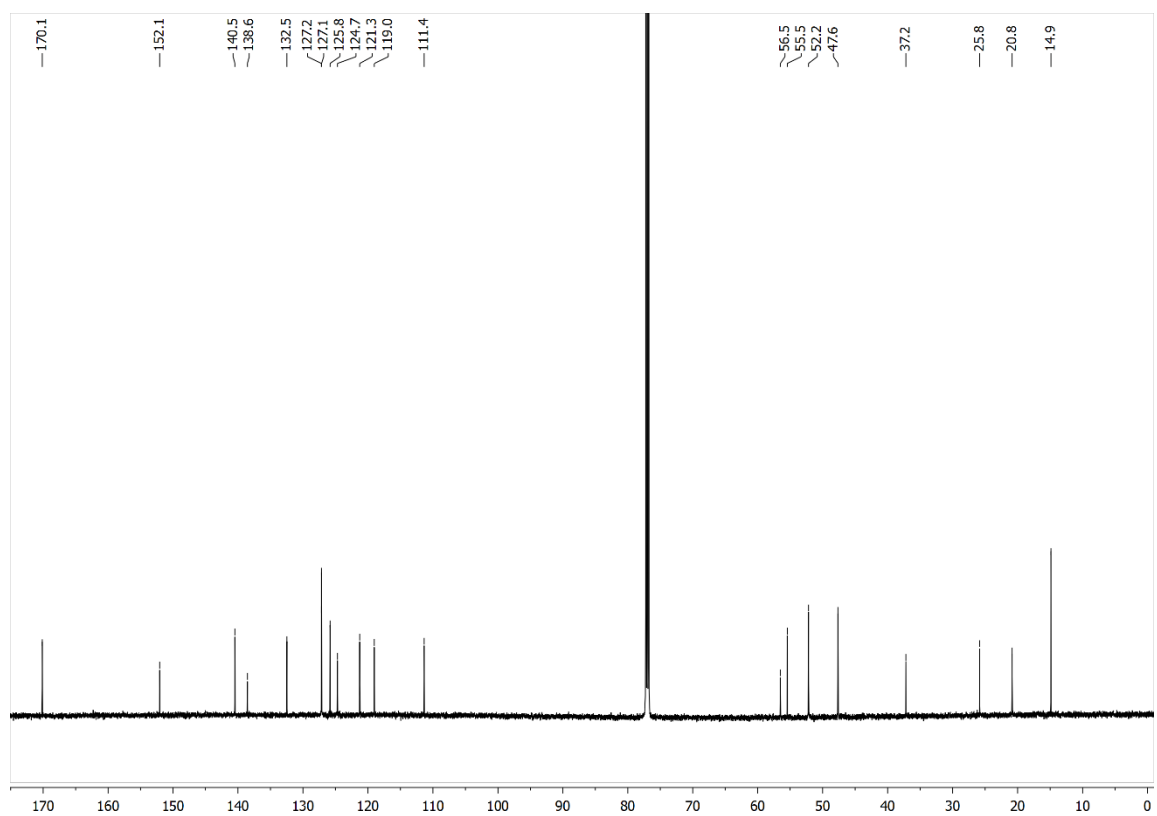
^a IP accumulation determined by applying the IP-One[®] assay (from Cisbio) with HEK 239T cells co-transfected with the cDNA of the dopamine D_{2S} receptor and that of the hybrid G-protein G α_{qj5HA} . ^b β -arrestin recruitment measured using the PathHunter[®] complementation assay (from DiscoverX) consisting of (EA)- β -arrestin-2-HEK293 cells and the transiently transfected vector D2SR-ARMS2-PK2. ^c E_{max} value \pm S.E.M. derived from 4 to 8 individual experiments each done in quadruplicate relative to the maximum effect of quinpirole. ^d E_{max} value \pm S.E.M. derived from 4 to 8 individual experiments each done in quadruplicate relative to the maximum effect of the reference ligand quinpirole. ^e Open state in *E*-configuration. ^f Open state in *Z*-configuration.

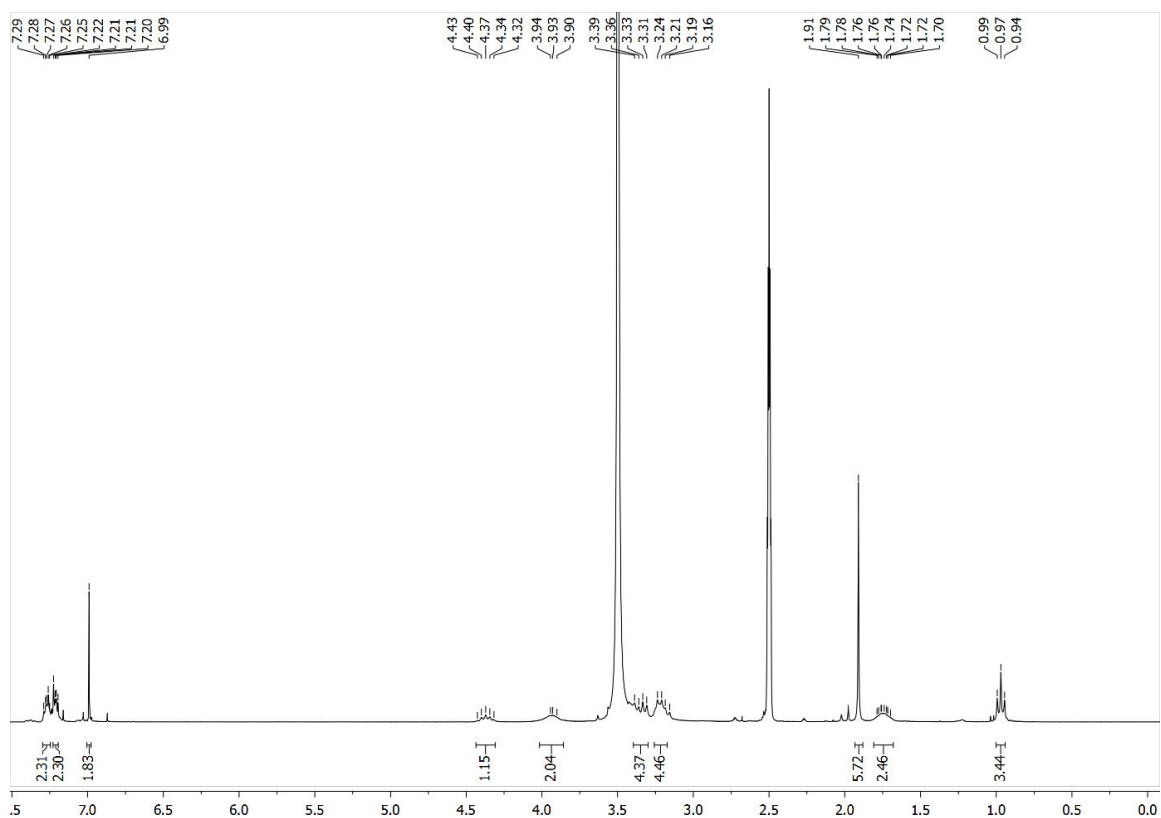
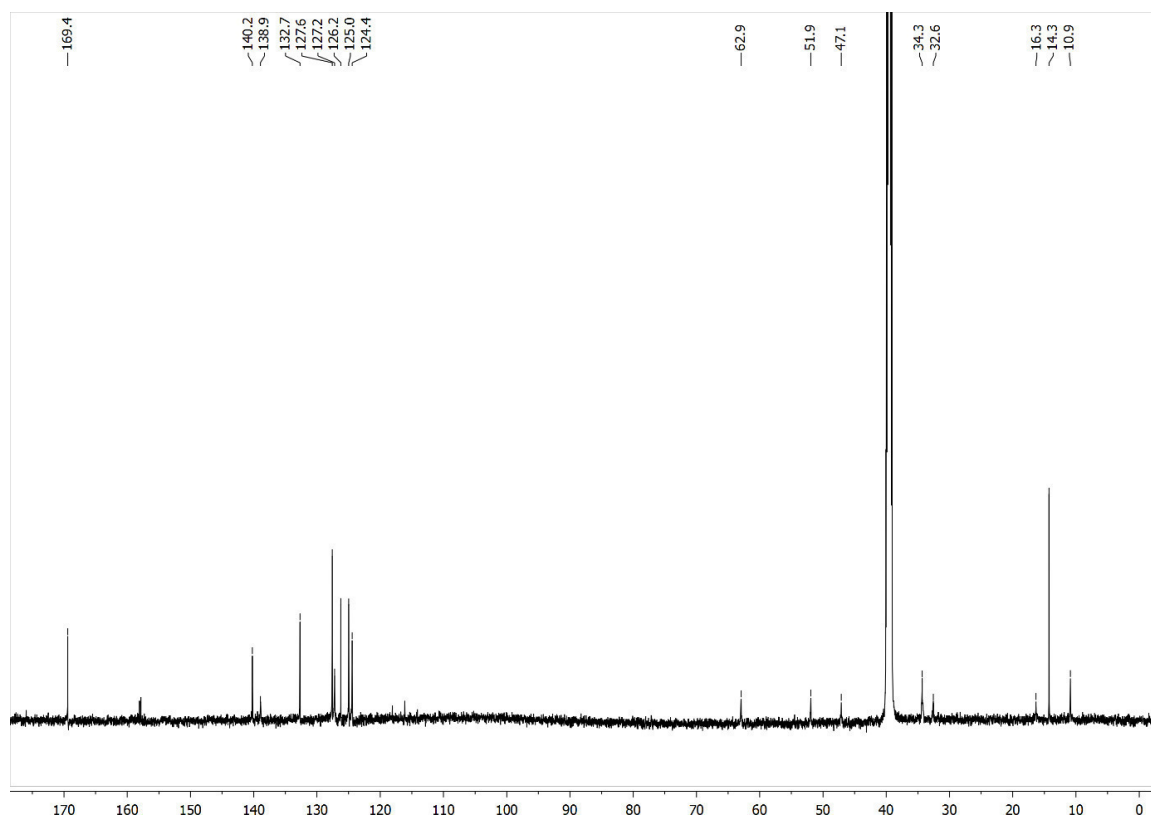
SI6: D_{2S} receptor competition binding experiments**Table SI6.** Receptor binding affinities (K_i values) of the most promising photoswitchable ligands **27**, **29**, **45** and **52** in the open and closed state at the human dopamine D_{2S} receptor.

| comp. | photoactive state | D _{2S} binding ^a |
|------------------------|-------------------|--------------------------------------|
| | | K_i [nM \pm SEM] ^b |
| 27 | open | 9.1 \pm 1.0 |
| | closed | 9.1 \pm 1.6 |
| 29 | open | 11 \pm 2.5 |
| | closed | 12 \pm 4.3 |
| 45 | open | 15 \pm 2.6 |
| | closed | 15 \pm 2.8 |
| 52 ^c | open | 17 \pm 8.0 |
| | closed | 14 \pm 3.6 |

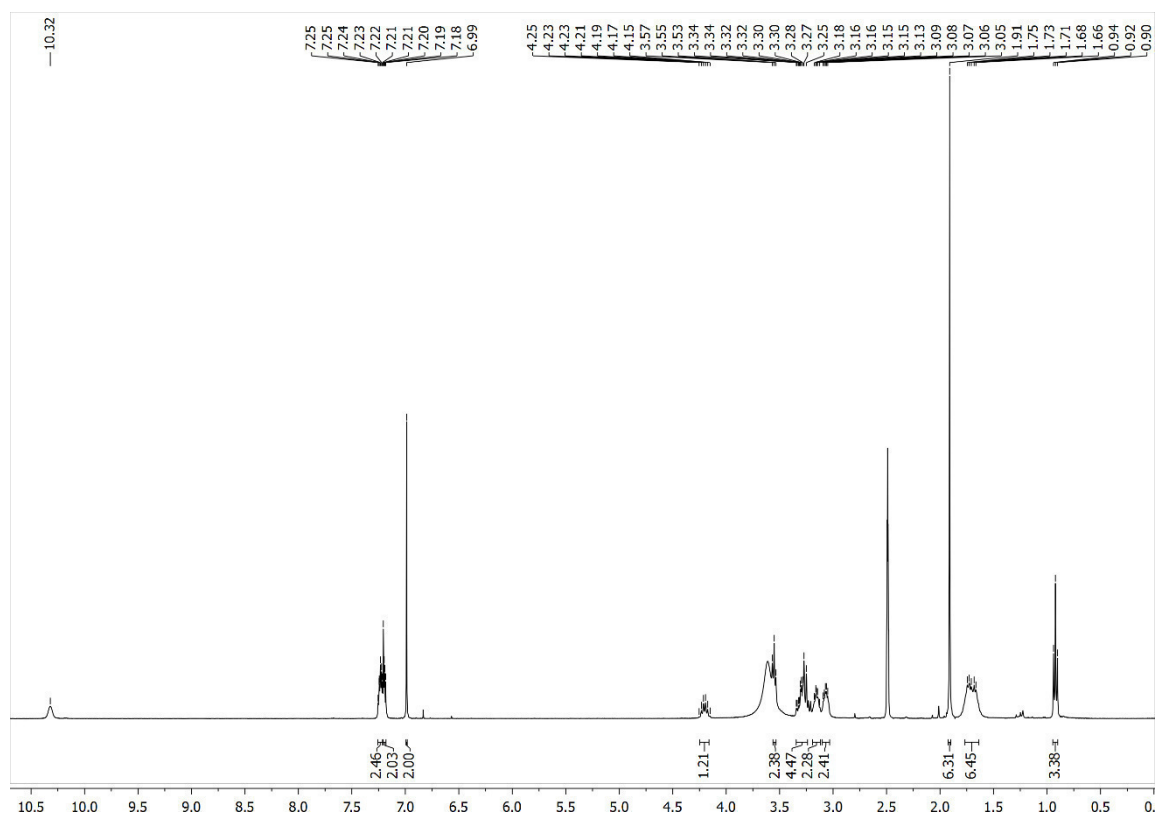
^a Binding data were measured with membrane preparations from CHO cells stably expressing the human D_{2S} receptor. ^b K_i values are derived from 4 to 6 individual experiments each done in triplicate. ^c The open isomer describes only the E-isomer.

S17: ^1H - and ^{13}C -NMR spectra of all photochromic ligands ^1H -NMR (600 MHz, CDCl_3) for compound **21**: ^{13}C -NMR (151 MHz, CDCl_3) for compound **21**:

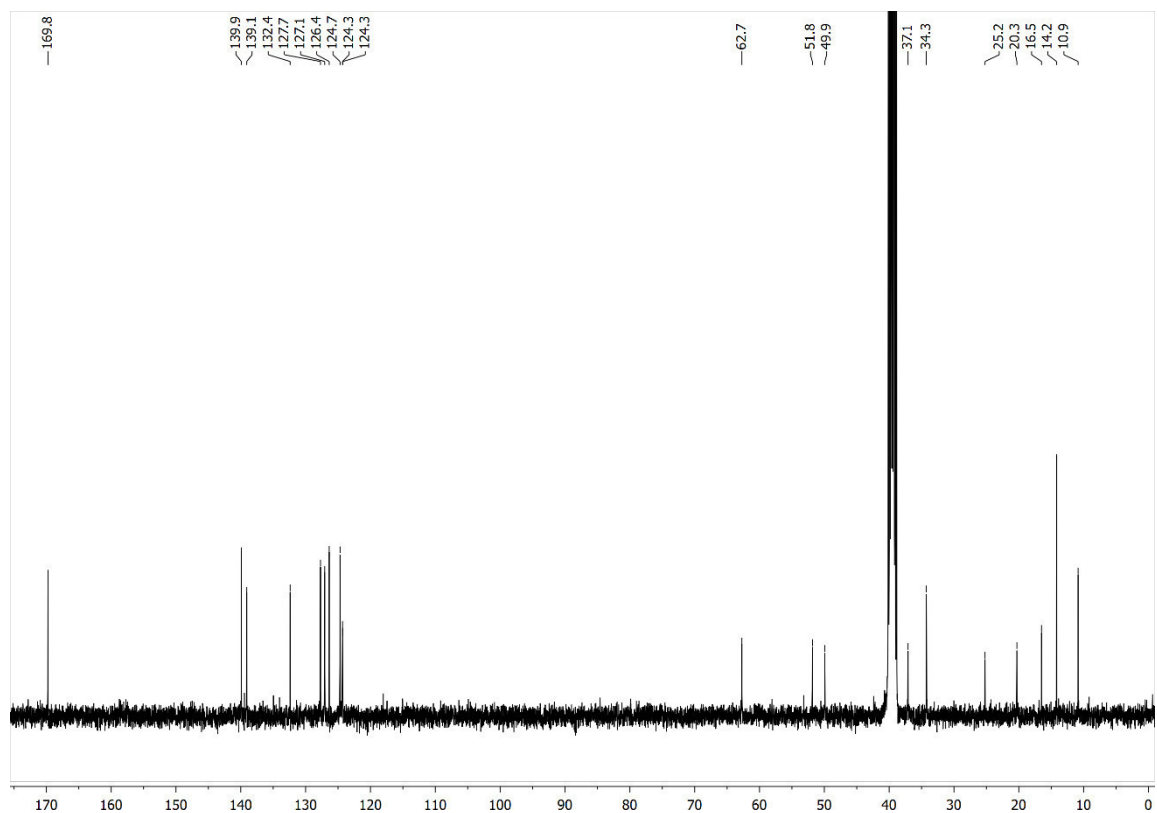
$^1\text{H-NMR}$ (600 MHz, CDCl_3) for compound **22**: $^{13}\text{C-NMR}$ (151 MHz, CDCl_3) for compound **22**:

$^1\text{H-NMR}$ (300 MHz, $\text{D}_6\text{-DMSO} + \text{D}_2\text{O}$) for compound **23**: $^{13}\text{C-NMR}$ (151 MHz, $\text{D}_6\text{-DMSO}$) for compound **23**:

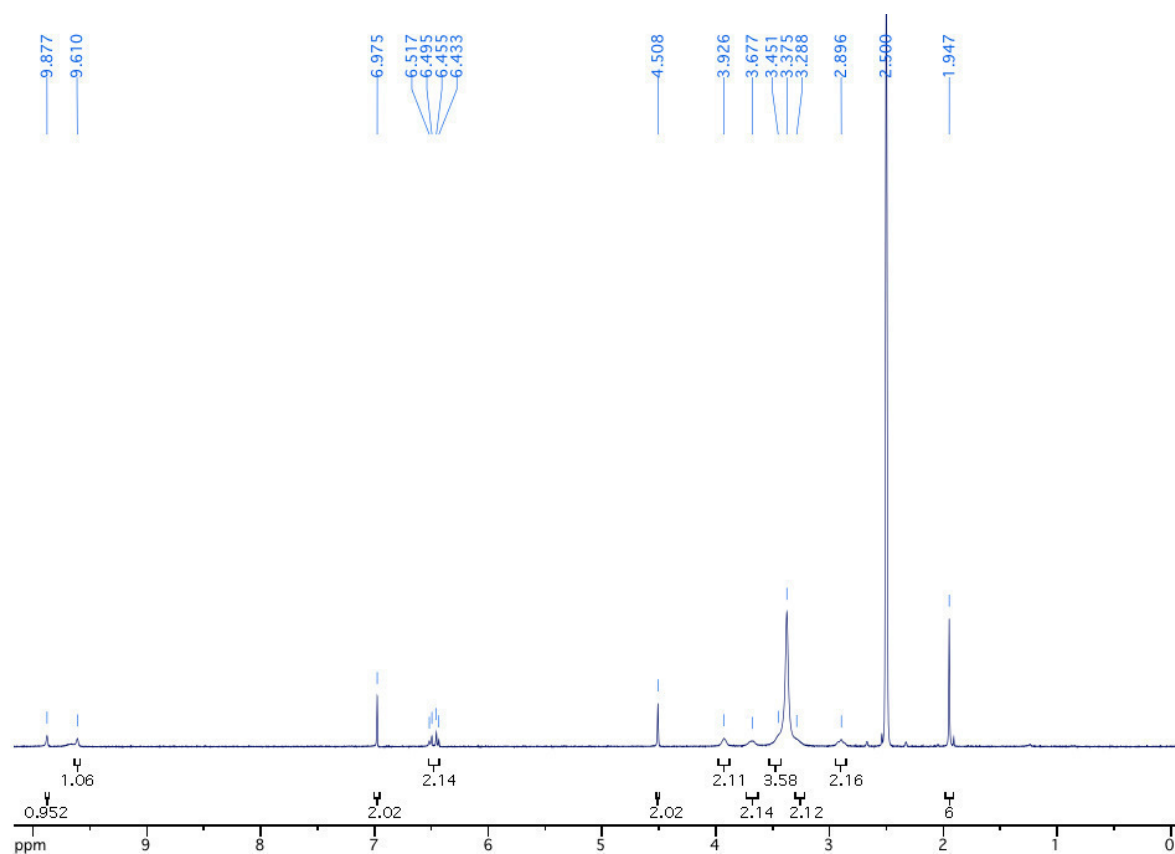
$^1\text{H-NMR}$ (400 MHz, $\text{D}_6\text{-DMSO}$) for compound **24**:



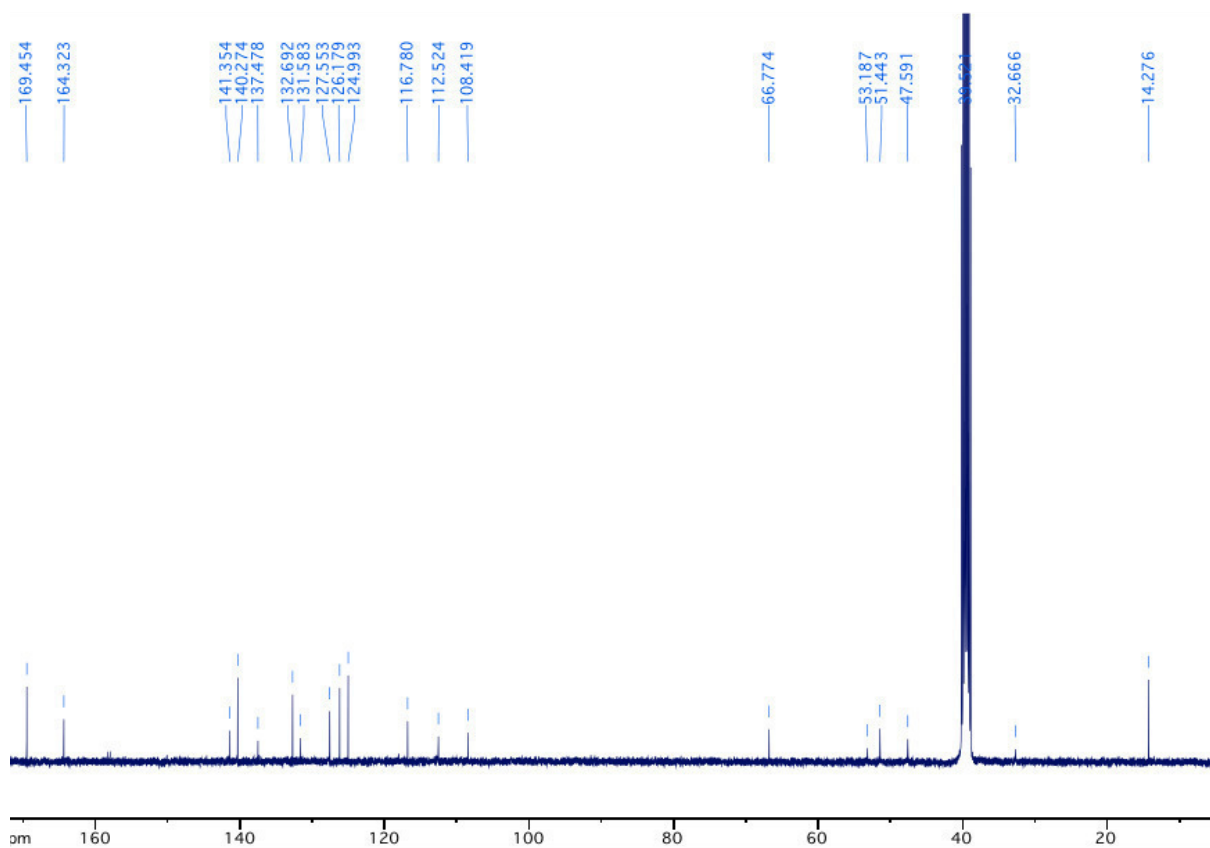
$^{13}\text{C-NMR}$ (101 MHz, $\text{D}_6\text{-DMSO}$) for compound **24**:

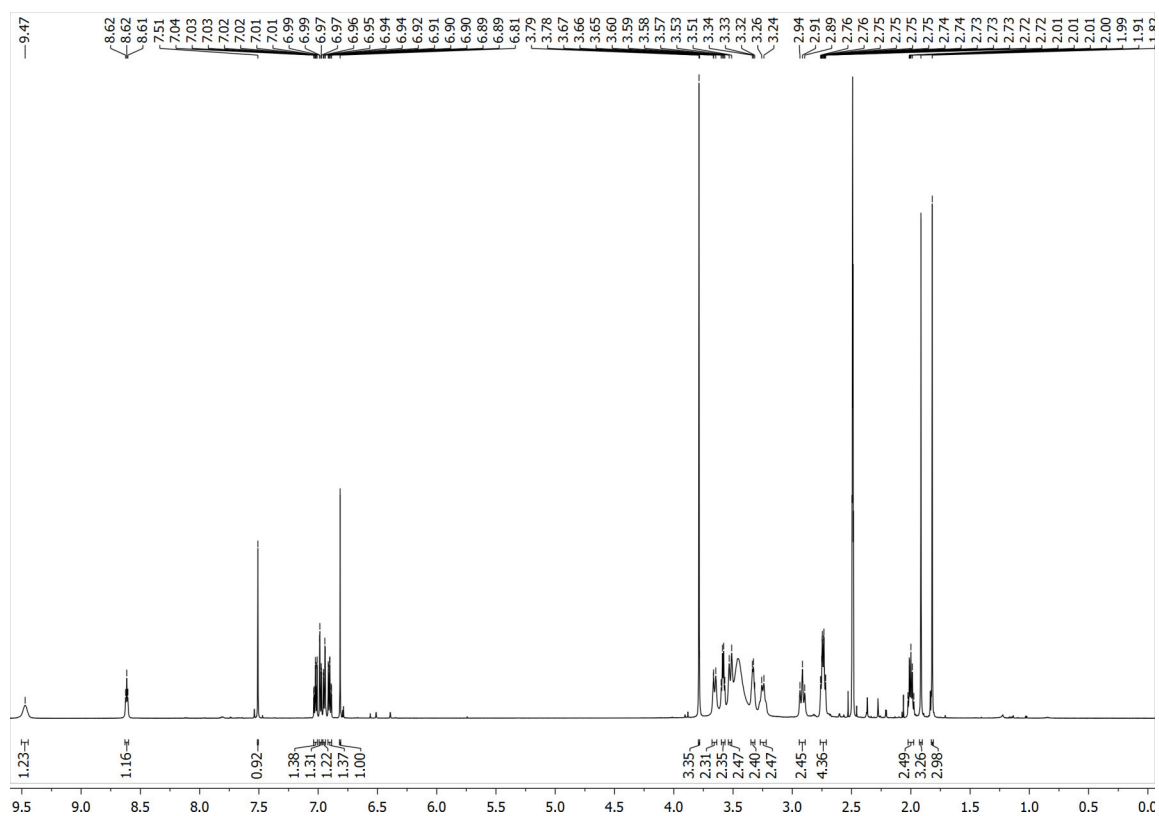
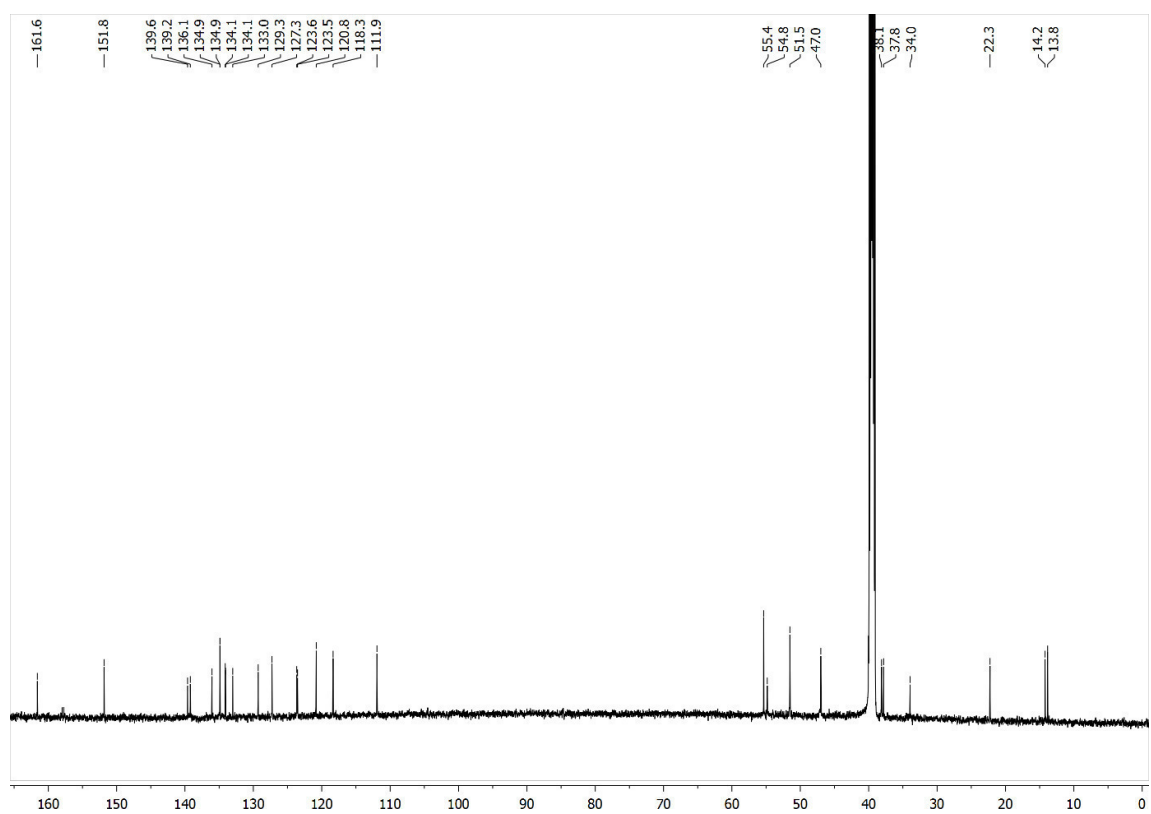


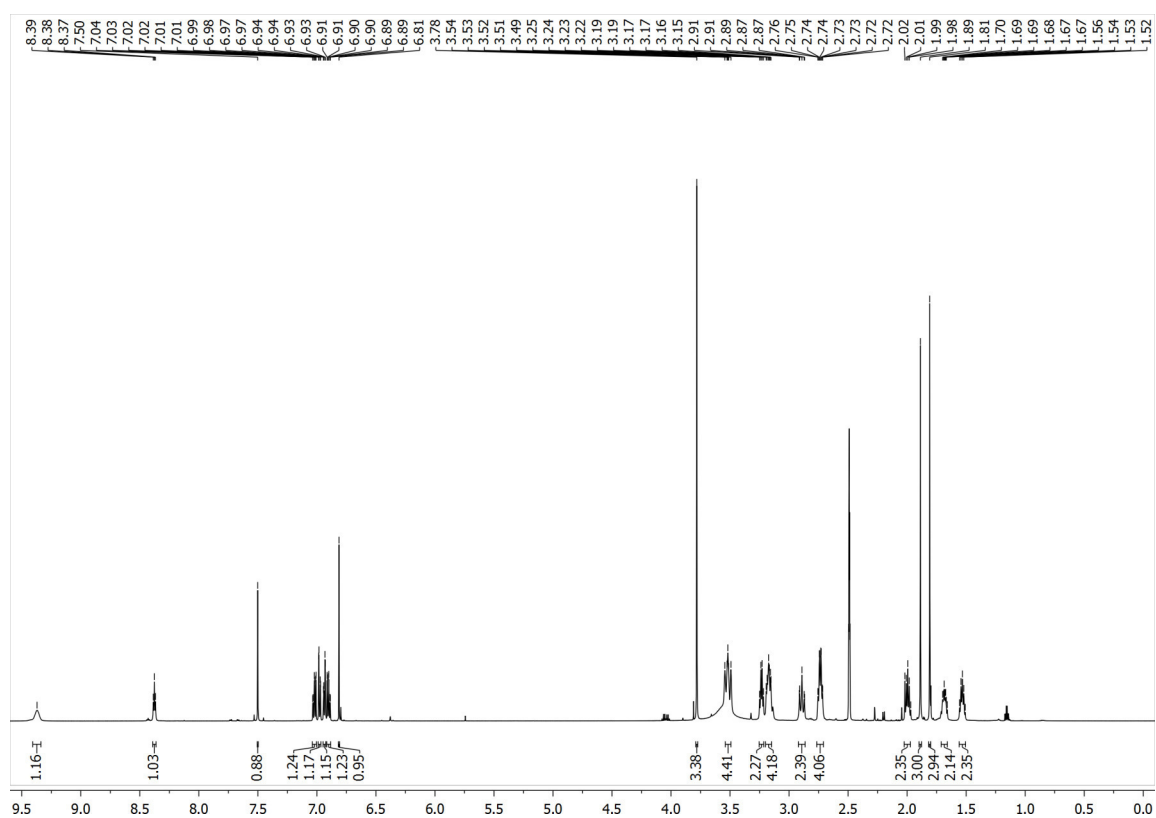
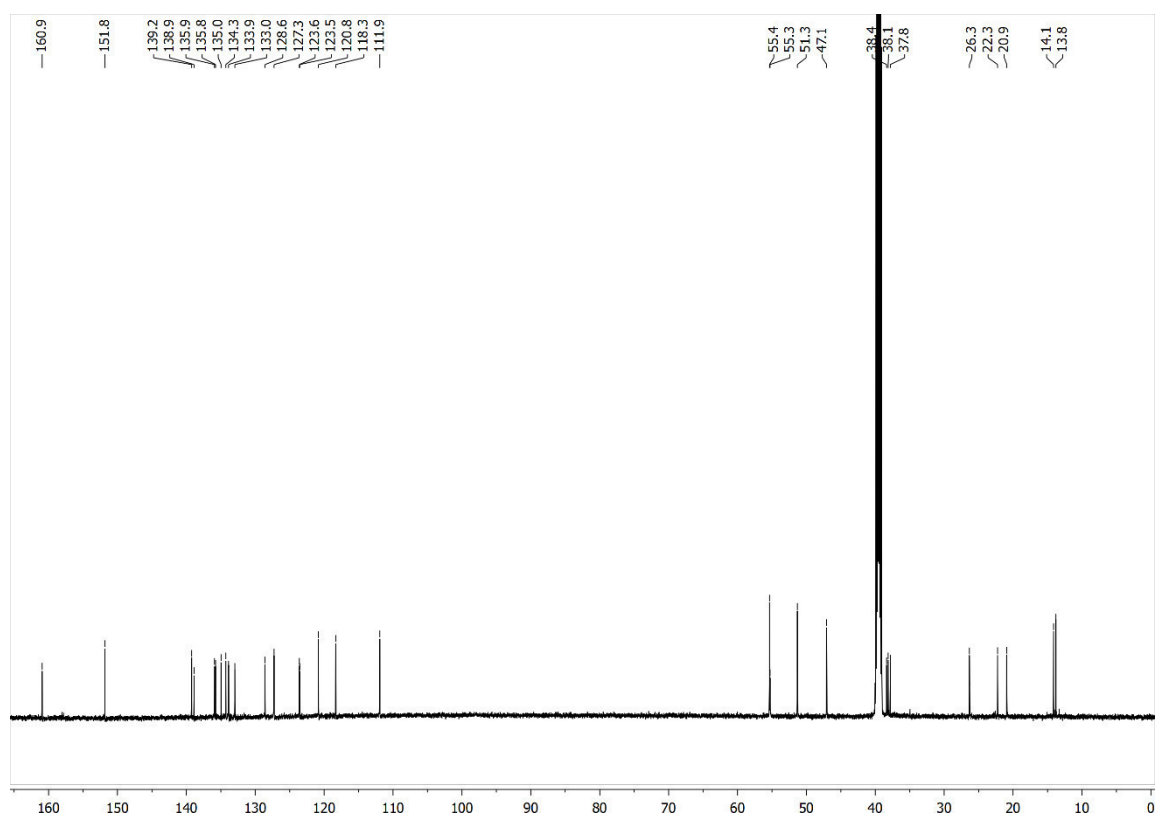
$^1\text{H-NMR}$ (400 MHz, $\text{D}_6\text{-DMSO}$) for compound **25**:



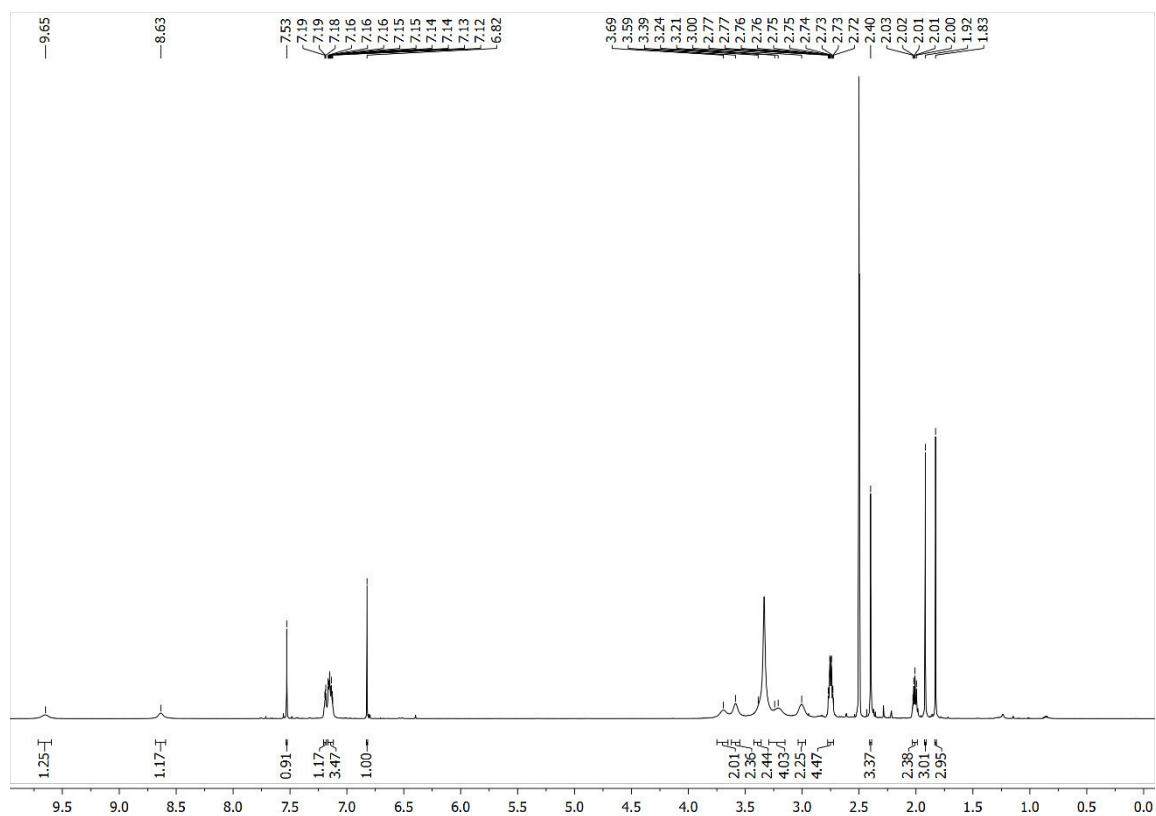
$^{13}\text{C-NMR}$ (151 MHz, $\text{D}_6\text{-DMSO}$) for compound **25**:



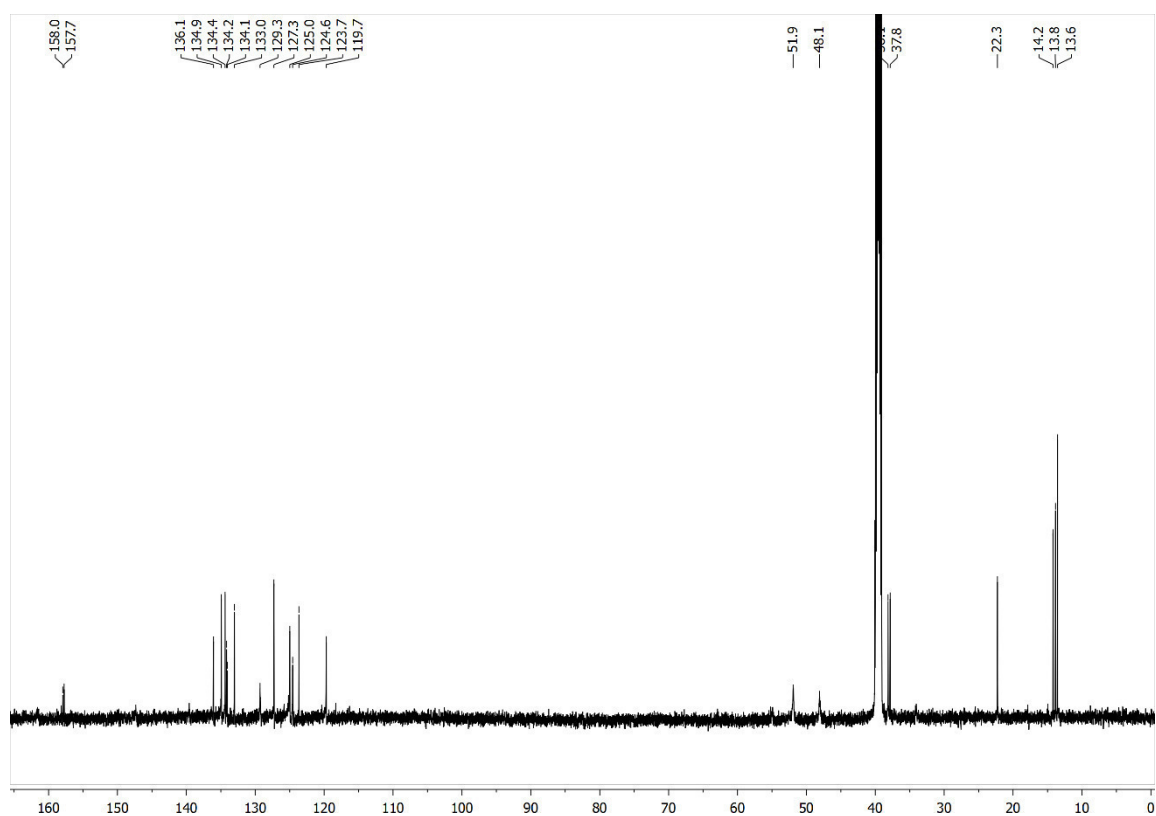
$^1\text{H-NMR}$ (600 MHz, $\text{D}_6\text{-DMSO}$) for compound **26**: $^{13}\text{C-NMR}$ (151 MHz, $\text{D}_6\text{-DMSO}$) for compound **26**:

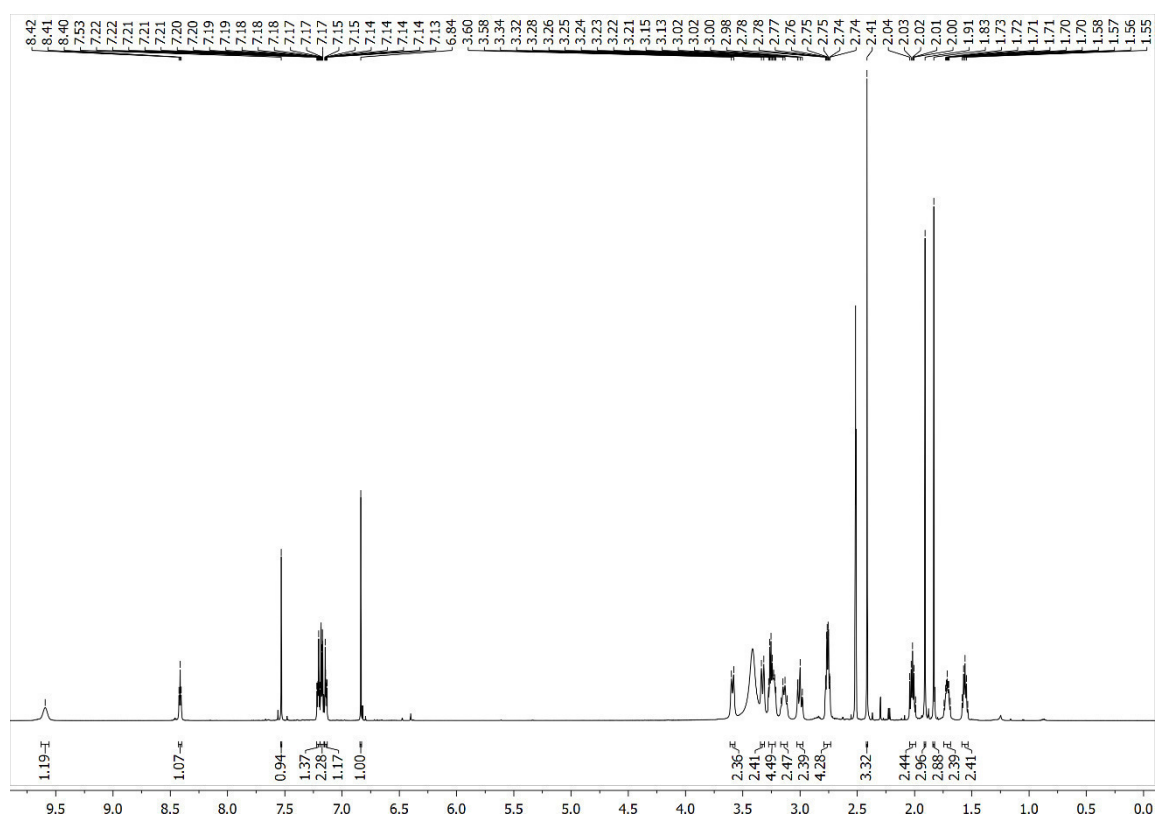
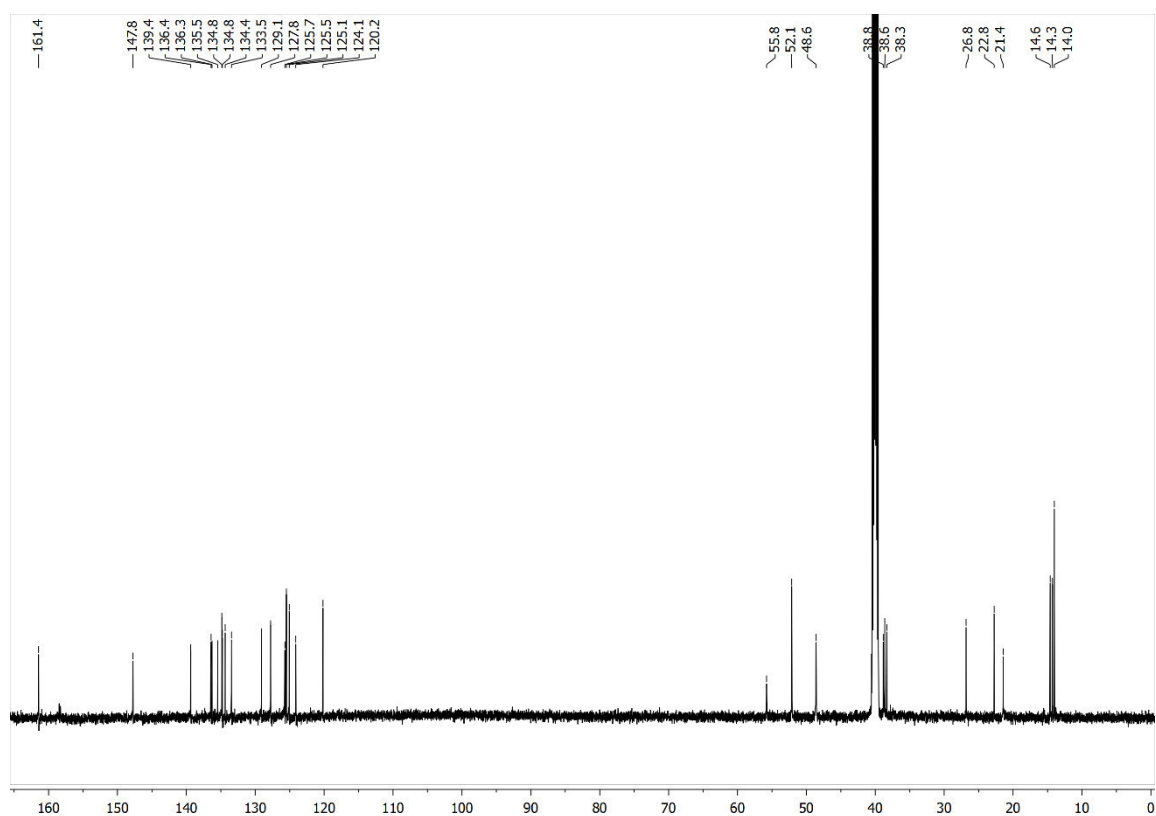
$^1\text{H-NMR}$ (600 MHz, $\text{D}_6\text{-DMSO}$) for compound **27**: $^{13}\text{C-NMR}$ (151 MHz, $\text{D}_6\text{-DMSO}$) for compound **27**:

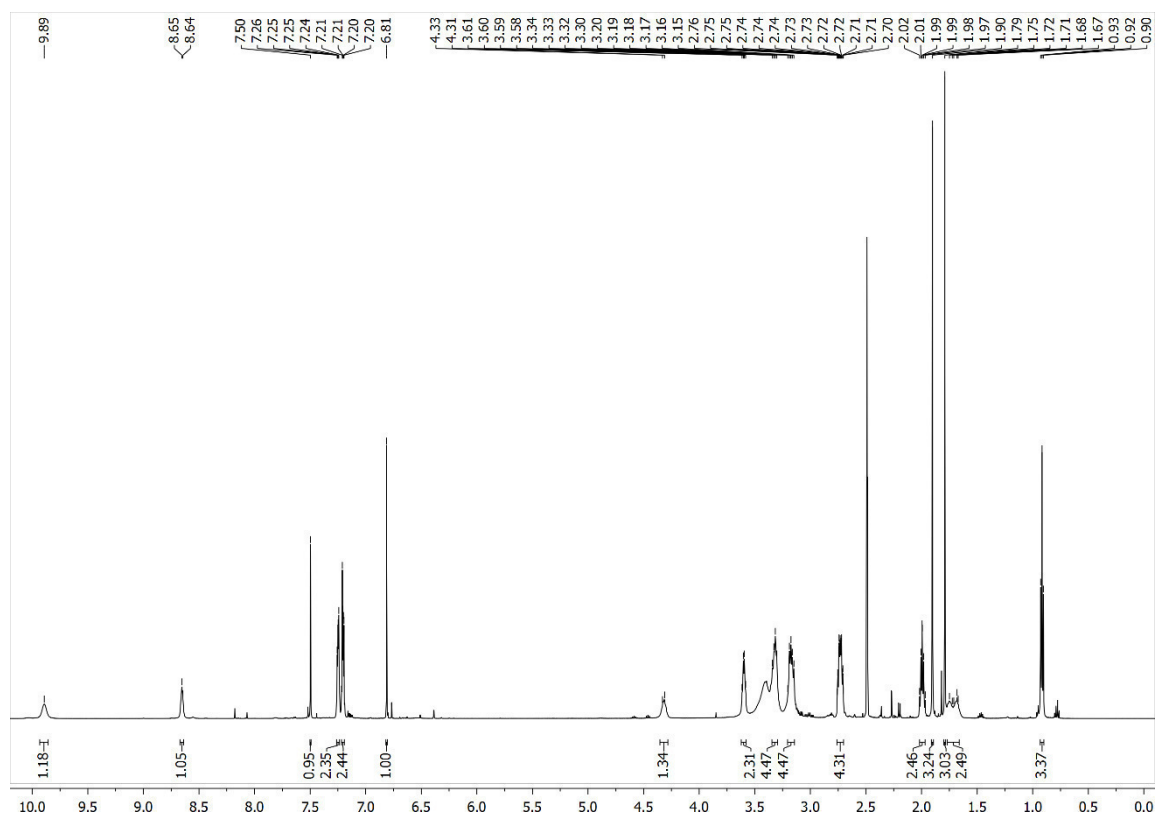
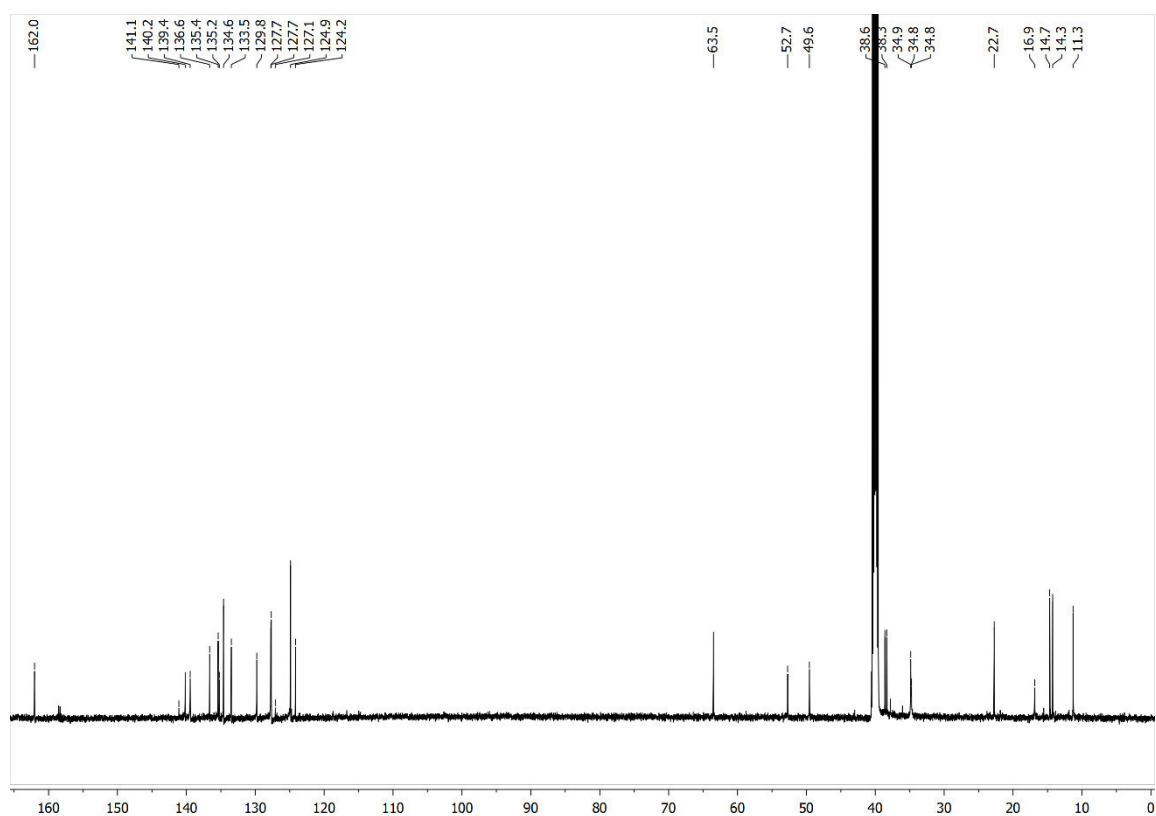
$^1\text{H-NMR}$ (600 MHz, $\text{D}_6\text{-DMSO}$) for compound **28**:

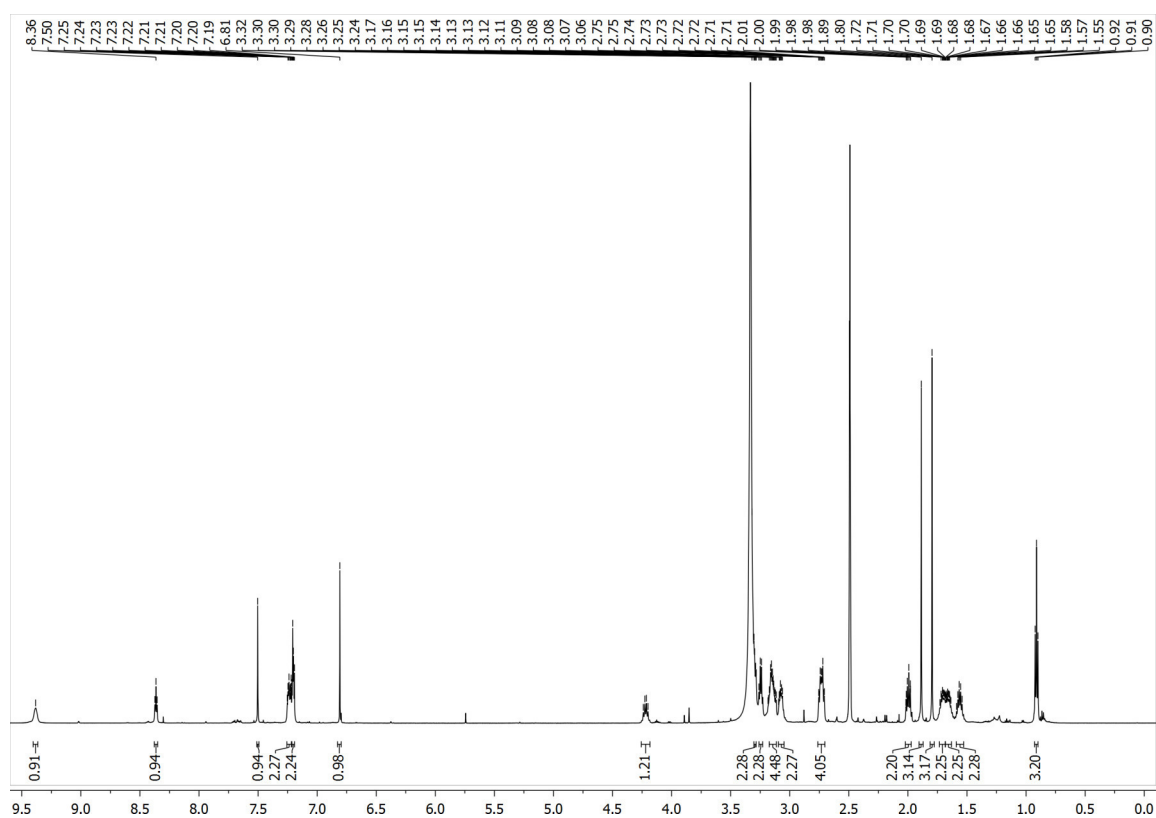
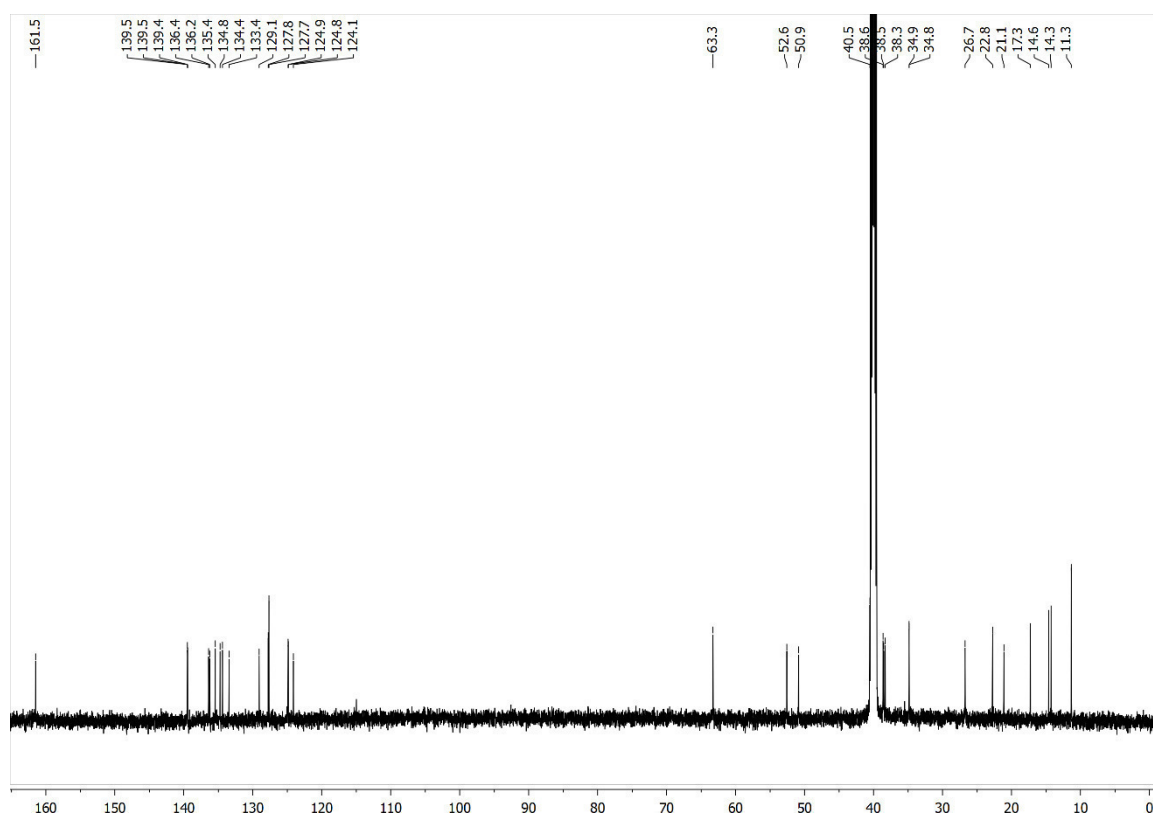


$^{13}\text{C-NMR}$ (151 MHz, $\text{D}_6\text{-DMSO}$) for compound **28**:

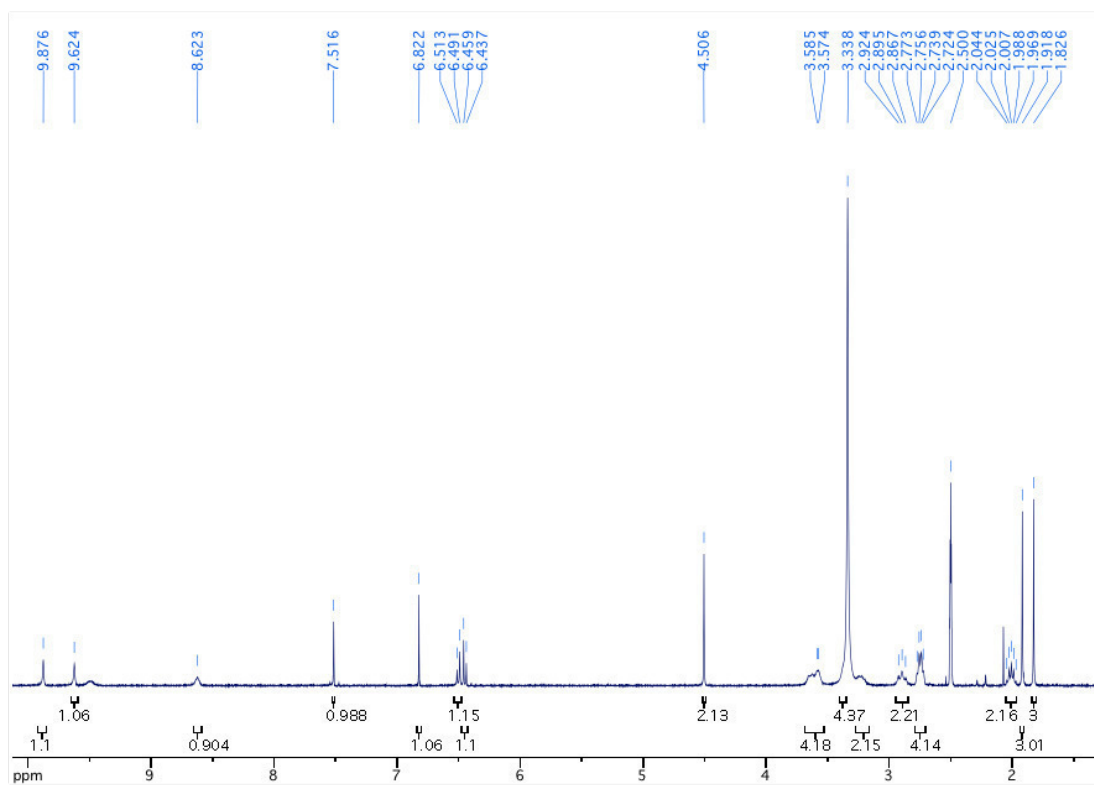


$^1\text{H-NMR}$ (600 MHz, $\text{D}_6\text{-DMSO}$) for compound **29**: $^{13}\text{C-NMR}$ (151 MHz, $\text{D}_6\text{-DMSO}$) for compound **29**:

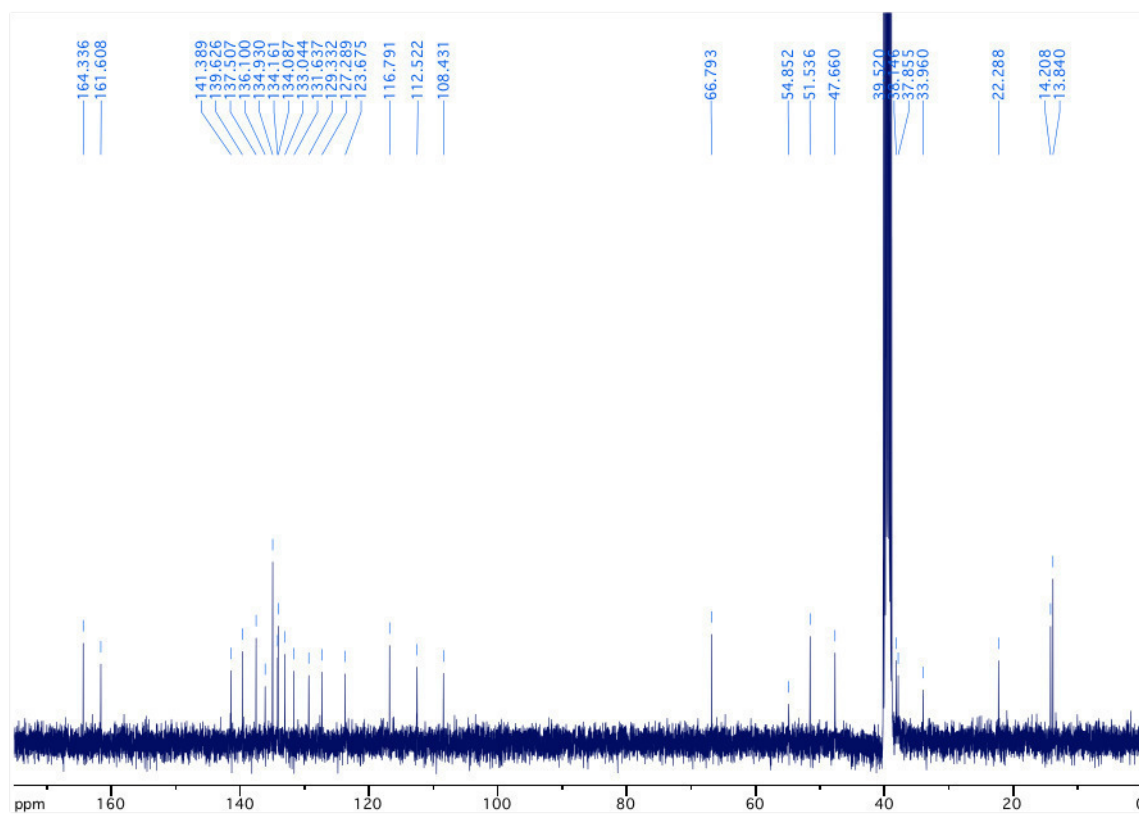
$^1\text{H-NMR}$ (600 MHz, $\text{D}_6\text{-DMSO}$) for compound **30**: $^{13}\text{C-NMR}$ (151 MHz, $\text{D}_6\text{-DMSO}$) for compound **30**:

$^1\text{H-NMR}$ (600 MHz, $\text{D}_6\text{-DMSO}$) for compound **31**: $^{13}\text{C-NMR}$ (151 MHz, $\text{D}_6\text{-DMSO}$) for compound **31**:

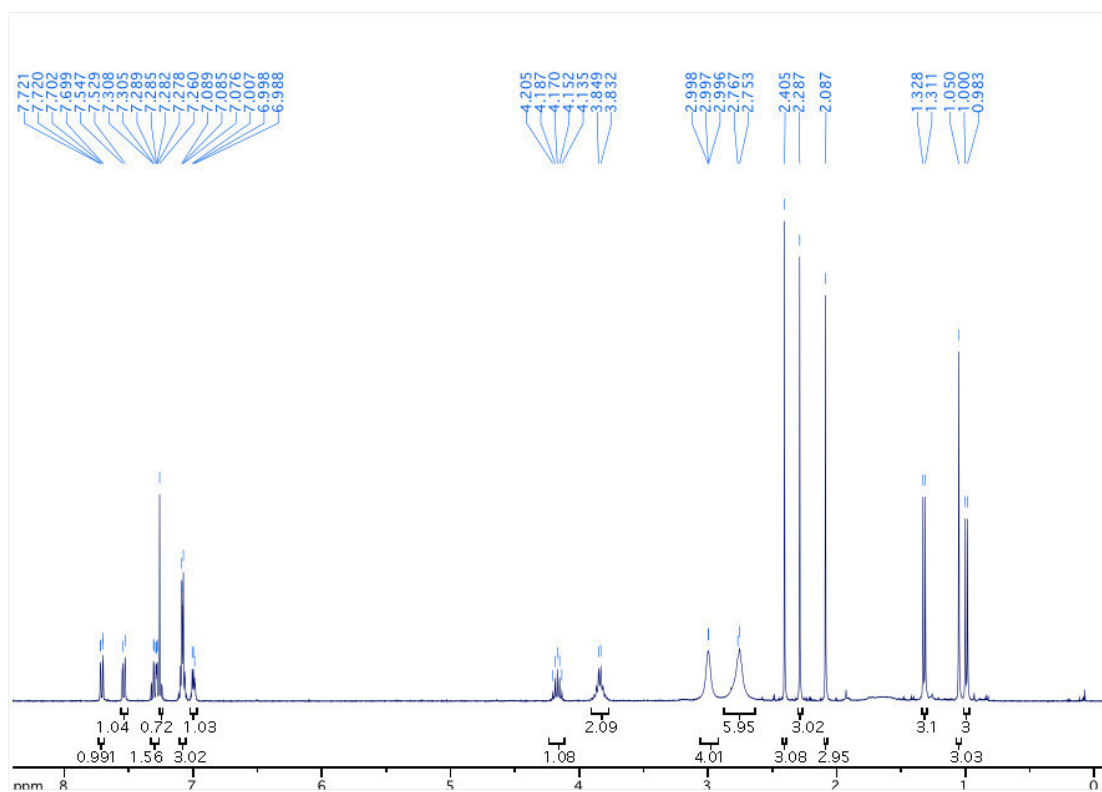
$^1\text{H-NMR}$ (400 MHz, $\text{D}_6\text{-DMSO}$) for compound **32**:



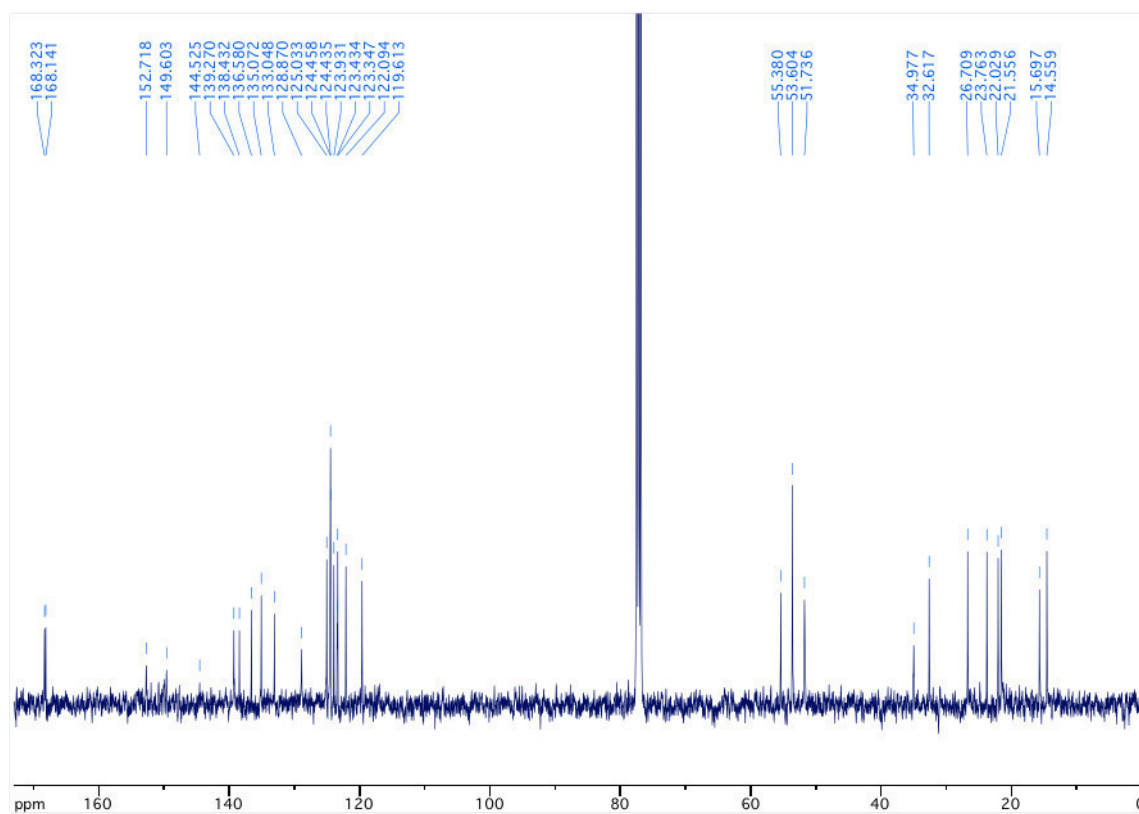
$^{13}\text{C-NMR}$ (151 MHz, $\text{D}_6\text{-DMSO}$) for compound **32**:



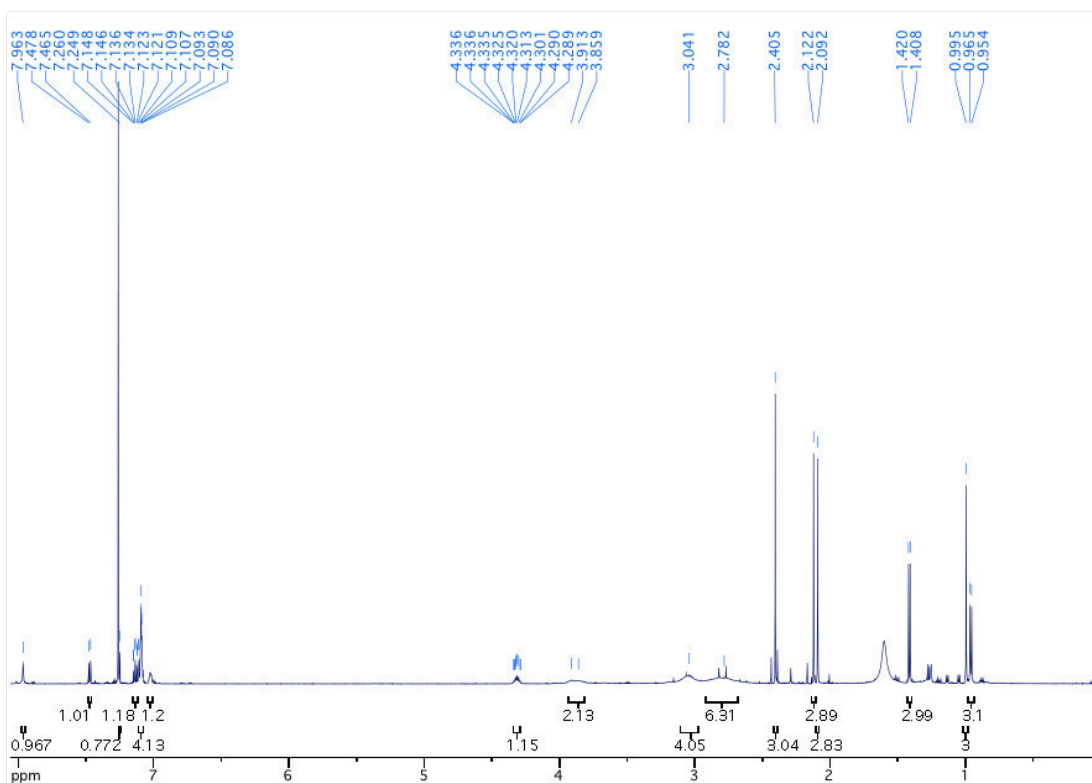
$^1\text{H-NMR}$ (400 MHz, CDCl_3) for compound **43**:



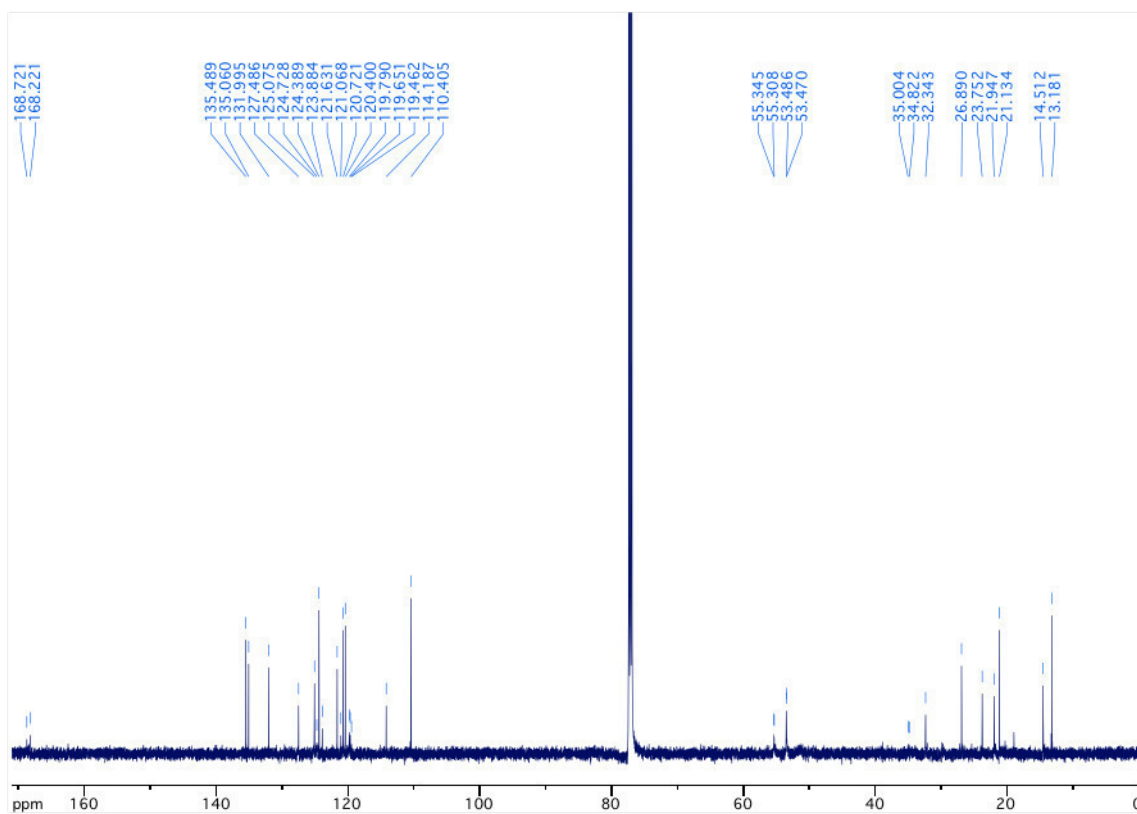
$^{13}\text{C-NMR}$ (101 MHz, CDCl_3) for compound **43**:



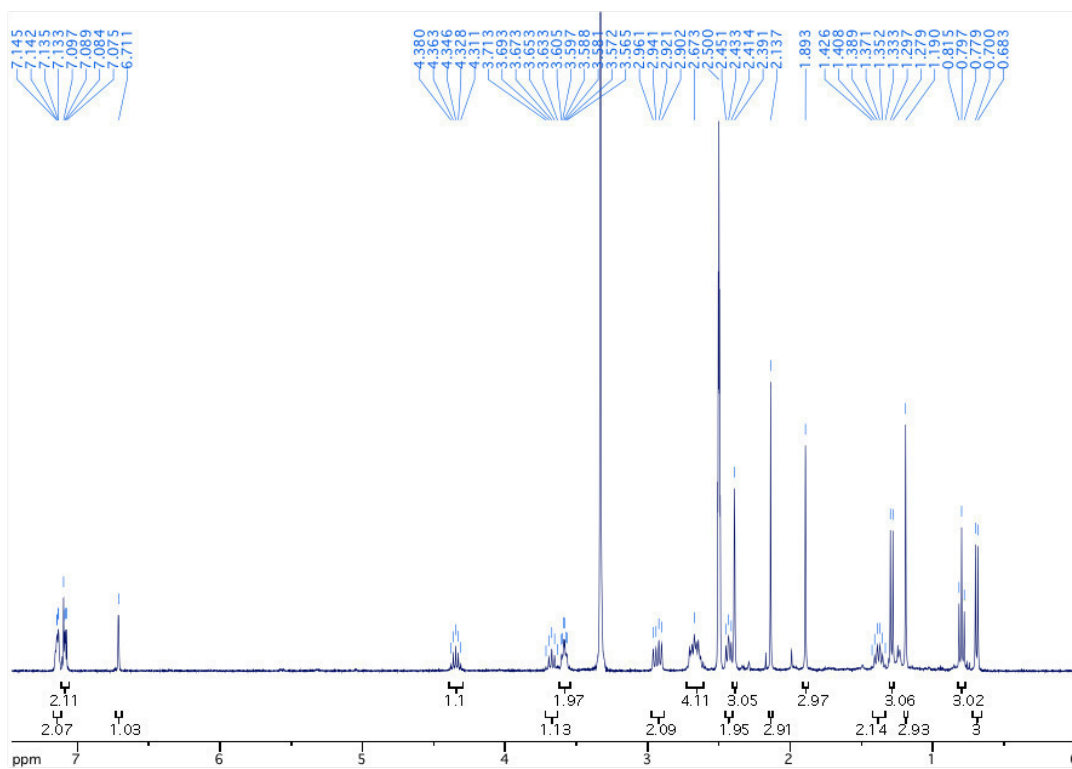
$^1\text{H-NMR}$ (600 MHz, CDCl_3) for compound **45**:



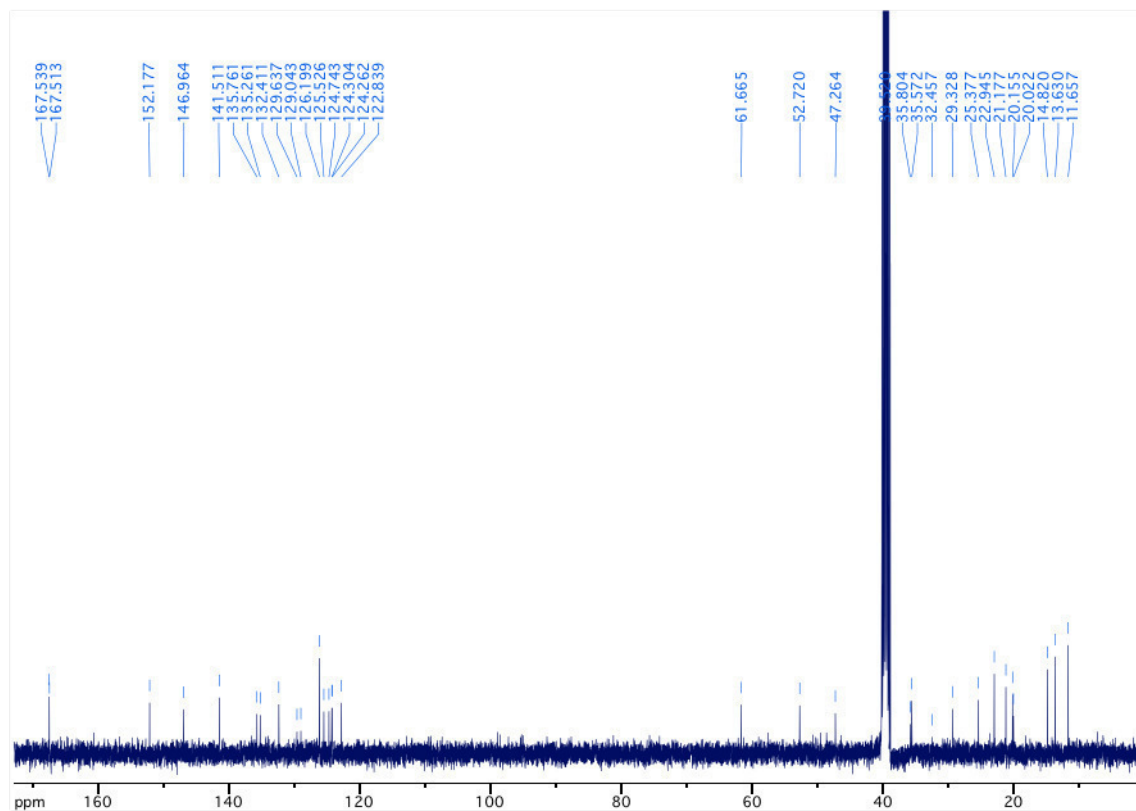
$^{13}\text{C-NMR}$ (151 MHz, CDCl_3) for compound **45**:



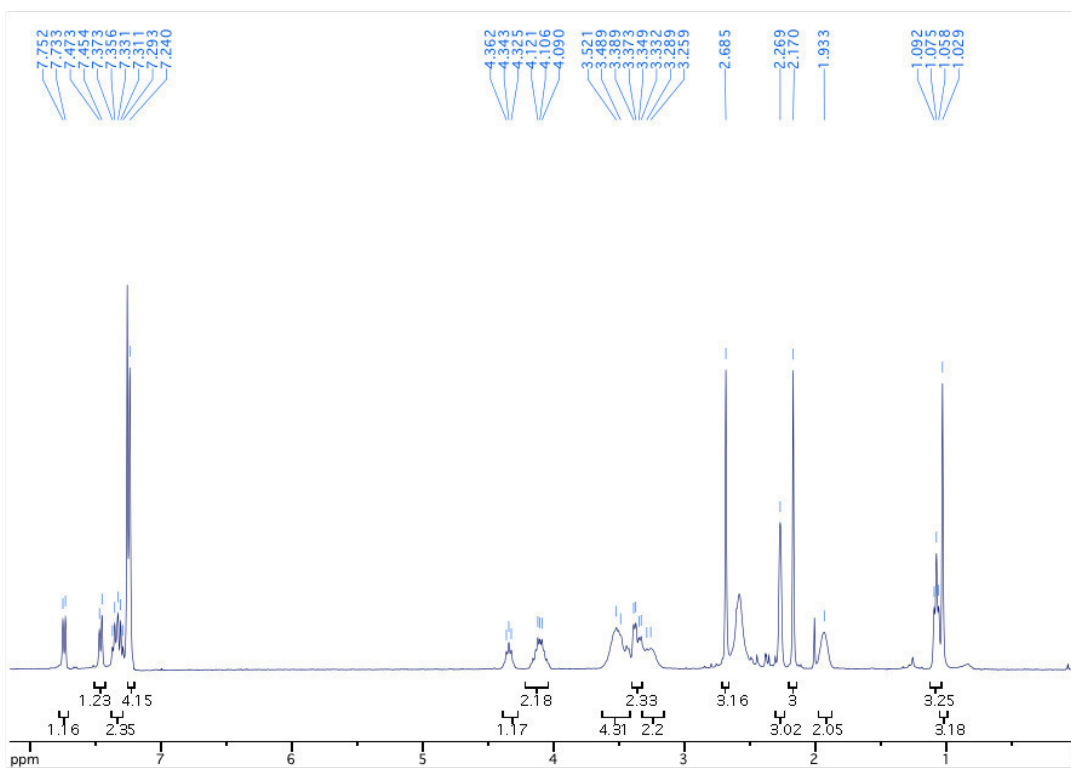
$^1\text{H-NMR}$ (400 MHz, $\text{D}_6\text{-DMSO}$) for compound **46**:



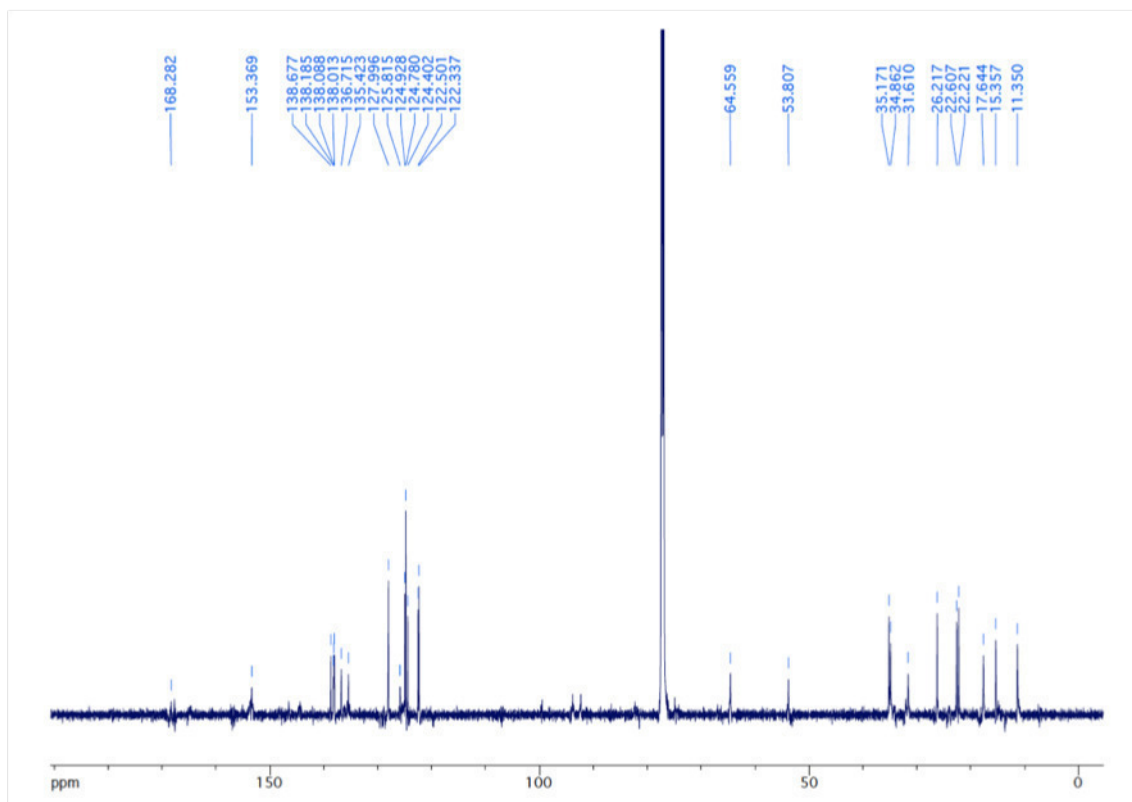
$^{13}\text{C-NMR}$ (151 MHz, $\text{D}_6\text{-DMSO}$) for compound **46**:



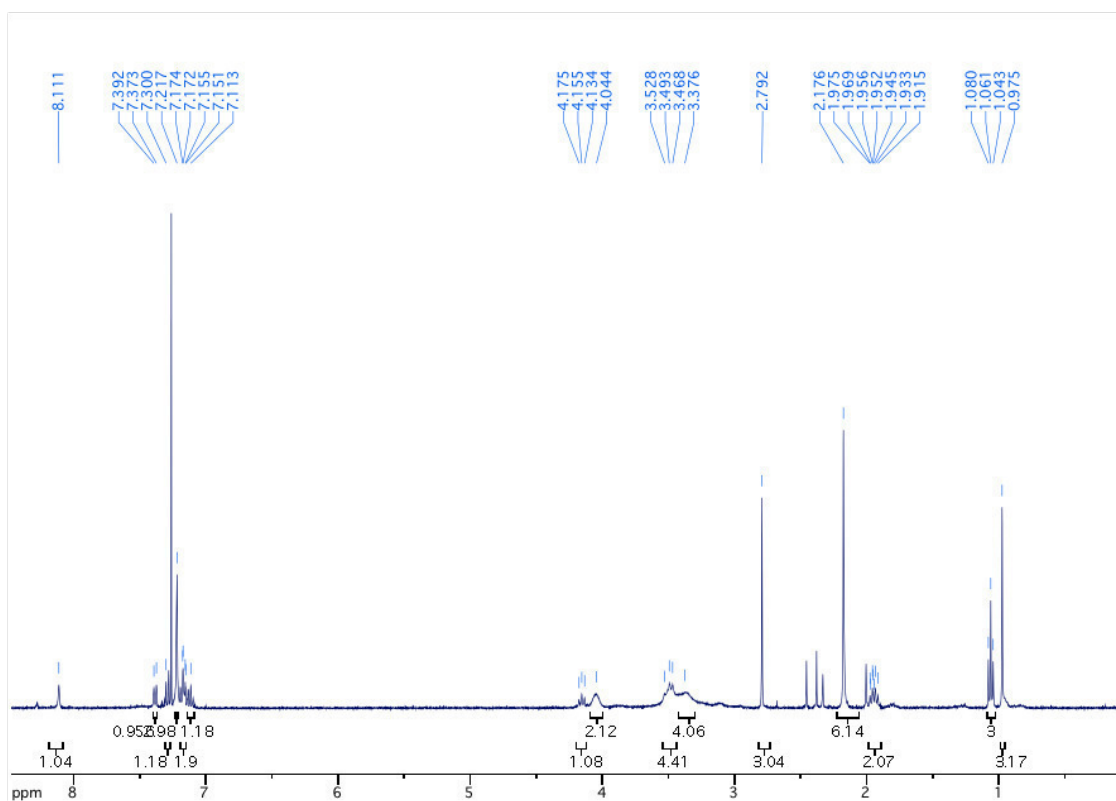
$^1\text{H-NMR}$ (400 MHz, CDCl_3) for compound **48**:



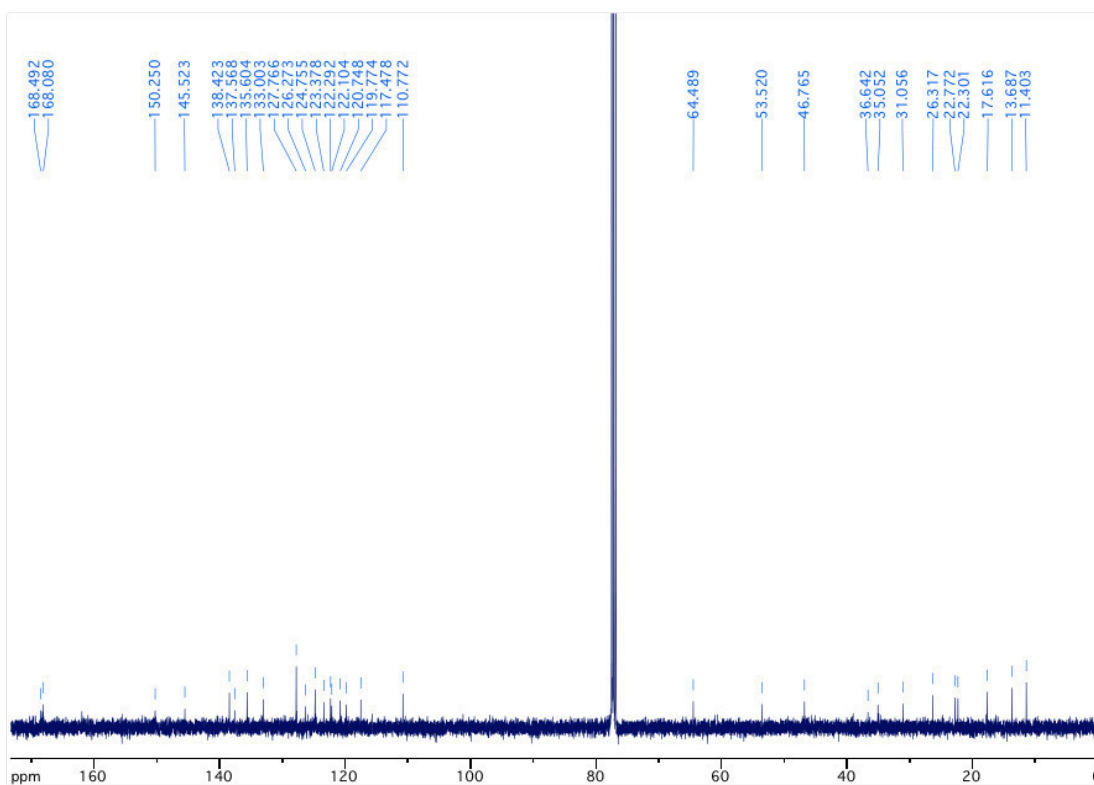
$^{13}\text{C-NMR}$ (151 MHz, CDCl_3) for compound **48**:



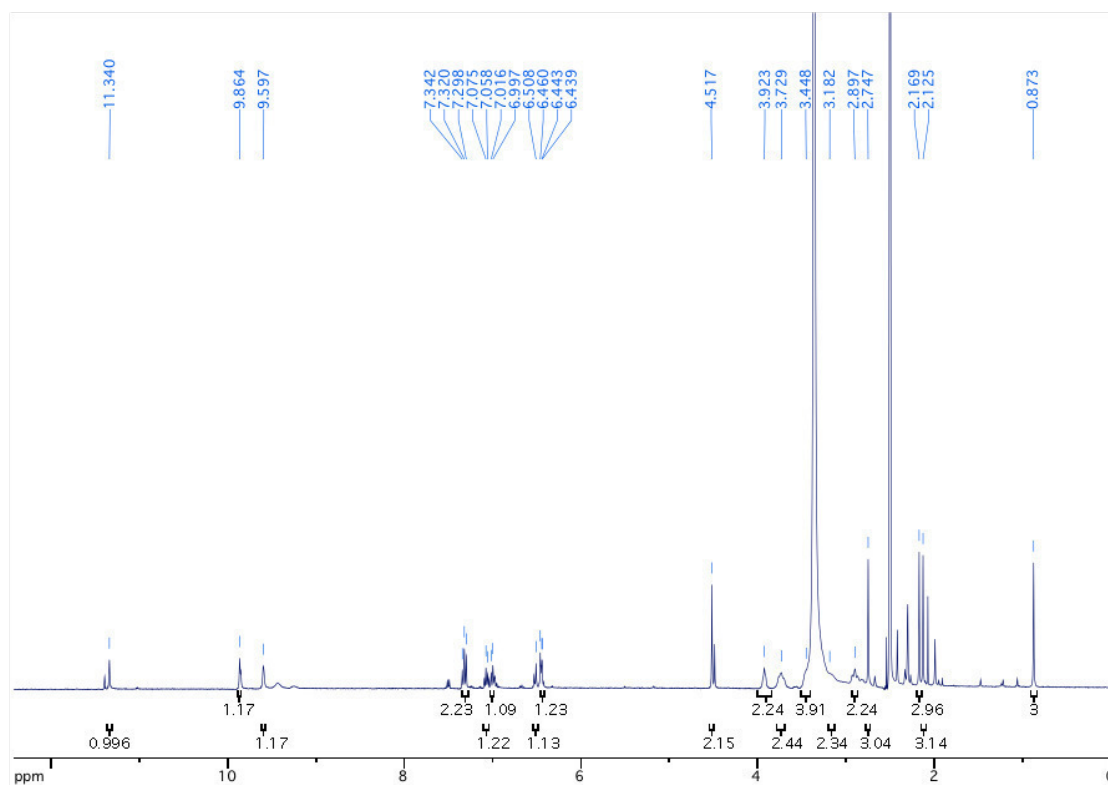
$^1\text{H-NMR}$ (400 MHz, CDCl_3) for compound **50**:



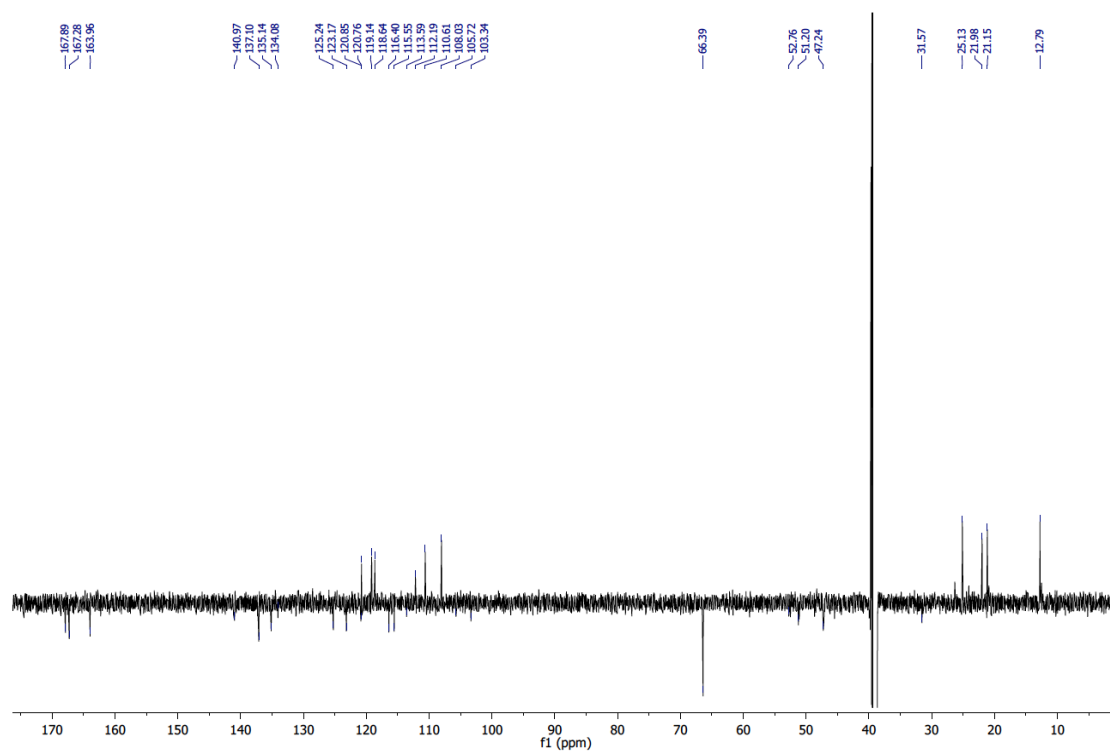
$^{13}\text{C-NMR}$ (151 MHz, CDCl_3) for compound **50**:



$^1\text{H-NMR}$ (600 MHz, $\text{D}_6\text{-DMSO}$) for compound **52**:



$^{13}\text{C-NMR}$ (151 MHz, $\text{D}_6\text{-DMSO}$) for compound **52**:



CHAPTER 2

2. Photochromic Peptidic NPY Y₄-Receptor Ligands

This chapter has been published as:

D. Lachmann, A. Konienzcy, M. Keller, B. König, *Org. Biomol. Chem.* **2019**, *17*, 2467

DL designed and synthesized all compounds, performed the corresponding photochemical measurements and wrote the manuscript. AK and MK did the biological investigations. BK supervised the project and is corresponding author.

1. Introduction

G protein coupled receptors (GPCRs) are known to bind a broad variety of ligands, among them peptides and small proteins acting as hormones, neurotransmitters or neuromodulators, and are therefore interesting drug targets.¹ Neuropeptide Y (NPY) is a 36-amino acid peptide, which is responsible for a variety of physiological functions in central and peripheral biological processes. In humans, NPY binds to at least four different GPCRs, the NPY receptor subtypes Y₁, Y₂, Y₄ and Y₅.² Recently, crystal structures of the human Y₁ receptor, bound to antagonists, were reported, allowing a better structure-based development of NPY receptor-addressing ligands.³ The Y₄R is considered to play an important role, for example, in the suppression of food intake and the regulation of energy metabolism.^{4,5} The primary natural ligand of the Y₄R is pancreatic polypeptide (PP), a peptide homologue of NPY, which exhibits higher Y₄R affinity compared to NPY.⁶ Detailed investigations of the physiological function of the Y₄R require selective Y₄R agonists and antagonists as pharmacological tools. Whereas several Y₄R agonists have been reported, Y₄R antagonists are lacking. Highly potent, dimeric peptidic NPY Y₄ receptor agonists, comprising two pentapeptides connected by an aliphatic linker (e.g. compound **1**, cf. **Figure 1**), were described to exhibit considerably higher Y₄R affinity (> 100fold) compared to the respective monomeric pentapeptide,^{2,7,8} revealing a contribution of both peptide moieties to Y₄R binding. Modifications of the pentapeptide moiety of the dimeric ligands, e.g. by introducing aza-amino acids, resulted in a decrease in Y₄R affinity.⁸ Aiming at a better understanding of structural requirements on high-affinity Y₄R agonists such as **1**, we replaced the highly flexible aliphatic linker in **1** by considerably less flexible moieties. For this purpose, we prepared the dimeric peptides **2-5** containing photochromic moieties (azobenzene, azopyrazole, dithienylethene (DTE) and fulgimide, respectively) instead of the suberyl linker in **1** (**Figure 1**).

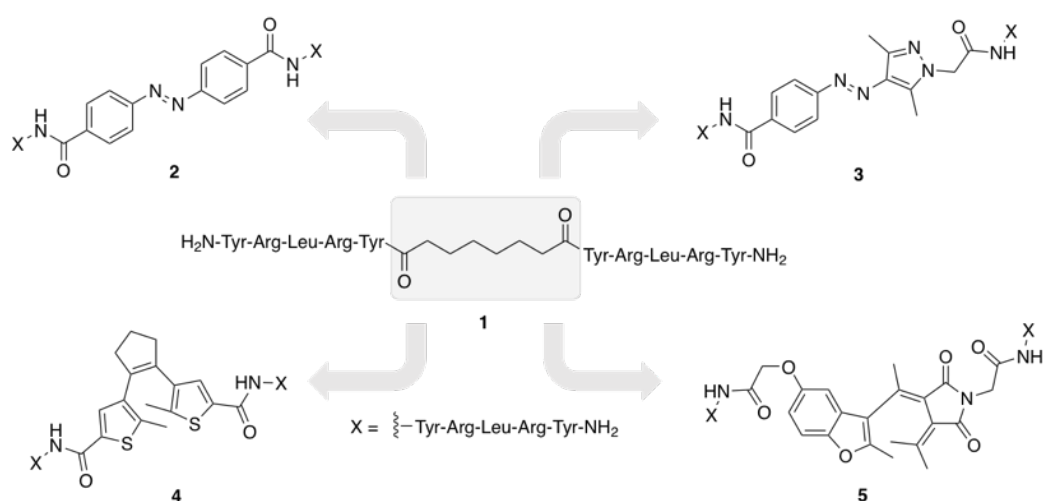


Figure 1. Schematic presentation of the rationale of the present study: replacement of the central suberyl moiety in **1** leads to four different photochromic peptidic Y₄R ligands (azobenzene **2**, azopyrazole **3**, dithienylethene **4** and fulgimide **5**).

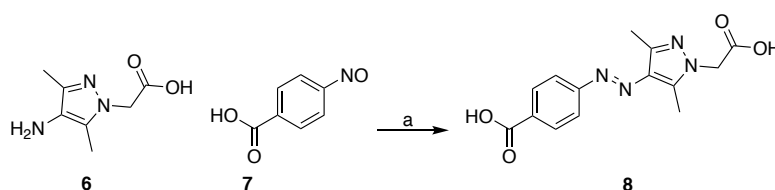
Besides exhibiting a high degree of rigidity, the photochromic scaffolds in **2-5** allow for two isomeric forms of **2-5**, which are accessible by irradiation with light: whereas the non-thermally stable azobenzene- and azopyrazole-type photochromic scaffolds account for changes in spatial orientation (*Z* vs. *E*), the thermally stable DTE and fulgimide structures enable, in particular, changes in flexibility/rigidity (open vs. closed). In addition, photochromic receptor ligands harbor the potential of switching between different modes of actions, i.e. between agonism and antagonism.^{9,10} Compounds **2-5** were characterized with respect to their photochemical properties as well as in terms of Y₄R affinity and agonism.

2. Discussion

A typical strategy towards light-switchable peptides is the incorporation of azobenzenes^{11,12} or dithienylethenes¹³ into the peptide backbone or side chains. However, these chromophores show limitation in their photophysical properties. Typically, azobenzenes do not fully interconvert to one isomer in their photostationary states and *Z*-isomers are thermally not stable.¹⁴ Photoisomers of dithienylethenes are thermally stable, but photodegradation may occur during isomerization.¹⁰ Azopyrazoles or fulgimides may overcome these limitations, but have so far not been used as photochromic moieties to modify peptides.

2.1 Synthesis

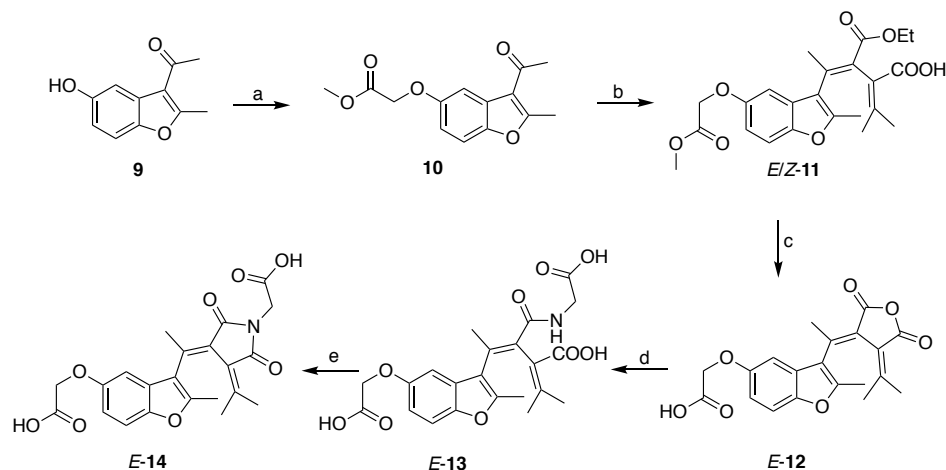
The dicarboxylic acid derivatives of the respective photochromic scaffolds were synthesized in order to use both carboxy moieties for peptide coupling. The azopyrazole precursor **8** was obtained by a Mills reaction of the nitroso compound **7** and the aminopyrazole **6** (**Scheme 1**).



Scheme 1. Synthesis of the azopyrazole precursor **8**. (a) Pyridine, NaOH, 2 h, 80 °C, 12%.

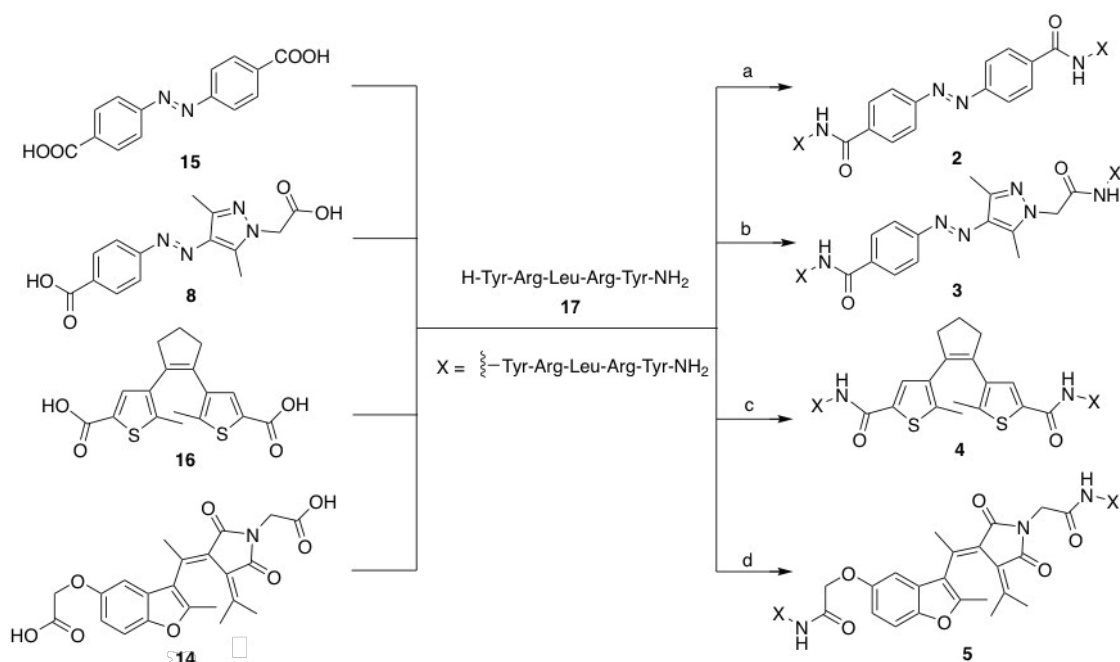
The benzofuryl core **9** was synthesized in a Nenitzescu type reaction, following literature procedures.¹⁵ Substitution of deprotonated compound **9** with methyl-2-bromoacetate gave precursor **10** in good yields. The heteroaromatic ketone **10** was used in a Stobbe condensation to form the monoesters *E/Z*-**11** with diethyl isopropylidene succinate and LDA as base at -78 °C. The monoesters *E/Z*-**11** were subsequently treated with KOH for saponification. Anhydride formation of the diacid gave the fulgides *E*-**12** and *Z*-**12** in a ratio of 40:60 (*Z* : *E*). Only the *E*-**12** isomer was used for further synthesis. Fulgimide precursor *E*-**14** was then

synthesized in three steps. First, ring opening of fulgide *E-12* with glycine methyl ester and subsequent saponification gave the regioisomeric succinamic acids **13**. The mixture was treated with acetic anhydride to obtain the target imide *E-14* (**Scheme 2**).



Scheme 2. Synthesis of the dicarboxy-fulgimide *E-14*. (a) Methyl-2-bromoacetate, NaH, DMF, 4 h, r.t., 83%. (b) Diethyl isopropylidenesuccinate, LDA, THF, 48 h, -78 °C → r.t. (c) KOH, H₂O, EtOH, 12 h, 70 °C; then DCC, CH₂Cl₂, 24 h, 40 °C (b-c, 5% overall yield). (d) Glycine methyl ester, DIPEA, 24 h, r.t.; then KOH, MeOH, 24 h, r.t., 83%. (e) Ac₂O, toluene, 2 h, 0 °C, 20%.

The azobenzene precursor **15** and the cyclopentene-DTE precursor **16** were synthesized according to literature reports.^{16,17} The synthesis of the pentapeptide **17** was carried out by manual solid phase supported peptide synthesis (SPPS) according to a standard protocol for Fmoc-strategy.² Every coupling step was performed twice, the pentapeptide was cleaved from the resin and the side-chain protecting groups were cleaved by TFA. Two equivalents of deprotected pentapeptide reacted with the pre-activated photochromic dicarboxylic acids to afford the respective target compounds **2-5**. The best yields for the azobenzene- **2** and azopyrazole **3**-based peptidic dimer were obtained applying PyBOB as the coupling reagent. The cyclopentene-DTE **4** and the fulgimide **5** were synthesized using HBTU or TBTU (**Scheme 3**).



Scheme 3. (a) PyBOB, HOBT, DIPEA, DMF, 24 h, r.t., 44%. (b) PyBOB, HOBT, DIPEA, DMF, 4 h, r.t., 63%. (c) HBTU, HOBT, DIPEA, DMF, 4 h, r.t., 33%. (d) TBTU, HOBT, DIPEA, DMF, 4 h, r.t., 43%.

2.2 Photophysical properties

All investigated photochromic peptidic ligands isomerize reversibly upon irradiation with UV-light and visible light in aqueous buffer in order to mimic the conditions of the biological assay. The azobenzene **2** could be toggled reversibly between its *Z*- (365 nm light) and *E*-isomer (455 nm light) in aqueous buffer and showed typical photophysical properties of an azobenzene as described in literature (**Figure 2a**).¹⁴

Azopyrazole **3** showed a light-responsive behavior, exhibiting high photostationary states (PSS) of 94% for the *E* to *Z* and 88% for the *Z* to *E* isomerization in aqueous buffer. The typically splitting of the *E*- and *Z*-isomer absorption band could be observed by UV-VIS spectroscopy measurements and is depicted in **Figure 2b**. The azobenzene **2** and arylazopyrazole **3** showed high fatigue resistance and very high thermal half-lives of 6.8 days (**2**) and 8.1 days (**3**) in aqueous buffer. It is literature known, that hydrophobic interactions between the peptide side chains and the aromatic rings provide additional free energy to stabilize the *Z*-isomer resulting in the observed long thermal half-lives in aqueous solution.¹⁸

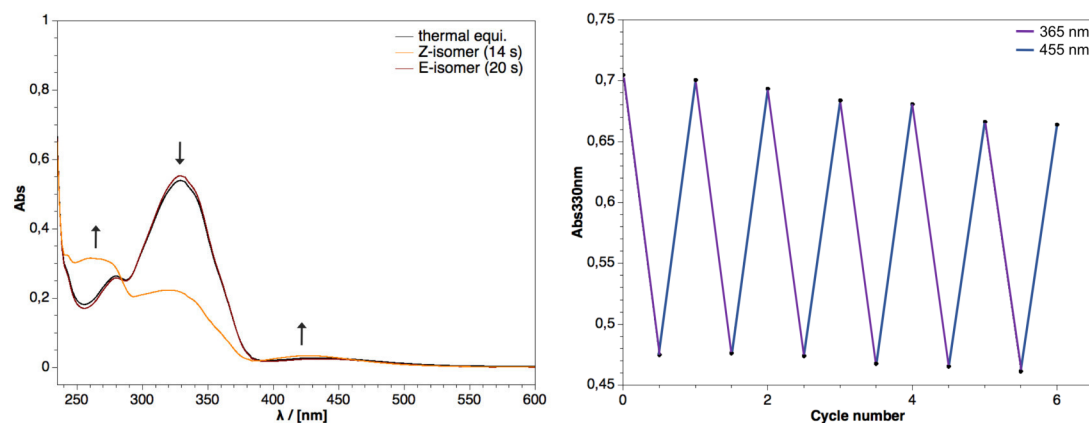
Table 1 summarizes the photophysical properties of the photochromic ligands **2** and **3**.

Table 1. Photochemical properties of azobenzene **2** and azopyrazole **3**.

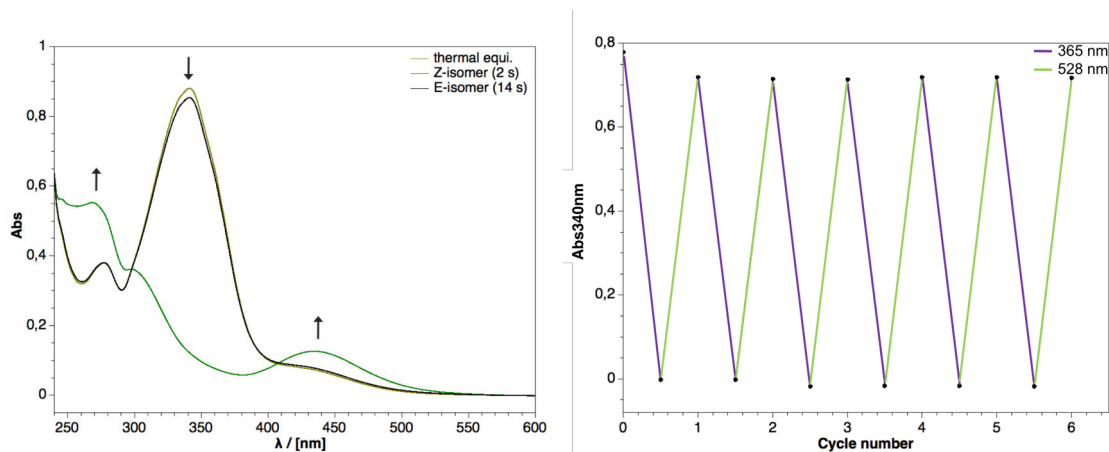
| Entry | Compd. | Solvent | λ_{\max} | | λ_{iso} [nm] | $t_{1/2}$ [d] | PSS | | QY | |
|-------|--------|-----------------------|------------------|-------------|--------------------------------|------------------|---|---|---------------------------|---------------------------|
| | | | (E) [nm] | (Z) [nm] | | | (E \rightarrow Z) ^[b] E:Z | (Z \rightarrow E) ^[b] E:Z | $\phi_{(E\rightarrow Z)}$ | $\phi_{(Z\rightarrow E)}$ |
| 1 | 2 | DMSO | 288, | 278, | 290, | 3.7 | 21:79 ^[c] | 96:4 ^[d] | 0.07 | 0.20 |
| | | | 338, | 328, | | | | | | |
| 2 | 2 | Buffer ^[a] | 282, | 278, | 281,390 | 6.8 | 32:68 ^[c] | 92:8 ^[d] | 0.06 | 0.16 |
| | | | 330, | 328, | | | | | | |
| 3 | 3 | DMSO | 351 | 278, 445 | 301, 418 | 1.1 | 5:95 ^[c] | 93:7 ^[e] | 0.65 | 0.40 |
| 4 | 3 | Buffer ^[a] | 275, | 275, | 297, | 8.1 | 6:94 ^[c] | 88:12 ^[e] | 0.15 | 0.13 |
| | | | 340 | 437 | | | | | | |

[a] Buffer: 25 mM HEPES, 2.5 mM CaCl₂, 1 mM MgCl₂, pH = 7.4, 0.4% DMSO; [b] PSS determination was done by HPLC at the appropriate isosbestic points at 15 °C; [c] Irradiation with 365 nm; [d] Irradiation with 455 nm; [e] Irradiation with 528 nm.

a)



b)



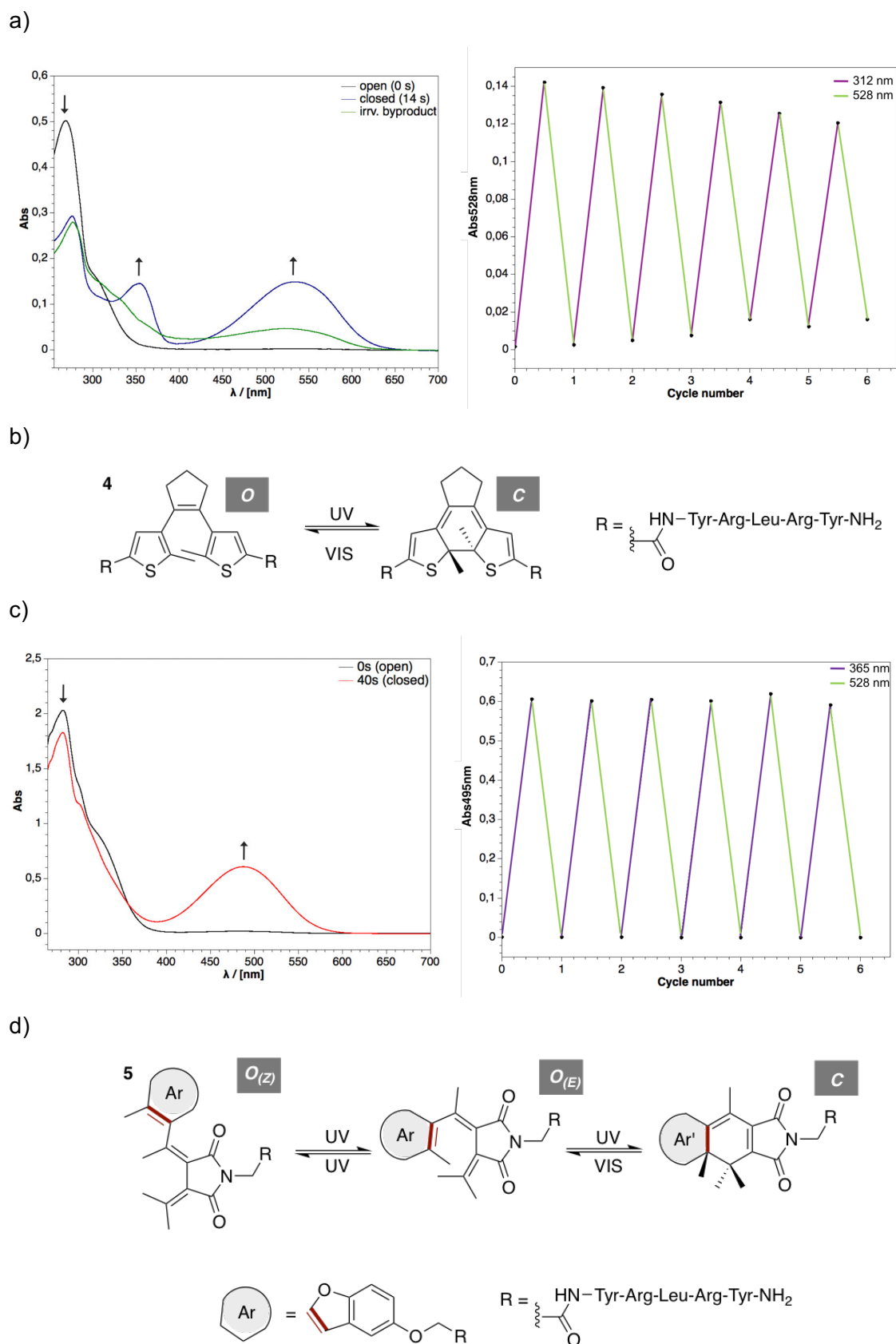


Figure 3. UV/VIS spectroscopy and cycle performance of the photochromic target ligands **4** and **5** in aqueous buffer. a) Cyclopentene-DTE **4** ($c = 20 \mu\text{M}$). b) Structure of the open (O) and closed (C) isomer of compound **4** toggling with 312 nm and 528 nm. c) Fulgimide **5** ($c = 20 \mu\text{M}$). d) Closed isomer (C) and open (O) isomers (E, Z) of fulgimide **5** switching with 365 nm and 528 nm.

Table 2. Photochemical properties of compound **4** and **5**.

| Entry | Compd. | Solvent | λ_{\max} | | Bypr. [nm] | λ_{iso} [nm] | PSS | | QY | |
|-------|--------|-----------------------|----------------------|----------------------|---------------|--------------------------------|---|--|---------------------------|---------------------------|
| | | | (<i>E</i>) [nm] | (<i>Z</i>) [nm] | | | (<i>O</i> → <i>C</i>) ^[b] O:C | (<i>C</i> → <i>O</i>) ^[b] O:C | $\phi_{(O\rightarrow C)}$ | $\phi_{(C\rightarrow O)}$ |
| 1 | 4 | DMSO | 268 | 533, 353, 276 | 277, 518 | 318 | 5:95 ^[c] | 98:2 ^[d] | 0.36 | 0.38 |
| 2 | 4 | Buffer ^[a] | 266 | 530, 350, 270 | 276, 528 | 310 | 8:92 ^[c] | 98:2 ^[d] | 0.64 | 0.27 |
| 3 | 5 | DMSO | 280 | 280, 487 | - | 356 | <i>Z</i> : <i>E</i> : <i>C</i> ^[e] 15:49:36 | <i>Z</i> : <i>E</i> : <i>C</i> ^[d] 15:85:0 | 0.17 | 0.10 |
| 4 | 5 | Buffer ^[a] | 278 | 279, 495 | - | 372 | <i>Z</i> : <i>E</i> : <i>C</i> ^[e] 16:49:35 | <i>Z</i> : <i>E</i> : <i>C</i> ^[d] 16:84:0 | 0.16 | 0.15 |

[a] Buffer: 25 mM HEPES, 2.5 mM CaCl₂, 1 mM MgCl₂, pH = 7.4, 0.4% DMSO; [b] PSS determination was done by HPLC at the appropriate isosbestic points at 25 °C; [c] Irradiation with 312 nm; [d] Irradiation with 528 nm; [e] Irradiation with 365 nm.

The photo-isomerization quantum yields of the photochromic NPY receptor ligands were determined in DMSO and aqueous buffer in a quantum yield determination setup (QYDS) and are summarized in **Table 2** and **3**.²⁰ The best results could be obtained for the *E*-*Z* isomerization of azopyrazole **3** in DMSO and the open-close reaction of the cyclopentene-DTE **4** in buffer.

2.3 Biological investigations

The photochromic peptides **2-5** were investigated with respect to their biological activities by radioligand competition binding experiments to estimate their binding affinity at the human Y₄R (for **2** and **3** additionally at the Y₁R), as well as in functional assays to study their capability of activating the Y₄R (for competition binding curves and concentration-effect curves see **Figures S7** and **S9-S11**, Supporting Information). The dissociation constants (*K_i* values) of *E*/*Z*-**2**, *E*/*Z*-**3**, *O*/*C*-**4** and *O*(*E*)/*C*-**5**, obtained from Y₄R binding studies, were comparable to that of the reference peptide **1** (**1**: *K_i* = 3.5 nM², **2-5**: *K_i* = 0.9-13 nM, **Table 3**), showing that the replacement of the suberyl moiety in **1** by various photochromic scaffolds (**8**, **12**, **15**, **16**) was well tolerated with respect to Y₄R binding. Differences in Y₄R affinity between *Z*- and *E*-isomers and *C*- and *O*-isomers were marginal (**Table 3**). These data suggest that the type of the linker (rigid vs. flexible, cyclic vs. acyclic), connecting the two pentapeptides, has little impact on the interaction of these ligands with the Y₄R. Presumably, one pentapeptide moiety, mimicking the C-terminus of the endogenous receptor ligands (hPP, NPY)^{3,21} occupies the orthosteric binding pocket of the Y₄R, while the second pentapeptidyl residue undergoes additional (allosteric)

interactions at the surface of the receptor. The flexibility of the peptide moieties possibly compensates reduced flexibility of the linker in **2-5**. Y₁R binding studies, exemplarily performed for *E/Z-2* and *E/Z-3*, revealed lower Y₁R affinities ($K_i > 400$ nM) compared to Y₄R affinities ($K_i < 5$ nM) (**Table 3**).

Table 3. NPY Y₄ receptor binding data (K_i values) and agonistic activities (EC_{50} values and intrinsic activities α) of hPP, **1**, *E/Z-2*, *E/Z-3*, *O/C-4* and *O_(E)/C-5*.

| Compd. | K_i Y ₄ R [nM] ^[a] | β -Arrestin 1 ^[b] | | β -Arrestin 2 ^[b] | | Aequorin ^[c] | | K_i Y ₁ R [nM] ^[d] |
|--------------------------|--|------------------------------------|----------|------------------------------------|----------|-------------------------|---------------------|--|
| | | EC_{50} [nM] | α | EC_{50} [nM] | α | EC_{50} [nM] | α | |
| hPP | 0.65 ± 0.13 | 2.2 ± 0.1 | 1 | 4.3 ± 0.3 | 1 | 9.7 ± 0.4 | 1 | 440 ± 74 ^[e] |
| 1 | 3.5 ± 0.6 ^[f] | n.d. | n.d. | n.d. | n.d. | 49 ± 13 ^[f] | 0.73 ^[f] | 720 ± 100 ^[f] |
| <i>E-2</i> | 4.4 ± 1.7 | 390 ± 90 | 0.78 | 470 ± 50 | 0.81 | 410 ± 60 | 0.72 | 1930 ± 370 |
| <i>Z-2</i> | 2.0 ± 0.4 | 270 ± 50 | 0.81 | 990 ± 120 | 0.78 | 290 ± 70 | 0.70 | 1550 ± 250 |
| <i>E-3</i> | 1.8 ± 0.1 | 250 ± 40 | 0.81 | 980 ± 250 | 0.80 | 150 ± 60 | 0.60 | 990 ± 250 |
| <i>Z-3</i> | 1.2 ± 0.1 | 180 ± 20 | 0.80 | 630 ± 180 | 0.71 | 800 ± 230 | 0.74 | 440 ± 220 |
| <i>O-4</i> | 6.9 ± 0.5 | 720 ± 30 | 0.66 | 100 ± 10 | 0.70 | 490 ± 190 | 0.60 | n.d. |
| <i>C-4</i> | 13 ± 4 | 830 ± 20 | 0.66 | 210 ± 60 | 0.68 | 1010 ± 310 | 0.66 | n.d. |
| <i>O_(E)-5</i> | 0.9 ± 0.1 | 700 ± 110 | 0.58 | 270 ± 40 | 0.63 | 670 ± 210 | 0.67 | n.d. |
| <i>C-5</i> | 1.7 ± 0.3 | 760 ± 130 | 0.54 | 440 ± 80 | 0.66 | 830 ± 120 | 0.77 | n.d. |

[a] Dissociation constant determined by competition binding with [³H]UR-KK200 at CHO-hY₄R-mtAEQ-G_{q15} cells. [b] Agonistic potencies (EC_{50}) and intrinsic activities (α) relative to 1 μ M hPP ($\alpha = 1$) determined in a β -arrestin 1/2 recruitment assay at HEK293T-ARRB1-Y₄R or HEK293T-ARRB2-Y₄R cells. [c] Agonistic potencies (EC_{50}) and intrinsic activities (α) relative to 1 μ M hPP ($\alpha = 1$) determined in a Ca²⁺-aequorin assay at CHO-hY₄R-mtAEQ-G_{q15} cells. [d] Dissociation constant determined by competition binding with [³H]UR-MK299 at SK-N-MC neuroblastoma cells. [e] Berlicki *et al.*² [f] Kuhn *et al.*² Data represent mean values ± SEM (K_i , EC_{50}) or mean values (α) from three or four experiments performed in triplicate.

In order to investigate whether the photochromic peptides **2-5** are Y₄R agonists, partial agonists or even antagonists, **2-5** were subjected to different functional assays measuring G-protein mediated signaling²³ (Ca²⁺-aequorin assay²⁴) or coupling of the receptor to arrestins²³ (β -arrestin 1 and 2 recruitment assay²⁵). As both assay types require an optical readout (measurement of bioluminescence), control experiments were performed with the physiological agonist hPP in the absence and presence of the photochromic scaffolds **8**, **14**, **15** and **16** at a concentration of 10 μ M. As demonstrated in **Figure S8** (Supporting Information) compounds **8**, **14**, **15** and **16** did not affect the assay readout. Like reference peptide **1** in the aequorin assay,² the photochromic Y₄R ligands *E/Z-2*, *E/Z-3*, *O/C-4* and *O_(E)/C-5* proved to be partial agonists in all functional assays with efficacies (α) ranging from 0.54 to 0.81 (**Table 3**, **Figures S9-S11**, Supporting Information). The differences in Y₄R potencies (EC_{50} values) between Z- and E-isomers and C- and O-isomers were marginal (**Table 3**) as in case of Y₄R binding affinities (K_i values). One reason for the discrepancies between K_i values and EC_{50}

values is the absence or presence of sodium ions in the used buffers for binding and functional assays, respectively, as discussed previously.^{2,25}

3. Conclusion

We successfully incorporated four different photochromic scaffolds into a dimeric peptidic Y₄R ligand resulting in the first azopyrazole and fulgimide containing bioactive peptides. All compounds were soluble and reversibly switchable in aqueous buffer. The photostationary states were excellent for the azobenzene-, azopyrazole- and dithienylethene-type ligands, and, additionally, the azobenzene and azopyrazole derivatives exhibited high thermal half-lives. Binding studies at the Y₄R showed that the highly flexible aliphatic linker in **1** is not a prerequisite for high Y₄R affinity of such dimeric ligands. All photochromic derivatives of **1** proved to be partial agonist when studied in functional assays with respect to Y₄R activation (**Table 3**). As some compounds proved to be weaker partial agonists than **1** (lower intrinsic activities compared to **1** in functional assays, e.g. **O-4**, cf. **Table 3**), this study might support the development of Y₄R antagonists, i.e. ligands, which give no response when studied in the agonist mode of functional assays.

4. Experimental Section

4.1 General Conditions

Compounds **7**²⁶, **9**¹⁷, **15**¹⁵ and **16**¹⁶ were synthesized to reported procedures. Starting materials were purchased from commercial suppliers and used without any further purification. Solvents were used in p.a. quality and dried according to common procedures, if necessary. Dry argon was used as inert gas atmosphere. Thin-layer chromatography (TLC) for reaction monitoring was performed with alumina plates coated with Merck silica gel 60 F₂₅₄ (layer thickness: 0.2 mm). The TLCs were analyzed under UV-light (254 nm, 365 nm) and with a staining solution (Ninhydrine). Automated flash column chromatography was performed with Sigma Aldrich MN silica gel 60M (0.040-0.063 mm, 230-400 mesh) as stationary phase, pre-packed Biotage SNAP cartridges (HP-Sphere 25µM) or a reversed phase column (KP-C18-HS) on a Biotage Isolera One system with UV-Vis detector. NMR spectra were recorded using a *Bruker Avance 300* (¹H: 300 MHz, ¹³C: 75 MHz, T = 295 K), *Bruker Avance 400* (¹H 400.1: MHz, ¹³C: 100.6 MHz, T = 300K) or a *Bruker Avance 600* (¹H: 600 MHz, ¹³C: 151 MHz, T = 295 K) instrument. The spectra are referenced against the NMR solvent and are reported as follows: ¹H: chemical shift δ (ppm), multiplicity, integration, coupling constant (*J* in Hz). ¹³C: chemical shift δ (ppm), abbreviations: (+) = primary/tertiary, (-) = secondary, (q) = quaternary carbon. The assignment resulted from DEPT, COSY, HMBC and HSQC experiments. Mass spectra were measured with a Finnigan MAT 95, Finnigan MAT SSQ 710 A, ThermoQuest Finnigan TSQ 7000 or an Agilent Q-TOF 6540 UHD instrument. Absorption spectra were recorded on

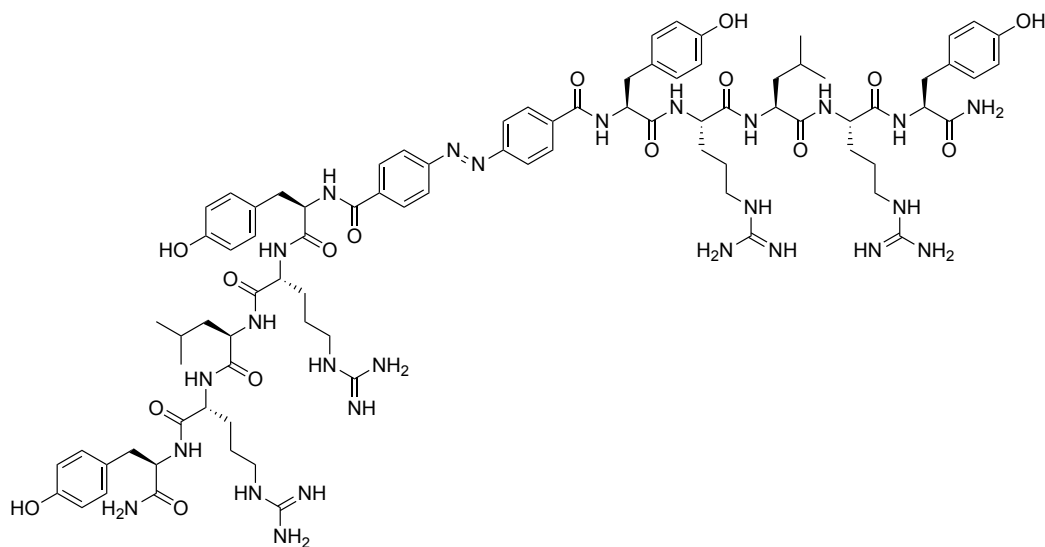
an Agilent Cary 100 Bio UV/Vis spectrophotometer in 10 mm quartz cuvettes. Preparative HPLC was performed on a *Agilent 1100 Series* (Column: *Phenomenex Luna 10*, C18, 100A, 250 x 21.2 mm, flow 20 mL/min, solvent A: H₂O [0.05 Vol% TFA], solvent B: MeCN). Photostationary states of the final compounds were measured on an *Agilent 1220 Infinity LC System* (column: *Phenomenex Luna*, 3 μ C18(2) 100A, 150 x 2.0 mm, 100 Å). All biological investigations were performed in the group of Dr. M. Keller at the pharmaceutical department of the University of Regensburg.

4.2 Synthesis procedures

General synthesis of the azo based peptides:

Dicarboxy-azobenzene **2**/-azopyrazole **3** (1.0 eq), PyBOP (2.2 eq), HOBt (2.2 eq) and DIPEA (2.0 eq) were dissolved in DMF (1 mL) for preactivation (10 min) at r.t. Pentapeptide **17** (2.0 eq) was dissolved in dry DMF (0.5 mL) and added to the mixture. After stirring for 24 h (**2**) / 4 h (**3**) at r.t., the mixture was filtered and purified by preparative HPLC (column: Luna 10, 250 x 21 mm; flow: 20 mL/min, solvent A: H₂O (0.05% TFA), solvent B: MeCN; gradient A/B: 0-15 min: 95/5, 15-20 min: 2/98).

Compound 2



C₈₆H₁₁₈N₂₆O₁₆, MW = 1772.06 g/mol, (4x TFA)

Slightly orange solid; yield: 44%. (HPLC: t_R = 7.6 min)

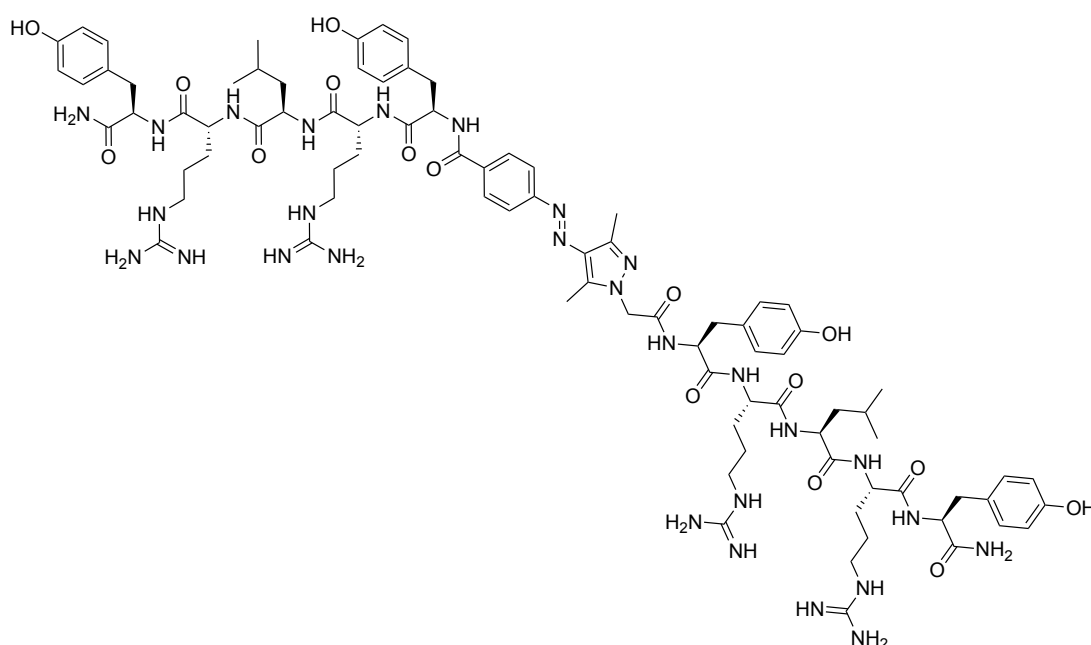
¹H-NMR (600 MHz, D₆-DMSO): δ = 0.83 (d, J = 6.5 Hz, 6H, CH₃(Leu)), 0.86 (d, J = 6.5 Hz, 6H, CH₃(Leu)), 1.38-1.47 (m, 8H, CH₂), 1.48-1.62 (m, 10H, CH₂), 1.62-1.68 (m, 2H, CH(Leu)), 2.69-2.75 (m, 2H, CH₂(Tyr)), 2.83-2.93 (m, 4H, CH₂(Tyr)), 2.95-3.02 (m, 2H, CH₂(Tyr)), 3.03-3.15 (m, 8H,

$\text{CH}_{2(\text{Arg})}$, 4.20 (q, $J = 7.0$ Hz, 2H, CH), 4.27-4.37 (m, 6H, CH), 4.60-4.70 (m, 2H, CH), 6.60-6.88 (m, 8H, $\text{CH}_{(\text{aromTyr})}$), 6.97 (d, $J = 8.6$ Hz, 4H, $\text{CH}_{(\text{aromTyr})}$), 7.16 (d, $J = 8.5$ Hz, 4H, $\text{CH}_{(\text{aromTyr})}$), 7.96 (d, $J = 8.5$ Hz, 4H, $\text{CH}_{(\text{aromazo})}$), 8.00 (d, $J = 8.6$ Hz, 4H, $\text{CH}_{(\text{aromazo})}$).

$^{13}\text{C-NMR}$ (151 MHz, $\text{D}_6\text{-DMSO}$): $\delta = 21.4$ (+), 23.1 (+), 24.2 (+), 24.9 (-), 25.1 (-), 28.9 (-), 29.0 (-), 36.2 (-), 36.8 (-), 40.5 (-), 40.8 (-), 51.0 (+), 52.3 (+), 53.9 (+), 55.5 (+), 114.9 (+), 122.5 (+), 128.3 (q), 129.4 (+), 130.8 (+), 136.5 (q), 153.3 (q), 155.8 (q), 156.7 (q), 165.6 (q), 170.8 (q), 171.1 (q), 171.7 (q), 172.0 (q), 172.7 (q).

HR-MS (ESI): calcd. for $\text{C}_{86}\text{H}_{118}\text{N}_{26}\text{O}_{16}$ ($\text{M}+3\text{H}$) $^{3+}$, $m/z = 591.3146$, found 591.3158

Compound 3



$\text{C}_{86}\text{H}_{122}\text{N}_{28}\text{O}_{16}$, MW = 1804.10 g/mol, (4x TFA)

White solid; yield: 63%. (HPLC: $t_R = 7.5$ min)

$^1\text{H-NMR}$ (600 MHz, $\text{D}_6\text{-DMSO}$): $\delta = 0.81$ -0.89 (m, 12H, $\text{CH}_3(\text{Leu})$), 1.39-1.47 (m, 4H, CH_2), 1.48-1.54 (m, 4H, CH_2), 1.58-1.78 (m, 6H, $\text{CH}_2+\text{CH}_{(\text{Leu})}$), 2.36 (s, 3H, CH_3), 2.37 (s, 3H, CH_3), 2.60-2.67 (m, 1H, CH_2), 2.68-2.74 (m, 2H, CH_2), 2.85 (dd, $J = 13.9$ Hz, 5.4 Hz, 2H, CH_2), 2.87-2.94 (m, 2H, CH_2), 2.95-2.99 (m, 1H, CH_2), 3.04-3.15 (m, 8H, $\text{CH}_2(\text{Arg})$), 4.21 (q, $J = 7.0$ Hz, 2H, CH), 4.28-4.35 (m, 6H, CH), 4.52-4.57 (m, 1H, CH), 4.61-4.66 (m, 1H, CH), 4.70-4.82 (m, 2H, $\text{CH}_2(\text{pyrazol})$), 6.61-6.67 (m, 8H, CH_{arom}), 6.97 (d, $J = 8.5$ Hz, 4H, CH_{arom}), 7.02 (d, $J = 8.5$ Hz, 2H, CH_{arom}), 7.15 (d, $J = 8.6$ Hz, 2H, CH_{arom}), 7.74-7.78 (m, 2H, CH_{arom}), 7.89-7.93 (m, 2H, CH_{arom}).

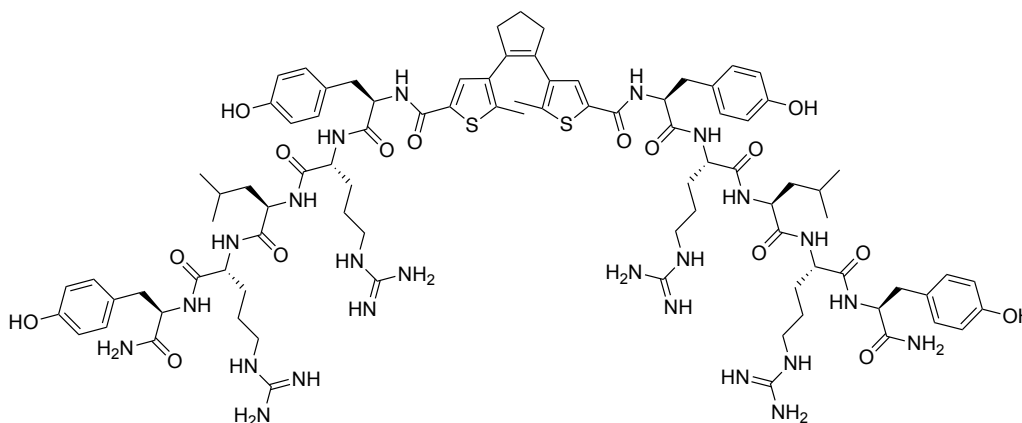
$^{13}\text{C-NMR}$ (151 MHz, $\text{D}_6\text{-DMSO}$): δ = 9.4 (+), 13.9 (+), 21.4 (+), 23.1 (+), 24.2 (+), 24.9 (-), 25.0 (-), 25.1 (-), 28.9 (-), 29.0 (-), 36.2 (-), 36.8 (-), 37.1 (-), 40.5 (-), 40.8 (-), 51.0 (+), 51.4 (-), 52.3 (+), 54.0 (+), 54.1 (+), 55.5 (+), 114.9 (+), 116.2 (q), 118.2 (q), 121.1 (+), 127.5 (q), 128.3 (q), 128.6 (+), 130.1 (+), 130.2 (q), 134.3 (q), 134.8 (q), 140.9 (q), 141.8 (q), 154.6 (q), 155.7 (q), 155.8 (q), 155.9 (q), 156.8 (q), 165.9 (q), 170.9 (q), 171.0 (q), 171.1 (q), 171.2 (q), 171.8 (q), 172.0 (q), 172.7 (q).

HR-MS (ESI): calcd. for $\text{C}_{86}\text{H}_{122}\text{N}_{28}\text{O}_{16}$ ($\text{M}+2\text{H}$) $^{2+}$, m/z = 902.4870, found 902.4880

General synthesis of the DTE/fulgimide based peptides:

Dicarboxy-fulgimide **5** or cyclopentene-DTE **4** (1.0 eq) was dissolved in dry DMF. TBTU (2.2 eq), HOBT (2.2 eq) and DIPEA (5.0 eq) were added and the mixture was stirred for 5 min at r.t. in the darkness. Pentapeptide **17** (2.0 eq) was added and the mixture was stirred at r.t. for 4 h. The reaction mixture was filtered and directly used for purification via preparative HPLC. (column: Luna 10, 250 x 21 mm; flow: 20 mL/min, solvent A: H_2O (0.05% TFA), solvent B: MeCN; gradient A/B: 0-15 min: 95/5, 15-20 min: 2/98).

Compound 4



$\text{C}_{89}\text{H}_{124}\text{N}_{24}\text{O}_{16}\text{S}_2$, MW = 1850.24 g/mol, (4x TFA)

Slightly red solid; yield: 33%. (HPLC: t_R = 8.7 min)

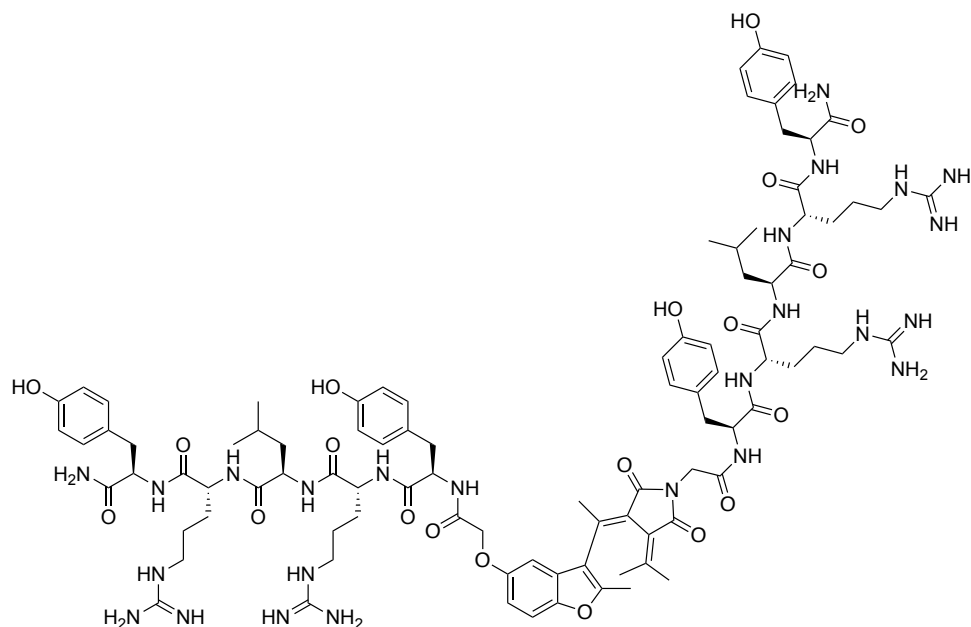
$^1\text{H-NMR}$ (600 MHz, $\text{D}_6\text{-DMSO}$): δ = 0.83 (d, J = 6.6 Hz, 6H, $\text{CH}_3(\text{Leu})$), 0.86 (d, J = 6.6 Hz, 6H, $\text{CH}_3(\text{Leu})$), 1.38-1.57 (m, 16H, CH_2), 1.63 (m, 2H, $\text{CH}(\text{Leu})$), 1.56-1.68 (m, 4H, CH_2), 1.69 (s, 6H, $\text{CH}_3(\text{DTE})$), 2.03-2.11 (m, 2H, $\text{CH}_2(\text{DTE})$), 2.68-2.93 (m, 12H, CH_2), 3.03-3.13 (m, 8H, $\text{CH}_2(\text{Arg})$), 4.12-4.24 (m, 2H, C_H), 4.25-4.35 (m, 6H, C_H), 4.51-4.57 (m, 2H, C_H), 6.61 (d, J = 8.5Hz, 4H,

$\text{CH}_{(\text{aromTyr})}$, 6.63 (d, $J = 8.5\text{Hz}$, 4H, $\text{CH}_{(\text{aromTyr})}$), 6.97 (d, $J = 8.5\text{Hz}$, 4H, $\text{CH}_{(\text{aromTyr})}$), 7.12 (d, $J = 8.6\text{Hz}$, 4H, $\text{CH}_{(\text{aromTyr})}$), 7.72 (s, 2H, $\text{CH}_{(\text{aromDTE})}$).

$^{13}\text{C-NMR}$ (151 MHz, $\text{D}_6\text{-DMSO}$): $\delta = 14.1$ (+), 21.4 (+), 22.1 (-), 23.1 (+), 24.1 (+), 24.9(-), 25.1(-), 28.9 (-), 29.0 (-), 36.3 (-), 36.8 (-), 38.6 (-), 40.5 (-), 40.8 (-), 50.9 (+), 52.2(+), 53.9 (+), 55.1(+), 114.9 (+), 127.5 (q), 128.28 (q), 129.3 (+), 130.0 (+), 134.0 (q), 135.3 (q), 136.1 (q), 138.9 (q), 155.7 (q), 155.8 (q), 156.7 (q), 160.9 (q), 170.8 (q), 171.1 (q), 171.7 (q), 172.0 (q), 172.7 (q).

HR-MS (ESI): calcd. for $\text{C}_{89}\text{H}_{124}\text{N}_{24}\text{O}_{16}\text{S}_2$ ($\text{M}+3\text{H}$) $^{3+}$, $m/z = 617.3111$, found 617.3096

Compound 5



$\text{C}_{94}\text{H}_{129}\text{N}_{25}\text{O}_{20}$, MW = 1929.22 g/mol, (4x TFA)

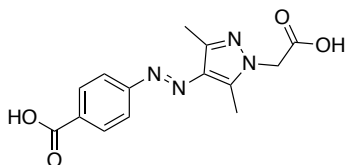
Slightly pink solid; yield: 43%. (HPLC: $t_R = 8.2$ min)

$^1\text{H-NMR}$ (600 MHz, $\text{D}_6\text{-DMSO}$): $\delta = 0.83\text{-}0.89$ (m, 12H, $\text{CH}_3(\text{Leu})$), 1.04 (s, 3H, $\text{CH}_3(\text{fulgimide})$), 1.38-1.56 (m, 16H, CH_2), 1.59-1.65 (m, 4H, CH_{Leu}), 1.62-1.70 (m, 4H, CH_2), 2.10 (s, 3H, $\text{CH}_3(\text{fulgimide})$), 2.16 (s, 3H, $\text{CH}_3(\text{fulgimide})$), 2.59-2.66 (m, 3H, $\text{CH}_3(\text{fulgimide})$), 2.68-2.74 (m, 4H, $\text{CH}_2(\text{Tyr})$), 2.84-2.87 (m, 4H, $\text{CH}_2(\text{Tyr})$), 3.05-3.10 (m, 8H, $\text{CH}_2(\text{Arg})$), 4.13 (s, 2H, $\text{CH}_2(\text{fulgimide})$), 4.20-4.23 (m, 2H, CH_{Leu}), 4.27-4.31 (m, 2H, $\text{CH}_2(\text{fulgimide})$), 4.31-4.35 (m, 6H, $\text{CH}_{\text{TyrArg}}$), 4.56 (s, 2H, $\text{CH}_2(\text{fulgimide})$), 4.53-4.60 (m, 2H, CH) 6.63 (d, 8H, $J = 8.1$ Hz, $\text{CH}_{(\text{aromTyr})}$), 6.79 (d, 1H, $J = 9.0$ Hz, $\text{CH}_{(\text{aromfulgimide})}$), 6.97 (d, 8H, $J = 8.1$ Hz, $\text{CH}_{(\text{aromTyr})}$), 7.10 (s, 1H, $\text{CH}_{(\text{aromFulgimid})}$), 7.42 (d, 1H, $J = 8.68$, $\text{CH}_{(\text{aromfulgimide})}$)

¹³C-NMR (151 MHz; D₆-DMSO): δ = 13.3 (+), 20.4 (+), 21.4 (+), 23.2 (+), 24.2 (+), 24.9 (-), 25.1 (-), 26.2 (+), 29.0 (-), 36.7 (-), 36.8 (-), 40.5 (-), 40.8 (-), 51.0 (+), 52.0 (+), 52.1 (+), 52.3 (+), 53.9 (+), 67.5 (-), 104.9 (+), 111.3 (+), 112.2 (+), 114.9 (+), 119.3 (q), 122.2 (q), 122.6 (q), 124.5 (q), 130.05 (q), 127.5 (+), 130.15 (q), 138.6 (q), 147.8 (q), 151.4 (q), 152.6 (q), 154.4 (q), 155.8 (q), 156.7 (q), 160.2 (q), 164.5 (q), 167.5 (q), 170.8 (q), 170.9 (q), 171.0 (q), 171.1 (q), 172.0 (q), 172.7 (q).

HR-MS (ESI): calcd. for C₉₄H₁₂₉N₂₅O₂₀ (M+3H)³⁺, m/z = 643.6688, found 643.6690

Compound 8: (E)-4-((1-(carboxymethyl)-3,5-dimethyl-1H-pyrazol-4-yl)diazenyl)-benzoic acid



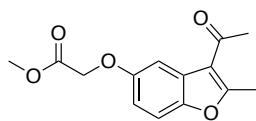
C₁₄H₁₄N₄O₄, MW = 302.29 g/mol

4-Nitrosobenzoic acid (200 mg, 1.32 mmol, 1.0 eq) was added to a stirred solution of 2-(4-amino-3,5-dimethyl-1H-pyrazol-1-yl)acetic acid (250 mg, 1.48 mmol, 1.1 eq) in pyridine (3 mL) and aqueous 40% NaOH (3 mL). The mixture was stirred at 80 °C for 2 h and subsequently cooled to r.t. Water was added and the mixture was extracted with EtOAc (4x 25 mL). The combined organic layers were dried over Na₂SO₄, filtered and the solvent was removed *in vacuo* to obtain the crude product. The crude product was purified by automated reversed phase column chromatography (H₂O + 0.05% TFA, MeCN: 10-98% MeCN) to yield the target compound **8** (48 mg, 0.15 mmol, 12%) as a yellow solid.

¹H-NMR (400 MHz; D₆-DMSO): δ = 13.18 (s, 2H), 8.07 (d, *J* = 8.7 Hz, 2H), 7.81 (d, *J* = 8.7 Hz, 2H), 4.97 (s, 2H), 2.54 (s, 3H), 2.39 (s, 3H).

¹³C-NMR (101 MHz; D₆-DMSO): δ = 9.5 (+), 13.9 (+), 39.5 (+), 50.6 (-), 121.5 (+), 130.5 (+), 131.1 (q), 135.0 (q), 141.2 (q), 141.8 (q), 155.5 (q), 166.9 (q), 169.1 (q).

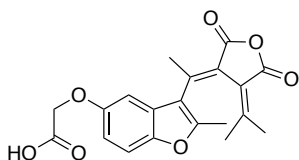
ESI-MS: m/z (%) = 303.10 (MH⁺)

Compound 10: methyl 2-((3-acetyl-2-methylbenzofuran-5-yl)oxy)acetate

$C_{14}H_{14}O_5$, MW = 262.26 g/mol

1-(5-hydroxy-2-methylbenzofuran-3-yl)ethan-1-one (**9**) (12.8 g, 67 mmol, 1.0 eq) was dissolved in DMF (150 mL) under argon atmosphere at 0 °C. NaH (2.5 g, 70 mmol, 1.1 eq) was added in portions and the suspension was stirred for 1 h at 0 °C. Methylbromoacetate (10.6 g, 69 mmol, 1.1 eq) was added and the mixture was stirred for 2 h at r.t. An aqueous HCl solution (2M, 200 mL) and H₂O (200 mL) were added to stop the reaction. The aqueous layer was extracted with EtOAc (3 x 200 mL) and the combined organic layers were dried over Na₂SO₄, filtered and the solvent was removed under reduced pressure. The crude product was purified by automated column chromatography (PE/EtOAc: gradient 0-60% EtOAc) to obtain the desired product **10** (14.6 g, 56 mmol, 83%).

Analytical data were in agreement with published data.²⁶

Compound 11: (E/Z)-2-((3-(1-(2,5-dioxo-4-(propan-2-ylidene)dihydrofuran-3(2H)-ylidene)-ethyl)-2-methylbenzofuran-5-yl)oxy)acetic acid

$C_{20}H_{18}O_7$, MW = 370.36 g/mol

To a solution of diisopropylamine (2.77 mL, 26.8 mmol, 1.6 eq) in tetrahydrofuran was added a 1.6 M solution of *n*-butyllithium in hexane (15.7 mL, 25.2 mmol, 1.5 eq) at -78 °C under nitrogen atmosphere. The mixture was stirred at this temperature for 30 min. Diethyl isopropylidenesuccinate (4.31 g, 20.1 mmol, 1.2 eq) was added and the mixture was stirred at -78 °C for 1h. Compound **10** (4.40 g, 16.8 mmol, 1.0 eq) was added and the mixture was allowed to warm to room temperature over night. The reaction mixture was stirred for 24 h at room temperature and quenched with an aqueous HCl-solution (2 M, 50 mL). The aqueous phase was extracted with ethyl acetate (3 x 100 mL) and the combined organic layers were dried over Na₂SO₄. The solvent was removed *in vacuo* to obtain the crude halfester mixture *E/Z*-**11** as intermediate.

Mixture **11** was dissolved in ethanol (40 mL) and after addition of KOH (23.5 g, 420 mmol, 25 eq) and H₂O (5 mL), the mixture was stirred for 12 h at 70 °C. The reaction mixture was poured

onto ice and quenched with an aqueous HCl-solution (2 M, 50 mL). The aqueous layer was extracted with ethyl acetate (3 x 50 mL) and the combined organic layers were washed with brine (30 mL) and dried over Na₂SO₄. The organic solvent was evaporated to get the crude diacid as a yellow solid. The diacid was suspended in dichloromethane (40 mL) and after added DCC (10.4 g, 50.4 mmol, 3.0 eq) the solution was stirred for 24 h at 40 °C. The solvent was removed *in vacuo* and the crude product was purified by automated flash column chromatography (PE/EtOAc: gradient 0-80% EtOAc) to obtain a slightly pink solid *E*-**12** (187 mg, 0.50 mmol, 3% overall yield *E*-isomer) and a white solid *Z*-**12** (124 mg, 0.34 mmol, 2% overall yield *Z*-isomer)

E-isomer

¹H-NMR (400 MHz, CDCl₃): δ = 1.90 (s, 3H, CH₃), 2.13 (s, 3H, CH₃), 2.20 (s, 3H, CH₃), 2.30 (s, 3H, CH₃), 4.59 (s, 2H, CH₂), 6.67 (d, 1H, *J* = 10.3 Hz, CH_{arom}), 6.75 (s, 1H, CH_{arom}), 7.13 (d, *J* = 8.9 Hz, 1H, CH_{arom}).

¹³C-NMR (151 MHz, CDCl₃): δ = 13.3 (+), 22.0 (+), 23.7 (+), 26.9 (+), 68.0 (-), 103.8 (+), 111.4 (+), 112.2 (+), 114.8 (q), 121.1 (q), 122.7 (q), 127.6 (q), 143.3 (q), 149.1 (q), 153.1 (q), 154.2 (q), 157.1 (q), 160.7 (q), 162.91 (q), 167.5 (q).

ESI-MS: *m/z* (%) = 369.10 (M-H)⁻

Z-isomer:

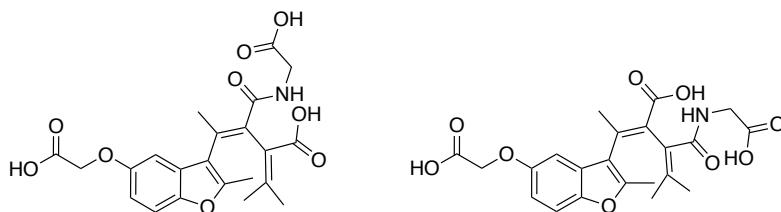
¹H-NMR (400 MHz; CDCl₃): δ = 1.14 (s, 3H), 2.24 (s, 3H), 2.29 (s, 3H), 2.73 (s, 3H), 4.69 (s, 2H), 6.70 (s, 1H), 6.94 (d, *J* = 7.0 Hz, 1H), 7.35 (d, *J* = 8.9 Hz, 1H).

¹³C NMR (101 MHz; CDCl₃): δ = 14.2 (+), 22.3 (+), 23.0 (+), 26.8 (+), 65.8 (-), 104.5 (+), 112.1 (+), 113.6 (+), 119.7 (q), 126.6 (q), 144.7 (q), 149.6 (q), 154.2 (q), 154.3 (q), 156.4 (q), 163.3 (q), 163.6 (q), 171.8 (q).

ESI-MS: *m/z* (%) = 369.11 (M-H)⁻

Compound *E-13*: (*E*)-4-(5-(carboxymethoxy)-2-methylbenzofuran-3-yl)-3-((carboxymethyl)carbamoyl)-2-(propan-2-ylidene)pent-3-enoic acid

Regioisomer 1 and 2



$C_{22}H_{23}NO_9$, MW = 445.42 g/mol

The fulgide *E-12* (120 mg, 0.32 mmol, 1.0 eq) was dissolved in MeCN (10 mL) and a mixture of DIPEA (0.28 mL, 1.62 mmol, 5.0 eq) and glycine methylester (122 mg, 0.97 mmol, 3.0 eq) in MeCN (8 mL) was added dropwise at 0 °C. The solution was stirred over night at r.t. The solvent was evaporated and the residue was quenched with 50 mL of H₂O and extracted with EtOAc (2x 70 mL). The aqueous layer was acidified with HCl (2 M) to pH 1 and extracted with EtOAc (3x 70 mL). The combined organic layers were dried over Na₂SO₄, filtered, and concentrated *in vacuo* to obtain the crude intermediate of amide acid ester. The residue was dissolved in MeOH and NaOH (64,8 mg, 1.62 mmol, 5.0 eq) was added to stir the solution over night at r.t. The solution was concentrated *in vacuo* and the resulting precipitate was dissolved in an aqueous solution of Na₂CO₃ (0.5 M, 50 mL) and extracted with EtOAc (3x 50 mL). After acidification of the aqueous layer with concentrated HCl to pH 1, the mixture was extracted again with EtOAc (3x 50 mL). The combined organic layers were dried over Na₂SO₄ and the solvent was concentrated *in vacuo*. The crude mixture was purified by automated reversed phase column chromatography (H₂O + 0.05% TFA, MeCN: 20-98% MeCN) to obtain the slightly yellowish product *E-13* (118 mg, 0.26 mmol, 83%).

Regioisomer 1

¹H-NMR (400 MHz; MeOD): δ = 1.89 (s, 3H), 2.06-2.09 (m, 6H), 2.35 (s, 3H), 4.06 (s, 2H), 4.65 (s, 2H), 6.87 (d, *J* = 8.8 Hz, 1H), 6.93 (s, 1H), 7.27 (d, *J* = 8.8 Hz, 1H).

¹³C-NMR (101 MHz; MeOD): δ = 12.9 (+), 21.4 (+), 21.6 (+), 22.1 (+), 41.8 (-), 66.7 (-), 104.6 (+), 111.8 (+), 113.2 (+), 118.4 (q), 128.8 (q), 130.2 (q), 135.2 (q), 140.3 (q), 144.0 (q), 150.5 (q), 152.8 (q), 155.4 (q), 171.3 (q), 171.5 (q), 172.5 (q), 172.8 (q).

ESI-MS: m/z (%) = 446.16 (MH^+)

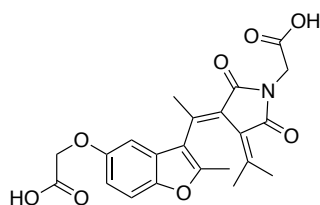
Regioisomer 2

1H -NMR (400 MHz; MeOD): δ = 1.88 (s, 3H), 1.91 (s, 3H), 2.21 (s, 3H), 2.29 (s, 3H), 4.04 (s, 2H), 4.64 (s, 2H), 6.87-6.88 (m, 1H), 6.93 (s, 1H), 7.28-7.24 (m, 1H).

^{13}C -NMR (101 MHz, MeOD): δ = 13.1 (+), 21.2 (+), 22.6 (+), 24.5 (+), 42.1 (-), 66.9 (-), 105.1 (+), 112.0 (+), 113.5 (+), 118.6 (q), 129.1 (q), 135.8 (q), 138.4 (q), 140.1 (q), 143.7 (q), 150.9 (q), 153.6 (q), 155.7 (q), 170.7 (q), 171.8 (q), 172.8 (q), 173.0 (q).

ESI-MS: m/z (%) = 446.14 (MH^+)

Compound *E-14*: (*E*)-2-(3-(1-(5-(carboxymethoxy)-2-methylbenzofuran-3-yl)ethylidene)-2,5-dioxo-4-(propan-2-ylidene)pyrrolidin-1-yl)acetic acid



$C_{22}H_{23}NO_9$, MW = 427.41 g/mol

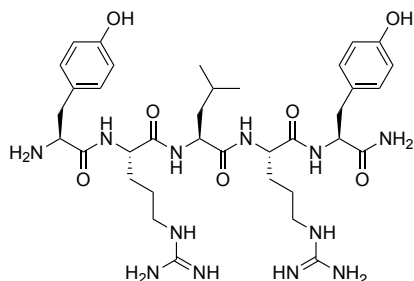
The amide acid *E-13* (118 mg, 0.26 mmol, 1 eq) was dissolved in toluene (30 mL) and after added acetic anhydride (10 mL) at 0 °C, the solution was stirred for 2 h at r.t. The reaction mixture was diluted with EtOAc (80 mL) and extracted with saturated $NaHCO_3$ (2x 50 mL) and H_2O (50 mL). The organic layer was dried over Na_2SO_4 , filtered and the solvent was evaporated. The crude product was purified by automated column chromatography ($CH_2Cl_2/MeOH$: 0-20% MeOH) and further purified by preparative HPLC (column: Luna 10, 250 x 21 mm; flow: 20 mL/min, solvent A: H_2O (0.05% TFA), solvent B: MeCN; gradient A/B: 0-15 min: 95/5, 15-20 min: 2/98; t_R = 11.8 min) to obtain the product *E-14* as a light red solid (22 mg, 0.05 mmol, 20%).

1H -NMR (400 MHz, D_6 -DMSO): δ = 1.07 (s, 3H, CH_3), 2.16 (s, 3H, CH_3), 2.18 (s, 3H, CH_3), 2.67 (s, 3H, CH_3), 4.23 (s, 2H, CH_2), 4.68 (s, 2H, CH_2), 6.88 (d, J 8.9 Hz, 1H, CH_{arom}), 7.01 (s, 1H, CH_{arom}), 7.43 (d, J 8.9 Hz, 1H, CH_{arom})

^{13}C -NMR (100 MHz, D_6 -DMSO): δ = 13.4 (+), 20.6 (+), 21.4 (+), 26.2 (+), 38.9 (-), 65.3 (-), 104.5 (+), 111.3 (+), 112.4 (+), 119.4 (q), 122.7 (q), 124.3 (q), 127.0 (q), 139.3 (q), 148.6 (q), 149.1 (q), 152.7 (q), 154.2 (q), 166.8 (q), 167.3 (q), 168.8 (q), 170.3 (q)

ESI-MS: m/z (%) = 385.23 (MH^+)

Compound 17: (S)-N-((S)-1-amino-3-(4-hydroxyphenyl)-1-oxopropan-2-yl)-2-((S)-2-((S)-2-((S)-2-amino-3-(4-hydroxyphenyl)propanamido)-5-guanidinopentanamido)-4-methylpentanamido)-5-guanidinopentanamide



$C_{36}H_{56}N_{12}O_7$, MW = 768.92 g/mol, (2x TFA salt)

Manual SPPS applying the Fmoc strategy on a Fmoc-Sieber-PS resin (loading, 0.85 mmol/g, 250 mg, 0.43 mmol, 1.0 eq) was used for the peptide synthesis. Discardit II syringes (20 mL) were equipped with 35 μ M polyethylene frits and used as reaction vessels. A mixture of DMF/NMP (8:2) was used as solvent and protected standard L-amino acids (5 eq) were preactivated with HBTU (5.0 eq)/HOBt (5.0 eq)/DIPEA (10 eq) for 7 min and added to the resin. Coupling was performed at r.t. for 1.5 h and every coupling step was done twice. After the coupling step, the resin was washed with DMF/NMP (8:2) and treated with 20% piperidine in DMF/NMP (8:2) at r.t. (2x, each step 10 min) for Fmoc deprotection. This step was followed by a DMF/NMP (8:2) wash (2x). After the last coupling step and Fmoc deprotection, the resin was washed with DCM (2x). The peptide was cleaved from the resin with CH_2Cl_2 /TFA (97:3) at r.t. (8x 10 min) and filtered. The combined filtrates were poured onto water and the organic solvent was removed in vacuo. The aqueous layer was lyophilized and subsequently purified by automated reversed phase column chromatography (H_2O + 0.05% TFA, MeCN: 30-98% MeCN) to obtain the side chain protected peptide. The protected peptide was dissolved in a mixture of TFA/ H_2O (95/5, 5 mL) and stirred at r.t. for 4 h. Water was added and removed by lyophilisation. The product was purified by automated reversed phase column chromatography (H_2O + 0.05% TFA, MeCN: 10-98% MeCN) to obtain the product **17** as a white solid (204 mg, 0.26 mmol, 62%).

1H -NMR (400 MHz; D_6 -DMSO): δ = 0.86 (dd, J = 15.3, 6.5 Hz, 6H), 1.69-1.44 (m, 11H), 2.84-2.74 (m, 3H), 2.98 (dd, J = 14.2, 4.3 Hz, 1H), 3.02-3.12 (m, 4H), 3.97 (t, J = 6.0 Hz, 1H), 4.19 (q, J = 6.8 Hz, 1H), 4.27-4.40 (m, 3H), 6.65 (dd, J = 16.9, 8.4 Hz, 4H), 6.99 (dd, J = 15.5, 8.4 Hz, 4H).

^{13}C -NMR (101 MHz; D_6 -DMSO): δ = 21.52 (+), 23.28 (+), 24.43 (+), 25.02 (-), 25.12 (-), 29.14 (-), 29.44 (-), 36.34 (-), 36.94 (-), 40.55 (-), 40.63 (-), 40.75 (-), 51.32 (+), 52.35 (+), 52.53

(+), 53.60 (+), 54.20 (+), 115.10 (+), 115.52 (+), 124.72 (q), 127.68 (q), 130.25 (+), 130.74 (+), 155.98 (q), 156.73 (q), 156.95 (q), 156.99 (q), 168.21 (q), 171.01 (q), 171.17 (q), 172.33 (q), 173.05 (q).

ESI-MS: m/z (%) = 385.23 (M+2H⁺)²⁺

4.3 Assays

NPY Y₄ receptor radioligand binding assay

Radioligand competition binding experiments at the Y₄ receptor were performed as previously described using CHO-hY₄R-mtAEQ-G_{q15} cells and [³H]UR-KK200 (K_d = 0.67 nM, concentration = 1 nM) as radioligand.² Immediately prior to the experiment, *Z*-isomers* of **2** and **3** were generated from the respective *E*-isomers (10 or 30 μM in binding buffer) by irradiation with UV light (λ = 365 nm) in open polypropylene reaction vessels for 40 s. The closed forms* of **4** and **5** were generated from the respective 'open' isomers (5 mM in DMSO/H₂O, 1:1) by irradiation with UV light (**4**: λ = 312 nm, **5**: λ = 365 nm). All solutions of **2-5** (both isomeric forms) were kept in the dark. Assays were performed in the dark using a red LED (λ = 650 nm) to maintain visibility for the operator. Specific binding data were analyzed by a four parameter logistic fit (log(inhibitor) vs response – variable slope; GraphPad Prism 5.0, GraphPad Software, San Diego, CA) to obtain IC₅₀ values. The latter were converted to K_i values according to the Cheng-Prusoff equation.²⁷

*Note: for an approximation of achieved *E/Z* ratios and *O/C* ratios (PSS) see **Table 1** and **2**.

NPY Y₁ receptor radioligand binding assay

Radioligand competition binding experiments at the Y₁ receptor were performed as previously described, using SK-N-MC neuroblastoma cells and [³H]UR-MK299 (K_d = 0.044 nM, concentration = 0.15 nM) as radioligand,²⁸ with the following modification: experiments were performed in the dark using a red LED (λ = 650 nm) to maintain visibility for the operator. The *Z*-isomers of **2** and **3** were generated as described under 'NPY Y₄ receptor radioligand binding assay'. Binding data of **3** were analyzed as in case of Y₄ receptor binding. In case of **2** (incomplete displacement [³H]UR-MK299) pIC₅₀ values were determined by plotting log($B/(B_0 - B)$) (B = specifically bound [³H]UR-MK299 in the presence of **2**; B_0 = specifically bound [³H]UR-MK299 in the absence of **2**) versus log(concentration of **2**) followed by linear regression. Resulting pIC₅₀ values (pIC₅₀ = intercept with the X-axis) were transformed to IC₅₀ values and the latter were converted to K_i values according to the Cheng-Prusoff equation.

β -Arrestin recruitment assay

The β -arrestin 1 and 2 recruitment assays were performed with HEK293T-ARRB1-Y₄R or HEK293T-ARRB2-Y₄R cells as previously reported²⁵ with the following modification: experiments were performed in the dark using a red LED ($\lambda = 650$ nm) to maintain visibility for the operator. The Z-isomers of **2** and **3** as well as the closed forms of **4** and **5** were prepared as described under 'NPY Y₄ receptor radioligand binding assay'. Measured bioluminescences were normalized (100% = bioluminescence obtained from 1 μ M hPP, 0% = basal effect in the absence of agonist; GraphPad Prism 5.0) and relative cellular responses were plotted against log(concentration of agonist) followed by fitting according to a four-parameter logistic equation (log(agonist) vs response - variable slope; GraphPad Prism 5.0). Resulting pEC₅₀ values were converted to EC₅₀ values. Efficacies α (maximum effect relative to 1 μ M hPP) were calculated from the upper curve plateaus ($\alpha = \text{'top'}/100$).

Aequorin assay

The Ca²⁺-aequorin assay was performed with CHO-hY₄R-mtAEQ-G_{q15} cells as previously reported.²⁴ The Z-isomers of **2** and **3** as well as the closed forms of **4** and **5** were prepared as described under 'NPY Y₄ receptor radioligand binding assay'. Areas under the curve were determined using Sigma Plot 12.5 (Systat Software, Chicago, IL). Fractional bioluminescences were normalized (100% = fractional bioluminescence obtained from 1 μ M hPP, 0% = basal effect in the absence of agonist; GraphPad Prism 5.0) and relative responses were plotted against log(concentration of agonist) followed by fitting according to a four-parameter logistic equation (log(agonist) vs response - variable slope; GraphPad Prism 5.0). Resulting pEC₅₀ values were converted to EC₅₀ values. Efficacies α (maximum effect relative to 1 μ M hPP) were calculated from the upper curve plateaus ($\alpha = \text{'top'}/100$).

5. Literature

- 1 K. B. Sickert, A. G. Beck-Sickinger, *Trends in Pharmacological Sciences* **2010**, *31*, 434
- 2 K. K. Kuhn, T. Ertl, S. Dukorn, M. Keller, G. Bernhardt, O. Reiser, A. Buschauer, *J. Med. Chem.* **2016**, *59*, 6045
- 3 Z. Yang, S. Han, M. Keller, A. Kaiser, B. J. Bender, M. Bosse, K. Burkert, L. M. Kögler, D. Wiffling, G. Bernhardt, N. Plank, T. Littmann, P. Schmidt, C. Yi, Y. Beibei, R. Zhang, B. Xu, D. Larhammar, R. C. Stevens, D. Huster, J. Meiler, Q. Zhao, A. G. Beck-Sickinger, A. Buschauer, B. Wu, *Nature* **2018**, *556*, 520
- 4 L. Zhang, M.S. Bijker, H. Herzog, *Pharmacol. Ther.* **2011**, *131*, 91
- 5 J.-B. Li, A. Asakawa, M. Terashi, K. Cheng, H. Chaolu, T. Zoshiki, M. Ushikai, S. Sheriff, A. Balasubramaniam, A. Inui, *Peptides* **2010**, *31*, 1706
- 6 I. Lundell, A. G. Blomqvist, M. M. Berglund, D. A. Schober, D. Johnson, M. A. Statnick, R. A. Gadski, D. R. Gehlert, D. Larhammer, *J. Biol. Chem.* **1995**, *270*, 29123
- 7 A. Balasubramaniam, D. E. Mullins, S. Lin, W. Zhai, Z. Tao, V. C. Dhawan, M. Guzzi, J. J. Knittel, K. Slack, H. Herzog, E. M. Parker, *J. Med. Chem.* **2006**, *49*, 2661
- 8 K. K. Kuhn, T. Littmann, S. Dukorn, M. Tanaka, M. Keller, T. Ozawa, G. Bernhardt, A. Buschauer, *ACS Omega* **2017**, *2*, 3616
- 9 X. Gómez-Santacana, S.M. de Munnik, P. Vijayachandran, D. Da Costa Pereira, J. P. M. Bebelman, I. J. P. de Esch, H. F. Vischer, M. Wijtman, R. Leurs, *Angew. Chem. Int. Ed.* **2018**, *57*, 11608
- 10 D. Lachmann, C. Studte, B. Männel, H. Harald, P. Gmeiner, B. König, *Chem. Eur. J.* **2017**, *23*, 13423
- 11 A. Prestel, H. M. Möller, *Chem. Commun.* **2016**, *52*, 701
- 12 Ch. Hoppmann, P. Schmieder, P. Domaing, G. Vogelreiter, J. Eichhorst, B. Wiesner, I. Morano, K. Rück-Braun, M. Beyermann, *Angew. Chem. Int. Ed.* **2011**, *50*, 7699
- 13 K. Fujimoto, T. Maruyama, Y. Okada, T. Itou, M. Inouye, *Tetrahedron* **2013**, *69*, 6170
- 14 H. M. D. Bandara, S. C. Burdette, *Chem. Soc. Rev.* **2012**, *41*, 1809
- 15 F. Strübe, S. Rath, J. Mattay, *Eur. J. Org. Chem.* **2011**, *24*, 4645
- 16 J. Li, I. Cvrtila, M. Colomb-Delsuc, E. Otten, S. Otto, *Chem. Eur. J.* **2014**, *20*, 15709
- 17 L. N. Lucas, J. H. D. de Jong, J. H. van Esch, R. M. Kellogg, B. L. Feringa, *Eur. J. Org. Chem.* **2003**, 155
- 18 E. J. Chambers, I. S. Haworth, *J. Chem. Soc., Chem. Commun.* **1994**, *0*, 1631
- 19 J. Levitz, M. Herder, B. M. Schmidt, L. Grubert, M. Paetzel, J. Schwarz, S. Hecht, *J. Am. Chem. Soc.* **2015**, *137*, 2738
- 20 U. Megerle, R. Lechner, B. König, E. Riedle, *Photochem. Photobiol. Sci.* **2010**, *9*, 1400

-
- 21 N. Merten, D. Lindner, N. Rabe, H. Römler, K. Mörl, T. Schöneberg, A. G. Beck-Sickinger, *J. Biol. Chem.* **2007**, *282*, 7543
 - 22 I. Berlicki, M. Kaske, R. Gutiérrez-Abad, G. Bernhardt, O. Illa, R. M. Ortuno, C. Cabrele, A. Buschauer, O. Reiser, *J. Med. Chem.* **2013**, *56*, 8422
 - 23 W. I Weis, B. K. Kobilka, *Annu. Rev. Biochem* **2018**, *87*, 897
 - 24 R. Ziemek, E. Schneider, A. Kraus, Ch. Cabrele, A. G. Beck-Sickinger, G. Bernhardt, A. Buschauer, *J. Recept. Signal Transduction Res.* **2007**, *27*, 217
 - 25 S. Dukorn, T. Littmann, M. Keller, K. Kuhn, Ch. Cabrele, P. Baumeister, G. Bernhardt, A. Buschauer, *Bioconjugate Chem.* **2017**, *28*, 1291
 - 26 O.A. Onuchina, S. A. Zaitsev, A. P. Arzamastev, M. A. Kalinkina, V. G. Granik, *Pharm Chem J* **2006**, *40*, 530
 - 27 Y.-Ch. Cheng, W. H. Prusoff, *Biochem. Pharmacol.* **1973**, *22*, 3099
 - 28 M. Keller, S. Weiss, C. Hutzler, K. K. Kuhn, C. Mollereau, S. Dukorn, L. Schindler, G. Bernhardt, B. König, A. Buschauer, *J. Med. Chem.* **2015**, *58*, 8834

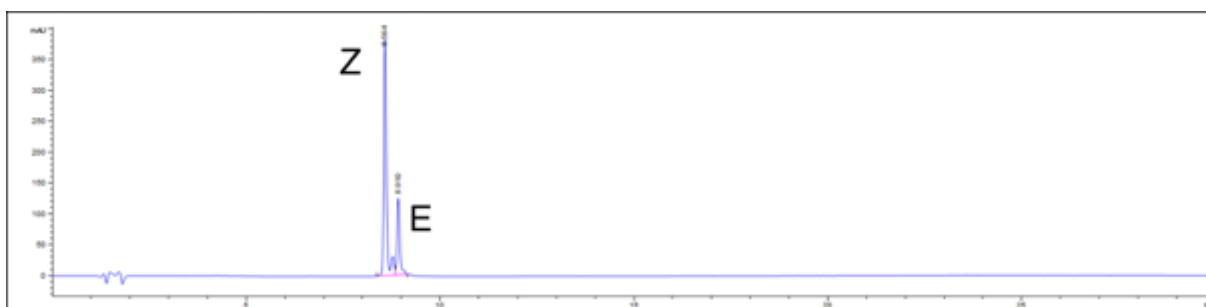
6. Supporting information

6.1 PSS determination via HPLC

Azobenzene **2**

The photochemical isomerization of compound **2** is depicted in **Figure S1**. The $E \rightarrow Z$ isomerization was performed with a 365 nm LED (SSC VIOSYS, 700 mA, 1250 mW) and the $Z \rightarrow E$ isomerization with a 455 nm LED (OSRAM Oslon SSL 80 blue, 1000 mA, 1480 mW). Conditions analytical HPLC: column *Phenomenex Luna*, 3 μ C18(2) 100A, 150 x 2.0 mm, 100 Å, 15 °C, solvent A: H₂O (0.05% TFA), solvent B: MeCN; gradient A/B: 0-20 min: 90/10, 20-30 min: 2/98.

a)



b)

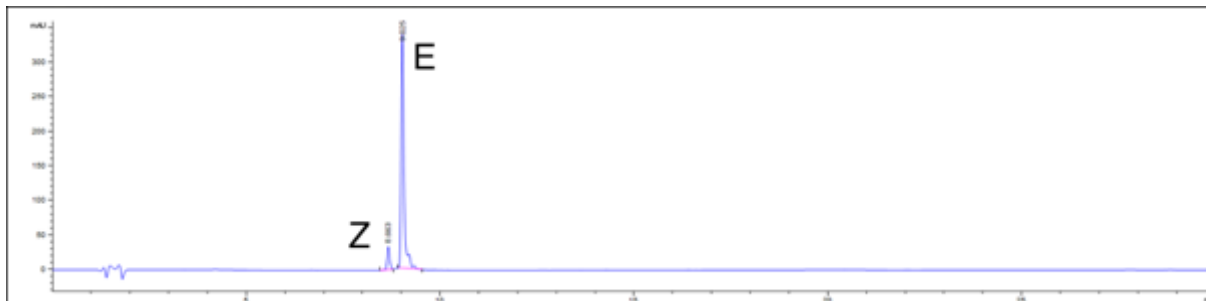
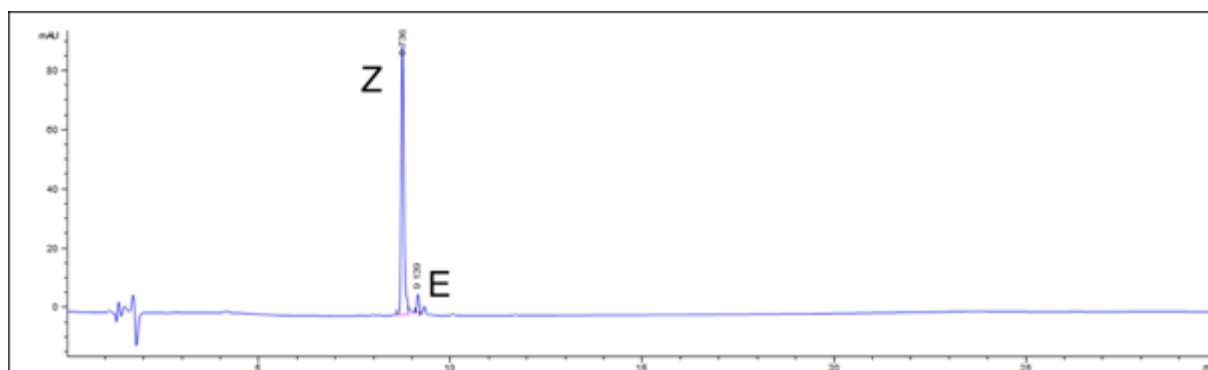


Figure S1. PSS determination via HPLC measurements at the isosbestic point of azobenzene **2** ($t_{R(E)} = 9.0$ min, $t_{R(Z)} = 8.6$ min). a) $E \rightarrow Z$ isomerization. b) $Z \rightarrow E$ isomerization.

Azopyrazole **3**

The photochemical isomerization of compound **3** is depicted in **Figure S2**. The $E \rightarrow Z$ isomerization was performed with a 365 nm LED (SSC VIOSYS, 700 mA, 1250 mW) and the $Z \rightarrow E$ isomerization with a 528 nm LED (OSRAM Oslon SSL 80 green, 500 mA, 34 mW). Conditions analytical HPLC: column *Phenomenex Luna*, 3 μ C18(2) 100A, 150 x 2.0 mm, 100 Å, 15 °C, solvent A: H₂O (0.05% TFA), solvent B: MeCN; gradient A/B: 0-20 min: 90/10, 20-30 min: 2/98.

a)



b)

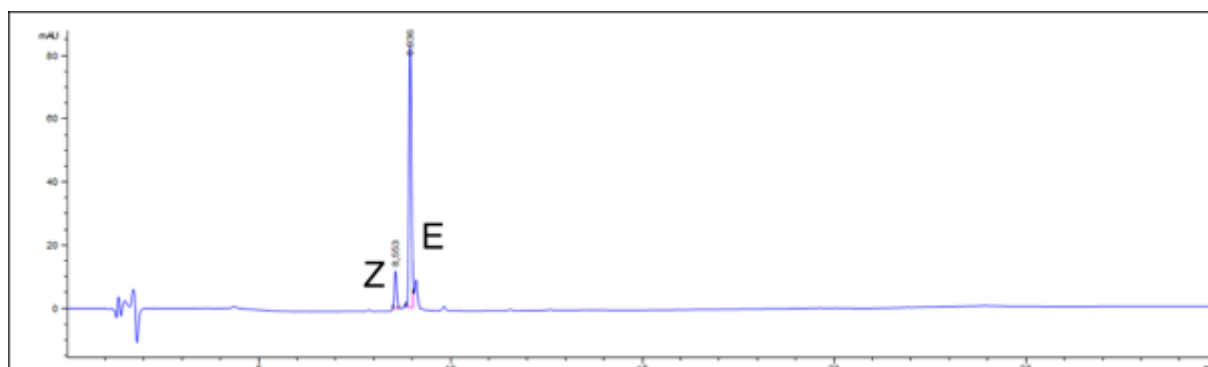
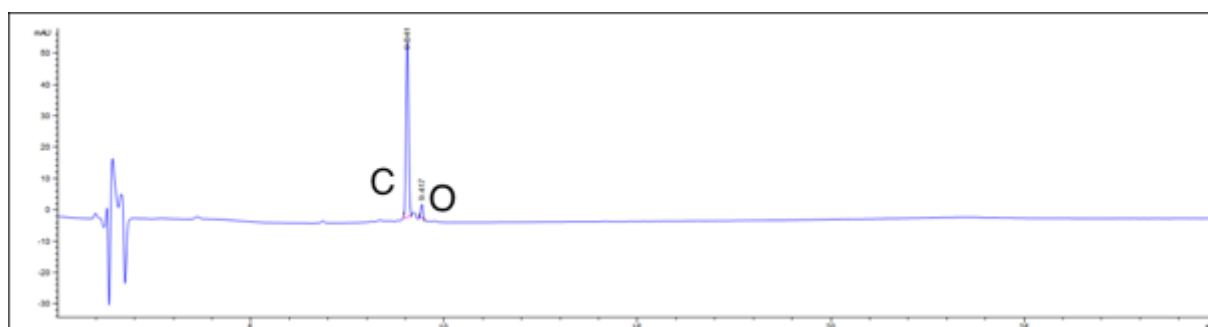


Figure S2. PSS determination via HPLC measurements at the isosbestic point of azopyrazole **3** ($t_{R(E)} = 8.9$ min, $t_{R(Z)} = 8.6$ min). a) $E \rightarrow Z$ isomerization. b) $Z \rightarrow E$ isomerization.

Dithienylethene **4**

The photochemical isomerization of compound **4** is depicted in **Figure S3**. The $O \rightarrow C$ isomerization was performed with a 312 nm tube lamp (Herolab hand-held lamp UV-6 M, 6 W) and the $C \rightarrow O$ isomerization with a 528 nm LED (OSRAM Oslon SSL 80 green, 500 mA, 34 mW). Conditions analytical HPLC: column *Phenomenex Luna*, 3 μ C18(2) 100A, 150 x 2.0 mm, 100 Å, 25 °C, solvent A: H₂O (0.05% TFA), solvent B: MeCN; gradient A/B: 0-20 min: 90/10, 20-30 min: 2/98

a)



b)

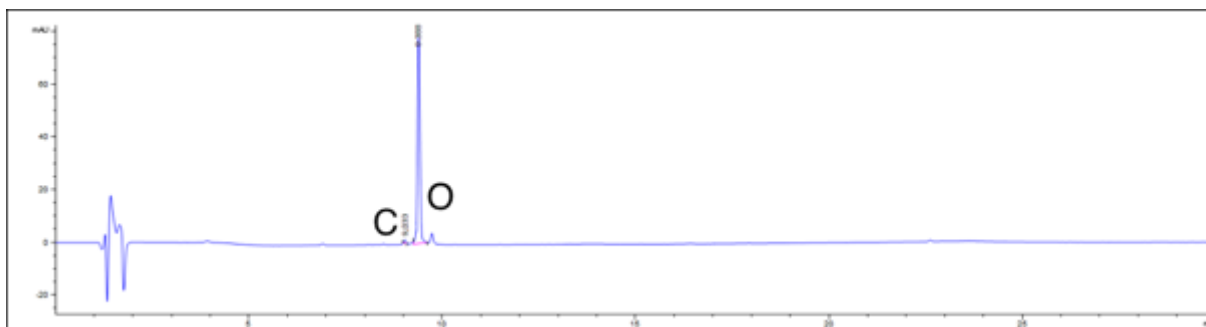
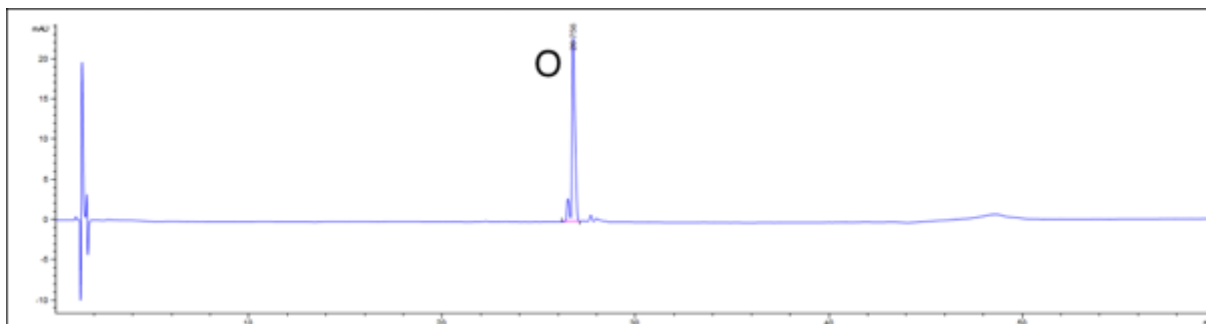


Figure S3. PSS determination via HPLC measurements at the isosbestic point of compound **4** ($t_{R(O)} = 9.4$ min, $t_{R(C)} = 9.0$ min). a) $O \rightarrow C$ isomerization. b) $C \rightarrow O$ isomerization.

Fulgimide **5**

The photochemical isomerization of compound **5** is depicted in **Figure S4**. The $O \rightarrow C$ isomerization was performed with a 365 nm LED (SSC VIOSYS, 700 mA, 1250 mW) and the $C \rightarrow O$ isomerization with a 528 nm LED (OSRAM Oslon SSL 80 green, 500 mA, 34 mW). Conditions analytical HPLC: column *Phenomenex Luna*, 3 μ C18(2) 100A, 150 x 2.0 mm, 100 Å, 15 °C, solvent A: H₂O (0.05% TFA), solvent B: MeCN; gradient A/B: 0-40 min: 90/10, 40-50 min: 55/45, 50-60 min: 2/98).

a)



b)

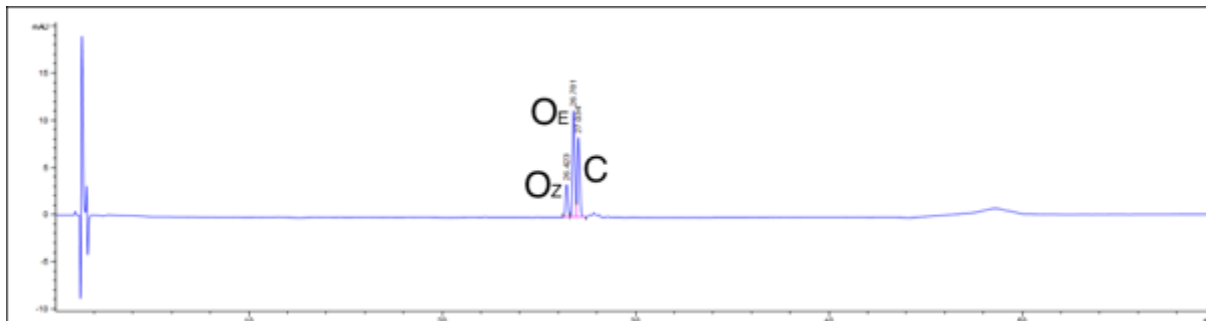
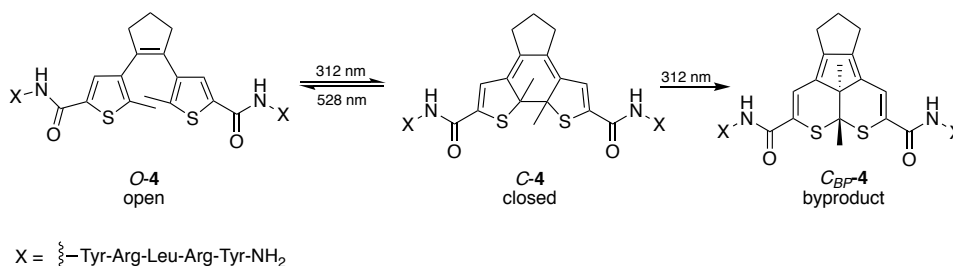


Figure S4. PSS determination via HPLC measurements at the isosbestic point of compound **5** ($t_{R(Z)} = 26.4$ min, $t_{R(E)} = 26.8$ min, $t_{R(C)} = 27.0$ min). a) $O \rightarrow C$ isomerization. b) $C \rightarrow O$ isomerization.

6.2 Byproduct formation of compound 4



Scheme S1. Formation of an irreversible byproduct C_{BP-4} upon irradiation with light of 312 nm (Herolab hand-held lamp UV-6 M, 6 W) after 5 min.

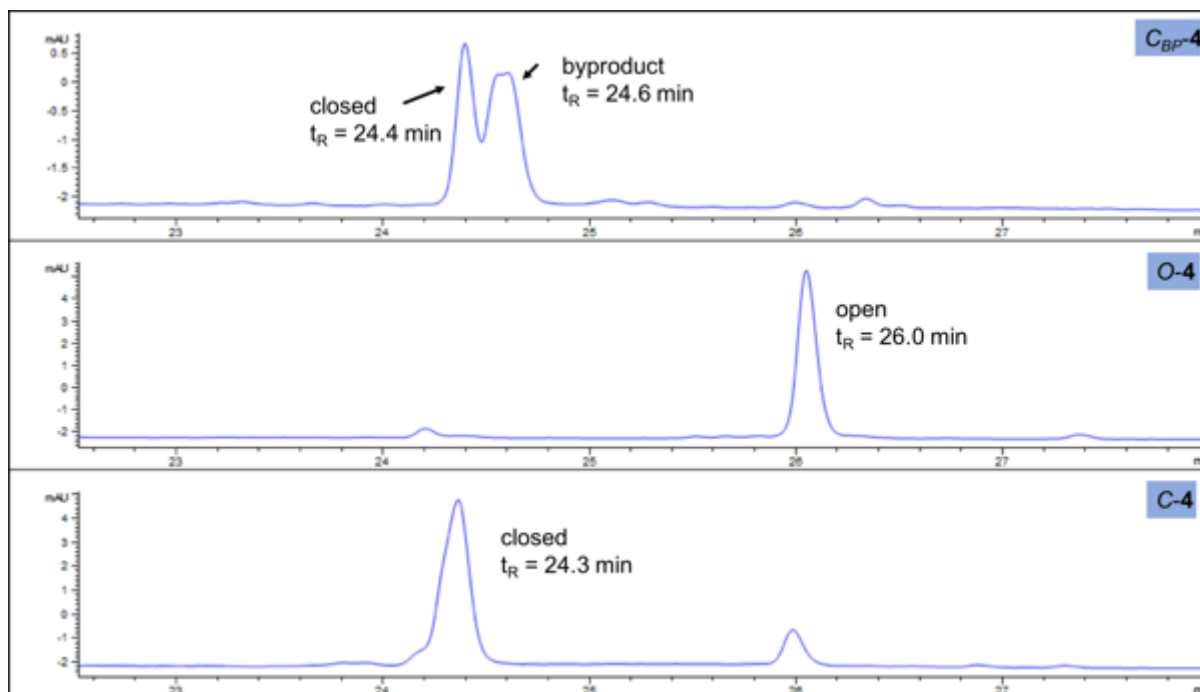
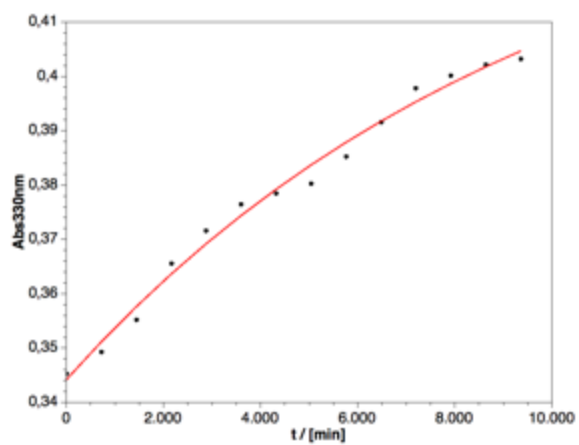


Figure S5. HPLC measurements, the three chromatograms are depicted to show the byproduct formation. Chromatogram C_{BP-4} was measured after 5 min irradiation with 312 nm light. (Method HPLC: column *Phenomenex Luna*, 3 μ C18(2) 100A, 150 x 2.0 mm, 100 \AA , 25 $^{\circ}\text{C}$, solvent A: H_2O (0.05% TFA), solvent B: MeCN; gradient A/B: 0-40 min: 90/10, 40-50 min: 55/45, 50-60 min: 2/98)

6.3 Thermal half-life of compound 2 and 3

To determine the thermal half-lives, the samples were first irradiated until the photostationary state (PSS) was reached. The samples were left for thermal relaxation at 25 $^{\circ}\text{C}$ and the recovery of the absorbance of the *E*-isomer at λ_{max} was measured. The calculation of the thermal half-life was done by fitting the data with an exponential function (**Figure S6**).

a)



b)

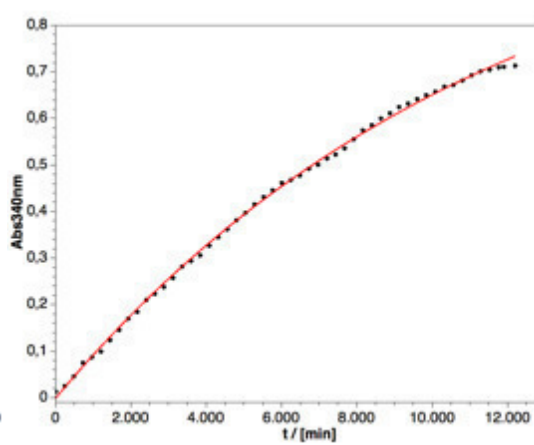


Figure S6. Half-life determination of the azo based compounds. a) Azobenzene 2; b) Azopyrazole 3.

6.4 Biological characterization

Displacement curves from radioligand competition binding assays and concentration-effect curves from functional assays.

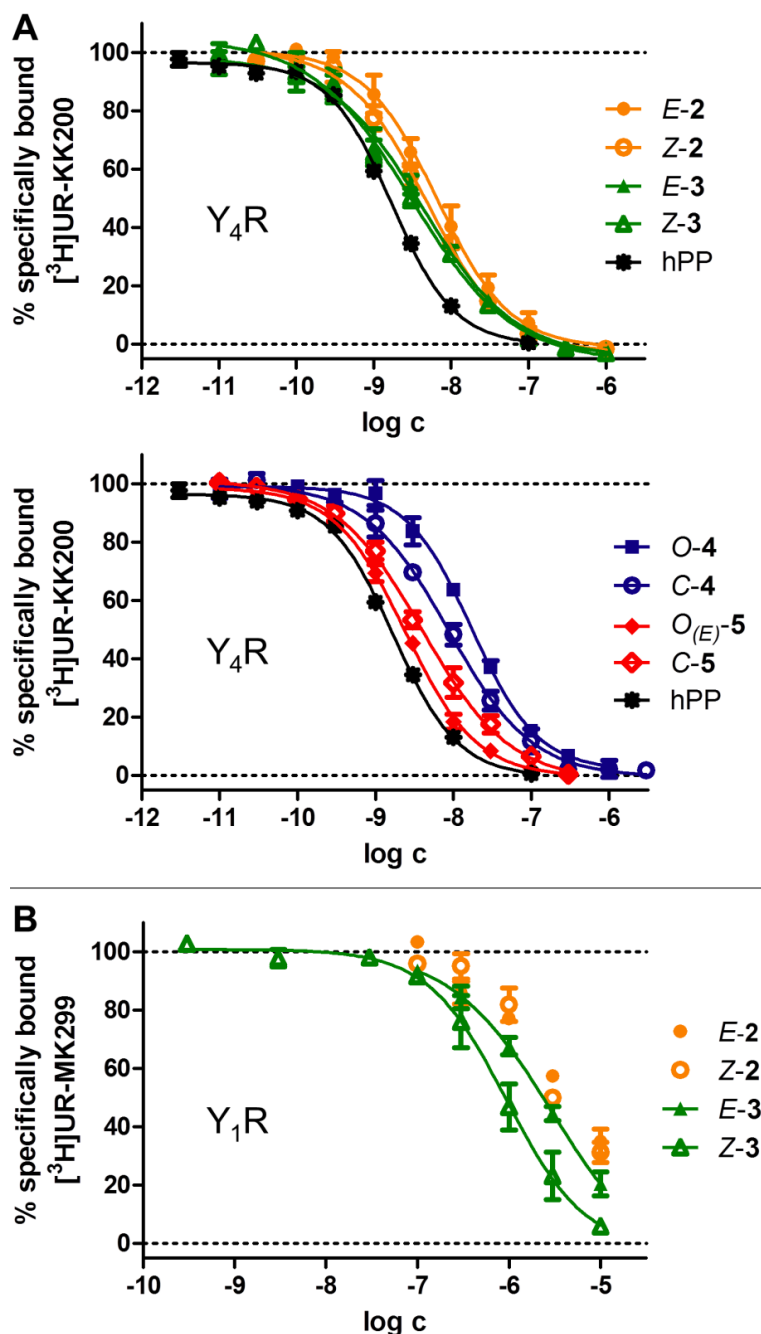


Figure S7. A: Displacement curves obtained from competition binding experiments with the Y₄R radioligand [³H]UR-KK200 ($K_d = 0.67$ nM, $c = 1$ nM) and *E/Z-2**, *E/Z-3**, *O/C-4** and *O_(E)/C-5** performed at CHO-hY₄R-mtAEQ-G_{q15} cells. B: Displacement curves obtained from competition binding experiments with the Y₁R radioligand [³H]UR-MK299 ($K_d = 0.044$ nM, $c = 0.15$ nM) and *E/Z-2** and *E/Z-3** performed at SK-N-MC neuroblastoma cells. Data (A, B) represent means \pm SEM from three or four independent experiments performed in triplicate. Data were analyzed by four parameter logistic fits (GraphPad Prism 5.0). In B, data of *E/Z-2* did not allow an analysis by a four parameter logistic fit.

*For an approximation of achieved *E/Z* and *O/C* ratios (PSS) see **Tables 1** and **2** (main article).

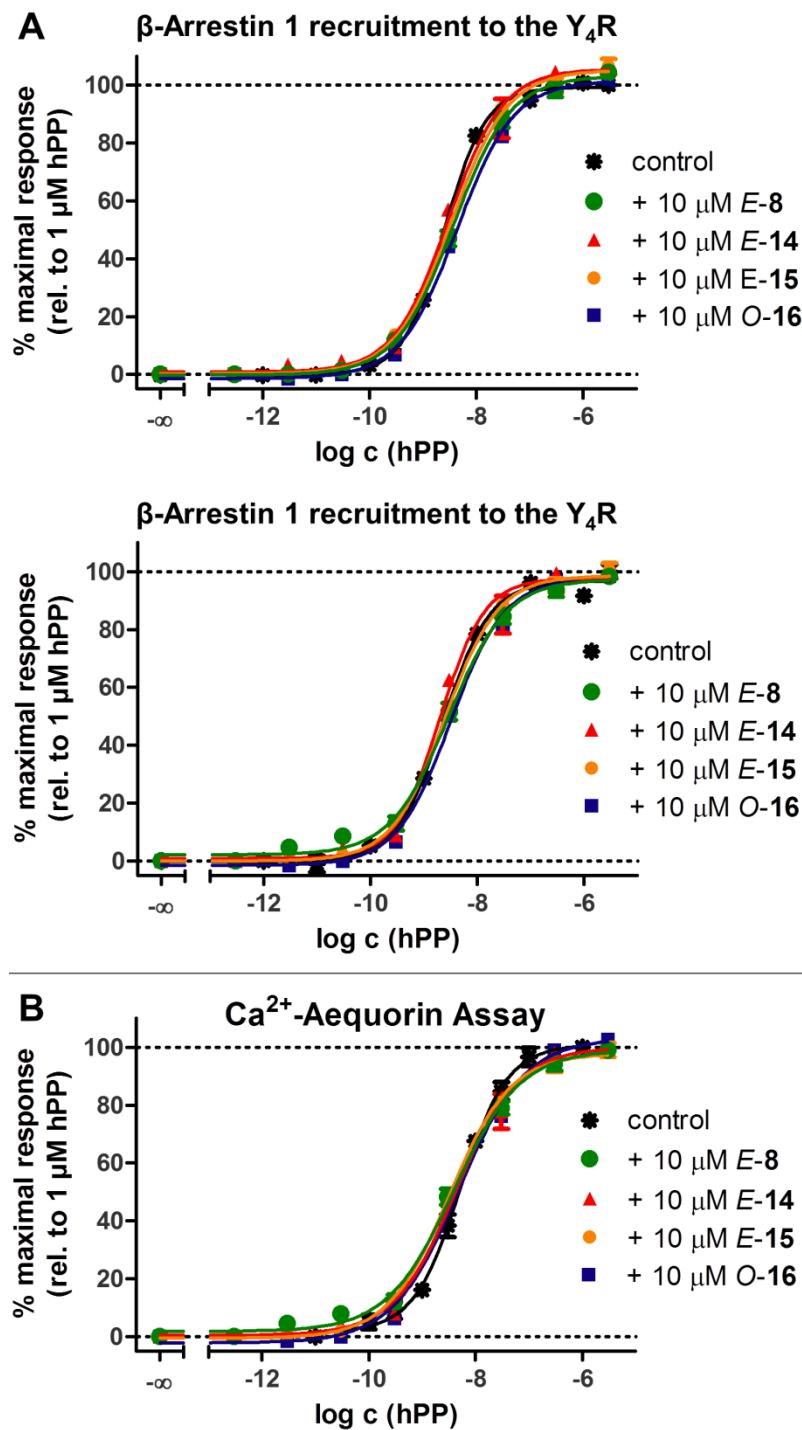


Figure S8. Control experiments to investigate whether the photochromic core structures **8**, **14**, **15** and **16** influence the readout of the functional Y_4R aequorin and arrestin assay. A: Concentration-response curves of hPP (β -arrestin 1 and 2 recruitment assay using HEK293T-ARRB1- Y_4R or HEK293T-ARRB2- Y_4R cells) in the absence and presence of E-8, E-14, E-15 and O-16. B: Concentration-response curves of hPP (Ca^{2+} -aequorin assay using CHO-h Y_4R -mtAEQ- G_{q5} cells) in the absence and presence E-8, E-14, E-15 and O-16. Data (A, B) represent means \pm SEM from three or four independent experiments performed in triplicate. Data were analyzed by four parameter logistic fits (GraphPad Prism 5.0). Cellular responses were normalized to the effect of hPP elicited at a concentration of 1 μM . In both assays, E-8, E-14, E-15 and O-16 did not affect the assay readout.

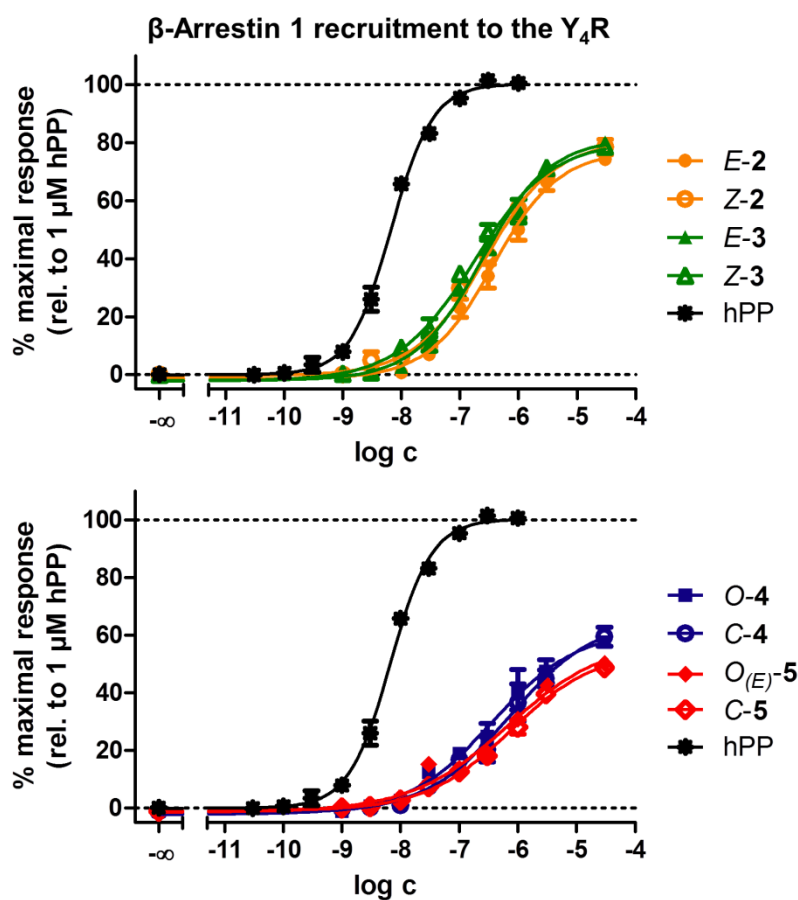


Figure S9. Y_4R functional activities (concentration-response curves) of $E/Z-2^*$, $E/Z-3^*$, $O/C-4^*$ and $O_{(E)}/C-5^*$ and the endogenous agonist hPP determined by measuring β -arrestin 1 recruitment to the Y_4R using HEK293T-ARRB1- Y_4R cells. Data represent means \pm SEM from three or four independent experiments performed in triplicate. Data were analyzed by four parameter logistic fits (GraphPad Prism 5.0). Cellular responses were normalized to the effect of hPP elicited at a concentration of 1 μ M.

*For an approximation of achieved E/Z and O/C ratios (PSS) see **Tables 1** and **2** (main article).

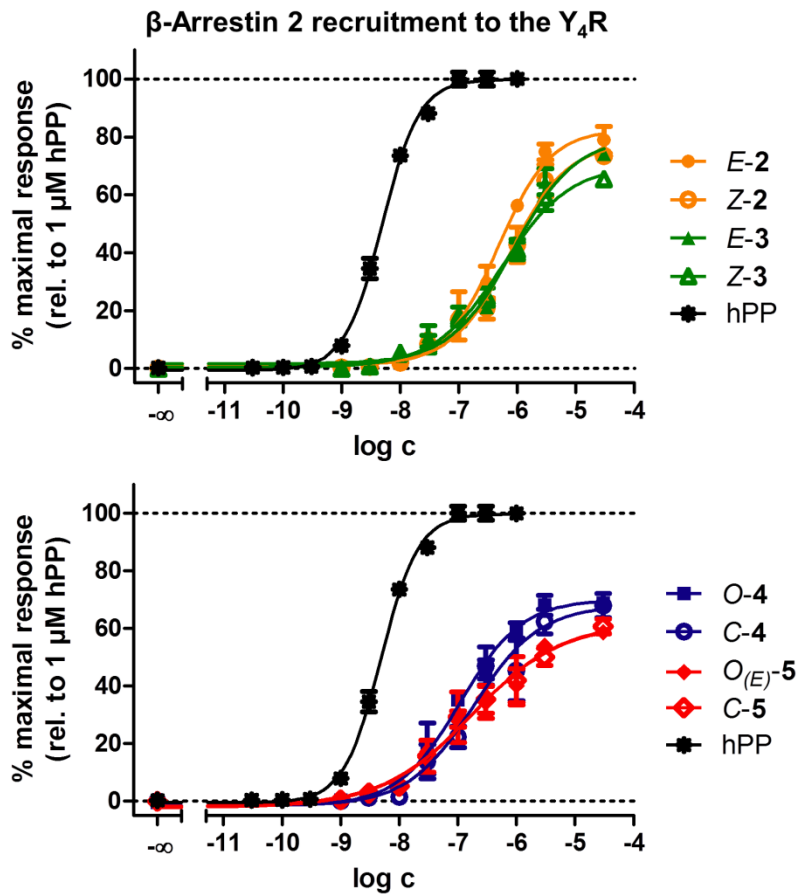


Figure S10. Y_4R functional activities (concentration-response curves) of $EIZ-2^*$, $EIZ-3^*$, $OIC-4^*$ and $O_{(E)}/C-5^*$ and the endogenous agonist hPP determined by measuring β -arrestin 2 recruitment to the Y_4R using HEK293T-ARRB2- Y_4R cells. Data represent means \pm SEM from three or four independent experiments performed in triplicate. Data were analyzed by four parameter logistic fits (GraphPad Prism 5.0). Cellular responses were normalized to the effect of hPP elicited at a concentration of 1 μ M.

*For an approximation of achieved EIZ and OIC ratios (PSS) see **Tables 1** and **2** (main article).

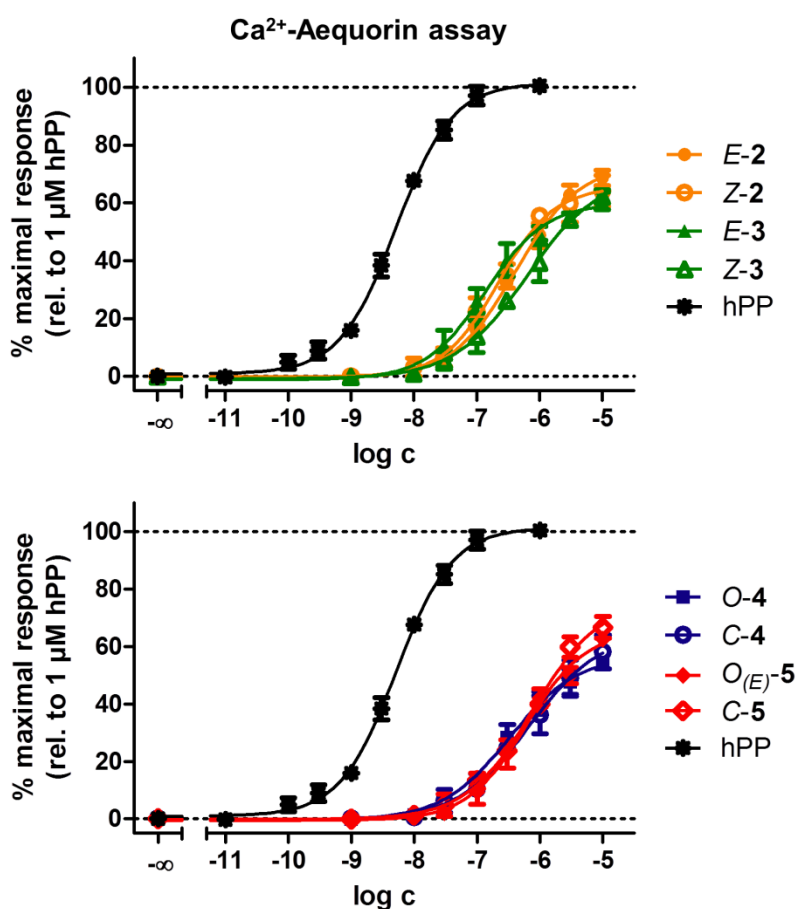
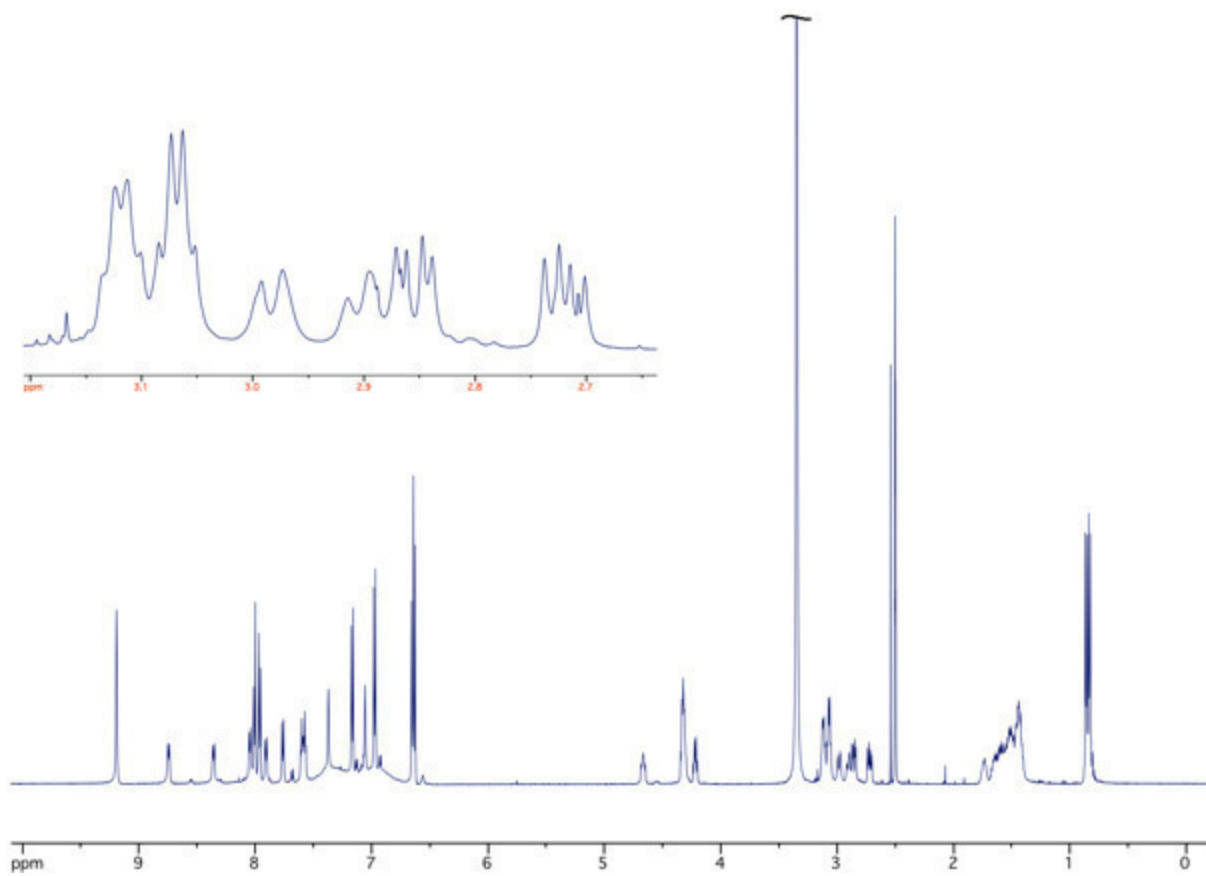
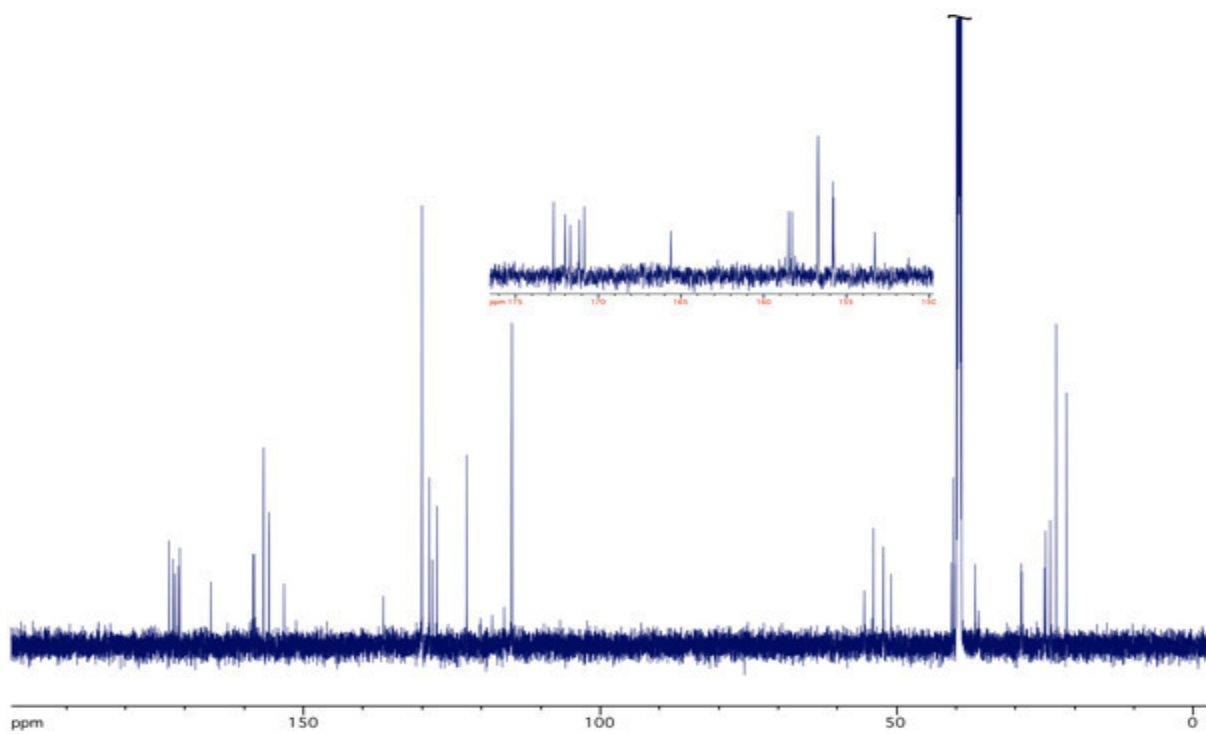
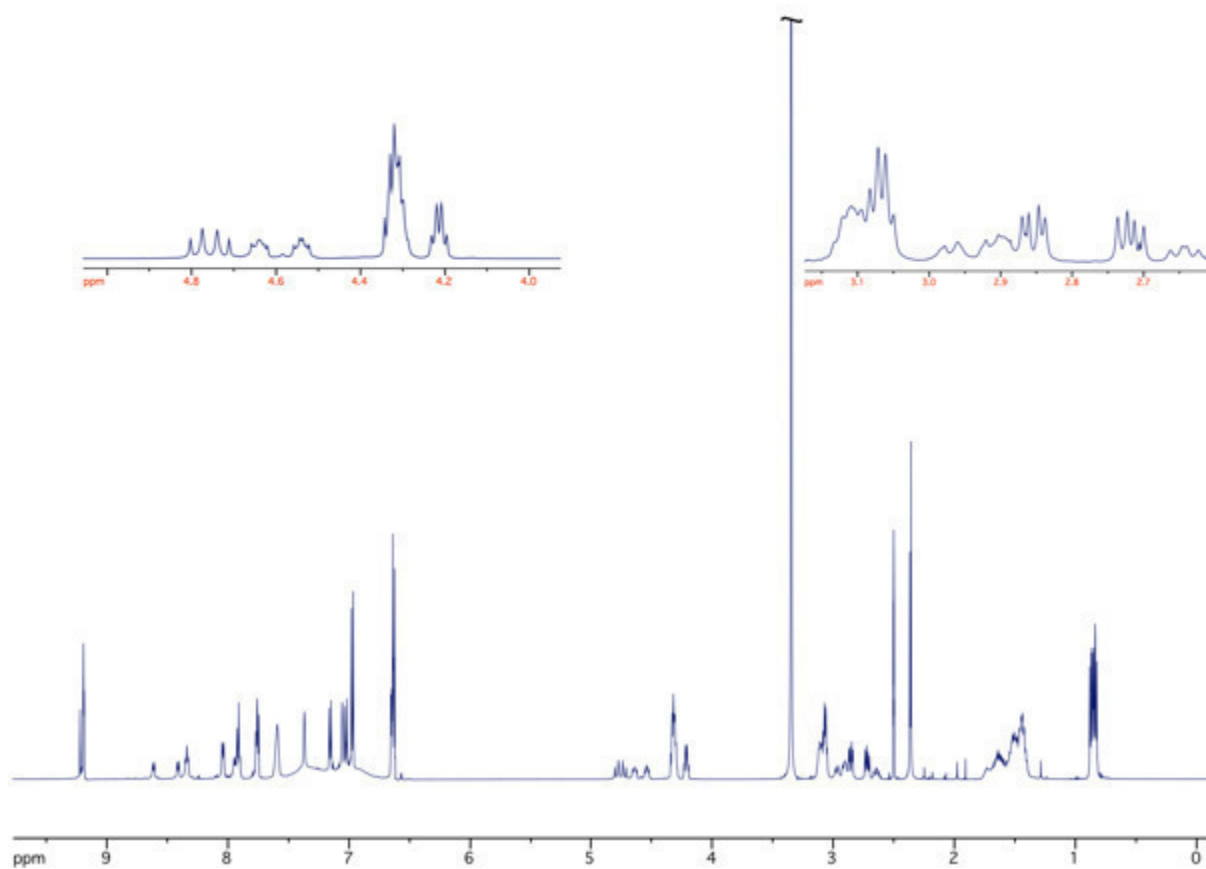
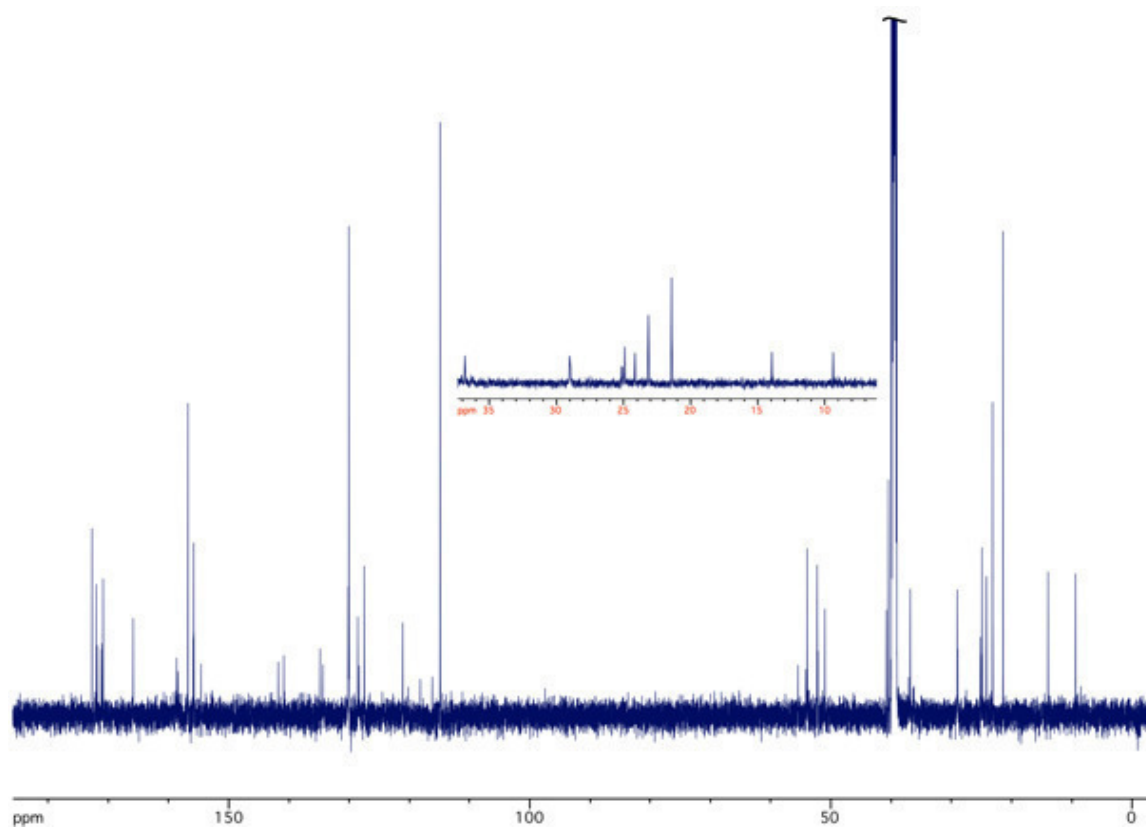


Figure S11. Y₄R functional activity (concentration-response curve) of *E/Z-2**, *E/Z-3**, *O/C-4** and *O_(E)/C-5** and the endogenous agonist hPP determined by measuring the intracellular Ca²⁺ mobilization in an aequorin assay using CHO-hY₄R-mtAEQ-G_{qi5} cells. Data represent means ± SEM from three or four independent experiments performed in triplicate. Data were analyzed by four parameter logistic fits (GraphPad Prism 5.0). Cellular responses were normalized to the effect of hPP elicited at a concentration of 1 μM.

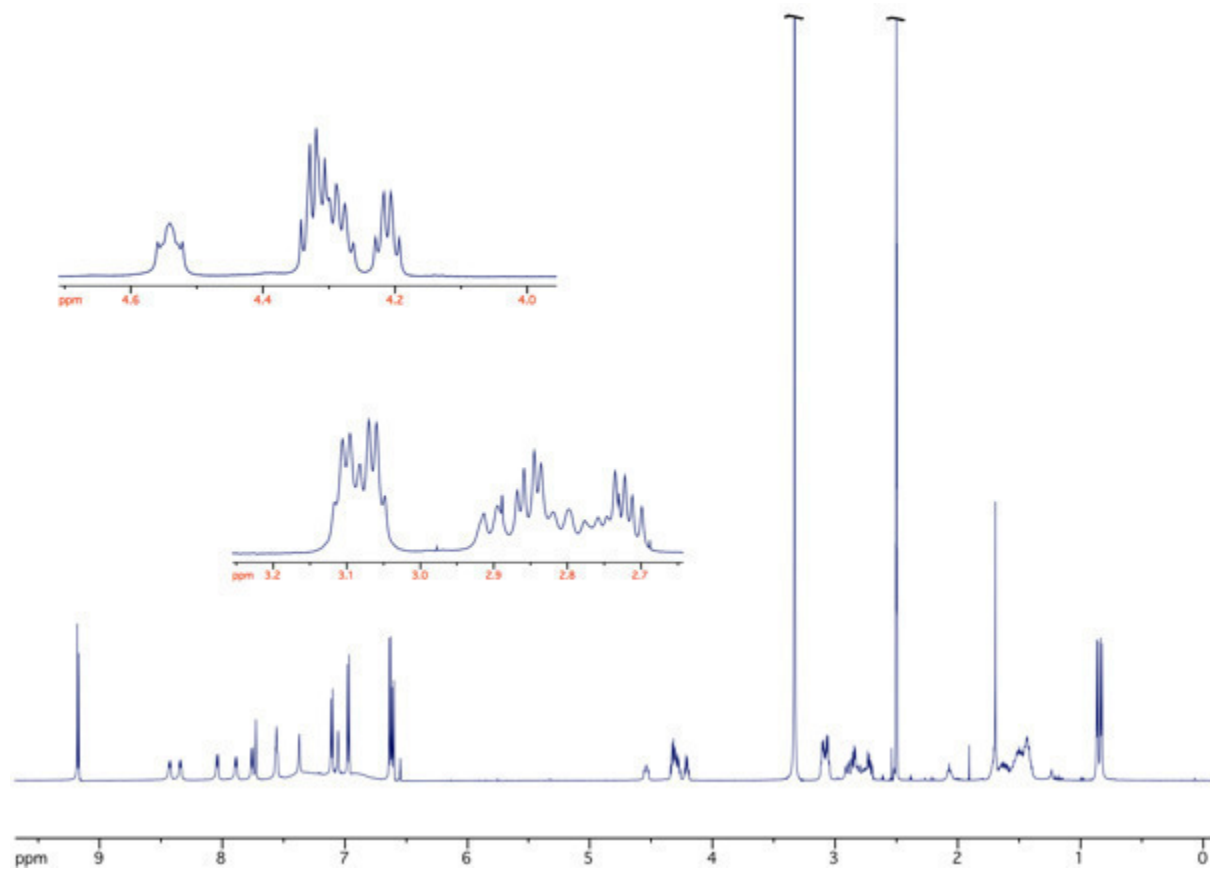
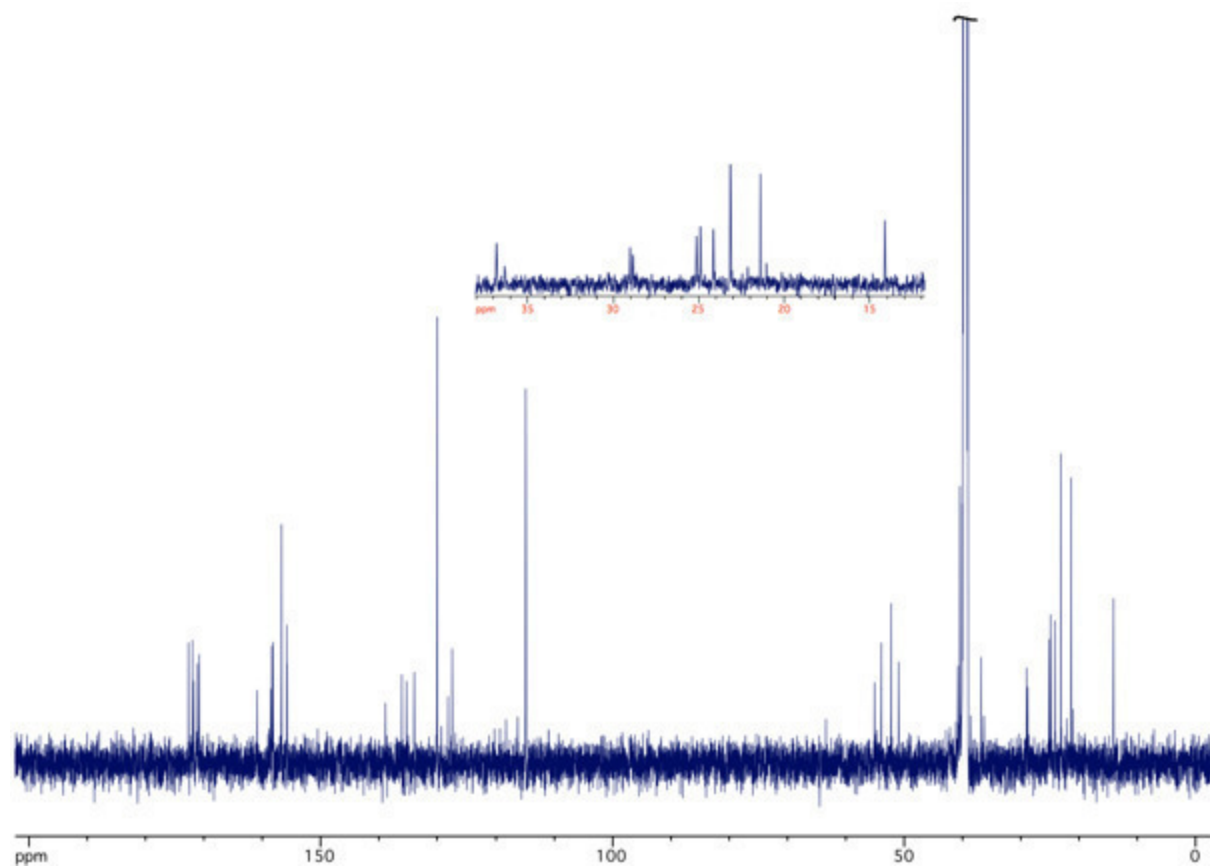
*For an approximation of achieved *E/Z* and *O/C* ratios (PSS) see **Tables 1** and **2** (main article).

7. NMR-spectraCompound **2** ^1H ($\text{D}_6\text{-DMSO}$, 600 MHz) ^{13}C ($\text{D}_6\text{-DMSO}$, 151 MHz)

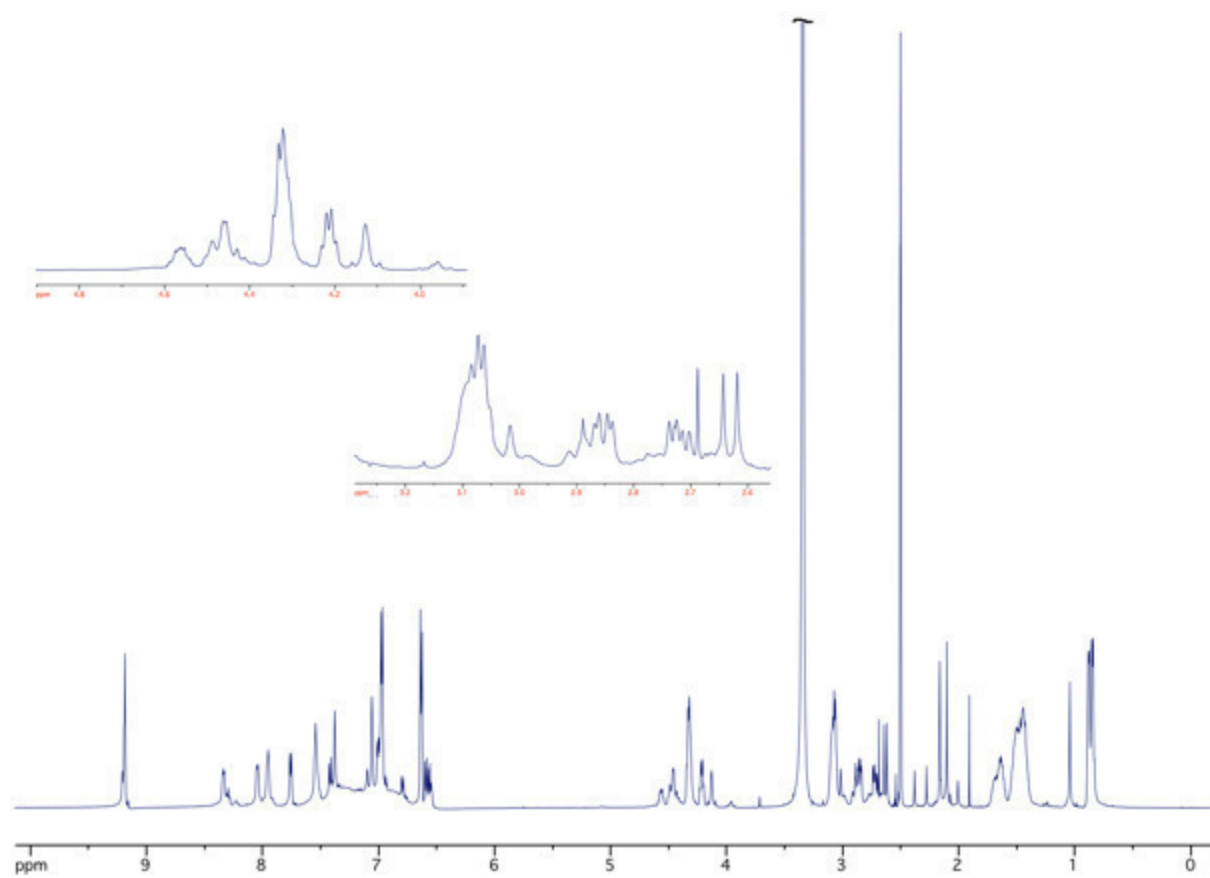
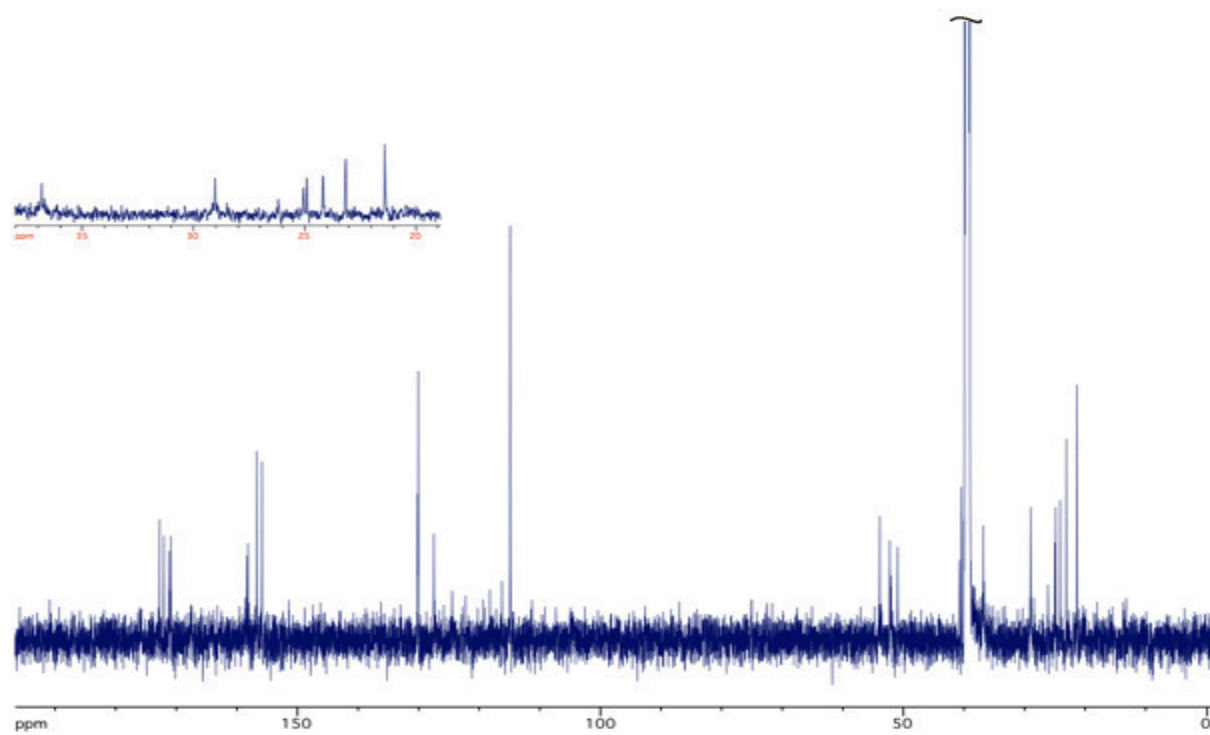
Compound 3

 ^1H ($\text{D}_6\text{-DMSO}$, 600 MHz) ^{13}C ($\text{D}_6\text{-DMSO}$, 151 MHz)

Compound 4

 ^1H ($\text{D}_6\text{-DMSO}$, 600 MHz) ^{13}C ($\text{D}_6\text{-DMSO}$, 151 MHz)

Compound 5

 ^1H ($\text{D}_6\text{-DMSO}$, 600 MHz) ^{13}C ($\text{D}_6\text{-DMSO}$, 151 MHz)

CHAPTER 3

3. Covalent binding photochromic GPCR-Ligands for single molecule spectroscopy

This chapter was in collaboration with the group of Prof. P. Gmeiner (University of Erlangen) and Prof. B. K. Kobilka (Stanford University School of Medicine).

D. Lachmann, R. Lahmy, J. Kaindl, M. Masureel, H. Hübner, P. Gmeiner, B. K. Kobilka, B. König

DL synthesized compounds **1 – 27, 29 – 49, 56, 58** and performed the corresponding photochemical measurements. RL synthesized compounds **28, 50 – 54** and performed the corresponding photochemical measurements. JK did the computational chemistry studies. MM did the single molecule fluorescence spectroscopy studies. BK supervised the project.

1. Introduction

Photochromic ligands are small molecules that act directly on endogenous proteins.¹ Several clinically significant receptors^{2,3} and ion channels^{4,5} have been targeted by photoresponsive molecules in the past but photochromic ligands are limited to a narrow concentration range and dilution in tissue reduces their efficacy.¹ In order to obtain photochromic ligands that are not diffusion limited, a series of covalent photoswitchable ligands were developed. They could be extremely useful in the functional dissection of closely related receptor subtypes, since selectivity can be achieved through covalent attachment to genetically engineered mutant receptors.^[L105a] These photochromic tethered ligands were comprised of a bioactive photoswitchable moiety and a reactive functionality that could covalently interact with certain amino acid residues in the target receptor binding site. To date, the majority of reports of such covalent ligands have been described for targeting G protein coupled receptors (GPCRs).^{7,8} GPCRs are transmembrane proteins that translate extracellular signals, including ions, hormones and peptides into intracellular responses and thus play a central role in many physiological and pathophysiological processes. Furthermore, they represent the largest group of targets for drug discovery over a broad spectrum of diseases.^{8,9} Even though GPCRs are an important class of receptors that have been heavily investigated, the molecular mechanisms responsible for ligand-dependent signalling still remain to be poorly understood. Controlling the diffusion by covalently binding ligands that could be triggered by light would offer a new way investigating the effects of ligand binding on receptor structure, dynamics and G-protein coupling.¹¹

Single-molecule fluorescence spectroscopy (SMFS) has become widely used for quantifying the conformational heterogeneity and structural dynamics of biomolecules *in vitro* and has been applied for studying GPCRs.¹⁰ In combination with this technique, covalent photochromic ligands could be used in a range of dynamic studies, localization and protein-protein associations to explore receptor-drug interactions.¹² Additionally, SMFS could be employed in another important study to attain key information on the process of ligand switching. It is currently believed that photoisomerization occurs once the ligand leaves the binding pocket, but it may be indeed possible that switching can proceed when bound to the receptor.¹³

The β_2 -adrenergic receptor (β_2 -AR) and the μ -opioid receptor (μ OR) are well-known receptors and both play a therapeutically very important role. The availability of X-ray crystal structures has allowed for structural insight that is beneficial when designing probe compounds.^{14,15} The highly potent β_2 -AR agonist BI-167107 and the μ -opioid receptor agonist fentanyl were chosen as good templates for the incorporation of photoswitches. In this project disulfide- and maleimide-modified azopyrazoles were incorporated into the structure of BI-167107¹⁶ and fentanyl¹⁷ to obtain covalent photochromic ligands. Disulfides were chosen as a covalent

tethering group due to their chemoselectivity for cysteine residues, while maleimides offer also the formation of a covalent bond to amino acids like lysine.

2. β_2 -Adrenergic receptor

β_2 -Adrenergic receptors belong to the family A of GPCRs and activate intracellular G-proteins upon binding catecholamine agonists, such as adrenaline and noradrenaline. The β_2 -adrenergic receptor is one of the best characterized GPCRs due to its role in several important physiological systems.¹⁸ The receptor plays a very important therapeutic role in the peripheral regulation of smooth muscle contraction, for instance in asthma. Furthermore, the β_2 -ARs are also widely expressed within the CNS, where they mediate a number of immunomodulatory, neuroprotective and cognitive enhancing effects.¹⁹ Synthetic ligands have been developed that either activate or inhibit the β_2 -AR, for example salmeterol, carazolol and BI-167107.

In order to target the β_2 -AR in our investigations, a mutation of H93C (Histidine 93C) to cysteine was performed. The covalent ligand for the β_2 -AR is modelled on the highly potent agonist BI-167107 and is designed to contain an azopyrazole as the photochromic scaffold and a disulfide (1) or a maleimide (2) as the covalent binding moiety (**Figure 1**).

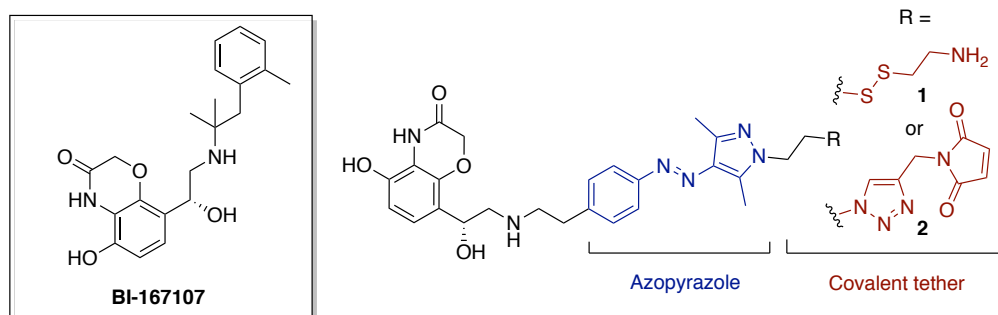


Figure 1. Target covalent photochromic β_2 -AR ligands **1** and **2** derived from the highly potent agonist BI-167107.

2.1 Molecular docking studies

Weichert *et al.* demonstrated that it is possible to covalently attach an agonist to the H93^{2,64}C mutant of the β_2 -AR while maintaining receptor affinity and activation.²⁰ We planned to adapt this approach to the structure of BI-167107 and further incorporated a photoswitch in the ligand.

To improve the design of these compounds and to better understand potential binding interactions, we performed covalent docking studies. Interestingly, **1** showed almost ideal binding behavior in these docking studies. When covalently attached to the H93C mutant receptor, the *Z*-conformation of compound **1**, displayed a binding mode comparable to BI-167107. In contrast, the *E*-conformation was predicted not to bind to the orthosteric site

(**Figure 2**). The results indicated that these ligands may indeed have a biologically active and inactive state, which is central in our investigations.

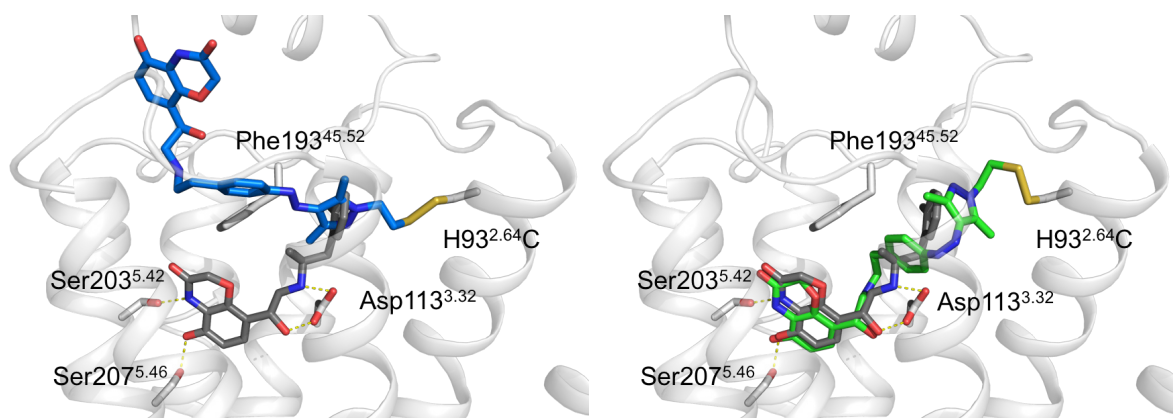


Figure 2. Superimposition of the bound compounds *E*-1- β_2 -AR (left) and *Z*-1- β_2 -AR (right) complex and the BI167107 (grey) active state structure of the β_2 -AR mutant H93C.

Compound **2** bearing a maleimide as the reactive group showed only minor docking differences between the isomers when covalently bound to the receptor. As the maleimide also binds covalently to other nucleophilic residues, we additionally considered two lysine residues as covalent attachment points. Lys97 in the extracellular loop 1 (ECL1) and Lys305^{7.32} in transmembrane helix (TM) 7. When considering the H93C as the anchor point, neither the *E*- nor the *Z*-conformation of ligand **2** resulted in a binding mode in the orthosteric binding site. When covalently attached to the two lysine residues, the predicted binding modes of ligand **2** were comparable to BI-167107 for both the *E*- and *Z*-conformations (**Figure 3**).

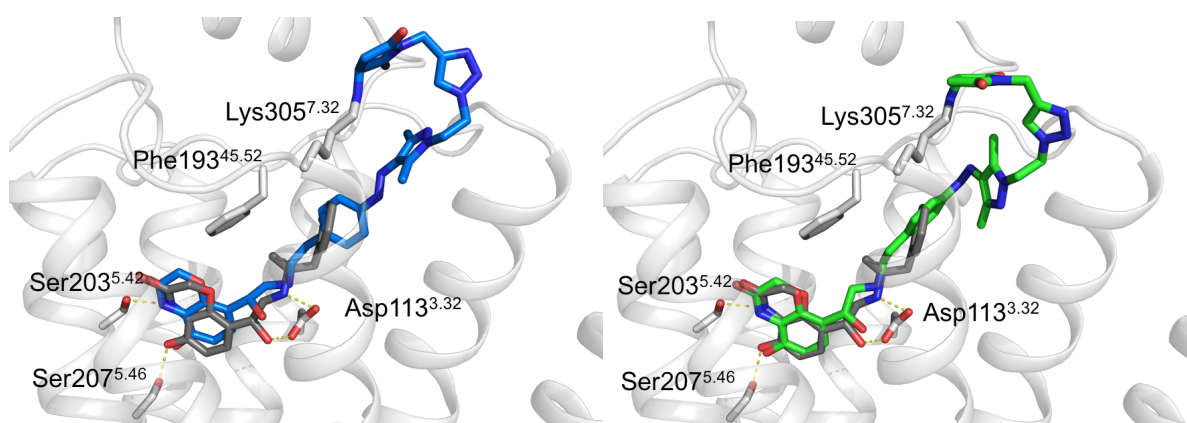
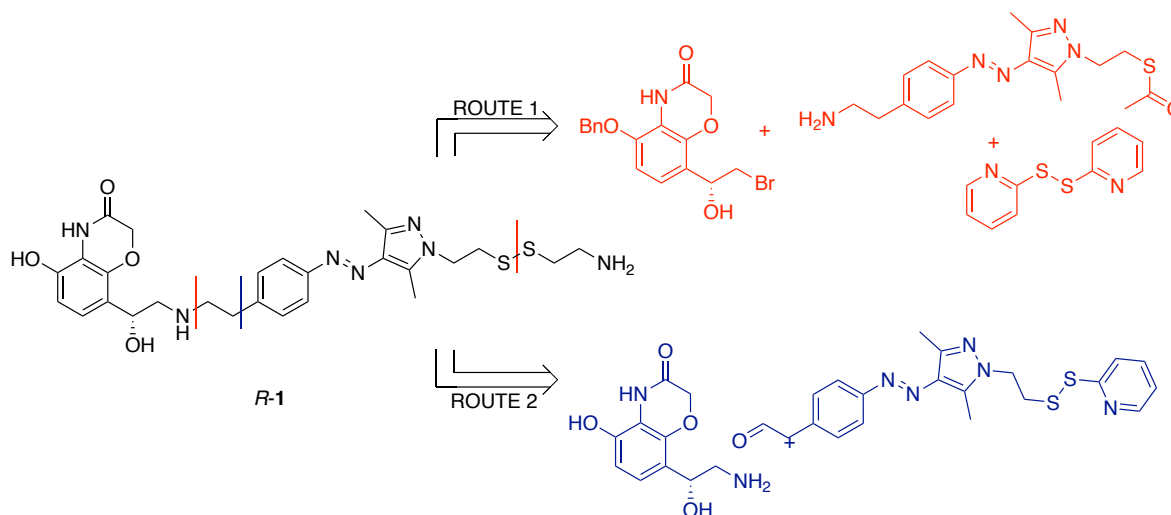


Figure 3. The *E*-isomer (left) and the *Z*-isomer (right) of **2** superimposed over BI-167107 (grey) bound to the β_2 -AR mutant H93C.

2.2 Synthesis of the photochromic β_2 -AR ligands

Retrosynthetic analysis of compound **1** followed two main routes (**Scheme 1**). In the first approach, the benzoxazinone and the azopyrazole is synthesized individually in parallel. The photochromic moiety and the benzoxazinone is connected in an S_N -type reaction to form a non-covalent hydroxyl precursor. The last steps would be the disulfide synthesis and the Bn-deprotection. In the second route two precursors are synthesized and the final step would be a reductive amination.

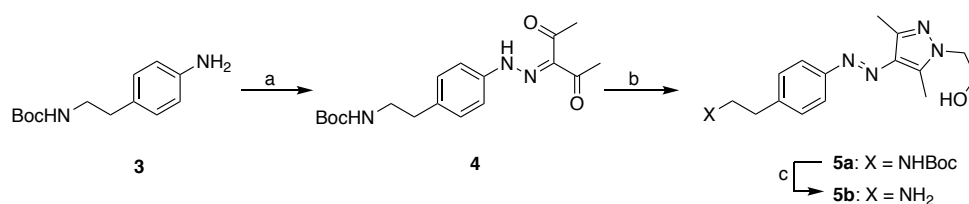


Scheme 1. Retrosynthetic analysis of compound **1** presenting two possible strategies.

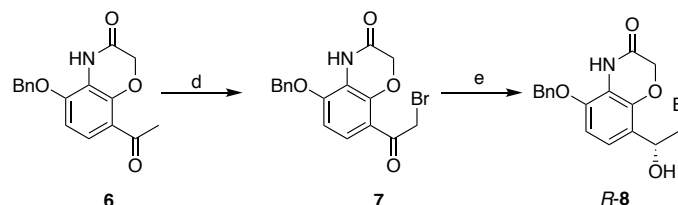
For compound **2** similar approaches could be considered or using an azopyrazole azide and an alkyne maleimide to attach the covalent moiety via a click reaction.

Following route 1, azopyrazole **5** was successfully synthesized via diazotization and subsequently condensation in good yield (**Scheme 2A**). The benzoxazinone scaffold **6** was synthesized according to a published synthetic route described by Pappano *et al.*²² Highly selective α -bromination of ketone **6** could be done to obtain the α -bromoketone **7**. The α -brominated ketone **7** was transformed into its secondary alcohol in a stereoselective reduction (Corey-Bakshi-Shibata, CBS) to form the enantiomerically pure compound *R*-**8** (**Scheme 2B**).²³ The enantiomeric excess (ee) was determined by chiral HPLC and revealed excellent ee values of 95% and is described in more detail in the Supplementary Figure **SI-1**.

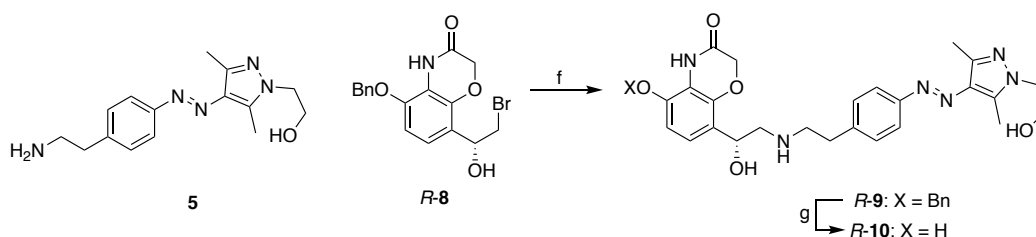
A)



B)



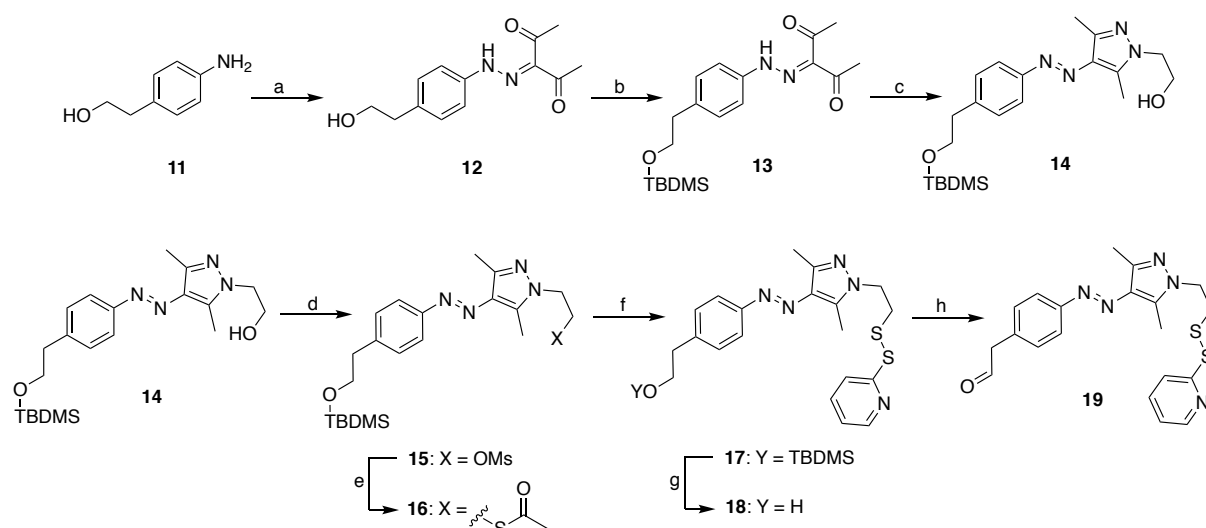
C)



Scheme 2. Precursor synthesis of ligand **1** and **2** following route 1. A) Azopyrazole synthesis: (a) NaNO₂, H₂O, HCl, AcOH, 1 h, 0 °C, then acetylacetone, NaOAc, EtOH, 1 h, r.t. 60%. (b) 2-Hydrazinoethanol, EtOH, 3 h, reflux, 45%. (c) TFA, CH₂Cl₂, 1 h, r.t., 98 %. B) Benzoxazinone precursor: (d) CuBr₂, EtOAc, 50 °C, 24 h, 67%. (e) THF-BH₃, (R)-(+)-2-Methyl-CBS-oxazaborolidine, THF, Ar, 2.5 h, r.t., 64%. C) Synthesis of *R*-**10**: (f) K₂CO₃, KI, MeCN, 12 h, 70 °C, 5%. (g) Pd/C, H₂, MeOH, 5 min, r.t. 23%.

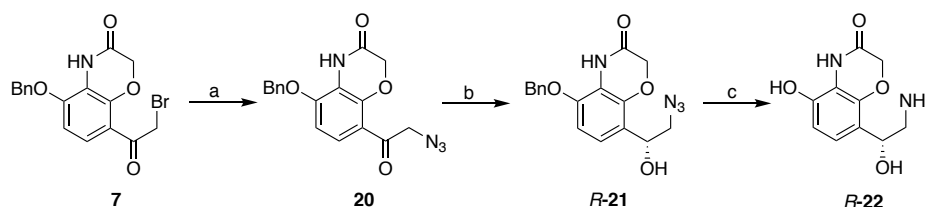
The hydroxy intermediate *R*-**9** was formed in an S_N-reaction under basic conditions and utilizing KI as a catalyst. Low yields were obtained and the subsequent Bn-deprotection showed only poor reproducibility. As the reaction of the azopyrazole with the pharmacophoric moiety *R*-**8** showed only low yields, as well as the deprotection of *R*-**9**, a better approach may be to first introduce the covalent moiety and do the coupling of pharmacophore and photoswitch at the last step of the synthesis. This approach is described in route 2.

The intermediate **12** was synthesized in a similar way to compound **4**. The hydroxyl moiety of **12** was then protected with TBDMS-Cl and condensation with hydrazinoethanol yielded the azopyrazole **14**. The mesitylation of compound **14** and subsequent nucleophilic replacement gave the thioester **16**. The thioester **16** was transformed to the thiopyridil disulfide **17** via methanolysis. Deprotection and oxidation with Dess-Martin Periodane of compound **18** yielded the aldehyde **19** in very good yields (**Scheme 3**).



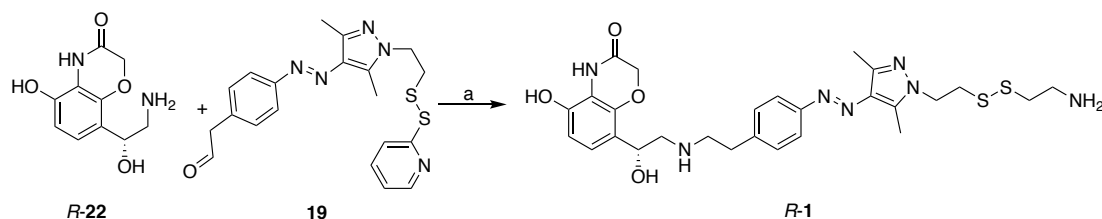
Scheme 3. Synthesis of the thiopyridyl-azopyrazole **19**. (a) NaNO_2 , H_2O , HCl , AcOH , 1 h, 0°C , then acetylacetone, NaOAc , EtOH , 30 min, r.t. 84%. (b) TBDMS-Cl, imidazole, DMF, 2 h, r.t., 29%. (c) 2-Hydrazinoethanol, EtOH , 3 h, reflux, 45%. (d) MsCl , NEt_3 , CH_2Cl_2 , 1 h, 0°C , 84%. (e), KSAc , acetone, 3 h, reflux, 74%. (f) 2-Aldrithiole, NaOMe , MeOH , 24 h, r.t., N_2 , 94%. (g) TBAF, THF, 3 h, r.t., 56%. (h) DMP, CH_2Cl_2 , Ar, 1 h, 0°C , 91%.

Azide **R-21** was synthesized in two steps via nucleophilic displacement of the bromine of **7** and subsequent enantioselective CBS-reduction of the ketone **20**. Simultaneous cleavage of the benzyl protection group and the reduction of the azide of compound **R-22** was accomplished by a transfer hydrogenation with good yields (**Scheme 4**).



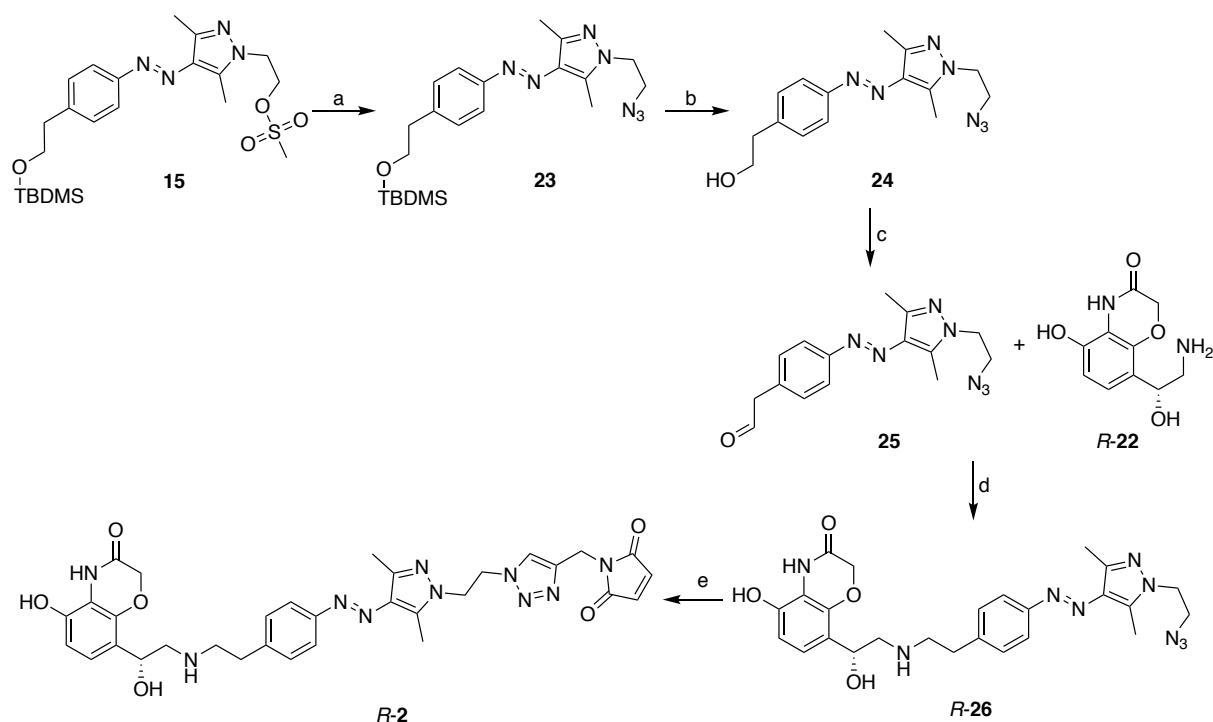
Scheme 4. Synthesis of precursor **R-22**. (a) NaN_3 , DMF, 2 h, r.t., 90%. (b) THF-BH_3 , (R)-(+)-2-Methyl-CBS-oxazaborolidine, THF, Ar, 2.5 h, r.t., 25%. (c) Pd/C , Et_3SiH , MeOH , 1 h, r.t., 89%.

To avoid regioselectivity problems, compound **19** containing a protected disulfide instead of the cysteamine containing disulfide moiety was used for the reductive amination. Treating the thiopyridyl group containing intermediate with cysteamine resulted in the formation of the target disulfide **R-1** (**Scheme 5**).



Scheme 5. Target ligand synthesis in a reductive amination of compound **R-22** and **19**. (a) NaBH_3CN , MeOH/MeCN, 16 h, r.t., then cysteamine, MeOH, 1 h, r.t., 4%.

The synthesis of the covalent β_2 -AR ligand **R-2** was done in a similar way as **R-1**. The deprotected benzoxazinone **R-22** was converted to the intermediate **R-26** in a reductive amination with the azopyrazole-aldehyde **24** in acceptable yields. The crude **R-26** was converted to the desired β_2 -AR ligand **R-2** by applying click chemistry. The Cu(II) salt was pre-complexed with TBTA and mixed with the *N*-propargylmaleimide and the azide **R-26** followed by the addition of Na-ascorbate to initiate the click reaction (**Scheme 6**).



Scheme 6. Synthesis of the maleimide based ligand **R-2**. (a) NaN_3 , DMSO, 24 h, 60 °C, Ar, 82%. (b) TBAF, THF, 24 h, r.t. 87%. (c) DMP, CH_2Cl_2 , Ar, 1 h, 0 °C, 92%. (d) $\text{NaHB}(\text{OAc})_3$, THF/MeCN, r.t., Ar. (e) *N*-Propargylmaleimide, CuSO_4 , TBTA, Na-ascorbate, $t\text{BuOH}/\text{THF}/\text{H}_2\text{O}$, 2 h, r.t., Ar, 25%(over d-e).

2.3 Photophysical investigations

The azopyrazoles were chosen as the photochromic scaffold in the target β_2 -AR ligands due to their excellent photochromic properties. The absorbance bands of the *E*- and *Z*-isomer of compounds **1**, **2** and **10** showed better separated absorption bands compared to the *E*- and

Z-isomers of azobenzenes (**Figure 2**).²⁴ This resulted in excellent PSS values for both the *E* to *Z* and the *Z* to *E* isomerization. Also, the thermal isomerization rate of the azopyrazoles **1**, **2** and **10** exhibited high values up to $t_{1/2} = 13.4$ days in aqueous buffer. **Table 1** summarizes the photochromic properties of compounds **1**, **2** and **10**. The cycle performance of compounds **1**, **2** and **10** was investigated during alternate irradiation with light of 365 nm for 1 second and 528 nm for 70 seconds (**SI-2**) and all compounds showed high fatigue resistance.

Table 1. Photochemical data of synthesized compounds **1**, **2** and **10**.

| Entry | Ligand | Solvent | λ_{\max} | λ_{\max} | λ_{iso} | $t_{1/2}$ | PSS | |
|----------|-----------|-----------------------|----------------------|----------------------|------------------------|-----------|---|---|
| | | | (<i>E</i>) [nm] | (<i>Z</i>) [nm] | [nm] | | (<i>E</i> → <i>Z</i>) ^[a,b] <i>E</i> : <i>Z</i> | (<i>Z</i> → <i>E</i>) ^[a,c] <i>E</i> : <i>Z</i> |
| 1 | 1 | DMSO | 343 | 293, 443 | 300, 414 | 7.0 | 1:99 | 86:14 |
| 2 | 1 | Buffer ^[d] | 335 | 292, 436 | 296, 400 | 2.9 | 13:87 | 90:10 |
| 3 | 2 | DMSO | 342 | 276, 445 | 300, 417 | 25.5 | 14:86 | 91:9 |
| 4 | 2 | Buffer ^[d] | 336 | 249, 431 | 297, 408 | 13.4 | 13:87 | 90:10 |
| 5 | 10 | DMSO | 263, 242 | 442 | 301, 412 | 5.6 | 15:85 | 99:1 |
| 6 | 10 | Buffer ^[d] | 262, 338 | 438 | 299, 402 | 11.3 | n.d. | n.d. |

[a] Determined by HPLC measurements at 25 °C, *E/Z* ratio detected at the isosbestic points. [b] The *E*→*Z* isomerization was done with a LED of 365 nm. [c] The *Z*→*E* isomerization was done with a LED of 528 nm. [d] Tris buffer: 50 mM Tris, 1 mM EDTA, 1 mM MgCl₂, 0.1% DMSO.

The reason for the high thermal stability of the *Z*-isomer can be due to a combined effect of steric and electronic effects, as well as hydrogen bonding.²⁵

2.4 Biological investigations

Radioligand binding studies at the β_2 -AR¹⁹ were performed to study the individual ligand receptor interactions of the covalent photochromic ligands **1**, **2** and the non-covalent ligand **10**. The covalent ligands **1** and **2** were also investigated towards binding to the β_2 -AR mutants β_2 -AR^{H93C} and β_2 -AR^{K305C} in which the specific positions, the amino acids were mutated to cysteine providing selective covalent binding.^{26,27} Individual testing of every isomer was done and the *E*-isomer of **1** showed high affinity at the β_2 -AR receptors but only slight affinity

changes when focusing on the Z-isomer. Initial functional experiments were done without focusing on the covalent binding of the target compounds **1** and **2**. The efficacy of the compounds was investigated in a β -arrestin recruitment assay (PathHunter assay, Eurofins) and the ligands displayed similar efficacies being partial agonists. Similar to the binding data, also the efficacies showed only 2- or 3-fold difference between the individual isomers.

Table 2. Radioligand binding data for ligands **1**, **2** and **10** towards β_2 -AR, β_2 -AR^{H93C}, β_2 -AR^{K305C} and receptor activation data for β -arrestin recruitment at the β_2 -AR.

| Entry | Ligand | Binding $K_i \pm \text{SEM}$ [nM] ^[a] | | | β -arrestin recruitment EC_{50} [nM] ^[b] | |
|----------|----------------|---|-------------------------------|--------------------------------|--|----------|
| | | β_2 -AR | β_2 -AR ^{H93C} | β_2 -AR ^{K305C} | β_2 -AR | α |
| 1 | Norepinephrine | 4700 \pm 1193 | n.d. | n.d. | 6700 | 1.00 |
| 2 | <i>E</i> -1 | 0.88 \pm 0.14 | 1.5 \pm 0.13 | 0.45 \pm 0.14 | 190 | 0.76 |
| 3 | <i>Z</i> -1 | 1.4 \pm 0.09 | 0.84 \pm 10 | 0.37 \pm 0.09 | 110 | 0.72 |
| 4 | <i>E</i> -2 | 30 \pm 7.9 | 28 \pm 9.6 | 16 \pm 11 | 670 | 0.90 |
| 5 | <i>Z</i> -2 | 85 \pm 39 | 50 \pm 13.4 | 190 \pm 20 | 1000 | 0.73 |
| 6 | <i>E</i> -10 | 91 \pm 12 | n.d. | n.d. | 670 | 0.82 |
| 7 | <i>Z</i> -10 | 700 \pm 108 | n.d. | n.d. | 2100 | 0.88 |

[a] Binding data determined by competition binding with [³H]CGP12177; K_i values in nM \pm standard error of the mean (SEM) derived from 2 to 4 individual experiments each performed in triplicate; n.d. = not determined. [b] EC_{50} values and intrinsic activities (α) relative to Norpinephrine.

The idea of the covalent ligands is, that the azopyrazole is connecting the pharmacophore with the covalent tether and therefore geometric changes should effect binding or activation when toggling between the two photoisomers. Experiments, focusing on efficient and irreversible blocking of radioligand binding have to be done utilizing the covalent tether.

2.5 Single molecule spectroscopy

Receptor activation assays were done on a detergent-purified receptor (wild type, without mutation) in solution (Stanford, Kobilka lab). The readout of this assay is based on a single-molecule FRET to probe conformational transitions.¹¹ The dye Atto655 is covalently linked to the end of TM6 (L266C) of the β_2 -AR and the fluorescence (655nm) is quenched by an engineered tryptophan in TM5 (L320W) in the inactive state. Upon activation, TM6 moves towards and away from L320W, releasing the fluorescence quenching. Initial experiments were done with the non-covalent binding photochromic ligand **10**. In the experiment, the

fluorescence intensities indicates the conformational changes occurring when a ligand is bound to the receptor.

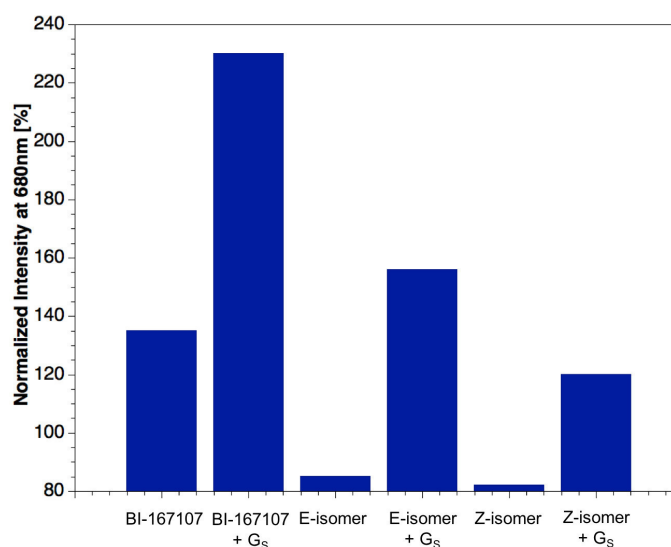


Figure 4. Comparison of the normalized fluorescence intensity of the high potent agonist BI-167107 and *E/Z*-isomers of compound **10** with absence and presence of the G_S-protein.

The experiments in absence of a G-protein showed that the binding to β_2 -AR of the ligands is possible. In accordance to the radioligand binding studies of the β_2 -AR receptor (wild type, see **Table 2**, entry 6 and 7) the *E*-isomer showed better binding than the *Z*-isomer of compound **10**. In the presence of the G-protein the *E*- and *Z*-isomer of **10** appear to enable G-protein coupling, although to a much lower extent than the high potent agonist BI-167107 (**Figure 4**). This suggests that both photoisomers behave like partial agonists and since both isomers gave similar responses and enable G-protein coupling, it might be difficult to use them to selectively turn activation on or off.

3. μ -Opioid receptor

The μ -opioid receptor (μ OR) is one of the oldest and most important drug targets due to its primary responsibility for the effects of opium. The activation of the G_i coupled GPCR displays powerful analgesic and sedation effects, as well as euphoria and physical dependence.²⁹ Besides the historic opiate Morphine, which is an alkaloid from the opium poppy that mainly targets the μ OR, more potent synthetic opioid agonists have been developed, including BU72, pethidine, tapentadol and fentanyl. To sever the analgesic properties of opioids from their euphoric and addictive side effects lots of research towards analgesics with reduced side effects was done.³⁰ Recent studies have suggested that opioid-induced analgesia results from μ OR G-protein signalling, while many side effects may be caused via β -arrestin pathway signalling downstream of μ OR activation.³¹ To get a better understanding of the different activation pathways, photochromic ligands could support the investigation of the μ OR. Recently, reversible photochromic fentanyl-azobenzenes were developed by Trauner *et al.* and studied by electrophysiology.³⁰ Based on the structure of this photochromic azobenzene-fentanyl, we developed a covalent ligand bearing an azopyrazole as the photochromic moiety. Targeting different amino acids in the binding pocket, three different covalent groups were used: Disulfide (**27**), maleimide (**28**) and an *N*-hydroxysuccinimide (NHS) ester **29** (**Figure 5**).

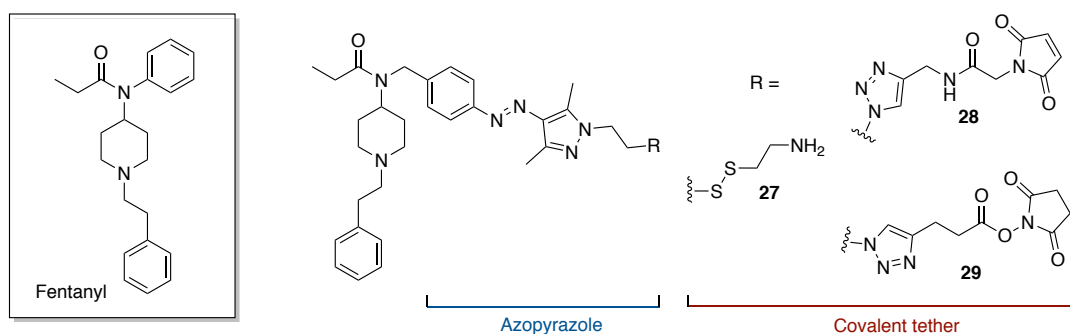


Figure 5. Fentanyl derived covalent target structures **27**, **28** and **29** bearing an azopyrazole as the photochromic scaffold.

3.1 Docking studies towards the μ OR

Manglik *et al.* successfully applied the N^{2.63}C mutant in order to achieve covalent binding of the PZM29 ligand to the receptor bearing a disulphide.³¹

We designed potential covalent agonists bearing an azopyrazole addressing this mutation. In the presented docking studies, depicted in **Figure 6**, the active state μ OR crystal structure in complex with agonist BU72 was used. At first, we confirmed our design utilizing covalent docking for compounds **27** and **28**. We were encouraged by the docking results for compound **27**, as the *Z*-conformation displayed a receptor ligand conformation showing a canonical salt-bridge to Asp3.32, which was not observed for the respective *E*-conformation. This suggested

that when covalently attached to the receptor, the ligand is able to form favorable ligand receptor conformations and may allow the receptor activation only when switched to the Z-conformation, which is desirable (**Figure 6**).

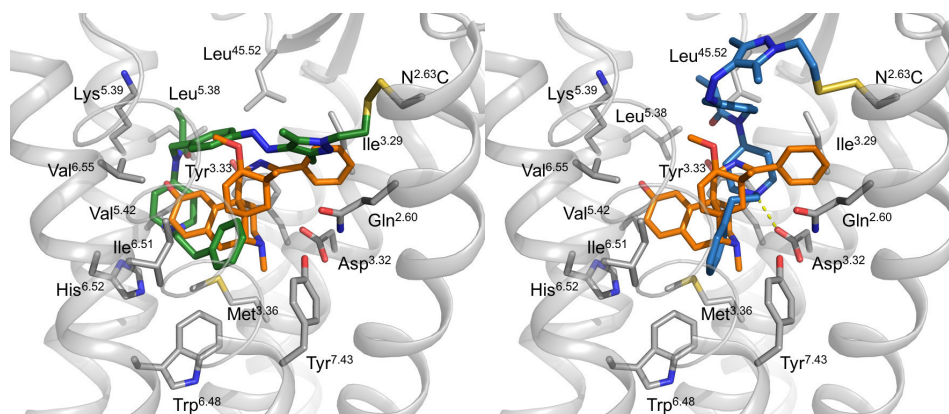
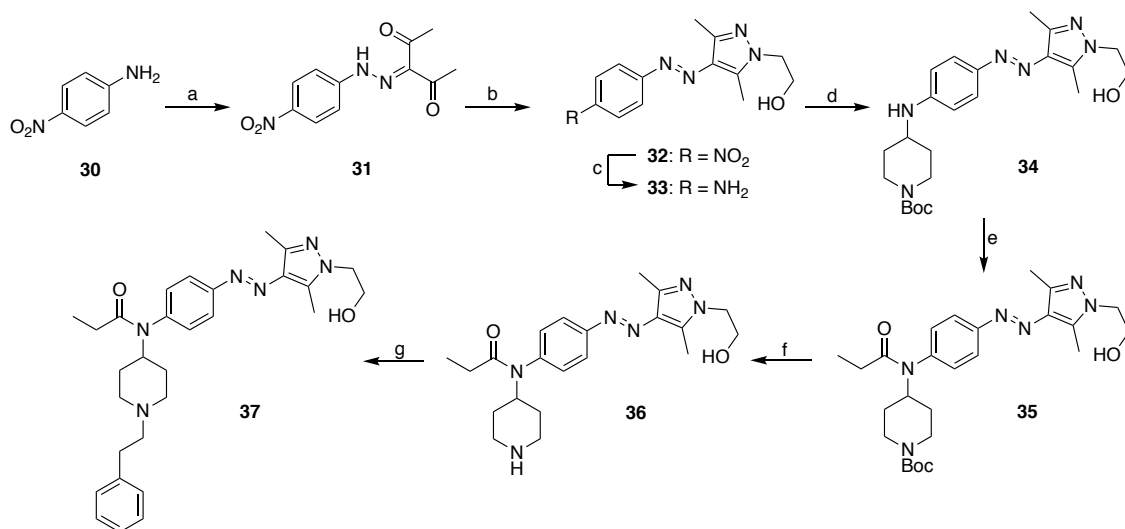


Figure 6. Docking pose of compound *E*-27 (left, green) and compound *Z*-27 (right, blue). The co-crystallized agonist BU72 is shown as orange sticks.

For compound **28** bearing the maleimide tether-group the docking results were rather ambiguous when considering the attachment to the latter cysteine mutant. Neither the *E*- nor the *Z*-conformation showed the salt-bridge to Asp3.32 in our docking studies (**SI-3**). As the maleimide is also able to address other nucleophilic amino acids, such as lysine residues, the next step would be to consider additional residues for a covalent attachment. As compound **29** exhibited a very reactive tether that does not favor any mutant, we did not consider any docking studies for this ligand.

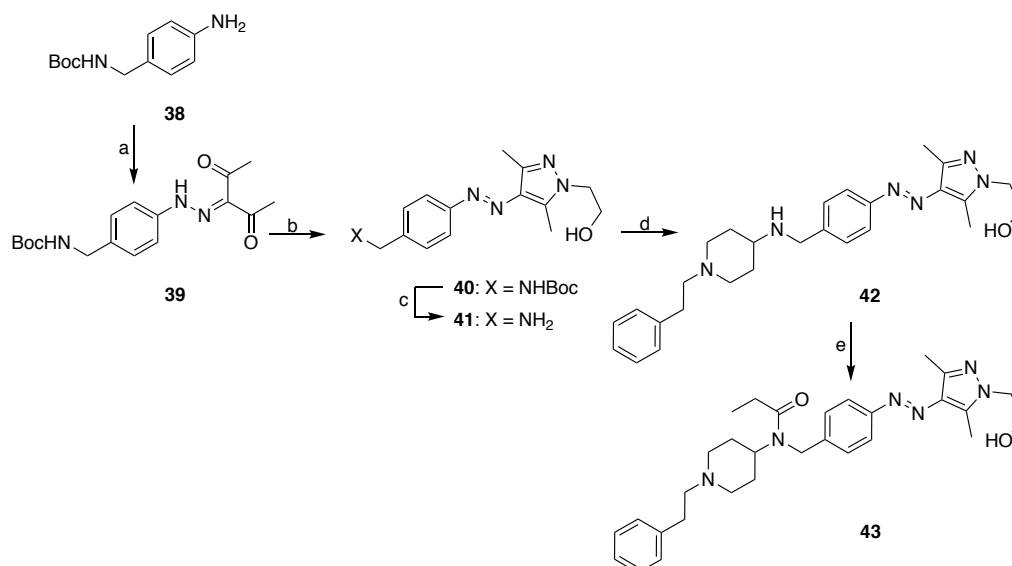
3.2 Synthesis of the azopyrazole based fentanyl derivatives

The first approach in synthesizing the covalent ligands was similar to the recent publication of Trauner *et al.*³⁰ First, the photochromic moiety **33** was formed in the diazotization of nitroaniline, followed by subsequent coupling with acetylacetone. Second, the pharmacophoric moiety was attached with reductive amination and acylation of the secondary amine of **36** (**Scheme 7**). The attachment of the covalent tether should be done as the last step, avoiding side reactions of the reactive covalent binding groups.



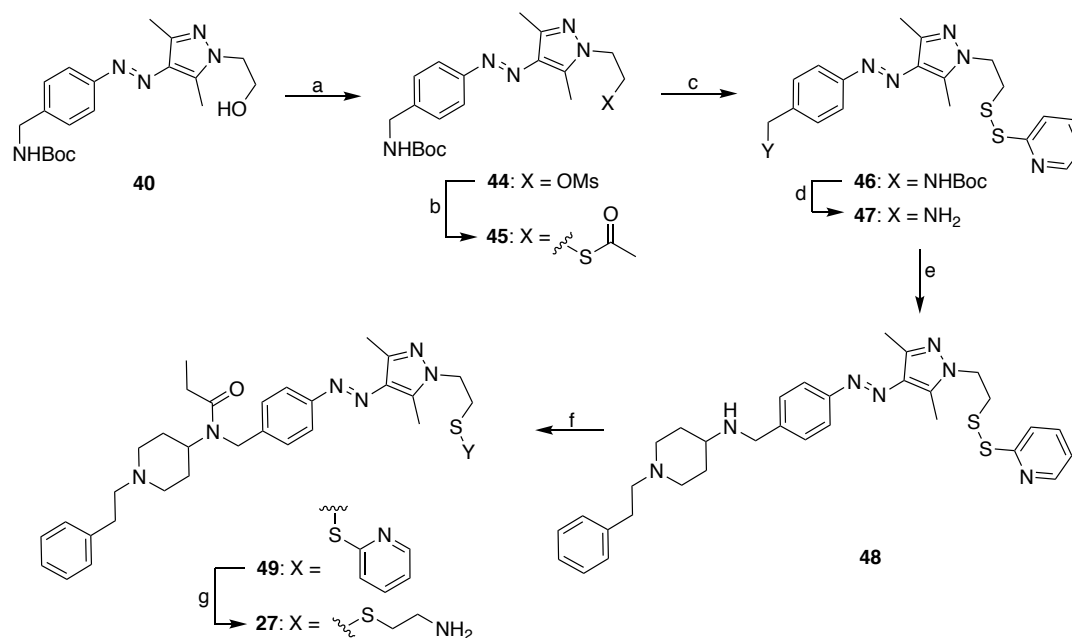
Scheme 7. Synthesis of the photofentanyl precursor **37**. (a) NaNO₂, HCl, H₂O, AcOH, 45 min, 0 °C, then NaOAc, EtOH, 1 h, 0 °C, 92%. (b) Hydrazinoethanol, EtOH, 3 h, reflux, 53%. (c) Na₂S₂, THF/H₂O, 3 h, 80 °C, 93%. (d) Tert-butyl-4-oxopiperidine-1-carboxylate, NaHB(OAc)₃, AcOH, DCE, 24 h, r.t., 77%. (e) Propionyl anhydride, DMAP, toluene_{dry}, N₂, 24 h, r.t., 59%. (f) TFA, CH₂Cl₂, 1 h, r.t., 87%. (g) Phenylacetaldehyde, NaHB(OAc)₃, AcOH, DCE, 24 h, r.t., 45%.

Initial determination of the photochromic properties of compound **37** showed only a very short thermal half-life of 37 seconds for the Z-isomer. As this half-life did not fit to the conditions of the biological assay, a structural modification to enhance the photochemical properties was performed. In order to improve thermal stability of the Z-isomer, an aminomethyl scaffold was utilized instead of the aniline, isolating the azopyrazole and the amide.³² We did not expect a significant loss of potency when changing the structure, as it was previously reported that using an aminomethyl scaffold should only slightly change the biological properties.³³



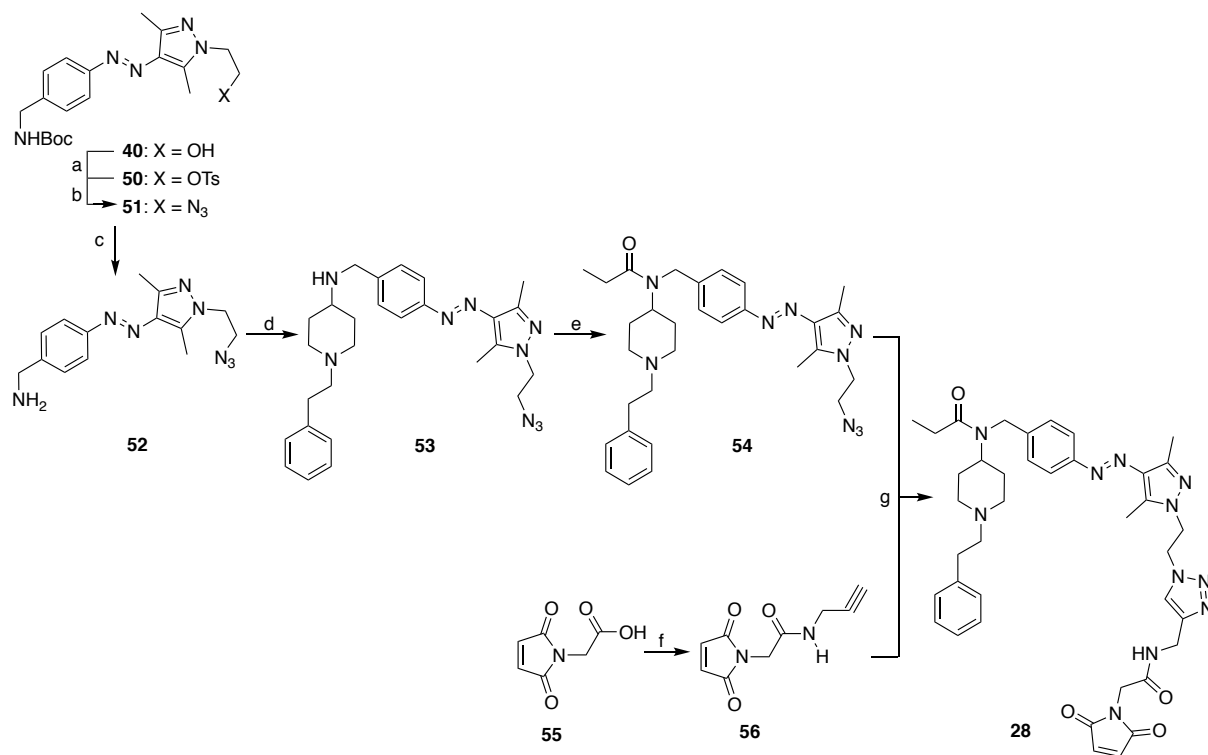
Scheme 8. Synthesis of the methylene analog **43** to fentanyl photoswitch **37**. (a) HCl, NaNO₂, AcOH, 0 °C, 0.75 h, and then acetylacetone, NaOAc, EtOH, 0.5 h, r.t., 90%. (b) Hydrazinoethanol, EtOH, 3 h, reflux, 63%. (c) TFA, CH₂Cl₂, 1 h, r.t., 95%. (d) 1-Phenethyl-4-piperidone, NaHB(OAc)₃, AcOH, DCE, 20 h, r.t., 37%. (e) Prop₂O, DMAP, DIPEA, 24 h, r.t., and then KOH, MeOH, H₂O, 24 h, r.t., 7%.

The synthetic route for synthesizing the covalent target structures follows a similar strategy as used in the synthesis of the β_2 -AR ligands. The disulfide moiety of compound **27** was introduced by the thiopyridyl strategy.



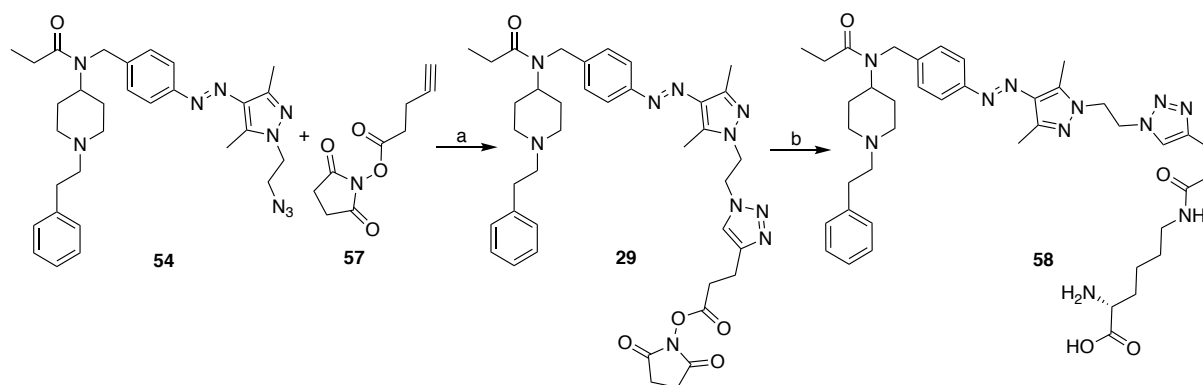
Scheme 9. Synthesis of target compound **27**. (a) MsCl, NEt₃, CH₂Cl₂, 1 h, r.t., 97%. (b) KSAc, acetone, 3 h, reflux. (c) 2-Aldrithiol, NaOMe, MeOH, 20 h, r.t., 67%(over b+c). (d) TFA, CH₂Cl₂, 1 h, r.t. 95%. (e) 1-Phenethyl-4-piperidone, NaHB(OAc)₃, AcOH, DCE, 20 h, r.t., Ar, 88%. (f) Propionylchloride, NEt₃, CH₂Cl₂, 10 min, r.t., 95%. (g) Cysteamine, MeOH, 1.0 h, r.t., Ar, 95%.

The maleimide derivative was synthesized via Cu^I-assisted click chemistry. First, compound **40** was converted to the corresponding azide **51**. The pharmacophoric core was then formed in a reductive amination, followed by an acylation to obtain intermediate **54**. Cycloaddition with alkyne **56**, which was obtained by the amide formation of the activated carboxylic acid **55** and propargylamine, gave the target triazole **28** (Scheme 10).



Scheme 10. Fentanyl azopyrazole-maleimide **28** synthesis. (a) TsCl, Et₃N, CH₂Cl₂, r.t., 16 h, 76%. (b) NaN₃, NaI, DMSO, 65 °C, 24 h, N₂, 72%. (c) TFA, CH₂Cl₂, 0 °C → r.t., 1 h, 99%. (d) 1-Phenethyl-4-piperidone, NaHB(OAc)₃, AcOH, DCE, 16 h, r.t., 64%. (e) Propionyl chloride, Et₃N, CH₂Cl₂, r.t., 1 h, N₂, 71%. (f) Oxalylchloride, THF, 2 h, Ar, r.t., then propargylamine, DMF, 30 min, Ar, r.t., 40%. (g) CuSO₄, TBTA, Na-ascorbate, ^tBuOH/THF/H₂O, 5 h, r.t., Ar, 47%.

Another approach was to covalently target the wild type receptor that have no overexpression of a mutant. *N*-hydroxylsuccinimide (NHS) esters react with reactive amines and hydroxyl groups that are presented in several amino acid side chains. We synthesized a NHS ester, containing the azopyrazole-fentanyl, in a click reaction strategy without TBTA using azide **54** and alkyne **57** (Scheme 11).



Scheme 11. Synthesis of the photochromic fentanyl NHS ester derivative **29** and the conversion with lysine to proof the reactivity. (a) CuSO_4 , Na-ascorbate, $t\text{-BuOH/THF/H}_2\text{O}$, 7 min, r.t. 99%(conversion). (b) *L*-Lysine, buffer.

With LC-MS monitoring, it was found that the click reaction was already finished after 7 minutes, where afterwards the NHS ester began to hydrolyze (**Figure 7**). Purification with preparative HPLC was not possible due to the fast degradation of the target compound.

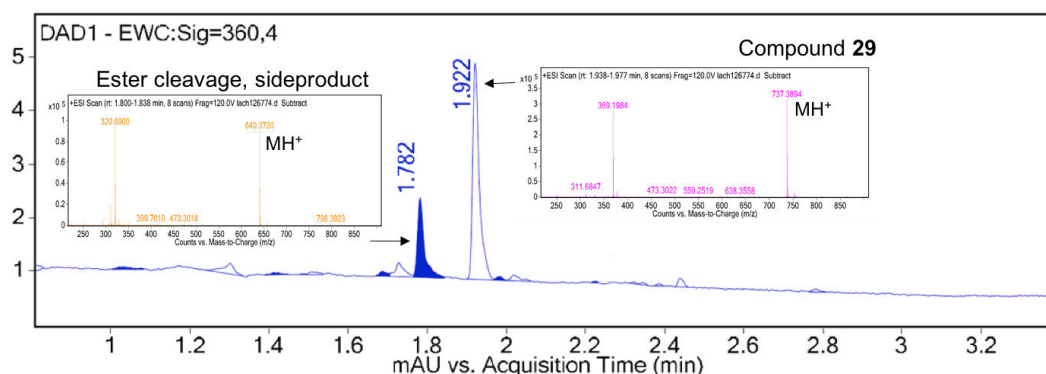


Figure 7. LC-MS analysis of compound **29** reaction mixture after 10 min. Hydrolysis of compound **29** could already be detected after 3 more minutes.

In order to characterize and prove the reactivity of the NHS ester, *L*-Lysine was added to an aliquot of the reaction mixture in buffer forming the stable derivative **58**. The *L*-Lysine adduct **58** was characterized by LC-MS analysis (**Figure 8**).

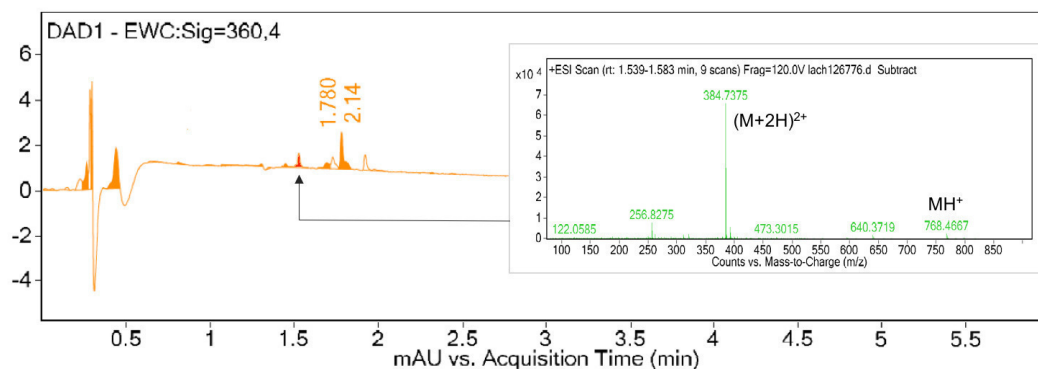


Figure 8. Example reaction to form the *L*-Lysine adduct **58**. The sample was taken after 15 min.

As significant hydrolysis of compound **29** started already after 10 min, it is not suitable for use in a biological assay.

3.3 Photophysical investigations

UV/VIS spectroscopy was carried out to investigate the photochemical properties of photochromic ligands **37**, **43**, **54** and **27 - 28**. All switches showed the characteristic changes in the absorbance, which is a significant decrease and a slight blue-shift of the $\pi \rightarrow \pi^*$ band from 340 to 300 nm and an increase of the $n \rightarrow \pi^*$ band to approximately 440 nm. All photochemical properties are summarized in **Table 4** and UV/VIS spectra are depicted in the **SI-4**. For initial biological studies, compound **37** was investigated and the thermal half-life of the *Z*-isomer was only 37 seconds (**Figure 9a**). Unfortunately, the PSS of **37** could not be determined by HPLC nor by NMR spectroscopy with continuous irradiation in MeOD at lower temperatures.

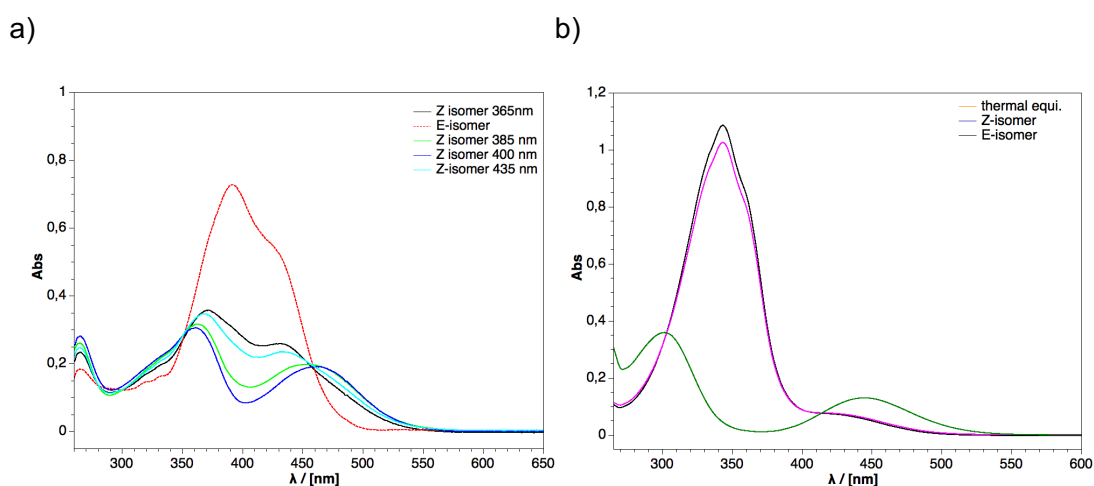


Figure 9. a) UV-VIS spectrum of azopyrazole **37** in DMSO; spectra were recorded under continuous irradiation with 365, 385, 400 and 435 nm to obtain the PSS (*E*→*Z*). b) UV-VIS spectrum of compound **43** showing excellent splitting of the *E*- and *Z*-isomer absorbance band.

The installed push-pull system could be a reason for this short thermal half-life. The aniline acts as an electron donor, and the second aromatic moiety consisting of a pyrazole acts as electron acceptor. In addition, the redshift in absorption observed for compound **37**, is typical for a push-pull system.^{34,35} The structurally modified azopyrazole **43**, containing an additional methylene group, showed long thermal half-lives in DMSO and buffer (**Figure 9b**). The resulting thermal half-lives for compound **54**, **27** and **28**, exhibiting the additional methylene group, were very high from 1.7 days to 241 days, which were similar to the results obtained for the β_2 -AR ligands. These properties are an advantage, because continuous irradiation is not required during the assay, which may cause problems for the biological testing.

Table 4. Photochemical properties of fentanyl derivatives **37**, **43**, **54** and **27-28**.

| Entry | Ligand | Solvent | λ_{\max} | λ_{\max} | λ_{iso} | $t_{1/2}$ | PSS | |
|-------|--------|-----------------------|------------------|---------------------|------------------------|-----------|-------------------------------|-------------------------------|
| | | | (E) [nm] | (Z) [nm] | | | (E→Z) ^[b,c] E:Z | (Z→E) ^[b,d] E:Z |
| 1 | 37 | DMSO | 235, 391 | 264, 358, 452 | 458 | 37 s | 20:80 ^[e] | 99:1 |
| 2 | 43 | DMSO | 341 | 297, 444 | 300, 411 | 1.7 d | 17:83 | 79:21 |
| 3 | 43 | Buffer ^[a] | 343 | 301, 444 | 303, 414 | 8.0 d | 21:79 | 97:3 |
| 4 | 27 | DMSO | 342 | 300, 445 | 301, 414 | 18.8 d | 20:80 | 95:5 |
| 5 | 27 | Buffer ^[a] | 342 | 299, 442 | 302, 413 | 43.8 d | 10:90 | 91:9 |
| 6 | 54 | DMSO | 342 | 299, 442 | 299 | 13.3 d | 11:89 | 90:10 |
| 7 | 54 | Buffer ^[a] | 336 | 300, 437 | 292, 417 | 241 d | 9:91 | 83:17 |
| 8 | 28 | DMSO | 342 | 298, 443 | 300, 412 | 11.8 d | 8:92 | 86:14 |
| 9 | 28 | Buffer ^[a] | 337 | 300, 432 | 295, 405 | 34.8 d | 9:91 | 89:11 |

[a] Tris buffer: 50 mM Tris, 1 mM EDTA, 1 mM MgCl₂, 0.1% DMSO. [b] PSS was determined by HPLC measurement at 25 °C. [c] Irradiation wavelength: 365 nm. [d] Irradiation wavelength: 528 nm. [e] Estimated PSS by UV-VIS measurements, irradiation wavelength, 400 nm.

All photochromic ligands exhibited high photostationary states, with PSS values greater than 80% for both the *E* to *Z* and the *Z* to *E* photoisomerization. In addition, all compounds were toggled between the two isomers six times showing high fatigue resistance and no degradation. The cycle performances are depicted in the supporting information (**SI-4**).

3.4 Biological investigations

To evaluate ligand affinity for the μ OR and the mutant μ OR^{N127C} ligands **37**, **43**, **54** and **27-28** were studied towards their abilities to displace [³H]diprenorphine from the receptor.³¹ The binding data of compound **Z-37** was recorded under permanent irradiation with light of 400 nm and could not be used due to cell damages. The hydroxyl fentanyl **43** showed only low binding affinity and no differences between the *E* and *Z* isomer. The disulfide-fentanyl **27** showed good binding for the *E* isomer at the μ OR wild type and the *Z* isomer, obtained after irradiation with light of 365 nm, exhibited a 6-fold lower binding. Generally, ligands **27** and **28** showed better binding at the μ OR^{N127C}.

Table 5. Radioligand binding data and functional investigations for the photochromic fentanyl ligands **37**, **43**, **54** and **27-28**.

| Entry | Ligand | Binding $K_i \pm \text{SEM}$ [nM] ^[a] | | Activation IP-one ^[b] | |
|-------|----------------------|---|---------------------------|--------------------------------------|----------|
| | | μ OR | μ ORN ^{127C} | EC ₅₀ [nM] ^[c] | α |
| 1 | Morphine | 52 ± 4.8 | 32 ± 10.9 | 20 | 1 |
| 2 | <i>E</i> - 37 | 970 ± 246 | n.d. | n.d. | n.d. |
| 3 | <i>E</i> - 43 | 3000 ± 168 | n.d. | n.d. | n.d. |
| 4 | <i>Z</i> - 43 | 2900 ± 698 | n.d. | n.d. | n.d. |
| 5 | <i>E</i> - 27 | 53 ± 8.3 | 19 ± 1.7 | 270 | 0.93 |
| 6 | <i>Z</i> - 27 | 310 ± 229 | 42 ± 229 | 350 | 0.94 |
| 7 | <i>E</i> - 28 | 1100 ± 474 ^[d] | 240 ± 21 ^[d] | 29 | 0.12 |
| 8 | <i>Z</i> - 28 | 2700 ± 458 | 170 ± 21 | 0 | 0 |

[a] Binding data determined by competition binding with [³H]diprenorphine; K_i values in nM ± standard error of the mean (SEM) derived from 3 to 18 individual experiments each performed in triplicate; n.d. = not determined. [b] IP accumulation determined by applying the IP-One assay (from Cisbio) with HEK 239T cells co-transfected with the cDNA of the individual opioid receptor and that of the hybrid G-protein G α q15HA. [c] EC₅₀ values and intrinsic activities (α) relative to Morphine. [d] K_i values in nM ± standard deviation (SD) derived from 2 individual experiments each performed in triplicate.

The functional investigations towards G protein mediated signalling was done in an IP-One accumulation (Cisbio) assay.²⁸ It was found that both isomers of compound **27** have intrinsic activities > 90% but no difference between their isomers. In accordance to the biological

investigations of the β_2 -AR, the formation of the covalent bond has to be considered in further experiments.

4. Conclusion and Outlook– β_2 -AR and μ OR

In summary, we have incorporated azopyrazoles into the structures of the highly potent agonists BI-167107 and fentanyl to obtain photochromic covalent ligands. The concept of the photochromic covalent ligands uses the azopyrazole as connecting moiety between the pharmacophore and a tethering position. Geometric changes of the azopyrazole should effect binding or activation when toggling between the two photoisomers. The different synthetic routes were investigated in parallel to the synthesis of the pharmacophoric moiety and the covalent groups, including the disulfide and the maleimide. The crucial step for the β_2 -AR ligands was accomplished in a reductive amination reaction connecting the photoresponsive tether and the pharmacophoric moiety as the final step. For the synthesized μ OR-ligands, either working with a disulfide protection group for the disulfide derivative or a post functionalization via a click-reaction for the maleimide or the NHS ester showed to be the best synthetic routes. The photochemical characterization of the photochromic ligands revealed high fatigue resistance and high thermal half-lives for the azopyrazoles. The fentanyl-derivative **37** has a very short thermal half-life due to the push-pull system. It could successfully be replaced by an azopyrazole exhibiting an additional methylene group. Initial biological investigations showed good binding affinities for both the covalent β_2 -AR and μ OR ligands towards the wild type receptor and much higher affinities for their corresponding mutant receptors. Functional studies on β -arrestin recruitment for the β_2 -AR and G-protein signalling for the μ OR showed high intrinsic activities for the BI-derivatives **1** and **2** and the fentanyl-derivatives **27** and **28**. However, the differences in efficacy between the *E*- and *Z*-isomers were only marginal.

Further investigations will focus on irreversible blocking of radioligand binding in radioligand depletion assays to get more insight into the covalent nature of the ligands. In addition, to only measure the efficacies of the covalently bound ligand, the receptor has to be blocked with an inverse agonist first. In order to determine the efficiency of the covalent binding, one could compare the covalently modified ligands to the non-covalent derivatives **10** (β_2 -AR) and **43** (μ OR).

5. Experimental section

General experimental procedures

Commercial reagents and starting materials were purchased from *Acros Organics*, *Alpha-Aesar*, *Sigma Aldrich*, *TCI*, *Fisher* and were used without further purification. Solvents were used in p.A. quality and dried according to common procedures if necessary. Technical solvents were used for automated flash column chromatography without further purification.

Flash column chromatography was performed on a *Biotage Isolera One* automated flash purification system with UV/Vis detector using *Macherey Nagel* silica gel 60 M (40-63 μm , 230-400 grain diameter) for normal phase chromatography. For reversed phase chromatography *Biotage SNAP* Cartridges KP-C18-HS were used. Thin layer chromatography (TLC) analyses were performed on silica gel 60 F-254 with a 0.2 mm layer thickness. Visualization was done by UV-light (254 nm, 312 nm or 365 nm) or staining with a vanillin- H_2SO_4 solution (0.5 g vanillin, 85 mL ethanol, 10 mL conc. acetic acid, 3 mL conc. H_2SO_4). For analytic HPLC measurements an *Agilent UHPLC-MSD-System* (column: *Phenomenex Luna C18(2)*, 150x2.00mm, 100A) and *Agilent 1220 Infinity LC System* (column: *Phenomenex Luna*, 3 μ C18(2) 100A, 150 x 2.0 mm, 100 Å, 40 °C) were used. Preparative HPLC was done using *Agilent 1100 Series* with a *Phenomenex Luna 10* (C18, 100A, 250 x 21.2 mm).

NMR spectra were recorded on a *Bruker Avance 600* (^1H 600.1 MHz, ^{13}C 150.1 MHz, T = 300K), *Bruker Avance 400* (^1H 400.1 MHz, ^{13}C 100.6 MHz, T = 300K) or *Bruker Avance 300* (^1H 300.1 MHz, ^{13}C 75.5 MHz, T = 300K). The chemical shifts are reported in δ [ppm] relative to tetramethylsilane as external standard. The multiplicity is abbreviated as “s” (singlet), “d” (doublet), “t” (triplet), “sep” (septet), “q” (quartet) and “m” (multiplet). The carbon NMR signals assignment (+) = primary/tertiary, (-) = secondary and (q) = quaternary resulted from DEPT, HSQC, HMBC experiments. Mass spectra were recorded on an *Agilent Q-TOF 6540 UHD* (ESI-MS, APCI-MS), *Finnigan MAT95* (EI-MS) or *Finnigan MAT SSQ 710 A* (EI-MS, CI-MS).

The IR-spectra were recorded on an *Agilent Technologies Cary 630 FTIR* instrument. The UV/VIS absorption spectra were recorded using a *Varian Cary 100 UV/Vis/NIR* spectrometer in 10 mm quartz cuvettes. The biological investigations were done in Erlangen at the group of Prof. P. Gmeiner (labs of Dr. H. Hübner) and in Stanford, group of Prof. B. K. Kobilka.

5.1 Synthesis

Compound **6**²², **20**³⁶, *R-21*¹⁹ and **31**³⁷ were synthesized according to literature.

General procedures:

GP1: Diazotization

The aniline-derivative (1.0 eq) was dissolved in a mixture of acetic acid (2 mL/mmol) and conc. HCl (0.25 mL/mmol) at 0 °C. A solution of NaNO₂ (1.2 eq) in a minimum amount of water was added and the mixture was stirred for 45 min at 0 °C. To a suspension of acetylacetone (1.3 eq) and NaAcO (3.0 eq) in EtOH (2 mL/mmol) the diazonium mixture was added and the resulting reaction mixture was stirred for 1 h at r.t. Ice water was added and the formed precipitate was separated by vacuum filtration followed by washing steps with H₂O and hexane. After drying under vacuum the target compounds were obtained as yellow-orange crystals.

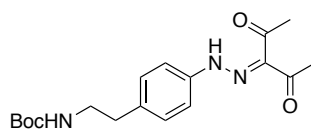
GP2: Pyrazole formation

A solution of the corresponding diketone (1.0 eq) and 2-hydrazinoethanol (1.1 eq) in EtOH (50 mL) was refluxed for 3 h. The solvent was evaporated and the title compound was obtained as an orange solid with purification (column chromatography) when necessary.

GP3: Boc-deprotection

The Boc-amine (1.0 eq) was dissolved in CH₂Cl₂ at r.t. and TFA (1 mL/mmol) was added to stir the solution at r.t. for 1 h (TLC monitoring!). An aqueous NaOH (2M) solution (20 mL/mmol) was added and extraction with CH₂Cl₂ was done. The combined organic layers were dried over Na₂SO₄ and the solvent was removed under reduced pressure to afford the target compounds as yellow solids.

Compound 4: *tert*-butyl (4-(2-(2,4-dioxopentan-3-ylidene)hydrazineyl)phenethyl)-carbamate



C₁₈H₂₅N₃O₄, MW = 347.42 g/mol

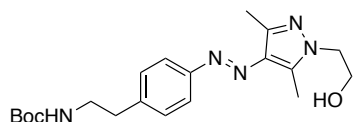
GP1, aniline derivative **3**, yield: 60%, yellow crystals.

¹H-NMR (400 MHz; CDCl₃): δ = 1.43 (s, 9H), 2.48 (s, 3H), 2.60 (s, 3H), 2.80 (t, *J* = 7.0 Hz, 2H), 3.41-3.32 (m, 2H), 7.23 (d, *J* = 8.4 Hz, 2H), 7.35 (d, *J* = 8.5 Hz, 2H).

¹³C-NMR (101 MHz, CDCl₃): δ = 26.8 (+), 28.5 (+), 31.8 (+), 35.9 (-), 41.9 (-), 95.6 (q), 116.6 (+), 130.2 (+), 133.3 (q), 137.1 (q), 140.2 (q), 156.0 (q), 162.8 (q), 198.0 (q).

ESI-MS: m/z (%) = 348.19 (M+H⁺)

Compound 5a: tert-butyl (E)-4-((1-(2-hydroxyethyl)-3,5-dimethyl-1H-pyrazol-4-yl)diazenyl)phenethyl)carbamate



C₂₀H₂₉N₅O₃, MW = 387.48 g/mol

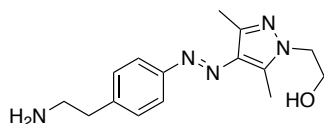
GP2, starting material **4**, yield: 45%, orange solid.

¹H-NMR (400 MHz; CDCl₃): δ = 1.24 (s, 9H), 2.28 (s, 3H), 2.42 (s, 3H), 2.65-2.63 (m, 2H), 3.21-3.13 (m, 2H), 3.77-3.73 (m, 2H), 4.01-3.08 (m, 2H), 7.08 (d, *J* = 8.2 Hz, 2H), 7.51 (d, *J* = 8.3 Hz, 2H).

¹³C-NMR (101 MHz, CDCl₃): δ = 9.6 (+), 13.7 (+), 28.1 (+), 35.6 (-), 41.4 (-), 50.6 (-), 60.2 (-), 78.8 (q), 121.6 (+), 129.1 (+), 134.5 (q), 139.7 (q), 140.5 (q), 142.0 (q), 151.9 (q), 198.9 (q).

ESI-MS: m/z (%) = 388.24 (M+H⁺)

Compound 5b: (E)-2-(4-((4-(2-aminoethyl)phenyl)diazenyl)-3,5-dimethyl-1H-pyrazol-1-yl)ethan-1-ol



C₁₅H₂₁N₅O, MW = 287.37 g/mol

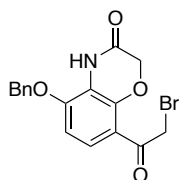
GP3, starting material **5a**, yield 98%, yellow solid.

¹H-NMR (400 MHz; CDCl₃): δ = 2.49 (s, 3H), 2.59 (s, 3H), 2.78 (t, *J* = 6.6 Hz, 2H), 2.96-2.94 (m, 2H), 4.05-4.01 (m, 2H), 4.17-4.12 (m, 2H), 7.28-7.26 (m, 2H), 7.70 (d, *J* = 7.7 Hz, 2H).

¹³C-NMR (101 MHz, CDCl₃): δ = 10.0 (+), 14.1 (+), 40.0 (-), 43.6 (-), 50.4 (-), 61.5 (-), 122.0 (+), 129.5 (+), 135.1 (q), 139.5 (q), 141.5 (q), 141.6 (q), 142.9 (q), 152.3(q).

ESI-MS: m/z (%) = 288.18 ($M+H^+$)

Compound 7: 5-(benzyloxy)-8-(2-bromoacetyl)-2H-benzo[*b*][1,4]oxazin-3(4*H*)-one



$C_{17}H_{14}BrNO_4$, MW = 376.21 g/mol

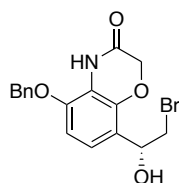
Compound **6** (4.1 g, 13.7 mmol, 1.0 eq) was dissolved in EtOAc (150 mL) at r.t. and subsequently $CuBr_2$ (4.6 g, 20.6 mmol, 1.5 eq) was added to stir the mixture at 50 °C for 24 h. The solvent was reduced *in vacuo* and the crude mixture was directly used for automated column chromatography (PE/EtOAc, 0-50% EtOAc) to afford the target compound **7** (3.5 g, 9.3 mmol, 67%) as a white solid.

1H -NMR (400 MHz; $CDCl_3$): δ = 7.64 (d, J = 8.9 Hz, 1H), 7.45-7.38 (m, 5H), 6.77 (d, J = 8.9 Hz, 1H), 5.17 (s, 2H), 4.75 (s, 2H), 4.50 (s, 2H)

^{13}C -NMR (101 MHz; $CDCl_3$): δ = 189.6 (q), 163.3 (q), 149.8 (q), 144.2 (q), 135.0 (q), 129.1 (q), 128.1 (q), 126.6 (+), 117.6 (+), 116.2 (q), 106.6 (+), 71.6 (-), 67.5 (-), 36.5 (-)

ESI-MS: m/z (%) = 276.02 ($M+H^+$)

Compound 8: (*R*)-5-(benzyloxy)-8-(2-bromo-1-hydroxyethyl)-2H-benzo[*b*][1,4]-oxazin-3(4*H*)-one



$C_{17}H_{16}BrNO_4$, MW = 378.22 g/mol

To a stirred solution of compound **7** (2.2 g, 5.9 mmol, 1.0 eq) and CBS-solution (0.6 mL, c = 1 M in toluene, 0.6 mmol, 0.1 eq) in anhydrous THF, BH_3 -THF complex (6.4 mL, c = 1 M in THF, 6.4 mmol, 1.1 eq) was added dropwise over 2 h at r.t. under Ar-atmosphere. The mixture was stirred for 0.5 h at r.t. and was then quenched by MeOH (3 mL). The solvent was evaporated and the crude product was used for automated column chromatography (PE/EtOAc, 0-60%

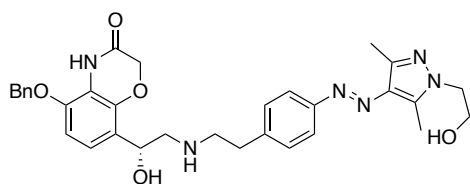
EtOAc) without any further workup. Compound **8** (1.4 g, 3.7 mmol, 64%) was obtained as a white solid.

¹H-NMR (400 MHz; CDCl₃): δ = 2.72-2.72 (m, 1H), 3.52 (dd, J = 10.2 Hz, 8.4 Hz, 1H), 3.69 (dd, J = 10.3 Hz, 3.5 Hz, 1H), 4.68-4.57 (m, 2H), 5.10 (s, 2H), 5.13-5.11 (m, 1H), 6.68 (d, J = 8.7 Hz, 1H), 7.09 (d, J = 8.6 Hz, 1H), 7.40 (d, J = 1.9 Hz, 5H), 7.85 (s, 1H)

¹³C-NMR (101 MHz; CDCl₃): δ = 39.2 (-), 67.3 (-), 68.9 (+), 71.2 (-), 106.1 (+), 115.8 (+), 121.0 (q), 121.5 (+), 128.0 (+), 128.8 (+), 129.0 (+), 135.8 (q), 140.9 (q), 145.7 (q), 163.7 (q).

ESI-MS: m/z (%) = 378.03 (M+H⁺)

Compound 9: (R,E)-5-(benzyloxy)-8-(1-hydroxy-2-((4-((1-(2-hydroxyethyl)-3,5-dimethyl-1H-pyrazol-4-yl)diazenyl)phenethyl)amino)ethyl)-2H-benzo[b][1,4]oxazin-3(4H)-one



C₃₂H₃₆N₆O₅, MW = 584.68 g/mol

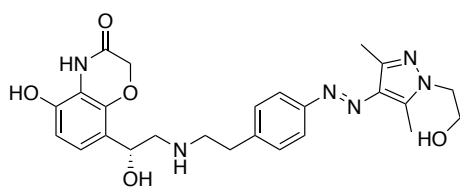
Compound **8** (121 mg, 0.32 mmol, 1.1 eq) and **5** (80 mg, 0.28 mmol, 1.0 eq) were dissolved in anhydrous MeCN (20 mL) at r.t. under nitrogen atmosphere. K₂CO₃ (44 mg, 0.32 mmol, 1.1 eq) and KI (5.3 mg, 0.032 mmol, 0.1 eq) were added and the mixture was refluxed for 3 h. The solvent was evaporated and the residue was dissolved in water to do an extraction with CH₂Cl₂ (3x 10 mL). The combined organic layers were dried over Na₂SO₄ and the solvent was reduced *in vacuo*. The crude product was first purified by automated column chromatography (CH₂Cl₂/MeOH, 0-10% MeOH, + 0.1% NEt₃) and second by RP chromatography (H₂O+TFA 0.05%/MeCN 10-98% MeCN). Lyophilization afforded compound **9** (15 mg, 0.026 mmol, 9%) as a yellowish solid.

¹H-NMR (400 MHz; MeOD): δ = 7.73 (d, J = 8.3 Hz, 2H), 7.48 (d, J = 7.2 Hz, 2H), 7.43-7.29 (m, 5H), 7.05-7.03 (m, 1H), 6.83 (dd, J = 9.8 Hz, 5.7, 1H), 5.29 (s, 2H), 4.63-4.60 (m, 2H), 4.62-4.58 (m, 1H), 4.19 (t, J = 5.3 Hz, 2H), 3.98 (m, 1H), 4.00-3.94 (t, J = 5.3 Hz, 2H), 3.90-3.85 (m, 1H), 3.32-3.24 (m, 2H), 3.23-3.24 (m, 2H), 3.13-3.05 (m, 2H), 3.04-3.29 (m, 2H), 2.68 (s, 3H), 2.46 (s, 3H)

¹³C-NMR (101 MHz, MeOD): δ = 10.0 (+), 14.1 (+), 52.2 (-), 59.8 (+), 61.8 (-), 67.5 (-), 68.2 (-), 70.0 (-), 71.8 (-), 108.6 (+), 114.0 (q), 122.2 (+), 123.2 (+), 123.9 (q), 128.8 (+), 129.1 (+), 129.7 (+), 130.4 (+), 135.9 (q), 137.8 (q), 139.2 (q), 142.4 (q), 143.4 (q), 148.6 (q), 153.1 (q), 167.0 (q).

ESI-MS: m/z (%) = 585.28 ($M+H^+$)

Compound 10: (*R,E*)-5-hydroxy-8-(1-hydroxy-2-((4-((1-(2-hydroxyethyl)-3,5-dimethyl-1*H*-pyrazol-4-yl)diazenyl)phenethyl)amino)ethyl)-2*H*-benzo[*b*][1,4]oxazin-3(4*H*)-one



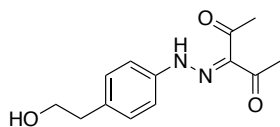
$C_{25}H_{30}N_6O_5$, MW = 494.55 g/mol

To a solution of compound **9** (15 mg, 0.026 mmol, 1.0 eq) in MeOH (5 mL), Pd/C (0.1 eq) was added and the mixture was treated with a H_2 -balloon for 5 min at r.t. The mixture was filtered over *celite*, washed with MeOH and the solvent was evaporated. The crude product was purified by preparative HPLC (column: Luna 10, 250 x 21 mm; flow: 20 mL/min, solvent A: H_2O (0.05% TFA), solvent B: MeCN; gradient A/B: 0-15 min: 95/5, 15-20 min: 2/98) to obtain compound **62** (3 mg, 6.1 mmol, 23%) as a white solid.

¹H-NMR (400 MHz; MeOD): δ = 7.73 (d, J = 8.3 Hz, 2H), 7.31 (d, J = 8.3 Hz, 2H), 6.95 (d, J = 8.6 Hz, 1H), 6.61 (d, J = 8.5 Hz, 1H), 4.62-4.58 (m, 2H), 4.57-4.55 (m, 1H), 4.17 (t, J = 5.3 Hz, 2H), 3.99 (dd, J = 11.7 Hz, 8.4 Hz, 1H), 3.90 (t, J = 5.3, 2H), 3.89-3.85 (s, 1H), 3.26-3.15 (m, 2H), 3.13-3.06 (m, 1H), 3.05-2.99 (m, 1H), 2.63 (s, 3H), 2.46 (s, 3H)

¹³C-NMR (151 MHz, MeOD): δ = 10.0 (+), 14.1 (+), 33.0 (-), 40.7 (-), 47.8 (-), 52.2 (-), 55.8 (+), 61.8 (-), 68.2 (-), 110.2 (+), 114.2 (q), 123.3 (+), 125.3 (q), 126.7 (+), 130.5 (+), 129.0 (q), 134.4 (q), 137.7 (q), 141.0 (q), 141.9 (q), 143.1 (q), 152.7 (q), 164.6 (q).

ESI-MS: m/z (%) = 495.24 ($M+H^+$)

Compound 12: 3-(2-(4-(2-hydroxyethyl)phenyl)hydrazineylidene)pentane-2,4-dione

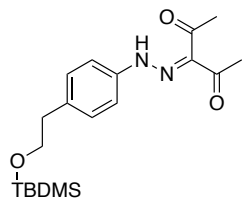
$C_{13}H_{16}N_2O_3$, MW = 248.28 g/mol

GP1, aniline derivative **11**, yield: 84%, yellow crystals.

1H -NMR (400 MHz; $CDCl_3$): δ = 2.48 (s, 3H), 2.60 (s, 3H), 2.88 (t, J = 6.5 Hz, 2H), 3.88 (t, J = 6.5 Hz, 2H), 7.28 (d, J = 8.5 Hz, 2H), 7.36 (d, J = 8.5 Hz, 2H).

^{13}C -NMR (101 MHz, $CDCl_3$): δ = 26.8 (+), 31.8 (+), 38.8 (-), 63.7 (-), 116.6 (+), 130.4 (+), 133.3 (q), 136.7 (q), 140.3 (q), 198.0 (q).

ESI-MS: m/z (%) = 249.13 ($M+H^+$)

Compound 13: 3-(2-(4-(2-((*tert*-butyldimethylsilyl)oxy)ethyl)phenyl)hydrazine-ylidene)pentane-2,4-dione

$C_{19}H_{30}N_2O_3Si$, MW = 362.55 g/mol

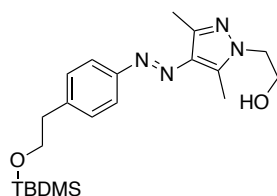
Compound **12** (15.2 g, 61.0 mmol, 1.0 eq) was dissolved in DMF (150 mL) at r.t. under Ar-atmosphere. Imidazole (8.3 g, 122 mmol, 2.0 eq) and TBDMS-Cl (9.2 g, 61 mmol, 1.0 eq) were added and the mixture was stirred at r.t. for 2 h. Water was added and the mixture was extracted with CH_2Cl_2 (3x 150 mL). The combined organic layers were again extracted with H_2O (3x 100 mL). The organic layer was dried over Na_2SO_4 and the solvent was evaporated under reduced pressure to yield the product **13** (6.4 g, 17.7 mmol, 29%) as a yellow oil.

1H -NMR (400 MHz; $CDCl_3$): δ = 0.00 (s, 6H), 0.86 (s, 9H), 2.48 (s, 3H), 2.59 (s, 3H), 2.81 (t, J = 6.7 Hz, 2H), 3.80 (t, J = 6.8 Hz, 2H), 7.24 (d, J = 8.5 Hz, 2H), 7.33 (d, J = 8.5 Hz, 2H).

^{13}C -NMR (101 MHz, $CDCl_3$): δ = -5.3 (+), 18.4 (q), 26.0 (+), 26.8 (+), 31.8 (+), 39.2 (-), 64.4 (-), 116.3 (+), 130.5 (+), 133.12 (q), 137.6 (q), 139.9 (q), 197.9 (q).

ESI-MS: m/z (%) = 363.21 ($M+H^+$)

Compound 14: (E)-2-(4-((4-(2-((tert-butyl dimethylsilyl)oxy)ethyl)phenyl)-diazenyl)-3,5-dimethyl-1H-pyrazol-1-yl)ethan-1-ol



$C_{21}H_{34}N_4O_2Si$, MW = 402.61 g/mol

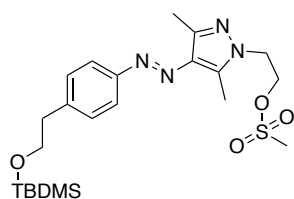
GP2, starting material **13**, yield: 45%, purification: automated column chromatography (PE/EtOAc, 5-80% EtOAc), orange crystals.

1H -NMR (400 MHz; $CDCl_3$): δ = 0.00 (s, 6H), 0.88 (s, 9H), 2.49 (s, 3H), 2.59 (s, 3H), 2.87 (t, J = 6.9 Hz, 2H), 3.84 (t, J = 6.9 Hz, 2H), 4.04 (t, J = 4.8 Hz, 2H), 4.13 (t, J = 4.8 Hz, 2H), 7.29 (d, J = 8.3 Hz, 2H), 7.71 (d, J = 8.3 Hz, 2H).

^{13}C -NMR (101 MHz, $CDCl_3$): δ = -3.4 (+), 10.0 (+), 14.1(+), 25.8(+), 26.07 (q), 31.6 (-), 50.3 (-), 61.6 (-), 63.7 (-), 122.1 (+), 129.7 (+), 135.1 (q), 139.4 (q), 140.3 (q), 142.9 (q), 152.5 (q).

ESI-MS: m/z (%) = 403.25 ($M+H^+$)

Compound 15: (E)-2-(4-((4-(2-((tert-butyl dimethylsilyl)oxy)ethyl)phenyl)-diazenyl)-3,5-dimethyl-1H-pyrazol-1-yl)ethyl methanesulfonate



$C_{22}H_{36}N_4O_4SSi$, MW = 480.70 g/mol

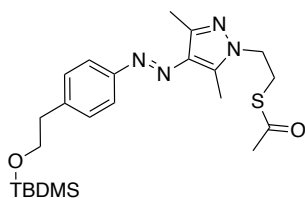
Compound **14** (100 mg, 0.25 mmol, 1.0 eq) was dissolved in CH_2Cl_2 (100 mL) and the mixture was cooled to 0 °C. Triethylamine (0.51 mL, 0.37 mmol, 1.5 eq) and methanesulfonyl chloride (0.21 mL, 0.26 mmol, 1.1 eq) were added and the mixture was warmed up to r.t. over 1 h. Water (100 mL) was added and the aqueous layer was extracted with CH_2Cl_2 (2x 100 mL). The combined organic layers were dried over Na_2SO_4 and the solvent was removed under reduced pressure to obtain a yellow oil as the product **15** (101 mg, 0.21 mmol, 84%).

¹H-NMR (400 MHz; CDCl₃): δ = 0.00 (s, 6H), 0.88 (s, 9H), 2.49 (s, 3H), 2.63 (s, 3H), 2.89-2.85 (m, 5H), 3.84 (t, *J* = 6.9 Hz, 2H), 4.36 (t, *J* = 5.2 Hz, 2H), 4.63 (t, *J* = 5.2 Hz, 2H) 7.30 (d, *J* = 8.4 Hz, 2H), 7.71 (d, *J* = 8.4 Hz, 2H).

¹³C-NMR (101 MHz, CDCl₃): δ = -5.2 (+), 9.9 (+), 18.4 (q), 14.2 (+), 26.1 (+), 37.4 (+), 39.6 (-), 47.8 (-), 64.4 (-), 67.8 (-), 121.8 (+), 129.9 (+), 135.2 (q), 138.7 (q), 139.1 (q), 140.1 (q), 141.4 (q).

ESI-MS: *m/z* (%) = 481.23 (M+H⁺)

Compound 16: (*E*)-S-(2-(4-((4-(2-((*tert*-butyldimethylsilyl)oxy)ethyl)phenyl)-diazenyl)-3,5-dimethyl-1*H*-pyrazol-1-yl)ethyl) ethanethioate



C₂₃H₃₆N₄O₂SSi, MW = 460.71 g/mol

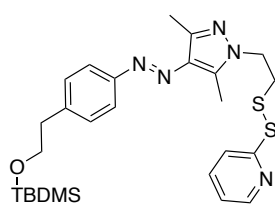
Potassium thioacetate (47.5 mg, 0.42 mmol, 2.0 eq) and compound **15** (100 mg, 0.21 mmol, 1.0 eq) were dissolved in acetone (50 mL) and the mixture was refluxed for 3 h. The reaction mixture was cooled to r.t. and the solvent was removed *in vacuo*. The residue was dissolved in water (80 mL) and extraction with CH₂Cl₂ (3x 50 mL) was done. The combined organic layers were dried (Na₂SO₄), filtrated and the solvent was removed under reduced pressure to obtain an orange solid as the product **16** (71.6 mg, 0.16 mmol, 74%).

¹H-NMR (400 MHz; CDCl₃): δ = 0.00 (s, 6H), 0.88 (s, 9H), 2.37 (s, 3H), 2.50 (s, 3H), 2.62 (s, 3H), 2.89-2.85 (m, 2H), 3.31 (t, *J* = 6.8, 2H), 3.84 (t, *J* = 7.0, 2H), 4.21 (t, *J* = 6.8, 2H), 7.29 (d, *J* = 7.5, 2H), 7.71 (d, *J* = 7.4, 2H).

¹³C-NMR (101 MHz, CDCl₃): δ = -5.2 (+), 10.0 (+), 14.0 (+), 18.5 (p), 26.1(+), 29.1 (-), 30.8(+), 39.6 (-), 47.9 (-), 64.5 (-), 113.0 (p), 121.9 (+), 122.1 (p), 129.9 (+), 139.3 (p), 141.3 (p), 143.0 (p), 195.7 (p).

ESI-MS: *m/z* (%) = 461.24 (M+H⁺)

Compound 17: (*E*)-2-((2-(4-((4-(2-((*tert*-butyldimethylsilyl)oxy)ethyl)phenyl)-diazenyl)-3,5-dimethyl-1*H*-pyrazol-1-yl)ethyl)disulfaneyl)pyridine



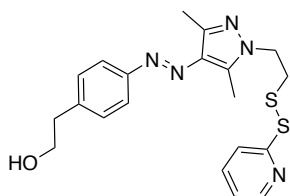
Compound **16** (60.0 mg, 0.15 mmol, 1.0 eq) and 2-aldrithiol (39.4 mg, 0.18 mmol, 1.2 eq) were dissolved in a 0.5 M NaOMe solution in MeOH (50 mL) under N_2 -atmosphere. The mixture was stirred 24 h at r.t. and the solvent was removed under reduced pressure. The crude product was purified by automated column chromatography (PE/EtOAc, 5-80% EtOAc) to obtain **17** (73.8 mg, 0.14 mmol, 94%) as a yellow oil.

$^1\text{H-NMR}$ (400 MHz; CDCl_3): δ = 0.00 (s, 6H), 0.88 (s, 9H), 2.49 (s, 3H), 2.58 (s, 3H), 2.87 (t, J = 6.9 Hz, 2H), 3.26 (t, J = 6.8 Hz, 2H), 3.84 (t, J = 6.9 Hz, 2H), 4.37 (t, J = 6.8 Hz, 2H), 7.13-7.09 (m, 1H), 7.30 (d, J = 8.3 Hz, 2H), 7.66-7.62 (m, 2H), 7.70 (d, J = 8.3 Hz, 2H), 8.49 (d, J = 4.8 Hz, 1H).

$^{13}\text{C-NMR}$ (101 MHz, CDCl_3): δ = -3.4 (+), 10.1 (+), 14.2 (+), 18.1 (q), 25.8 (+), 37.7 (-), 39.2 (-), 47.3 (-), 63.7 (-), 120.3 (+), 121.2 (+), 122.1 (+), 129.7 (+), 135.1 (q), 137.3 (+), 139.4 (q), 140.2 (q), 143.2 (q), 149.7 (+), 152.5 (q), 159.3 (q).

ESI-MS: m/z (%) = 528.23 ($\text{M}+\text{H}^+$)

Compound 18: (E)-2-(4-((3,5-dimethyl-1-(2-(pyridin-2-yl)disulfaneyl)ethyl)-1H-pyrazol-4-yl)diazenyl)phenyl)ethan-1-ol



Compound **17** (100 mg, 0.19 mmol, 1.0 eq) was dissolved in THF and a 1M TBAF solution in THF (1 mL) was added to stir the solution for 1 h at r.t. (TLC-monitoring!). Saturated NaCl-solution (50 mL) was added and the mixture was extracted with EtOAc (3x 50 mL). The combined organic layers were dried (Na_2SO_4), and concentrated under reduced pressure.

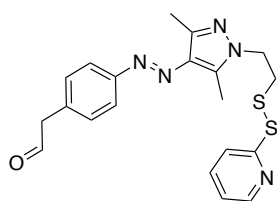
The residue was purified by automated column chromatography (PE/EtOAc, 10-80% EtOAc) to obtain **18** (50 mg, 0.12 mmol, 64%) as a yellow oil.

¹H-NMR (400 MHz; CDCl₃): δ = 2.44 (s, 3H), 2.53 (s, 3H), 2.88 (t, *J* = 6.6 Hz, 2H), 3.21 (t, *J* = 6.8 Hz, 2H), 3.85 (t, *J* = 6.6 Hz, 2H), 4.31 (t, *J* = 6.8 Hz, 2H), 7.06 (s, 1H), 7.27 (d, *J* = 8.3 Hz, 2H), 7.62-7.55 (m, 2H), 7.68 (d, *J* = 8.3 Hz, 2H), 8.42 (s, 1H).

¹³C-NMR (101 MHz, CDCl₃): δ = 10.0 (+), 14.1 (+), 37.6 (-), 39.1 (-), 47.2 (-), 63.5 (-), 120.2 (+), 121.2 (+), 122.0 (+), 129.6 (+), 135.0 (q), 137.3 (+), 139.3 (q), 140.3 (q), 143.1 (q), 149.9(+), 152.4 (q), 159.2 (q).

ESI-MS: *m/z* (%) = 414.14 (M+H⁺)

Compound 19: (*E*)-2-(4-((3,5-dimethyl-1-(2-(pyridin-2-yl)disulfaneyl)ethyl)-1*H*-pyrazol-4-yl)diazenyl)phenyl)acetaldehyde



C₂₀H₂₁N₅OS₂, MW = 411.54 g/mol

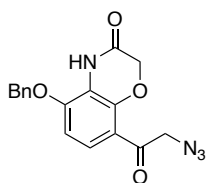
The alcohol **18** (50 mg, 0.12 mmol, 1.0 eq) was dissolved in CH₂Cl₂ (30 mL) under Ar-atmosphere and Dess Martin periodinane (76 mg, 0.18 mmol, 1.5 eq) was added to stir the mixture at 0 °C for 1.5 h. The reaction mixture was diluted with EtOAc (50 mL) and subsequently extracted with aqueous sat. Na₂S₂O₃ (50 mL), sat. NaHCO₃ (50 mL) and sat. NaCl (50 mL). The combined organic layers were dried over Na₂SO₄ and after filtration the solvent was removed under reduced pressure to get the crude compound **19** (45 mg, 0.11, 91%) as a yellow solid. Compound **19** was carried on to the reductive amination immediately for the formation of compound **1**.

¹H-NMR (400 MHz; CDCl₃): δ = 2.49 (s, 4H), 2.59 (s, 3H), 3.27 (t, *J* = 6.8 Hz, 2H), 3.75 (d, *J* = 2.3 Hz, 2H), 4.38 (t, *J* = 6.8 Hz, 2H), 7.13-7.10 (m, 1H), 7.31 (d, *J* = 8.4 Hz, 2H), 7.67-7.61 (m, 2H), 7.78 (d, *J* = 8.4 Hz, 2H), 8.49 (d, *J* = 4.7 Hz, 1H), 9.78 (s, 1H).

¹³C-NMR (101 MHz, CDCl₃): δ = 10.1 (+), 14.2 (+), 37.7 (-), 47.3 (-), 50.5 (-), 120.3 (+), 121.3 (+), 122.5 (+), 130.3 (+), 135.2 (q), 137.4 (+), 139.8 (q), 143.3 (q), 150.0 (+), 153.0 (q), 159.3 (q), 199.2 (q).

ESI-MS: m/z (%) = 412.13 ($M+H^+$)

Compound 20: 8-(2-azidoacetyl)-5-(benzyloxy)-2H-benzo[*b*][1,4]oxazin-3(4H)-one

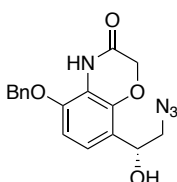


$C_{17}H_{14}N_4O_4$, MW = 338.32 g/mol

Compound **7** (800 mg, 2.13 mmol, 1.0 eq), NaN_3 (210 mg, 3.19 mmol, 1.5 eq) were dissolved in DMF (10 mL) and the mixture was stirred at r.t. for 2 h. The reaction was stopped by the addition of water and the formed precipitate was filtered, washed with ice-water and EtOH. The crude product was dried under vacuum to afford **20** (649 mg, 1.91 mmol, 90%) as a beige solid.

Analytical data were in agreement with published data 22.

5.1.17 Compound R-21: (*R*)-8-(2-azido-1-hydroxyethyl)-5-(benzyloxy)-2H-benzo[*b*][1,4]oxazin-3(4H)-one

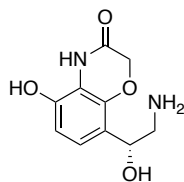


$C_{17}H_{16}N_4O_4$, MW = 340.34 g/mol

Compound **20** (400 mg, 1.2 mmol, 1.0 eq) and CBS-solution (0.12 mL, $c = 1$ M in toluene, 0.12 mmol, 0.1 eq) were dissolved in anhydrous THF under Ar-atmosphere at r.t. A solution of BH_3 -THF complex (1.4 mL, $c = 1$ M in THF, 1.4 mmol, 1.1 eq) in THF was added dropwise over 2 h at r.t. The mixture was stirred for 2.5 h at r.t. and was then quenched by MeOH (1.5 mL). The solvent was evaporated and the crude product was used for automated column chromatography (PE/EtOAc, 0-40% EtOAc) without any further workup. Compound **R-21** (102 mg, 0.31 mmol, 25%) was obtained as a beige solid.

Analytical data were in agreement with published data.¹⁹

Compound R-22: (R)-8-(2-amino-1-hydroxyethyl)-5-hydroxy-2H-benzo[b][1,4]oxazin-3(4H)-one

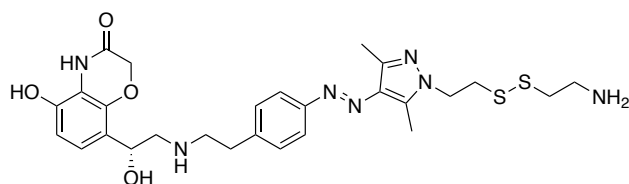


$C_{10}H_{12}N_2O_4$, MW = 224.22 g/mol

To a solution of *R-21* (50 mg, 0.16 mmol, 1.0 eq) in MeOH (5 mL) was added Pd/C (10 mol%) and Et_3SiH (0.13 mL, 0.8 mmol, 5.0 eq). The mixture was stirred for 1 h at r.t. and subsequently the charcoal was filtered off over celite. The solvent was removed *in vacuo* and the crude was purified by automated column chromatography ($CH_2Cl_2/(CH_2Cl_2, MeOH 10\% + 1\% NH_3)$, 0-80 %) to yield compound *R-22* (31 mg, 0.14 mmol, 89%) as a white solid.

Analytical data were in agreement with published data.³⁸

Compound R-1: (R,E)-8-(2-((4-((1-(2-((2-aminoethyl)disulfaneyl)ethyl)-3,5-di-methyl-1H-pyrazol-4-yl)diazenyl)phenethyl)amino)-1-hydroxyethyl)-5-hydroxy-2H-benzo[b][1,4]oxazin-3(4H)-one



$C_{27}H_{35}N_7O_4S_2$, MW = 585.74 g/mol

Compound *R-22* (25 mg, 0.11 mmol, 1.0 eq), **19** (46 mg, 0.11 mmol, 1.0 eq) and $NaCNBH_3$ (11 mg, 0.17 mmol, 1.5 eq) were dissolved in MeOH (10 mL) under Ar-atmosphere and stirred at r.t. for 16 h. The reaction mixture was diluted with EtOAc (20 mL) and extracted with sat. aqueous $NaHCO_3$ solution (50 mL) and H_2O (50 mL). The organic layer was dried over Na_2SO_4 , filtered and the solvent was removed *in vacuo*. The crude product was dissolved in MeOH (5 mL) and cysteamine hydrochloride (25 mg, 0.22 mmol, 2.0 eq) was added to stir the mixture for 1 h at r.t. The solvent was carefully removed *in vacuo* and the crude product was purified by preparative HPLC (column: Luna 10, 250 x 21 mm; flow: 20 mL/min, solvent A: H_2O (0.05% TFA), solvent B: MeCN; gradient A/B: 0-20 min: 90/10, 20-25 min: 2/98) to obtain *R-1* (2.6 mg, 4.4 μ mol, 4%) as a yellow solid.

1H -NMR (400 MHz; $DMSO-D_6$): δ = 2.38 (s, 3H), 2.59 (s, 3H), 2.96 (d, J = 6.8 Hz, 2H), 3.03-3.01 (m, 2H), 3.16-3.17 (m, 4H), 3.19 (t, J = 6.7 Hz, 4H), 4.22 (t, J = 0.6 Hz, 1H), 4.35 (t, J =

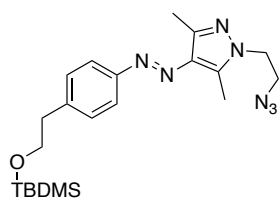
6.5 Hz, 2H), 4.57-4.51 (m, 2H), 6.57 (d, $J = 8.4$ Hz, 1H), 6.92 (d, $J = 8.5$ Hz, 1H), 7.40 (d, $J = 8.4$ Hz, 2H), 7.70 (d, $J = 8.3$ Hz, 2H),

$^{13}\text{C-NMR}$ (151 MHz, DMSO- D_6): $\delta = 9.4$ (+), 14.0 (+), 31.1 (-), 34.0 (-), 36.5 (-), 37.7 (-), 47.1 (-), 47.9 (-), 52.2 (-), 62.8 (+), 67.0 (-), 109.1 (+), 115.3 (q), 120.0 (+), 121.7 (+), 127.7 (q), 129.5 (+), 134.3 (q), 136.9 (q), 138.9 (q), 140.0 (q), 141.0 (q), 144.9 (q), 151.9 (q), 164.2 (q).

ESI-MS: m/z (%) = 586.23 ($\text{M}+\text{H}^+$)

HR-MS (ESI): calcd. for $\text{C}_{27}\text{H}_{35}\text{N}_7\text{O}_4\text{S}_2$ ($\text{M}+2\text{H}$) $^{2+}$, $m/z = 293.6169$, found 293.6173

Compound 23: (*E*)-1-(2-azidoethyl)-4-((4-(2-((*tert*-butyldimethylsilyl)oxy)ethyl)-phenyl)diazenyl)-3,5-dimethyl-1*H*-pyrazole



$\text{C}_{21}\text{H}_{33}\text{N}_7\text{OSi}$, MW = 427.63 g/mol

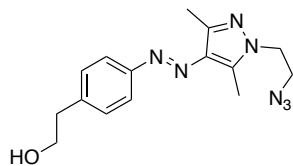
Compound **15** (200 mg, 0.42 mmol, 1.0 eq), NaN_3 (30 mg, 0.46 mmol, 1.1 eq) and NaI (69 mg, 0.46 mmol, 1.1 eq) were dissolved in DMSO under Ar-atmosphere to stir the mixture 24 h at 65 °C. The reaction was quenched by the addition of H_2O (50 mL) and subsequently the reaction mixture was extracted with EtOAc (3x 60 mL). The combined organic layers were dried (Na_2SO_4), filtered and the solvent was removed under reduced pressure. The crude product was purified by automated column chromatography (PE/EtOAc, 0-100% EtOAc), affording **23** (147 mg, 0.34 mmol, 82%) as a bright yellow solid.

$^1\text{H-NMR}$ (400 MHz; CDCl_3): $\delta = 0.00$ (s, 6H), 0.88 (s, 9H), 2.51 (s, 3H), 2.62 (s, 3H), 2.87 (t, $J = 6.9$ Hz, 2H), 3.77 (t, $J = 5.7$ Hz, 2H), 3.84 (t, $J = 6.9$ Hz, 2H), 4.16 (t, $J = 5.7$ Hz, 2H), 7.30 (d, $J = 8.3$ Hz, 2H), 7.72 (d, $J = 8.3$ Hz, 2H).

$^{13}\text{C-NMR}$ (101 MHz, CDCl_3): $\delta = -5.25$ (+), 9.94 (+), 14.20 (+), 18.47 (+), 26.06 (-), 39.55 (-), 47.84 (-), 50.83 (-), 64.44 (q), 121.81 (+), 129.81 (+), 135.22 (q), 139.67 (q), 141.18 (q), 143.36 (q), 152.22 (q).

ESI-MS: m/z (%) = 428.26 ($\text{M}+\text{H}^+$)

Compound 24: (E)-2-(4-((1-(2-azidoethyl)-3,5-dimethyl-1H-pyrazol-4-yl)-di-azeryl)-phenyl)ethan-1-ol



$C_{15}H_{19}N_7O$, MW = 313.37 g/mol

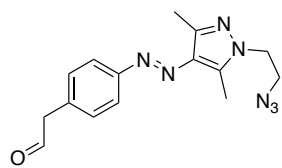
Azide **23** (1.2 g, 2.8 mmol, 1.0 eq) was dissolved in THF and a 1 M TBAF solution in THF (5 mL) was added to stir the mixture 24 h at r.t. The solvent evaporated and the crude was purified by automated column chromatography ($CH_2Cl_2/MeOH$, 0-10% MeOH) to afford compound **24** (764 mg, 2.4 mmol, 87%) as a yellow solid.

1H -NMR (400 MHz, $CDCl_3$): δ = 2.50 (s, 3H), 2.62 (s, 3H), 2.93 (t, J = 6.5, 2H), 3.77 (t, J = 5.7, 2H), 3.90 (t, J = 6.5, 2H), 4.16 (t, J = 5.6, 2H), 7.32 (d, J = 8.3, 2H), 7.74 (d, J = 8.3, 2H).

^{13}C -NMR (101 MHz, $CDCl_3$): δ = 9.9 (+), 14.2 (+), 39.1 (-), 47.8 (-), 50.8 (-), 63.6 (-), 122.1 (+), 129.7 (+), 135.2 (q), 139.9 (q), 140.4 (q), 152.4 (q).

ESI-MS: m/z (%) = 314.16 ($M+H^+$)

Compound 25: (E)-2-(4-((1-(2-azidoethyl)-3,5-dimethyl-1H-pyrazol-4-yl)di-azeryl)-phenyl)acetaldehyde



$C_{15}H_{17}N_7O$, MW = 311.35 g/mol

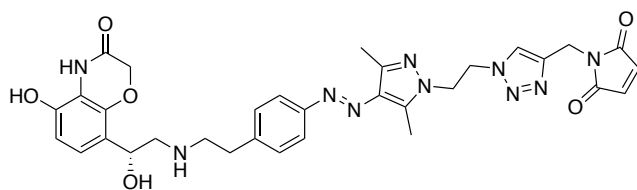
Compound **24** (40 mg, 0.13 mmol, 1.0 eq) was dissolved in CH_2Cl_2 (30 mL) under Ar-atmosphere and the solution was cooled to 0 °C. Dess Martin periodinane (81 mg, 0.19 mmol, 1.5 eq) was added and the mixture was stirred for 1.5 h. The reaction mixture was diluted with EtOAc (50 mL) and subsequently washed with aqueous sat. $Na_2S_2O_3$ (50 mL), sat. $NaHCO_3$ (50 mL) and sat. $NaCl$ (50 mL). The combined organic layers were dried (Na_2SO_4), filtered and the solvent was removed under reduced pressure to get the crude compound **25** (37 mg, 0.12 mmol, 92%) as a yellow solid. Compound **25** was carried on to the reductive amination immediately for the formation of compound **2**.

¹H-NMR (400 MHz; CDCl₃): δ = 2.50 (s, 3H), 2.62 (s, 3H), 3.82-3.74 (m, 4H), 4.22-4.14 (m, 2H), 7.30 (d, *J* = 8.3 Hz, 2H), 7.79 (s, 2H), 9.77 (s, 1H).

¹³C-NMR (101 MHz, CDCl₃): δ = 9.9 (+), 14.2 (+), 47.8 (-), 50.4 (-), 50.8 (-), 122.5 (+), 130.3 (+), 133.2 (q), 135.2 (q), 140.19 (q), 143.4 (q), 152.9 (q), 199.1 (+).

ESI-MS: *m/z* (%) = 312.14 (M+H⁺)

Compound 2: (*R,E*)-1-((1-(2-(4-((4-(2-((2-hydroxy-2-(5-hydroxy-3-oxo-3,4-dihydro-2*H*-benzo[*b*][1,4]oxazin-8-yl)ethyl)amino)ethyl)phenyl)diazenyl)-3,5-dimethyl-1*H*-pyrazol-1-yl)ethyl)-1*H*-1,2,3-triazol-4-yl)methyl)-1*H*-pyrrole-2,5-dione



C₃₂H₃₄O₁₀N₆, MW = 654.69 g/mol

Compound *R*-**22** (20 mg, 0.088 mmol, 1.1 eq), **25** (25 mg, 0.080 mmol, 1.0 eq) and Na(AcO)₃BH (19 mg, 0.088 mmol, 1.1 eq) were dissolved in dry THF/MeCN (1:1, 20 mL) under Ar-atmosphere. The reaction mixture was stirred at r.t. for 16 h and then diluted with EtOAc (30 mL). The mixture was extracted with sat. aqueous NaHCO₃ solution (50 mL) and water (50 mL). The organic layer was dried over Na₂SO₄ and the solvent was removed under reduced pressure. The crude intermediate **26** was dissolved in ^tBuOH, THF, H₂O (1:1:1, 5 mL) and *N*-propargylmaleimide (13 mg, 0.096 mmol, 1.2 eq), CuSO₄·5H₂O (4.3 mg, 0.026 mmol, 0.33 eq) and TBTA (17 mg, 0.026 mmol, 0.33 eq) were added. After 2 min, Na-ascorbate (5.3 mg, 0.026 mmol, 0.33 eq) was added and the mixture was stirred at r.t. for 2h. The reaction mixture was diluted with DMSO (1 mL) and directly used for purification with preparative HPLC (column: Luna 10, 250 x 21 mm; flow: 20 mL/min, solvent A: H₂O (0.05% TFA), solvent B: MeCN; gradient A/B: 0-20 min: 90/10, 20-25 min: 2/98) to obtain the desired product *R*-**2** (5.7 mg, 0.0087 mmol, 11%) as a yellow solid.

¹H-NMR (600 MHz; DMSO-*D*₆): δ = 2.13 (s, 3H, CH₃), 2.35 (s, 3H, CH₃), 3.02-2.97 (m, 2H, CH₂), 3.15-3.08 (m, 2H, CH₂), 3.25-3.19 (m, 2H, CH₂), 4.48 (t, *J* = 5.6 Hz, 2H, CH₂), 4.54 (d, *J* = 4.6 Hz, 2H, CH₂), 4.61 (s, 2H, CH₂), 4.77 (t, *J* = 5.6 Hz, 2H, CH₂), 5.09-5.07 (m, 1H, CH_{arom}), 5.96 (s, 1H, OH), 6.56 (d, *J* = 8.4 Hz, 1H, CH_{arom}), 6.93 (d, *J* = 8.5, 1H, CH_{arom}), 7.00 (s, 2H,

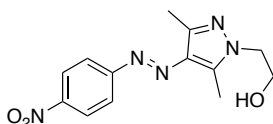
CH_{arom}), 7.00 (s, 2H, CH_{arom}), 7.39 (d, *J* = 8.3 Hz, 2H, CH_{arom}), 7.68 (d, *J* = 8.3 Hz, 2H, CH_{arom}), 7.88 (s, 1H), 7.88 (s, 1H), 8.64 (s, 1H, NH), 8.76 (s, 1H, OH), 9.98 (s, 1H, NH)

¹³C-NMR (151 MHz; DMSO-D₆): δ = 8.6 (+), 14.0 (+), 31.1 (-), 32.4 (-), 47.9 (-), 48.2 (-), 48.9 (-), 52.2 (-), 62.8 (+), 67.0 (-), 109.1 (+), 115.3 (q), 119.8 (q), 120.0 (+), 121.7 (+), 123.6 (+), 129.5 (+), 134.1 (q), 134.7 (+), 140.4 (q), 141.18 (q), 141.21 (q), 142.5 (q), 144.9 (q), 151.9 (q), 164.2 (q), 170.3 (q, = 3x C=O),

ESI-MS: *m/z* (%) = 655.27 (M+H⁺)

HR-MS (ESI): calcd. for C₃₂H₃₄N₁₀O₆ (M+H⁺), *m/z* = 655.2736, found 655.2731

Compound 32: (*E*)-2-(3,5-dimethyl-4-((4-nitrophenyl)diazenyl)-1*H*-pyrazol-1-yl)-ethan-1-ol



C₁₃H₁₅N₅O₃, MW = 289.30 g/mol

GP2, starting material **31**, yield: 98%, orange solid.

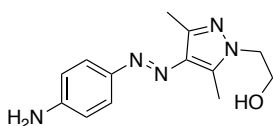
TLC: (PE/EtOAc, 3:1) R_f = 0.46

¹H-NMR (400 MHz; CDCl₃): δ = 2.51 (s, 3H), 2.64 (s, 3H), 4.07 (t, *J* = 4.8 Hz, 2H), 4.18 (t, *J* = 4.8 Hz, 2H), 7.87 (d, *J* = 9.0 Hz, 2H), 8.32 (d, *J* = 9.1 Hz, 2H).

¹³C-NMR (101 MHz; CDCl₃): δ = 10.1 (+), 14.3 (+), 50.6 (-), 61.5 (-), 122.5 (+), 124.8 (+), 136.3 (q), 141.5 (q), 143.8 (q), 147.1 (q), 157.2 (q),

ESI-MS: *m/z* (%) = 290.13 (M+H⁺)

Compound 33: (*E*)-2-(4-((4-aminophenyl)diazenyl)-3,5-dimethyl-1*H*-pyrazol-1-yl)-ethan-1-ol



C₁₃H₁₇N₅O, MW = 259.31 g/mol

Compound **32** (1.0 g, 3.5 mmol, 1.0 eq) was dissolved in a mixture of THF/H₂O (3:1 (v/v), 60 mL) and Na₂S (1.0 g, 12.8 mmol, 3.4 eq) was added to reflux the reaction mixture for 4 h. The mixture was cooled to r.t. and the organic solvent was removed in *vacuo*. Aqueous 1 M NaOH and EtOAc were added and after separation of the aqueous layer, the organic layer was extracted with sat. NaHCO₃ solution (1 x 50 mL) and sat. NaCl solution (1 x 50 mL). The organic layer was dried over Na₂SO₄ and after filtration the solvent was removed in *vacuo*. The crude product was purified by automated column chromatography (CH₂Cl₂/MeOH, 0-30% MeOH, + 0.1% NEt₃) to afford compound **33** (0.8 g, 0.2 mmol, 77%) as an orange solid.

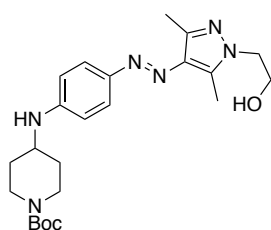
TLC: (CH₂Cl₂/MeOH, 20:1) R_f = 0.22

¹H-NMR (400 MHz; DMSO-D₆): δ = 2.34 (s, 3H), 2.51 (s, 4H), 3.71 (q, J = 5.5 Hz, 2H), 4.04 (t, J = 5.6 Hz, 2H), 6.62 (d, J = 8.8 Hz, 2H), 7.49 (d, J = 8.7 Hz, 2H).

¹³C-NMR (101 MHz; DMSO-D₆): δ = 9.5 (+), 13.9 (+), 50.9 (-), 60.1 (-), 113.4 (+), 123.2 (+), 133.8 (q), 138.0 (q), 139.9 (q), 143.8 (q), 150.8 (q).

ESI-MS: m/z (%) = 260.15 (M+H⁺)

Compound 34: *tert*-butyl (*E*)-4-((4-((1-(2-hydroxyethyl)-3,5-dimethyl-1*H*-pyrazol-4-yl)diazanyl)phenyl)amino)piperidine-1-carboxylate



C₂₃H₃₄N₆O₃, MW = 442.56 g/mol

Azopyrazol **33** (0.7 g, 2.7 mmol, 1.05 eq), Boc-piperidone (0.5 g, 2.6 mmol, 1.0 eq) and AcOH (169 μL, 2.7 mmol, 1.0 eq) were dissolved in dichloroethane (50 mL) at r.t. Na(AcO)₃BH (0.8 g, 3.5 mmol, 1.0 eq) was added in small portions over 15 min and the mixture was stirred for 24 h at r.t. The reaction mixture was diluted with EtOAc and the organic layer was extracted with 1 M NaOH (2 x 50 mL), sat. NaHCO₃ solution (1 x 50 mL) and sat. NaCl solution (1 x 50 mL). The organic layer was dried over Na₂SO₄ and after filtration the solvent was reduced in *vacuo*. The crude product was purified by automated column chromatography (CH₂Cl₂/MeOH,

0-10% MeOH, + 0.1% NEt₃) to afford the target compound **34** (0.8 g, 0.2 mmol, 77%) as a yellow solid.

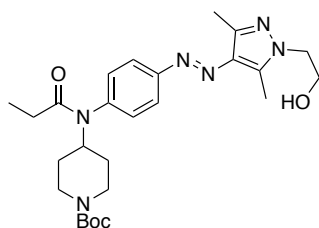
TLC: (CH₂Cl₂/MeOH, 20:1) R_f = 0.45

¹H-NMR (400 MHz; DMSO-D₆): δ = 1.32-1.20 (m, 2H), 1.41 (s, 9H), 1.96-1.86 (m, 2H), 2.34 (s, 3H), 2.51 (s, 3H), 3.01-2.84 (m, 2H), 3.70 (t, J = 5.6 Hz, 2H), 3.90-3.87 (m, 2H), 4.04 (t, J = 5.6 Hz, 2H), 6.67 (d, J = 8.9 Hz, 2H), 7.54 (d, J = 8.9 Hz, 2H).

¹³C-NMR (101 MHz; DMSO-D₆): δ = 9.5 (+), 13.9 (+), 28.1 (+), 31.5 (-), 42.7 (-), 48.6 (+), 50.9 (-), 60.1 (-), 78.6 (q), 112.0 (+), 123.3 (+), 133.8 (q), 138.0 (q), 139.9 (q), 143.7 (q), 149.3 (q), 153.9 (q),

ESI-MS: m/z (%) = 443.28 (M+H⁺)

Compound 35: tert-butyl (E)-4-(N-(4-((1-(2-hydroxyethyl)-3,5-dimethyl-1H-pyrazol-4-yl)diazenyl)phenyl)propionamido)piperidine-1-carboxylate



C₂₆H₃₈N₆O₄, MW = 498.63 g/mol

Compound **34** (1.1g, 2.5 mmol, 1.0 eq) was dissolved in anhydrous toluene (35 mL) under Ar-atmosphere. DMAP (0.62 g, 5.1 mmol, 2.0 eq), propionic anhydride (0.65 mL, 5.1 mmol, 2 eq) and NEt₃ (1.8 mL, 12.7 mmol, 5.0 eq) were added and the mixture was stirred over night at r.t. The solvent was evaporated and the crude product was purified by automated column chromatography (PE/EtOAc, 0-90% EtOAc) to obtain compound **35** (0.1 g, 0.31 mmol, 10%) as a yellowish oil.

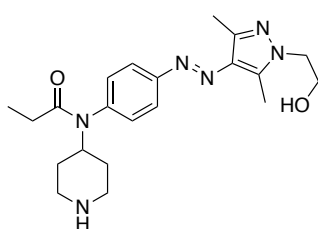
TLC: (PE/EtOAc, 1:1 + 1% NEt₃) R_f = 0.23

¹H-NMR (400 MHz; CDCl₃): δ = 1.25-1.21 (m, 3H), 1.40-1.29 (m, 2H), 1.45 (s, 9H), 2.08-2.03 (m, 2H), 2.32-2.26 (m, 2H), 2.46 (d, 3H), 2.54 (s, 3H), 2.93 (t, J = 11.9 Hz, 2H), 3.54-3.42 (m, 1H), 4.09-3.95 (m, 2H), 4.26 (t, J = 5.3 Hz, 2H), 4.41 (t, J = 5.3 Hz, 2H), 6.61 (d, J = 7.8 Hz, 2H), 7.66 (d, J = 7.9 Hz, 2H).

¹³C-NMR (101 MHz; CDCl₃): δ = 9.9 (+), 14.3 (+), 13.9 (+), 27.4, 28.5 (+), 32.3 (-), 47.5 (-), 50.1(+), 62.9 (-), 79.8 (q), 112.8 (+), 123.8 (+), 134.9 (q), 137.9 (q), 142.7 (q), 145.7 (q), 148.3 (q), 154.8 (q), 174.1 (q).

ESI-MS: m/z (%) = 499.30 (M+H⁺)

Compound 36: (E)-N-(4-((1-(2-hydroxyethyl)-3,5-dimethyl-1H-pyrazol-4-yl)di-azeryl)-phenyl)-N-(piperidin-4-yl)propionamide



C₂₁H₃₀N₆O₂, MW = 398.51 g/mol

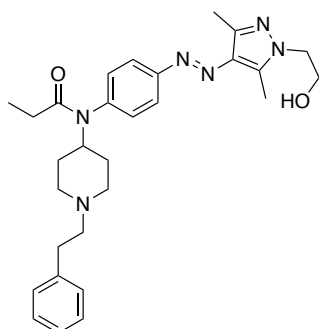
Compound **35** (196 mg, 0.39 mmol, 1 eq) was dissolved in a mixture of THF/CH₂Cl₂ (1:1). A solution of HCl in Dioxane (5 mL) was added and the mixture was stirred at r.t. for 1.5 h. The solvent was evaporated and the crude product was purified by RP chromatography (H₂O+TFA 0.05%/MeCN 10-98% MeCN). After lyophilization the product **36** (120 mg, 0.3 mmol, 77%) was obtained as a white solid.

1-H NMR (400 MHz; DMSO-D₆): δ = 0.98 (t, J = 7.5 Hz, 3H), 1.65-1.55 (m, 2H), 2.08-2.05 (m, 2H), 2.28 (q, J = 7.5 Hz, 2H), 2.34 (s, 3H), 2.51 (s, 3H), 3.04-3.01 (m, 2H), 3.33-3.30 (m, 2H), 3.63 (s, 1H), 4.27 (t, J = 5.0 Hz, 2H), 4.36-4.33 (m, 2H), 6.71 (d, J = 8.8 Hz, 2H), 7.56 (d, J = 8.8 Hz, 2H).

¹³C NMR (101 MHz; DMSO-D₆): δ = 8.8 (+), 9.3 (+), 13.9 (+), 26.7 (-), 28.3 (-), 42.1(-), 46.2 (+), 47.1 (-), 62.3 (-), 112.0 (+), 123.3 (+), 133.9 (q), 137.9 (q), 140.3 (q), 143.8 (q), 149.1 (q), 173.3 (q).

ESI-MS: m/z (%) = 399.25 (M+H⁺)

Compound 37: (E)-N-(4-((1-(2-hydroxyethyl)-3,5-dimethyl-1H-pyrazol-4-yl)-diazeryl)-phenyl)-N-(1-phenethylpiperidin-4-yl)propionamide



$C_{29}H_{38}N_6O_2$, MW = 502.66 g/mol

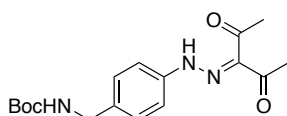
Compound **37** (1.6 g, 4.0 mmol, 1.0 eq) was dissolved in dichloroethane (100 mL) at r.t. Phenylacetaldehyde (0.72 g, 6.0 mmol, 1.5 eq) and $Na(AcO)_3BH$ (7.7 g, 36 mmol, 6 eq) were added and the mixture was stirred under Ar-atmosphere and r.t. over night. The reaction mixture was diluted with EtOAc and the organic mixture was extracted with 1 M NaOH (100 mL), sat. $NaHCO_3$ (100 mL) and brine (100 mL). The organic layer was dried over Na_2SO_4 , filtered and the solvent was evaporated. The crude product was purified by automated column chromatography ($CH_2Cl_2/MeOH$, 0-8% MeOH) to afford compound **38** (0.9 g, 1.8 mmol, 45%) as an orange solid.

1H -NMR (400 MHz; MeOD): δ = 1.06 (t, J = 7.6, 3H), 1.61-1.52 (m, 2H), 2.06 (d, J = 12.0, 2H), 2.29-2.21 (m, 2H), 2.31 (q, J = 7.6, 2H), 2.44 (s, 3H), 2.56 (s, 3H), 2.63-2.59 (m, 2H), 2.84-2.77 (m, 2H), 3.01 (d, J = 11.8 Hz, 2H), 3.41-3.34 (m, 1H), 4.28 (t, J = 5.2 Hz, 2H), 4.41 (t, J = 5.2 Hz, 2H), 6.68 (d, J = 8.9 Hz, 2H), 7.23-7.18 (m, 3H), 7.27 (d, J = 7.3 Hz, 2H), 7.64 (d, J = 8.8 Hz, 2H).

^{13}C -NMR (101 MHz; MeOD): δ = 9.3 (+), 9.9 (+), 14.0 (+), 28.1 (-), 32.7 (-), 34.2 (-), 48.4 (-), 50.5 (+), 53.4 (-), 61.6 (-), 63.7 (-), 113.4 (+), 124.8 (+), 127.2 (+), 129.5 (+), 129.8 (+), 135.7 (q), 139.5 (q), 141.2 (q), 143.2 (q), 146.0 (q), 151.2 (q), 175.5 (q).

ESI-MS: m/z (%) = 503.31 ($M+H^+$)

Compound 39: *tert*-butyl (4-(2-(2,4-dioxopent-3-ylidene)hydrazineyl)-benzyl)-carbamate



$C_{17}H_{23}N_3O_4$, MW = 333.39 g/mol

GP1, aniline derivative **38**, yield: 90%, yellow crystals.

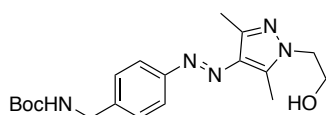
TLC: (CH₂Cl₂/MeOH, 20:1) R_f = 0.46

¹H-NMR (400 MHz; CDCl₃): δ = 1.46 (s, 9H), 2.48 (s, 3H), 2.59 (s, 3H), 4.34-4.22 (m, 2H) 7.32 (d, *J* = 8.6 Hz, 2H), 7.36 (d, *J* = 8.6 Hz, 2H).

¹³C-NMR (101 MHz, CDCl₃): δ = 26.8 (+), 28.5 (+), 31.8 (+), 44.3 (-), 79.8 (q), 116.6 (+), 128.9 (+), 133.4 (q), 137.0 (q), 140.9 (q), 198.1 (q).

ESI-MS: *m/z* (%) = 334.18 (M+H⁺)

Compound 40: *tert*-butyl (*E*)-(4-((1-(2-hydroxyethyl)-3,5-dimethyl-1*H*-pyrazol-4-yl)diazenyl)benzyl)carbamate



C₁₉H₂₇N₅O₃, MW = 373.46 g/mol

GP2, starting material **39**, yield 63%, yellow crystals.

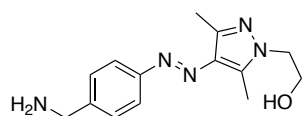
TLC: (CH₂Cl₂/MeOH, 20:1) R_f = 0.12

¹H-NMR (400 MHz; CDCl₃): δ = 1.46 (s, 9H), 2.47 (s, 3H), 2.58 (s, 3H), 4.01 (t, *J* = 4.9 Hz, 2H), 4.12 (t, *J* = 4.9 Hz, 2H), 4.35 (d, *J* = 5.3 Hz, 2H), 7.35 (d, *J* = 8.2 Hz, 2H), 7.72 (d, *J* = 8.3 Hz, 2H).

¹³C-NMR (101 MHz, CDCl₃): δ = 10.0 (+), 14.1 (+), 28.5 (+), 50.4 (-), 58.5 (-), 61.5 (-), 79.8 (q), 122.1 (+), 128.1 (+), 135.1 (q), 139.7 (q), 142.9 (q), 153.0 (q), 156.1 (q).

ESI-MS: *m/z* (%) = 374.22 (M+H⁺)

Compound 41: (*E*)-2-(4-((4-(aminomethyl)phenyl)diazenyl)-3,5-dimethyl-1*H*-pyrazol-1-yl)ethan-1-ol



C₁₄H₁₉N₅O, MW = 273.34 g/mol

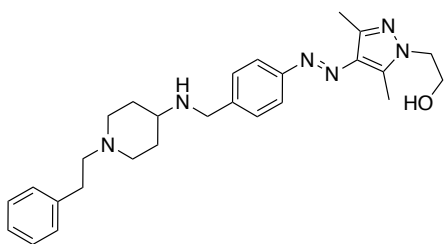
GP3, starting material **40**, yield: 95%, yellow crystals.

¹H-NMR (300 MHz; CDCl₃): δ = 2.46 (s, 3H), 2.58 (s, 3H), 3.84 (s, 2H), 3.99 (t, *J* = 4.9 Hz, 2H), 4.11 (t, *J* = 4.8 Hz, 2H), 7.32 (d, *J* = 8.6 Hz, 2H), 7.70 (d, *J* = 8.4 Hz, 2H).

¹³C-NMR (75 MHz, CDCl₃): δ = 10.0 (+), 14.1 (+), 46.2 (-), 50.7 (-), 61.2 (-), 122.1 (+), 127.6 (+), 135.0 (q), 139.8 (q), 142.7 (q), 144.4 (q), 152.6 (q).

ESI-MS: *m/z* (%) = 274.15 (M+H⁺)

Compound **42**: (*E*)-2-(3,5-dimethyl-4-((4-(((1-phenethylpiperidin-4-yl)amino)-methyl)-phenyl)diazenyl)-1*H*-pyrazol-1-yl)ethan-1-ol



C₂₇H₃₆N₆O, MW = 460.63 g/mol

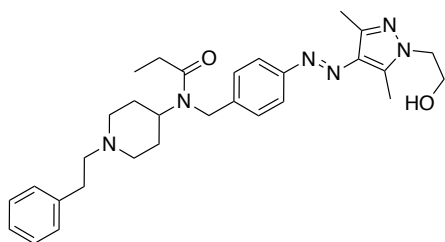
To a solution of azopyrazole **41** (600 mg, 1.61 mmol, 1.0 eq), phenethyl-4-piperidone (444 mg, 1.61 mmol, 1.0 eq) and AcOH (0.13 mL, 1.61 mmol, 1.0 eq) in dichloroethane (80 mL) was added Na(AcO)₃BH (651 mg, 3.07 mmol, 1.9 eq) in small portions over 15 min and the mixture was stirred for 24 h at r.t. The reaction mixture was diluted with EtOAc (120 mL) and the organic layer was extracted with 1 M NaOH (100 mL), sat. aqueous NaHCO₃ solution (100 mL) and sat. aqueous NaCl solution (100 mL). The organic layer was dried over Na₂SO₄ and after filtration the solvent was reduced *in vacuo*. The crude product was purified by automated column chromatography (CH₂Cl₂/MeOH, 0-20% MeOH, + 0.1% NEt₃) to afford the target compound **42** (270 mg, 0.59 mmol, 37%) as a yellow solid.

¹H-NMR (400 MHz; CDCl₃): δ = 1.52-1.41 (m, 2H), 1.92 (d, *J* = 10.2 Hz, 2H), 2.05 (t, *J* = 10.6 Hz, 2H), 2.49 (s, 3H), 2.57-2.53 (m, 2H), 2.59 (s, 3H), 2.82-2.74 (m, 3H), 2.95 (d, *J* = 11.8 Hz, 2H), 3.85 (s, 2H), 4.01 (t, *J* = 4.9 Hz, 2H), 4.12 (t, *J* = 4.8 Hz, 2H), 7.21-7.17 (m, 3H), 7.31-7.23 (m, 2H), 7.39 (d, *J* = 8.3 Hz, 2H), 7.73 (d, *J* = 8.3 Hz, 2H).

¹³C-NMR (101 MHz, CDCl₃): δ = 10.0 (+), 14.1 (+), 32.8 (-), 33.9 (-), 50.5 (-), 52.5 (-), 54.1 (+), 60.7 (-), 61.4 (-), 122.0 (+), 126.1 (+), 128.5 (+), 128.6 (+), 128.8 (q), 135.0 (q), 139.6 (q), 140.5 (q), 142.2 (q), 142.8 (q), 152.7 (q).

ESI-MS: m/z (%) = 461.30 (M+H⁺)

Compound 43: (E)-N-(4-((1-(2-hydroxyethyl)-3,5-dimethyl-1H-pyrazol-4-yl)diazenyl)-benzyl)-N-(1-phenethylpiperidin-4-yl)propionamide



C₃₀H₄₀N₆O₂, MW = 516.69 g/mol

Compound **42** (270 mg, 0.587 mmol, 1.0 eq), DMAP (86.0 mg, 0.704 mmol, 1.2 eq), propionic anhydride (90 μL, 0.704 mmol, 1.2 eq) and DIPEA (0.5 mL, 2.93 mmol, 5 eq) were dissolved in CH₂Cl₂ (10 mL) and stirred at r.t. for 24 h. The solvent was evaporated and the crude product was purified by automated column chromatography (CH₂Cl₂/MeOH, 0-5% MeOH) and preparative HPLC (column: Luna 10, 250 x 21 mm; flow: 20 mL/min, solvent A: H₂O (0.05% TFA)), solvent B: MeCN; gradient A/B: 0-15 min: 90/10, 15-20 min: 2/98; t_R = 10.0 min). The intermediate was dissolved in MeOH/H₂O (9:1, 10 mL) and KOH (164 mg, 2.93 mmol, 5.0 eq) was added to stir the mixture over night. The reaction mixture was acidified with 2M HCl and extracted with CH₂Cl₂ (3x 50 mL). The combined organic layers were dried over Na₂SO₄, filtered and the solvent was removed under reduced pressure to obtain compound **43** (20 mg, 0.038 mmol, 7%) as the desired product.

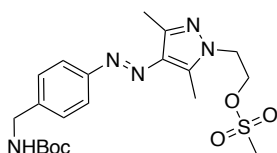
¹H-NMR (400 MHz; CDCl₃): δ = 1.12 (t, J = 7.2 Hz, 3H), 1.79 (d, J = 12.6 Hz, 2H), 2.33-2.29 (m, 2H), 2.53-2.40 (s, 5H), 2.58 (s, 3H), 2.78 (t, J = 10.3 Hz, 2H), 3.15 (s, 4H), 3.60-3.58 (m, 2H), 4.03 (t, J = 4.8 Hz, 2H), 4.14 (t, J = 4.8 Hz, 2H), 4.64 (s, 2H), 4.89 (s, 1H), 7.20 (d, J = 6.7 Hz, 2H), 7.28-7.26 (m, 5H), 7.72 (d, J = 8.4 Hz, 2H).

¹³C-NMR (101 MHz; CDCl₃): δ = 9.6 (+), 10.0 (+), 14.1 (+), 26.4 (-), 27.2 (-), 27.4 (-), 30.6 (-), 46.4 (-), 48.9 (+), 50.5 (-), 52.7 (-), 52.8 (-), 53.6 (-), 58.7 (-), 61.5 (-), 122.4 (+), 126.4 (+), 127.4(+), 128.8 (+), 129.1 (+), 135.1 (q), 136.1 (q), 139.2 (q), 139.9 (q), 142.9 (q), 153.0 (q), 175.4 (q),

ESI-MS: m/z (%) = 517.33 ($M+H^+$)

HR-MS (ESI): calcd. for $C_{30}H_{40}N_6O_2$ ($M+H^+$), m/z = 517.3286, found 517.3294

Compound 44: (*E*)-2-(4-((4-(((*tert*-butoxycarbonyl)amino)methyl)phenyl)-diazenyl)-3,5-dimethyl-1*H*-pyrazol-1-yl)ethyl 4-methylbenzenesulfonate



$C_{20}H_{29}N_5O_5S$, MW = 451.54 g/mol

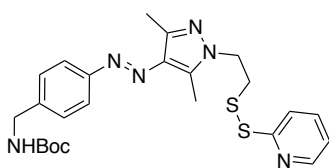
A solution of Compound **40** (4.0 g, 11.0 mmol, 1.0 eq) in CH_2Cl_2 (150 mL) was cooled to 0 °C and NEt_3 (2.2 mL, 16.5 mmol, 1.5 eq) and methanesulfonyl chloride (2.2 mL, 11.1 mmol, 1.05 eq) were added. The mixture was stirred and warmed up to r.t. over 1 h. Water (100 mL) was added and the aqueous layer was extracted with CH_2Cl_2 (2x 100 mL). The combined organic layers were dried over Na_2SO_4 and the solvent was removed under reduced pressure to obtain a yellow oil as the product **44** (4.8 g, 10.6 mmol, 97%).

1H -NMR (400 MHz; $CDCl_3$): δ = 1.47 (s, 9H), 2.49 (s, 3H), 2.62 (s, 3H), 2.87 (s, 3H), 4.39-4.31 (m, 4H), 4.63 (t, J = 5.2 Hz, 2H), 7.37 (d, J = 8.3 Hz, 2H), 7.74 (d, J = 8.4 Hz, 2H).

^{13}C -NMR (101 MHz, $CDCl_3$): δ = 9.9 (+), 14.2 (+), 28.6 (+), 37.4 (+), 44.5 (-), 47.8 (-), 67.8 (-), 79.8 (q), 122.2 (+), 128.1 (+), 135.3 (q), 140.4 (q), 143.5 (q), 152.9 (q), 156.0 (q), 162.7 (q).

ESI-MS: m/z (%) = 452.20 ($M+H^+$)

5.4.2 Compound 46: *tert*-butyl (*E*)-4-((3,5-dimethyl-1-(2-(pyridin-2-yl)disulfaneyl)ethyl)-1*H*-pyrazol-4-yl)diazenyl)benzyl)carbamate



$C_{24}H_{30}N_6O_2S_2$, MW = 498.66 g/mol

Potassium acetate (0.51 g, 3.79 mmol, 2.0 eq) was added to a stirred mixture of compound **44** (1.0 g, 1.89 mmol, 1.0 eq) in acetone (80 mL). The mixture was refluxed for 3 h and

subsequently cooled down to r.t. The solvent was removed under reduced pressure and the residue was dissolved in H₂O to do an extraction with EtOAc (3x 80 mL). The combined organic layers were dried (Na₂SO₄) and the solvent was removed *in vacuo* to obtain the intermediate **45** as an orange solid. Intermediate **45** was dissolved in a 0.5 M NaOMe solution in MeOH under Ar-atmosphere. 2-Aldrithiol (0.46 g, 2.08 mmol, 1.1 eq) was added and the mixture was stirred over night at r.t. The solvent was evaporated and the crude product was purified by automated column chromatography (PE/EtOAc, 5-80% EtOAc) to afford **26** (0.63 g, 1.26 mmol, 67%) as a yellow oil.

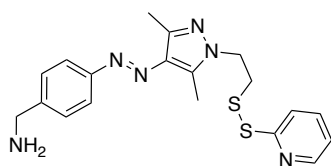
TLC: (CH₂Cl₂/MeOH, 20:1) R_f = 0.55

¹H-NMR (400 MHz; CDCl₃): δ = 1.47 (s, 9H), 1.66 (d, J = 0.3, 2H), 2.48 (s, 3H), 2.58 (s, 3H), 3.26 (t, J = 6.8, 2H), 4.37 (t, J = 6.8, 4H), 7.12-7.10 (m, 1H), 7.36 (d, J = 8.3, 2H), 7.65 (d, J = 1.4, 2H), 7.73 (d, J = 8.4, 2H), 8.50-8.48 (m, 1H).

¹³C-NMR (101 MHz, CDCl₃): δ = 10.2 (+), 14.4 (+), 28.7 (+), 37.8 (-), 44.7 (-), 47.4 (-), 79.9 (q), 120.4 (+), 121.3 (+), 122.3 (+), 128.2 (q), 135.3 (+), 137.4 (q), 143.3 (q), 150.1 (+), 159.4 (q), 171.4 (q),

ESI-MS: m/z (%) = 499.19 (M+H⁺)

Compound 47: (E)-4-((3,5-dimethyl-1-(2-(pyridin-2-yl)disulfaneyl)ethyl)-1H-pyrazol-4-yl)diazenyl)phenyl)methanamine



C₁₉H₂₂N₆S₂, MW = 398.55 g/mol

GP3, starting material **46**, yield: 95%, yellow crystals.

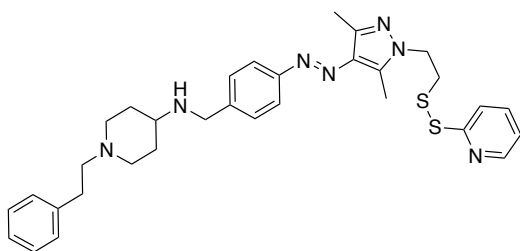
TLC: (CH₂Cl₂/MeOH 0.01 % Et₃N, 20:1) R_f = 0.09

¹H-NMR (400 MHz; CDCl₃): δ = 2.40 (s, 3H), 2.50 (s, 3H), 3.21 (t, J = 6.6, 2H), 4.33 (t, J = 6.6, 2H), 7.18-7.12 (m, 1H), 7.37 (d, J = 8.4, 2H), 7.69-7.66 (m, 4H), 8.47 (d, J = 4.9, 1H),

¹³C-NMR (CDCl₃, 101 MHz): δ = 10.0 (+), 13.9 (+), 37.7 (-), 43.5 (-), 47.1 (-), 121.0 (+), 121.7 (+), 122.5 (+), 129.9 (+), 133.4 (q), 135.0 (q), 138.3 (+), 140.4 (q), 143.2 (q), 149.1 (+), 153.8 (q), 158.8 (q).

ESI-MS: m/z (%) = 399.14 (M+H⁺)

Compound 48: (E)-N-(4-((3,5-dimethyl-1-(2-(pyridin-2-yl)disulfaneyl)ethyl)-1H-pyrazol-4-yl)diazenyl)benzyl)-1-phenethylpiperidin-4-amine



C₃₂H₃₉N₇S₂, MW = 585.83 g/mol

To a solution of 1-phenethylpiperidin-4-one (162 mg, 1.0 mmol, 1.0 eq) in dichloroethane (40 mL), was added sequentially compound **47** (400 mg, 1.0 mmol, 1.0 eq), NaHB(OAc)₃ (391 mg, 1.4 mmol, 1.4 eq) and AcOH (0.08 mL, 1.4 mmol, 1.0 eq) under Ar-atmosphere at r.t. The bright orange reaction mixture was stirred overnight at r.t. After 20 h, the reaction mixture was diluted with EtOAc (100 mL), washed with 1M NaOH (50 mL), aqueous sat. NaHCO₃ (50 mL), aqueous sat. NaCl solution (50 mL). The combined organic layers were dried (Na₂SO₄), filtered and concentrated *in vacuo*. The crude residue was purified by automated column chromatography (CH₂Cl₂/MeOH, 0-10% MeOH) to obtain **48** as an orange oil (342 mg, 0.58 mmol, 88%).

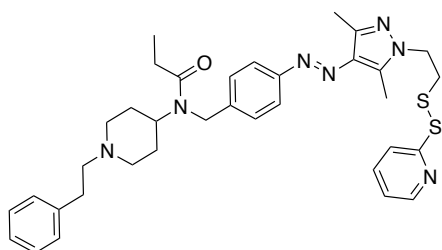
TLC: (CH₂Cl₂/MeOH 0.01 % Et₃N, 20:1) R_f = 0.05

¹H-NMR (400 MHz; CDCl₃): δ = 1.61-1.48 (m, 8.6, 2H), 2.01-1.93 (m, 2H), 2.17-2.08 (m, 2H), 2.50 (s, 3H), 2.58 (s, 3H), 2.61-2.50 (m, 1H), 2.63-2.61 (m, 2H), 2.85-2.80 (m, 2H), 3.04-2.97 (m, 2H), 3.26 (t, J = 6.8, 2H), 3.88 (s, 2H), 4.36 (t, J = 6.8, 2H), 7.11 (ddd, J = 5.9, 4.9, 2.5, 1H), 7.21-7.19 (m, 3H), 7.30-7.27 (m, 2H), 7.43 (d, J = 8.4, 2H), 7.65-7.62 (m, 2H), 7.76-7.74 (m, 2H), 8.48 (dt, J = 4.7, 1.4, 1H).

¹³C-NMR (101 MHz; CDCl₃): δ = 10.0 (+), 14.1 (+), 32.2 (-), 33.6 (-), 37.6 (-), 47.2 (-), 50.3 (-), 52.2 (-), 53.8 (+), 60.4 (-), 120.1 (+), 121.1 (+), 121.9 (+), 126.1 (+), 128.4 (+), 128.7 (+), 134.9 (q), 137.2 (+), 139.4 (q), 140.2 (q), 141.6 (q), 143.0 (q), 149.9 (+), 152.7 (q), 159.2 (q).

ESI-MS: m/z (%) = 586.28 ($M+H^+$)

Compound 49: (E)-N-(4-((3,5-dimethyl-1-(2-(pyridin-2-yl)disulfaneyl)ethyl)-1H-pyrazol-4-yl)diazenyl)benzyl)-N-(1-phenethylpiperidin-4-yl)propionamide



$C_{35}H_{43}N_7OS_2$, MW = 641.90 g/mol

Compound **48** (200 mg, 0.34 mmol, 1.0 eq) was dissolved in CH_2Cl_2 at r.t. and propionylchloride (40 μ L, 0.41 mmol, 1.2 eq) and NEt_3 (240 μ L, 1.71 mmol, 5.0 eq) were added to stir the mixture 10 min at r.t. The reaction was quenched by H_2O and extraction with CH_2Cl_2 (3x 50 mL) was done. The combined organic layers were dried over Na_2SO_4 and the solvent was removed under reduced pressure. The crude product was purified by automated reverse phase column chromatography (H_2O + 0.05% TFA/MeCN, 10-98% MeCN) to obtain target compound **49** (208 mg, 0.32 mmol, 95%) as a yellowish powder.

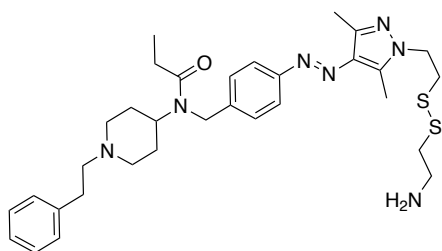
TLC: ($CH_2Cl_2/MeOH$, 0.01 % Et_3N , 20:1) R_f = 0.29

1H -NMR (400 MHz; MeOD): δ = 1.14 (t, J = 7.0 Hz, 3H), 2.03-1.93 (m, 2H), 2.23-2.07 (m, 2H), 2.44 (s, 3H), 2.50-2.45 (m, 2H), 2.62 (s, 3H), 2.68-2.63 (m, 2H), 3.06-2.99 (m, 2H), 3.17-3.07 (m, 2H), 3.36-3.32 (m, 2H), 3.67 (d, J = 11.4 Hz, 2H), 4.41 (t, J = 6.4 Hz, 2H), 4.52-4.44 (m, 1H), 4.70 (s, 2H), 7.29-7.21 (m, 4H), 7.35-7.29 (m, 3H), 7.39 (d, J = 8.0 Hz, 1H), 7.77-7.67 (m, 1H), 7.83-7.76 (m, 3H), 8.41 (d, J = 4.8 Hz, 1H).

^{13}C -NMR (101 MHz, MeOD): δ = 9.8 (+), 9.9, 14.1 (+), 28.0 (+), 31.4 (-), 39.1 (-), 48.7 (-), 48.8 (-), 49.1 (-), 53.5 (+), 59.0, 121.6 (+), 122.7 (+), 123.3 (+), 128.0 (+), 128.4 (+), 129.8 (+), 130.0 (+), 136.0(+), 137.4 (+), 139.4 (q), 140.7 (q), 141.6 (q), 143.7 (q), 150.4 (q), 154.4 (q), 177.2 (q).

ESI-MS: m/z (%) = 642.31 ($M+H^+$)

Compound 27: (E)-N-(4-((1-(2-((2-aminoethyl)disulfaneyl)ethyl)-3,5-dimethyl-1H-pyrazol-4-yl)diazenyl)benzyl)-N-(1-phenethylpiperidin-4-yl)propionamide



$C_{32}H_{45}N_7OS_2$, MW = 607.88 g/mol

Compound **49** (6.0 mg, 9.3 μ mol, 1.0 eq) was dissolved in MeOH (10 mL) at r.t. under Ar-atmosphere. Cysteamine hydrochloride (1.2 mg, 10 μ mol, 1.1 eq) was added and the mixture was stirred at r.t. for 0.5 h. The solvent was removed carefully and the crude product was purified by preparative HPLC (column: Luna 10, 250 x 21 mm; flow: 20 mL/min, solvent A: H₂O (0.05% TFA), solvent B: MeCN; gradient A/B: 0-15 min: 90/10, 15-20 min: 2/98; t_R = 7.9 min). Lyophilization afforded compound **27** (5.4 mg, 9.3 μ mol, 95%) as a pale yellow solid.

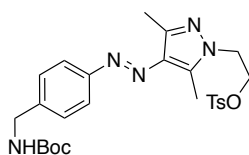
¹H-NMR (600 MHz; MeOD): δ = 1.13 (t, J = 7.4 Hz, 3H), 2.02-1.97 (m, 2H), 2.24-2.14 (m, 2H), 2.46-2.41 (m, 2H), 2.47 (s, 3H), 2.65 (s, 3H), 2.68-2.67 (m, 2H), 3.00-2.99 (m, 2H), 3.03-3.02 (m, 2H), 3.13-3.10 (m, 2H), 3.24-3.20 (m, 2H), 3.31-3.28 (m, 2H), 3.70-3.66 (m, 2H), 4.43 (t, J = 6.6 Hz, 2H), 4.52-4.46 (m, 1H), 4.71 (s, 2H), 7.28-7.24 (m, 3H), 7.35-7.31 (m, 2H), 7.39 (d, J = 8.2 Hz, 2H), 7.80 (d, J = 8.3 Hz, 2H).

¹³C-NMR (151 MHz, MeOD): δ = 9.7 (+), 9.8 (+), 14.0 (+), 27.5 (-), 27.8 (-), 28.1 (-), 31.3 (-), 35.0 (-), 37.8 (-), 39.0 (-), 45.2 (-), 48.3 (-), 49.0 (-), 52.4 (+), 53.4 (-), 58.9 (-), 123.2 (+), 127.8 (+), 128.2 (+), 129.6 (+), 129.9 (+), 135.9 (q), 137.3 (q), 140.6 (q), 141.7 (q), 143.7 (q), 154.3 (q), 177.2 (q).

ESI-MS: m/z (%) = 608.32 (M+H⁺)

HR-MS (ESI): calcd. for $C_{32}H_{45}N_7OS_2$ [MH⁺], m/z = 608.3200, found 608.3207

Compound 50: (E)-2-(4-((4-(((*tert*-butoxycarbonyl)amino)methyl)phenyl)-diazenyl)-3,5-dimethyl-1H-pyrazol-1-yl)ethyl 4-methylbenzenesulfonate



$C_{26}H_{33}N_5O_5S$, MW = 527.64 g/mol

To a solution of **40** (1.30 g, 3.48 mmol, 1.0 eq) in CH₂Cl₂ (80 mL), NEt₃ (1.46 mL, 10.4 mmol, 3.0 eq) was added, followed by the addition of p-toluenesulfonyl chloride (0.73 g, 3.83 mmol, 1.1 eq) at r.t. After 16 h of stirring, water was added (60 mL), and the mixture was extracted with CH₂Cl₂ (2x 40 mL). The combined organic layers were dried (Na₂SO₄), filtered and concentrated *in vacuo*. The crude residue was purified by automated column chromatography (CH₂Cl₂/MeOH, 0-20% MeOH) to obtain **50** as yellow crystals (1.40 mg, 2.65 mmol, 76%).

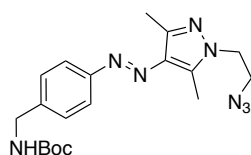
TLC: (CH₂Cl₂/MeOH, 20:1) R_f = 0.66

¹H-NMR (400 MHz, CDCl₃): δ = 1.48 (s, 9H), 2.34 (s, 3H), 2.35 (s, 3H), 2.54 (s, 3H), 4.27 (t, *J* = 4.92 Hz, 2H), 4.38 (br s, 2H), 4.43 (t, *J* = 4.94 Hz, 2H), 7.18 (d, *J* = 8.17 Hz, 2H), 7.39 (d, *J* = 8.13 Hz, 2H), 7.59 (d, *J* = 8.29 Hz, 2H), 7.76 (d, *J* = 8.29 Hz, 2H).

¹³C-NMR (101 MHz, CDCl₃): δ = 9.8 (+), 13.8 (+), 21.7 (+), 28.4 (+), 44.6 (-), 47.6 (-), 68.3 (-), 79.8 (q), 122.2 (+), 122.5 (q), 127.9 (+), 128.2 (+), 129.9 (+), 132.2 (q), 135.0 (q), 140.7 (q), 142.8 (q), 145.2 (q), 152.8 (q), 156.0 (q).

ESI-MS: m/z (%) = 528.23 (M+H⁺)

Compound 51: *tert*-butyl (*E*)-(4-((1-(2-azidoethyl)-3,5-dimethyl-1*H*-pyrazol-4-yl)-diaz-enyl)benzyl)carbamate



C₁₉H₂₆N₈O₂, MW = 398.47 g/mol

Compound **50** (1.30 g, 2.46 mmol, 1.0 eq) was dissolved in anhydrous DMSO (55 mL). NaN₃ (641 mg, 9.86 mmol, 4.0 eq) and NaI (369 mg, 2.46 mmol, 1.0 eq) were added and the reaction mixture was heated to 65 °C for 24 h under N₂ atmosphere. The reaction was allowed to cool to room temperature, water (50 mL) was added and the mixture was extracted with CH₂Cl₂ (2x 30 mL). The combined organic layers were dried (Na₂SO₄), filtered and concentrated *in vacuo*. The crude residue was purified by automated column chromatography (CH₂Cl₂/MeOH, 0-20% MeOH) to obtain **51** as a yellow oil (714 mg, 1.79 mmol, 72%).

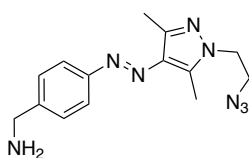
TLC: (CH₂Cl₂/MeOH, 20:1) R_f = 0.69

¹H-NMR (400 MHz, CDCl₃): δ = 1.46 (s, 9H), 2.49 (s, 3H), 2.61 (s, 3H), 3.77 (t, *J* = 5.68 Hz, 2H), 4.16 (t, *J* = 5.68 Hz, 2H), 4.36 (br s, 2H), 7.36 (d, *J* = 8.09 Hz, 2H), 7.74 (d, *J* = 8.33 Hz, 2H).

¹³C-NMR (101 MHz, CDCl₃): δ = 9.9 (+), 14.1 (+), 28.5 (+), 44.5 (-), 47.8 (-), 50.8 (-), 79.7 (+), 122.2 (+), 128.1 (+), 135.2 (q), 140.1 (q), 140.5 (q), 143.3 (q), 152.9 (q), 156.0 (q).

ESI-MS: *m/z* (%) = 399.23 (M+H⁺)

Compound 52: (*E*)-4-(((1-(2-azidoethyl)-3,5-dimethyl-1*H*-pyrazol-4-yl)-di-azeryl)phenyl)-methanamine



C₁₄H₁₈N₈, MW = 298.35 g/mol

GP3, starting material **51**, yield: 99%, yellow crystals.

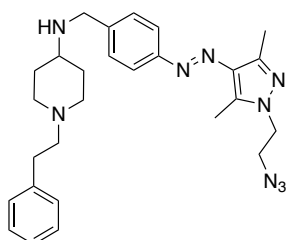
TLC: (CH₂Cl₂/MeOH 0.01 % Et₃N, 20:1) R_f = 0.07

¹H-NMR (400 MHz, CDCl₃): δ = 2.49 (s, 3H), 2.60 (s, 3H), 3.76 (t, *J* = 5.67 Hz, 2H), 3.91 (s, 2H), 4.15 (t, *J* = 5.67 Hz, 2H), 7.39 (d, *J* = 8.24 Hz, 2H), 7.74 (d, *J* = 8.32 Hz, 2H).

¹³C-NMR (101 MHz, MeOD): δ = 9.8 (+), 14.2 (+), 45.8 (-), 48.9 (-), 51.9 (-), 123.1 (+), 129.5 (+), 136.1 (q), 142.1 (q), 143.0 (q), 143.9 (q), 154.2 (q).

ESI-MS: *m/z* (%) = 299.17 (M+H⁺)

Compound 53: (*E*)-*N*-4-(((1-(2-azidoethyl)-3,5-dimethyl-1*H*-pyrazol-4-yl)di-azeryl)-benzyl)-1-phenethylpiperidin-4-amine



C₂₇H₃₅N₉, MW = 485.64 g/mol

To a solution of 1-phenethylpiperidin-4-one (465 mg, 2.29 mmol, 1.05 eq) in dichloroethane (10 mL), was added sequentially to **52** (650 mg, 2.18 mmol, 1.0 eq), NaHB(OAc)₃ (646 mg, 3.05 mmol, 1.4 eq) and AcOH (0.12 mL, 2.18 mmol, 1.0 eq). The bright orange reaction mixture was stirred overnight at r.t. After 15 h, the reaction mixture was diluted with EtOAc (2 x 10 mL), washed with 1M NaOH (5 mL), aqueous sat. NaHCO₃ (5 mL) and aqueous sat. NaCl (10 mL). The combined organic layers were dried (Na₂SO₄), filtered and concentrated *in vacuo*. The crude residue was purified by automated column chromatography (CH₂Cl₂/MeOH, 0-10% MeOH) to obtain **53** as an orange oil (680 mg, 1.40 mmol, 64%).

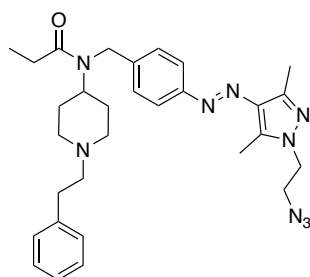
TLC: (CH₂Cl₂/MeOH, 0.01 % Et₃N, 20:1) R_f = 0.13

¹H-NMR (400 MHz; CDCl₃): δ = 1.28 (s, 2H), 1.84-1.81 (m, 2H), 2.18-2.14 (m, 2H), 2.49 (s, 3H), 2.60 (s, 3H), 2.79-2.71 (m, 1H), 2.88-2.78 (m, 2H), 3.00-2.92 (m, 2H), 3.22-3.10 (m, 2H), 3.76 (t, *J* = 5.7 Hz, 2H), 3.91 (s, 2H), 4.14 (t, *J* = 5.7 Hz, 2H), 7.23-7.16 (t, *J* = 5.9 Hz, 3H), 7.31-7.27 (d, *J* = 7.0 Hz, 2H), 7.48 (s, 2H), 7.76 (d, *J* = 8.3 Hz, 2H).

¹³C-NMR (101 MHz, CDCl₃): δ = 10.0 (+), 14.3 (+), 29.5 (-), 29.8 (-), 32.2 (-), 47.9 (-), 49.6 (-), 50.8 (-), 54.3 (+), 59.5 (-), 59.7 (-), 122.2 (+), 126.7 (+), 128.8 (+), 128.8 (+), 131.0 (q), 135.3 (q), 140.2 (q), 143.4 (q), 144.9 (q), 153.2 (q).

ESI-MS: *m/z* (%) = 486.31 (M+H⁺)

Compound 54: (*E*)-*N*-(4-(((1-(2-azidoethyl)-3,5-dimethyl-1*H*-pyrazol-4-yl)-diazenyl)-benzyl)-*N*-(1-phenethylpiperidin-4-yl)propionamide



C₃₀H₃₉N₉O, MW = 541.70 g/mol

To a solution of **53** (660 mg, 1.36 mmol, 1.0 eq) in anhydrous CH₂Cl₂ (15 mL), NEt₃ (0.37 mL, 2.72 mmol, 2.0 eq) was added, followed by propionyl chloride (0.24 mL, 2.72 mmol, 2.0 eq). The reaction mixture was allowed to stir for 24 h under N₂-atmosphere at r.t. Water was then added, and the organic phase was extracted with CH₂Cl₂ (2 x 10 mL). The pooled organic

phase was washed with sat. NaHCO₃ (1x 20 mL) and brine (1 x 20 mL). The combined organic layers were dried (Na₂SO₄), filtered and concentrated *in vacuo*. The crude residue was purified by automated column chromatography (CH₂Cl₂/MeOH, 0-10% MeOH) to obtain **54** as an orange oil (525 mg, 0.97 mmol, 71%).

TLC: (CH₂Cl₂/MeOH, 20:1) R_f = 0.31

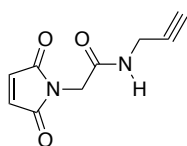
¹H-NMR (400 MHz; MeOD): δ = 1.22 (t, *J* = 7.4 Hz, 3H), 1.75-1.68 (m, 4H), 1.85-1.79 (m, 2H), 2.26-2.21 (m, 2H), 2.47 (s, 3H), 2.61-2.59 (m, 2H), 2.64 (s, 3H), 2.79-2.77 (m, 3H), 3.16-3.07 (m, 2H), 3.76-3.73 (m, 2H), 4.27-4.22 (m, 2H), 4.50 (s, 1H), 4.68 (s, 2H), 7.20-7.18 (m, 3H), 7.28-2.25 (s, 2H), 7.36 (d, *J* = 8.5 Hz, 2H), 7.79 (d, *J* = 8.3 Hz, 2H).

¹³C-NMR (101 MHz, CDCl₃): δ = 9.8 (+), 10.2 (+), 14.2 (+), 27.7 (-), 29.8 (-), 31.3 (-), 33.9 (-), 48.0 (-), 48.9 (-), 51.9 (-), 53.7 (-), 54.0 (+), 61.1 (-), 111.4 (q), 123.2 (+), 127.7 (+), 129.5 (+), 129.7 (+), 136.1 (q), 141.4 (q), 142.2 (q), 143.9 (q), 153.8 (q), 176.7 (q).

IR: $\tilde{\nu}$ [cm⁻¹]: 2934, 2803, 2102, 1733, 1640, 1558, 1502, 1409, 1375, 1282, 1233, 1200, 1118, 1077, 1032, 999, 936, 824, 749.

ESI-MS: *m/z* (%) = 542.34 (M+H⁺)

Compound **56**: 2-(2,5-dioxo-2,5-dihydro-1*H*-pyrrol-1-yl)-*N*-(prop-2-yn-1-yl)-acetamide



C₉H₈N₂O₃, MW = 192.17 g/mol

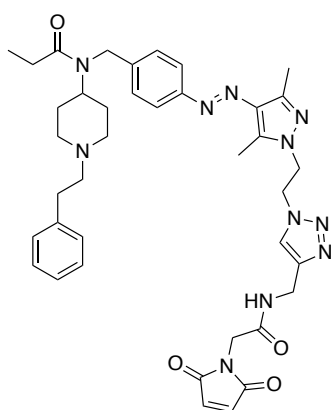
2-Maleimidoacetic acid **55** (100 mg, 0.65 mmol, 1.0 eq) was dissolved in a mixture of CH₂Cl₂/DMF (100:1, 5 mL) and oxalylchloride (124 mg, 0.97 mmol, 1.5 eq) was added dropwise. The reaction mixture was stirred for 2 h at r.t. and subsequently the solvent was removed under reduced pressure. The residue was dissolved in THF (4 mL) and was then added to a solution of *N*-propargylamine (50 μL, 0.78 mmol, 1.2 eq) and DIPEA (0.23 mL, 1.3 mmol, 2.0 eq) in THF (4 mL) at 0 °C. The mixture was stirred for 1 h at r.t., the solvent was removed *in vacuo* and the crude mixture was purified by automated column chromatography (PE/EtOAc, 0-80% EtOAc) to yield compound **56** (50 mg, 0.26 mmol, 40%) as a white powder.

¹H-NMR (400 MHz; CDCl₃): δ = 2.26 (t, *J* = 2.6 Hz, 1H), 4.07 (t, *J* = 2.6 Hz, 2H), 4.19 (s, 2H), 6.80 (s, 2H).

¹³C-NMR (101 MHz, CDCl₃): δ = 29.7 (-), 40.5 (-), 72.4 (+), 78.9 (q), 134.7 (+), 165.8 (q), 170.2 (q).

ESI-MS: *m/z* (%) = 193.06 (M+H⁺)

Compound 28: (*E*)-*N*-(4-((1-(2-(4-((2-(2,5-dioxo-2,5-dihydro-1*H*-pyrrol-1-yl)acetamido)methyl)-1*H*-1,2,3-triazol-1-yl)ethyl)-3,5-dimethyl-1*H*-pyrazol-4-yl)di-azeryl)-benzyl)-*N*-(1-phenethylpiperidin-4-yl)propionamide



C₃₉H₄₇N₁₁O₄, MW = 733.88 g/mol

Alkyne **56** (15.0 mg, 78.1 μmol, 1.0 eq) and azide **54** (48.6 mg, 89.8 μmol, 1.15 eq), were dissolved in a 3 mL mixture of ^tBuOH/H₂O/THF (1:1:1) under N₂-atmosphere. CuSO₄·5H₂O (1.95 mg, 7.81 μmol, 0.1 eq), TBTA (2.32 mg, 11.7 μmol, 0.15 eq), (+)-sodium-L-ascorbate (4.14 mg, 7.81 μmol, 0.1 eq) were then added. The reaction was allowed to stir for 16 h at room temperature. The crude was purified by preparative HPLC (column: Luna 10 250 x 21 mm; flow: 20 mL/min; solvent A: H₂O [0.05 Vol% TFA], solvent B: MeCN; gradient A/B: 0-20 min: 30/70, 20-25 min: 2/98, *t_R* = 10.9 min) to yield target compound **28** as an orange solid (27.0 mg, 36.8 μmol, 47%).

TLC: (CH₂Cl₂/MeOH, 20:1) R_f = 0.77

¹H-NMR (400 MHz; CDCl₃): δ = 1.15 (t, *J* = 7.4 Hz, 3H), 1.85-1.81 (m, 2H), 2.16-2.08 (m, 2H), 2.18 (s, 3H), 2.39 (q, *J* = 7.4 Hz, 2H), 2.52 (s, 3H), 2.79 (t, *J* = 11.6 Hz, 2H), 3.03 (dd, *J* = 10.6, 5.8 Hz, 2H), 3.17 (dd, *J* = 10.6, 5.9 Hz, 2H), 3.67 (d, *J* = 11.8 Hz, 2H), 4.05 (s, 2H), 4.41 (d, *J* = 5.8 Hz, 2H), 4.53 (t, *J* = 5.5 Hz, 2H), 4.59 (s, 2H), 4.86 (t, *J* = 5.5 Hz, 3H), 4.91 (s, 1H), 6.73

(s, 2H), 7.17-7.15 (m, 2H), 7.26-7.23 (m, 3H), 7.30 (dd, $J = 7.1, 5.6$ Hz, 2H), 7.74 (d, $J = 8.3$ Hz, 2H).

$^{13}\text{C-NMR}$ (101 MHz, CDCl_3): $\delta = 9.1$ (+), 9.7 (+), 14.0 (+), 26.7 (-), 27.2 (-), 30.6 (-), 34.4 (-), 40.3 (-), 46.4 (-), 48.1 (-), 49.0 (+), 49.9 (-), 52.8 (-), 58.6 (-), 117.1 (+), 122.7 (+), 126.5 (+), 128.7 (+), 129.2 (+), 134.6 (q), 135.6 (q), 139.2 (q), 140.6 (q), 144.2 (q), 152.9 (q), 166.7 (q), 170.2 (q), 175.6 (q).

ESI-MS: m/z (%) = 734.39 ($\text{M}+\text{H}^+$)

HR-MS (ESI): calcd. for $\text{C}_{39}\text{H}_{47}\text{N}_{11}\text{O}_4\text{S}_2$ [MH^+], $m/z = 734.3885$, found 734.3899

5.5 Molecular Docking

β_2 -AR

Docking studies were performed using the published active state β_2 -AR crystal structures in complex with BI (PDB entry 3P0G, 4LDE) (doi:10.1038/nature09648, doi:10.1038/nature12572). UCSF Chimera (doi:10.1002/jcc.20084) was used to introduce the $\text{N}^{2,63}\text{C}$ mutant, add missing sidechains and add hydrogens. The investigated compounds **1** and **2** were geometry-optimized by means of Gaussian 09²¹ at the B3LYP/6-31G(d) level attributing a formal charge of +1. Subsequently, the ligands were docked into the crystal structure utilizing the covalent docking procedure of the CCDC GOLD Suite v5.4. On the basis of the scoring function and the presence of the canonical salt bridge to Asp^{3,32}, we selected one final conformation for each ligand. Figures were prepared using PyMOL Molecular Graphics System, Version 2.1.1 (Schrödinger, LLC).

μOR

Docking studies were performed using the recently published active state μOR crystal structure in complex with BU72 (PDB entry 5C1M) (doi:10.1038/nature14886). UCSF Chimera (doi:10.1002/jcc.20084) was used to introduce the $\text{N}^{2,63}\text{C}$ mutant, add missing sidechains and add hydrogens. The investigated compounds **27** and **28** were geometry-optimized by means of Gaussian 09²¹ at the B3LYP/6-31G(d) level attributing a formal charge of +1. Subsequently, the ligands were docked into the crystal structure utilizing the covalent docking procedure of the CCDC GOLD Suite v5.4. On the basis of the scoring function and the presence of the canonical salt bridge to Asp^{3,32}, we selected one final conformation for each ligand. Figures were prepared using PyMOL Molecular Graphics System, Version 2.1.1 (Schrödinger, LLC).

6. Literature

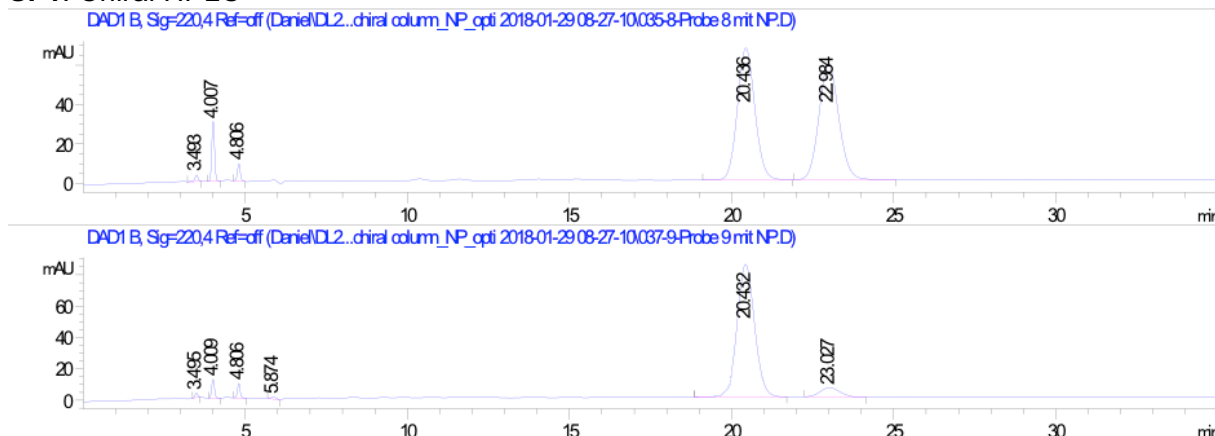
- 1 M. Izquierdo-Serra, A. Bautista-Barrufet, A. Trapero, A. Garrido-Charles, A. Liebaria, P. Gorostiza, *Nat. Commun.* **2015**, 1
- 2 D. Lachmann, C. Studte, B. Männel, H. Harald, P. Gmeiner, B. König, *Chem. Eur. J.* **2017**, 23, 13423
- 3 H. Farrants. V. A. Gutzeit, A. Acosta-Ruiz, D. Trauner, K. Johnsson, J. Levitz, J. Broichhagen, *ACS Chem. Biol.* **2018**, 13, 2682
- 4 A. Mourot, M. A. Kienzler, M. R. Banghart, T. Fehrentz, F. M. E. Huber, M. Stein, R. H. Kramer, D. Trauner, *ACS Chem. Neurosci.* **2011**, 9, 536
- 5 W.-Ch. Lin, M.-Ch. Tsai, R. Rajappa, R. H. Kramer, *J. Am. Chem. Soc.* **2018**, 140, 7445
- 6 M. Schönberger, *Dissertation*, **2014**, München
- 7 P. C. Donthamsetti, N. Winter, M. Schönberger, J. Levitz, Ch. Stanley, J. A. Javitch, E. Y. Isacoff, D. Trauner, *J. Am. Chem. Soc.* **2017**, 139, 18522
- 8 D. Weichert, P. Gmeiner, *ACS Chem. Biol.* **2015**, 10, 1376
- 9 B. Kobilka, *Angew. Chem. Int. Ed.* **2013**, 52, 6380
- 10 G. Peleg, P. Ghanouni, B. K. Kobilka, R. N. Zare, *PNAS* **2001**, 98, 15, 8569
- 11 G. G. Gregorio, M. Masureel, D. Hilger, D. S. Terry, M. Juette, H. Zhao, Z. Zhoun, J. M. Perez-Aguilar, M. Hauge, S. Mathiasen, J. A. Javitch, H. Weinstein, B. K. Kobilka, S. C. Banchar, *Nature* **2017**, 547, 68
- 12 B. Schuler, *Journal of Nanobiotechnology* **2013**, 11, S2
- 13 W. A. Velema, W. Szymanski, B. L. Feringa, *J. Am. Chem. Soc.* **2014**, 136, 2178
- 14 S. G. F. Rasmussen, B. T. DeVree, Y. Zou, A. C. Kruse, K. Y. Chung, T. S. Kobilka, F. S. Thian, P. S. Chae, E. Pardon, D. Calinski, J. M. Mathiesen, S. T. A. Shah, J. A. Lyons, M. Caffrey, S. H. Gellman, J. Steyaert, G. Skiniotis, W. I. Weis, R. K. Sunahara, B. K. Kobilka, *Nature*, **2011**, 477, 549
- 15 W. Huang, A. Manglik, A. H. Venkatakrisnan, T. Laeremans, E. N. Feinberg, A. L. Sanborn, H. E. Kato, K. E. Livingston, T. S. Thorsen, R. C. Kling, S. Granier, P. Gmeiner, S. M. Husbands, J. R. Traynor, W. I. Weis, J. Steyaert, R. O. Dror, B. K. Kobilka, *Nature* **2015**, 524, 315
- 16 S. G. F. Rasmussen, H.-J. Choi, J. J. Fung, E. Pardon, P. Casarosa, B. K. Kobilka, *Nature* **2011**, 469, 175
- 17 P.A.J. Janssen, *US Patent 3* **1965**, 164, 600
- 18 T. Warne, R. Moukhametzianov, J. G. Baker, R. Nehme, P. C. Edwards, A. G. W. Leslie, G. F. X. Schertler, Ch. G. Tate, *Nature* **2011**, 469, 241
- 19 D. Weichert, M. Stanek, H. Hübner, P. Gmeiner, *Bioorg. Med. Chem.* **2016**, 24, 2641
- 20 D. Weichert, A. C. Kruse, A. Manglik, Ch. Hiller, Ch. Zhang, H. Hübner, B. K. Kobilka, P. Gmeiner, *PNAS* **2014**, 111, 10744

- 21 Frisch, M. J., G. W. Trucks, H. B. Schlegel, G. E. Scuseria, M. A. Robb, J. R. Cheeseman, G. Scalmani, V. Barone, B. Mennucci, G. A. Petersson, H. Nakatsuji, M. Caricato, X. Li, H. P. Hratchian, A. F. Izmaylov, J. Bloino, G. Zheng, J. L. Sonnenberg, M. Hada, M. Ehara, K. Toyota, R. Fukuda, J. Hasegawa, M. Ishida, T. Nakajima, Y. Honda, O. Kitao, H. Nakai, T. Vreven, J. A. Montgomery, Jr., J. E. Peralta, F. Ogliaro, M. Bearpark, J. J. Heyd, E. Brothers, K. N. Kudin, V. N. Staroverov, R. Kobayashi, J. Normand, K. Raghavachari, A. Rendell, J. C. Burant, S. S. Iyengar, J. Tomasi, M. Cossi, N. Rega, J. M. Millam, M. Klene, J. E. Knox, J. B. Cross, V. Bakken, C. Adamo, J. Jaramillo, R. Gomperts, R. E. Stratmann, O. Yazyev, A. J. Austin, R. Cammi, C. Pomelli, J. W. Ochterski, R. L. Martin, K. Morokuma, V. G. Zakrzewski, G. A. Voth, P. Salvador, J. J. Dannenberg, S. Dapprich, A. D. Daniels, J. Farkas; Foresman, J. V. B.; Ortiz, J. Cioslowski and D. J. Fox (2009). "Gaussian 09, revision B.01." Gaussian, Inc.: Wallingford, CT.
- 22 R. F. Sweis, Z. Wang, M. Algire, C. H. Arrowsmith, P. J. Brown, G. G. Chiang, J. Guo, C. G. Jakob, M. Vedadi, W. N. Pappano, *ACS Med. Chem. Lett.* **2015**, *6*, 695
- 23 E. J. Corey, R. K. Bakshi, S. Shibata, *J. Am. Chem. Soc.* **1987**, *109*, 5551
- 24 C. E. Weston, A. Krämer, F. Colin, Ö. Yildiz, M. G. J. Baud, F.-J. Meyer-Almes, M. J. Fuchter, *ACS Infect. Dis.* **2017**, *3*, 152
- 25 S. Devi, M. Saraswat, S. Grewal, S. Venkataramani, *J. Org. Chem.* **2018**, *83*, 4307
- 26 D. M. Rosenbaum, Ch. Zhang, J. A. Jyons, R. Holl, D. Aragao, D. H. Arlow, S. G. F. Rassmussen, H.-J. Choi, B. T. DeVree, R. K. Sunahara, P. S. Chae, S. H. Gellman, R. O. Dror, D. E. Shaw, W. I. Weis, M. Caffrey, P. Gmeiner, B. K. Kobilka, *Nature* **2011**, *469*, 236
- 27 M. Masureel, Y. Zou, L.-P. Picard, E. v. d. Westhuizen, J. P. Mahoney, J. P. G. L. M. Rodrigues, T. J. Mildorf, R. O. Dror, D. W. Shaw, M. Bouvier, E. Pardon, J. Steyaert, R. K. Sunahara, W. I. Weis, C. Zhang, B. K. Kobilka, *Nat. Chem. Biol* **2018**, *14*, 1059
- 28 H. Liu, J. Hofmann, I. Fish, B. Schaaque, K. Eitel, A. Bartuschat, J. Kaindl, H. Rampp, A. Banerjee, H. Hübner, M. J. Clark, S. G. Vincent, J. T. Fisher, M. R. Heinrich, K. Hirata, X. Liu, R. K. Sunahara, B. K. Shoichet, B. K. Kobilka, P. Gmeiner, *PNAS* **2018**, *115*, 12046
- 29 W. Huang, A. Manglik, A. J. Venkatakrisnan, T. Laeremans, E. N. Feinberg, A. L. Sanborn, H. E. Kato, K. E. Livingston, T. S. Thorsen, R. C. Kling, S. Granier, P. Gmeiner, S. M. Husbands, J. R. Traynor, W. I. Weis, J. Steyaert, R. O. Dror, B. K. Kobilka, *Nature* **2015**, *524*, 315
- 30 M. Schönberger, D. Trauner, *Angew. Chem. Int. Ed.* **2014**, *53*, 3264
- 31 A. Manglik, H. Lin, D. K. Aryal, J. D. McCorvy, D. Dengler, G. Corder, A. Levit, R. C. Kling, V. Bernat, H. Hübner, X.-P. Huang, M. F. Sassano, P. M. Giguère, S. Löber, D.

-
- Duan, G. Scherrer, B. K. Kobilka, P. Gmeiner, B. L. Roth, B. K. Shoichet, *Nature* **2016**, 537, 185
- 32 L. Stricker, E.-C. Fritz, M. Peterlechner, N. L. Doltsinis, B. J. Ravoo, *J. Am. Chem. Soc.* **2016**, 138, 4547
- 33 G. Weltrowska, N. N. Chung, C. Lemieux, J. Guo, Y. Lu, B. C. Wilkes, P. W. Schiller, *J. Med. Chem.* **2010**, 53, 2875
- 34 C. E. Weston, R. D. Richardson, P. R. Haycock, A. J. P. White, M. J. Fuchter, *J. Am. Chem. Soc.* **2014**, 136, 11878
- 35 A. A. Beharry, G. A. Woolley, *Chem. Soc. Rev.* **2011**, 40, 4422
- 36 R. F. Sweis, Z. Wang, M. Algire, Ch. H. Arrowsmith, P. J. Brown, G. G. Chiang, J. Guo, C. G. Jakob, S. Kennedy, F. Li, D. Maag, B. Shaw, N. B. Soni, M. Vedadi, W. N. Pappano, *ACS Med. Chem. Lett.* **2015**, 6, 695
- 37 L. Stricker, M. Böckmann, T. M. Kirse, N. L. Doltsinis, B. J. Ravoo, *Chem. Eur. J.* **2018**, 24, 8639
- 38 L. Alcaraz, A. Bailey, R. Cox, P. Meghani, G. Pairaudeau, M. Stocks, *PCT Int. Appl.* **2007**, WO 2007102771 A1 20070913

7.Supporting information

SI-1: Chiral HPLC



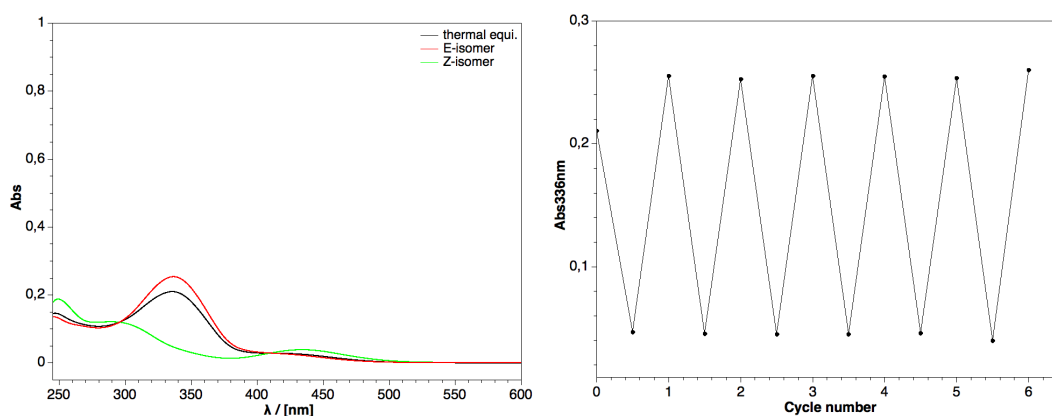
SI-2: Absorption spectra, cycle performance and thermal half-life of compounds **1**, **2** and **10**

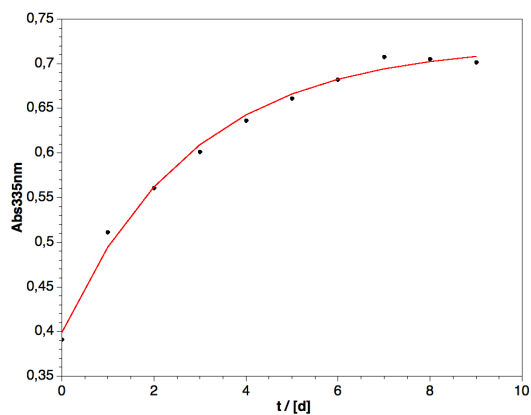
Absorption spectra, cycle performance and thermal half-life of compound **1,2** and **10** in aqueous tris-buffer ($c = 10 \mu\text{M}$). LEDs, used for isomerization:

$E \rightarrow Z$ isomerization: 365 nm LED (SSC VIOSYS, 700 mA, 1250 mW)

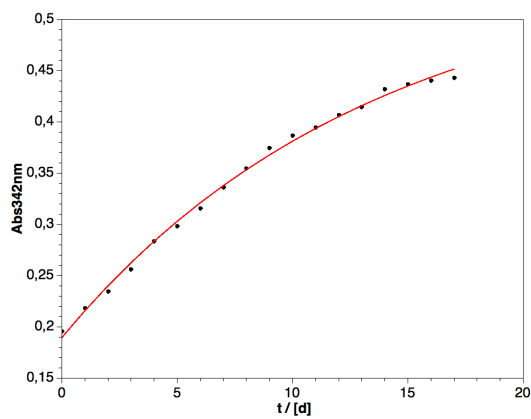
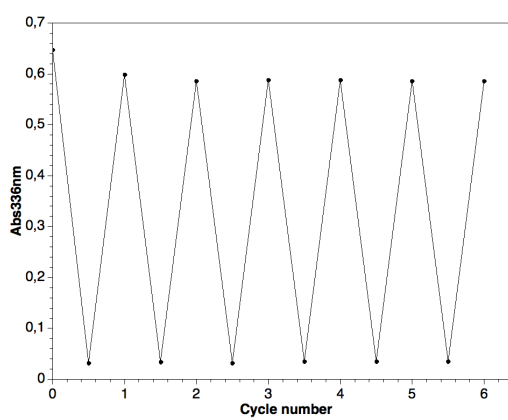
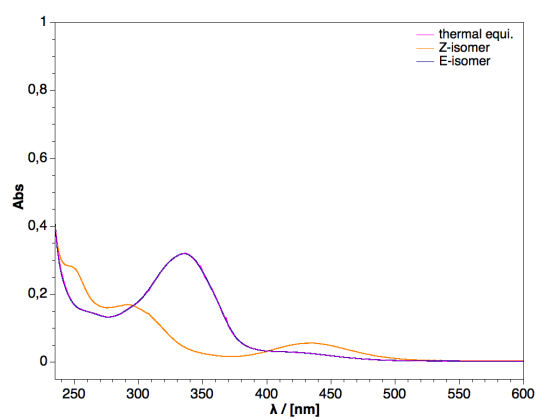
$Z \rightarrow E$ isomerization: 528 nm LED (OSRAM Oslon SSL 80 green, 500 mA, 34 mW)

Compound **1**

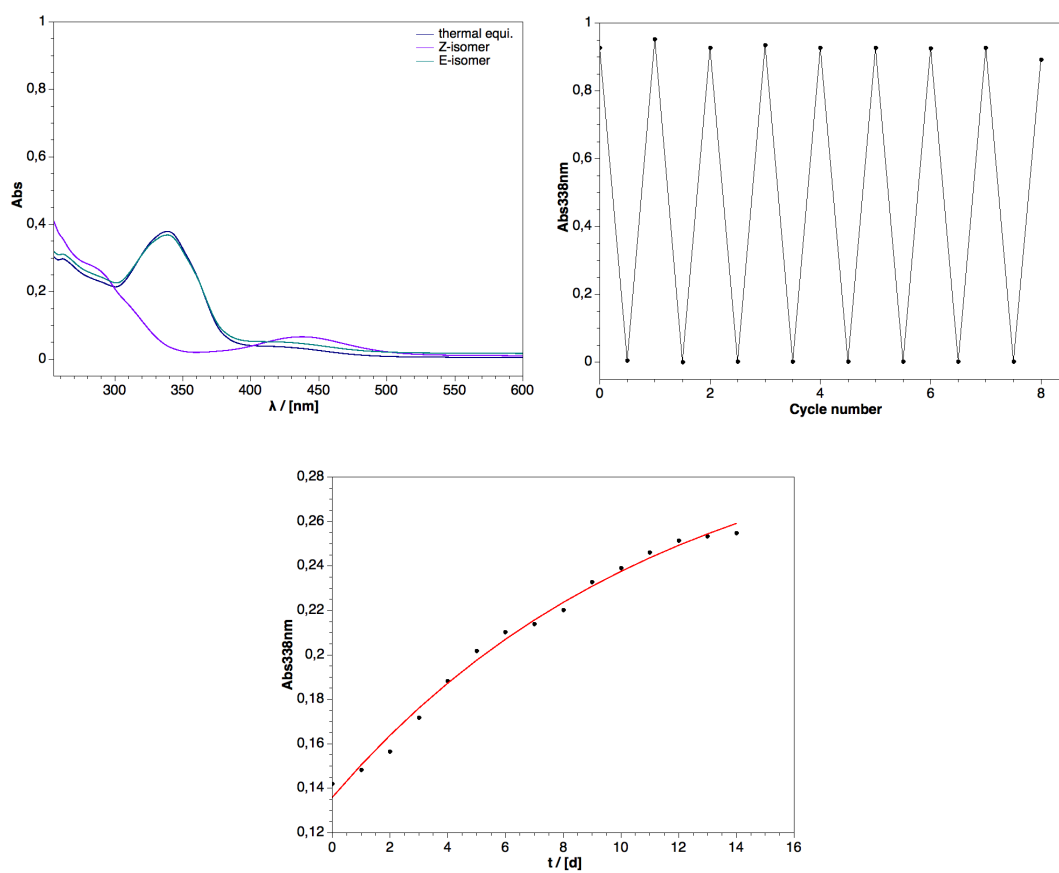
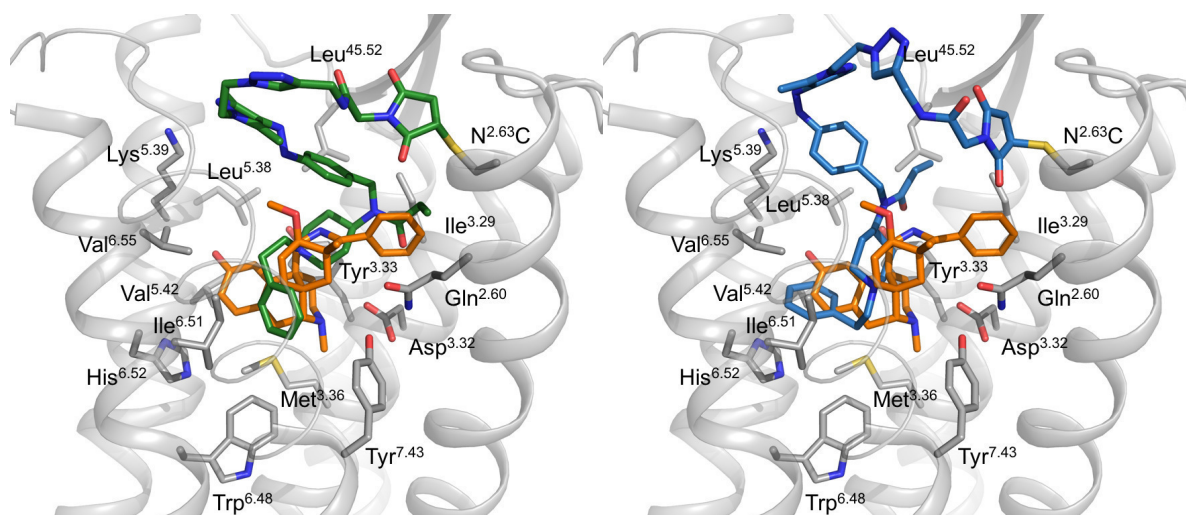




Compound 2



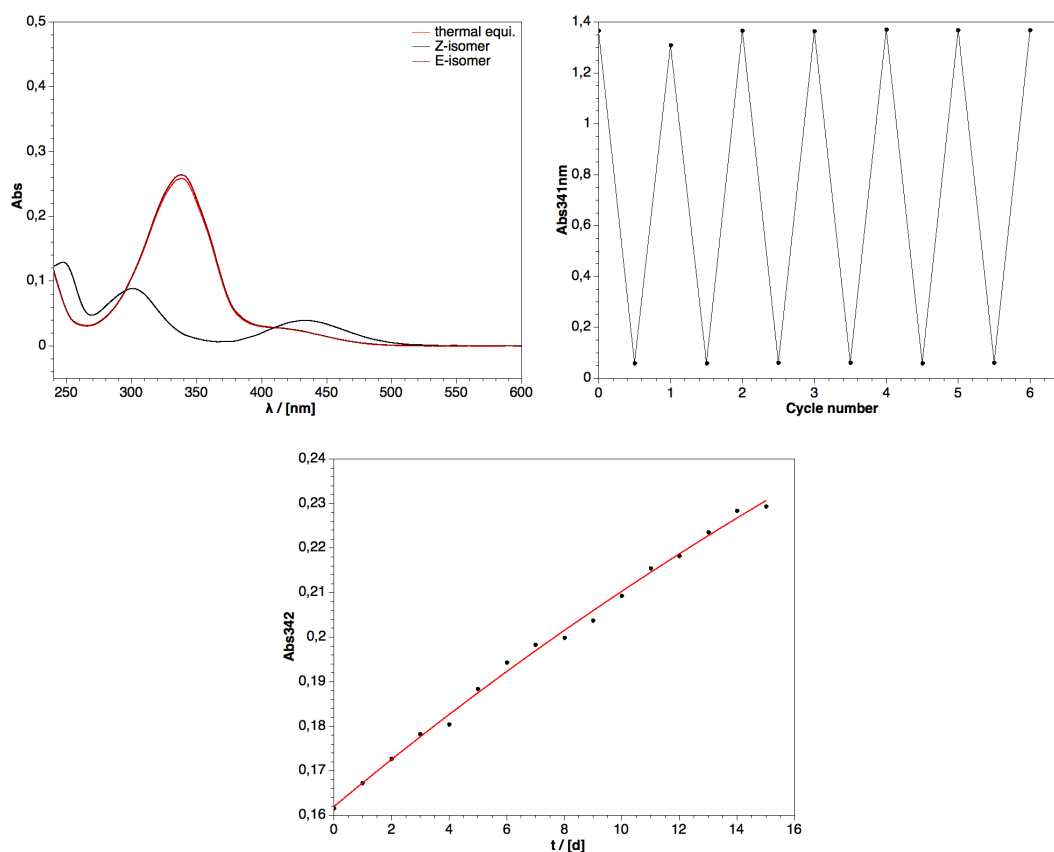
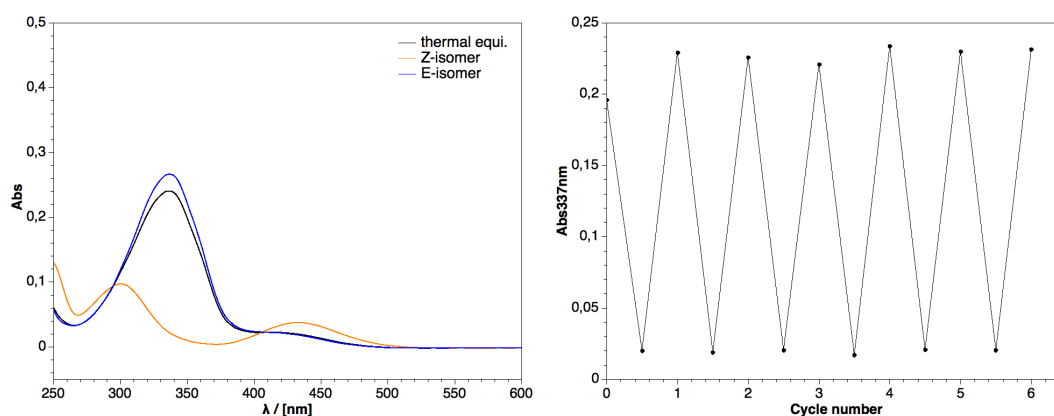
Compound 10

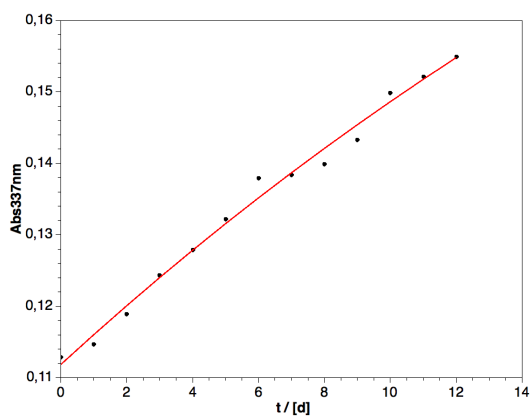
SI-3: Docking studies towards compound *E/Z*-28

Docking pose of compound *E*-28 (left, green) and compound *Z*-28 (right, blue). The co-crystallized agonist BU72 is shown as orange sticks.

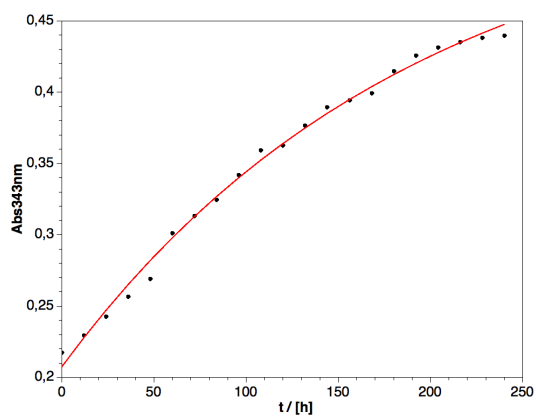
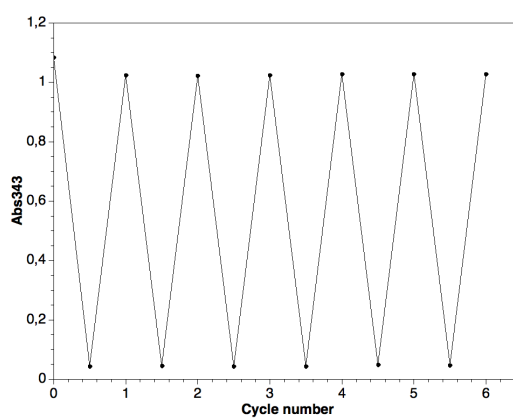
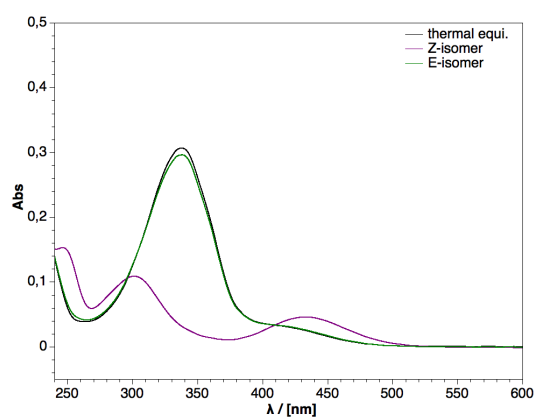
SI-4: UV/VIS-spectra, cycle performance and thermal half-life of compounds 43, 54 and 27 – 28

UV/VIS absorption spectra, cycle performance and thermal half-life of compounds **43**, **54**, **27** - **28** in aqueous tris-buffer. ($c = 10\mu\text{M}$) LEDs \rightarrow see **SI-4**.

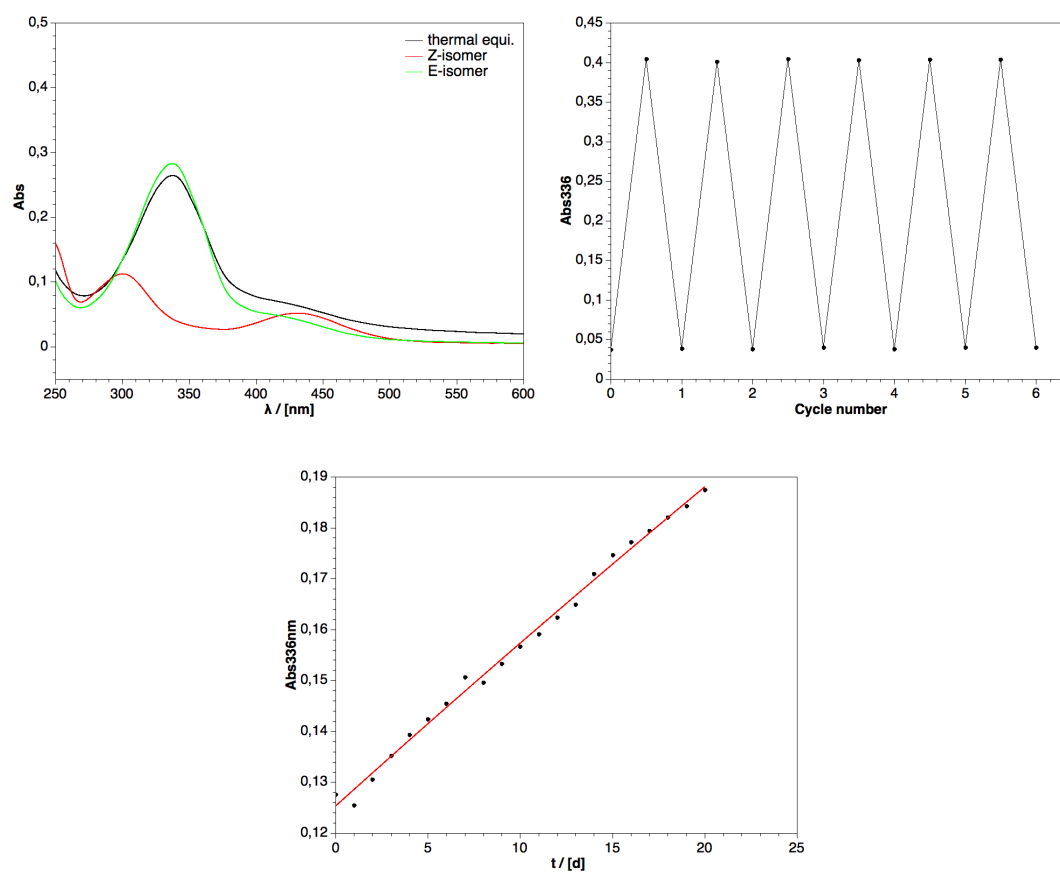
Compound 27**Compound 28**



Compound 43

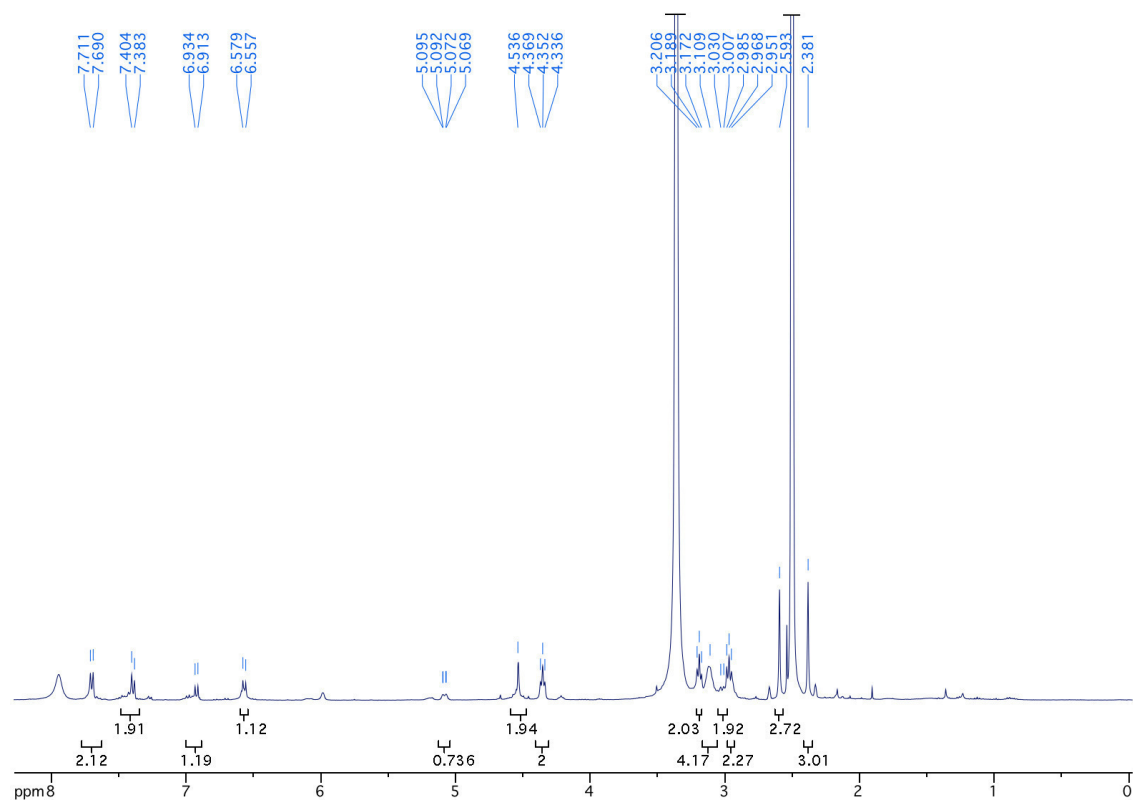
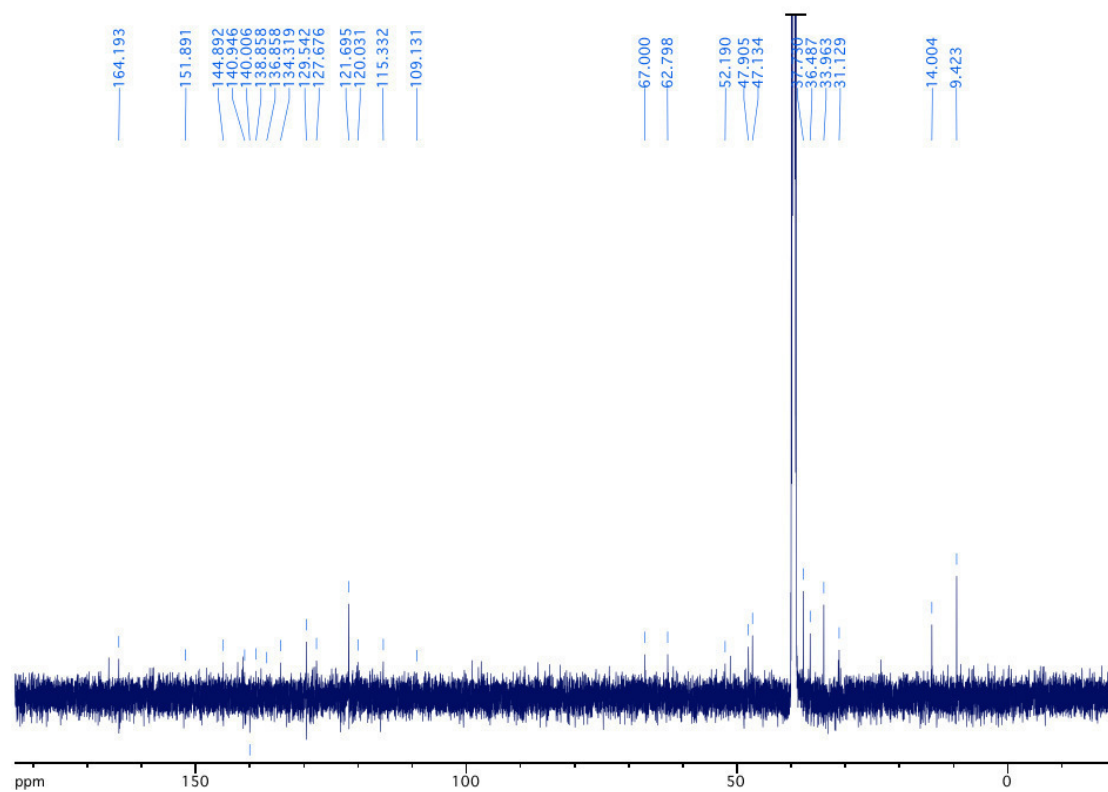


Compound 54

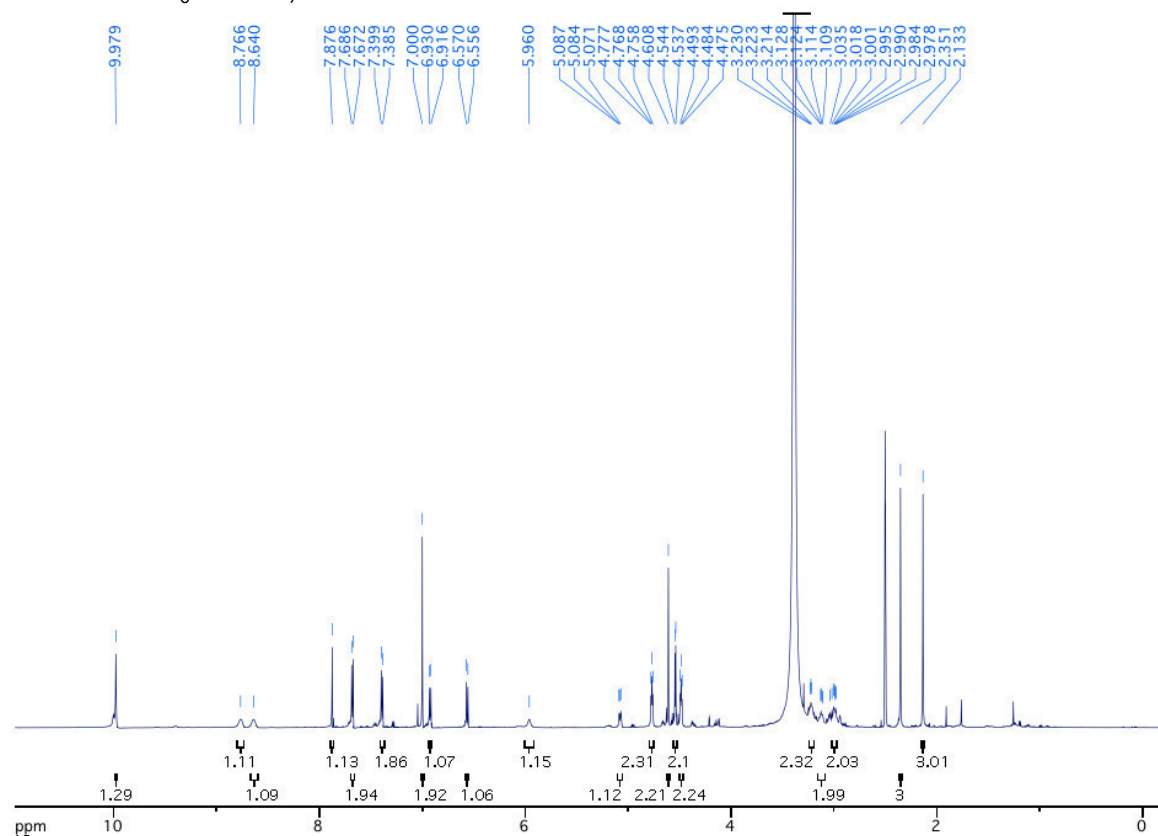
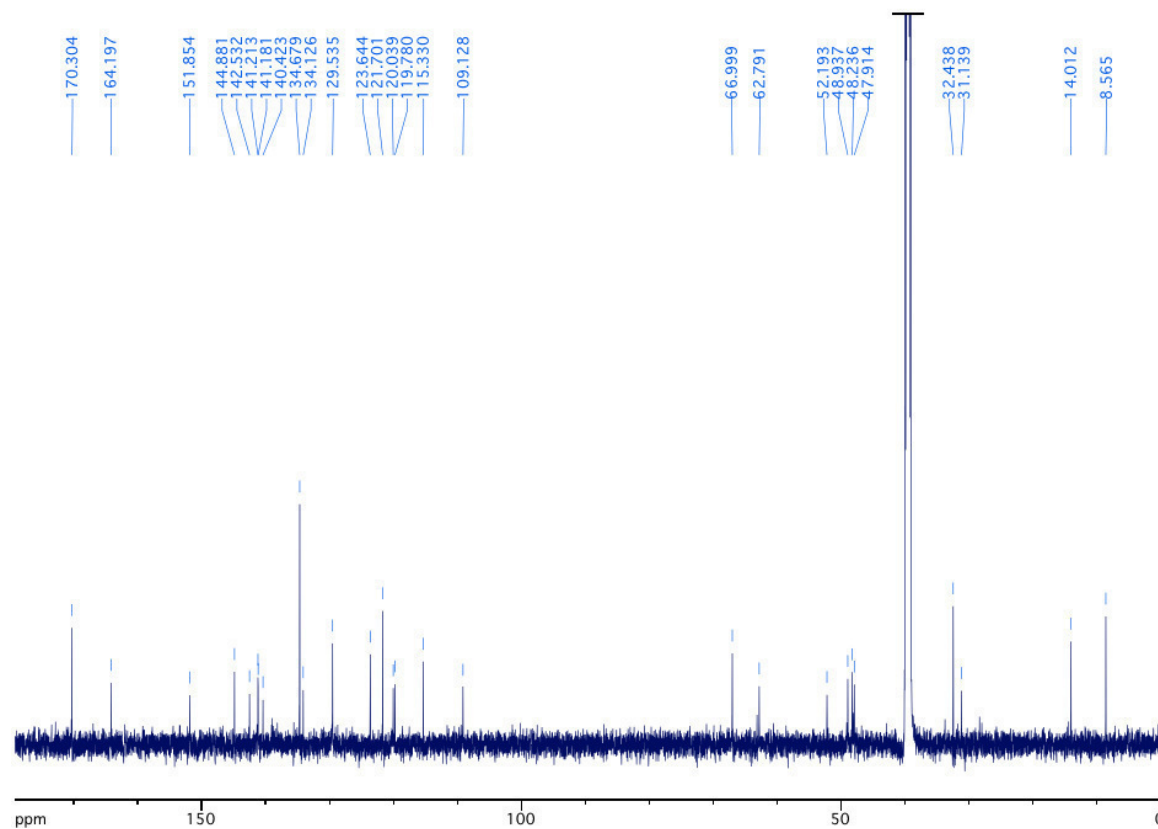


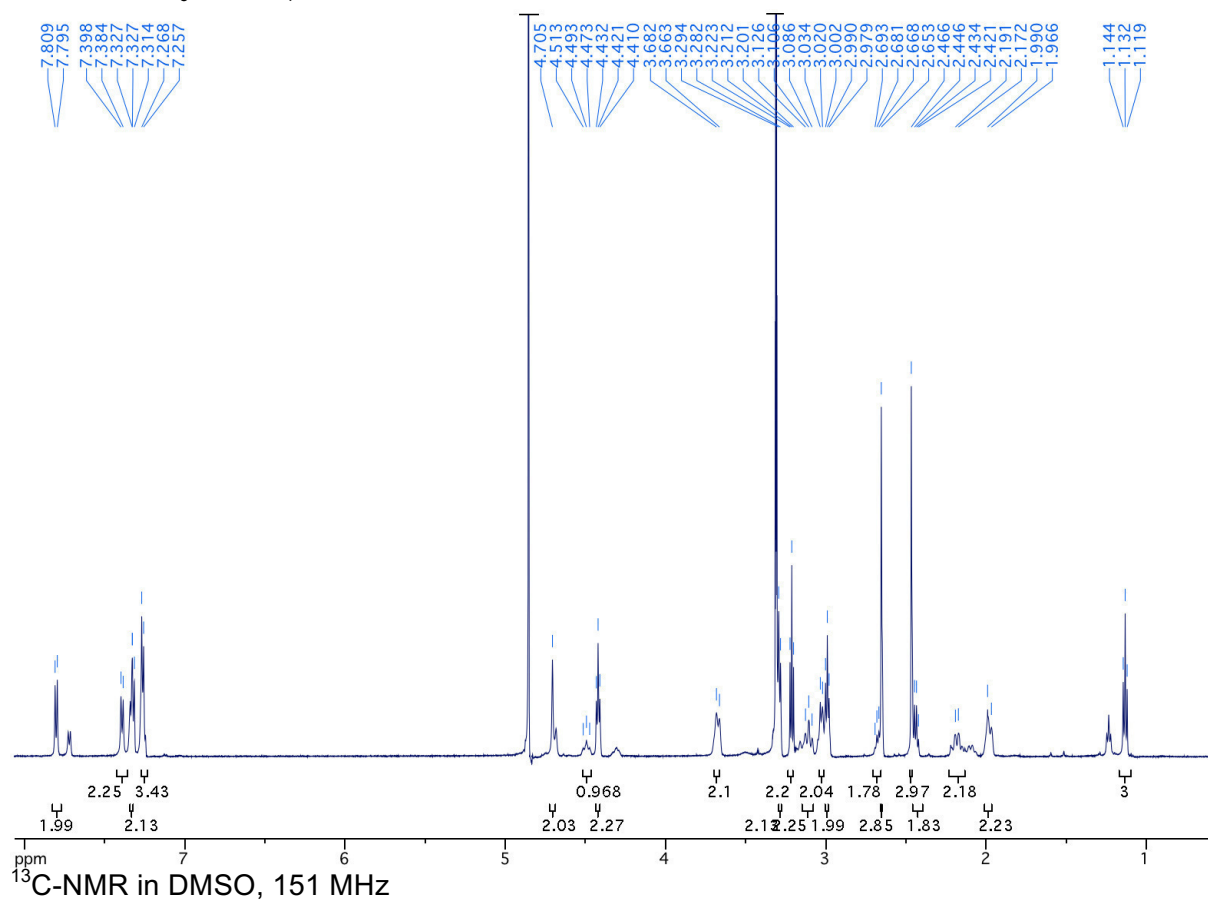
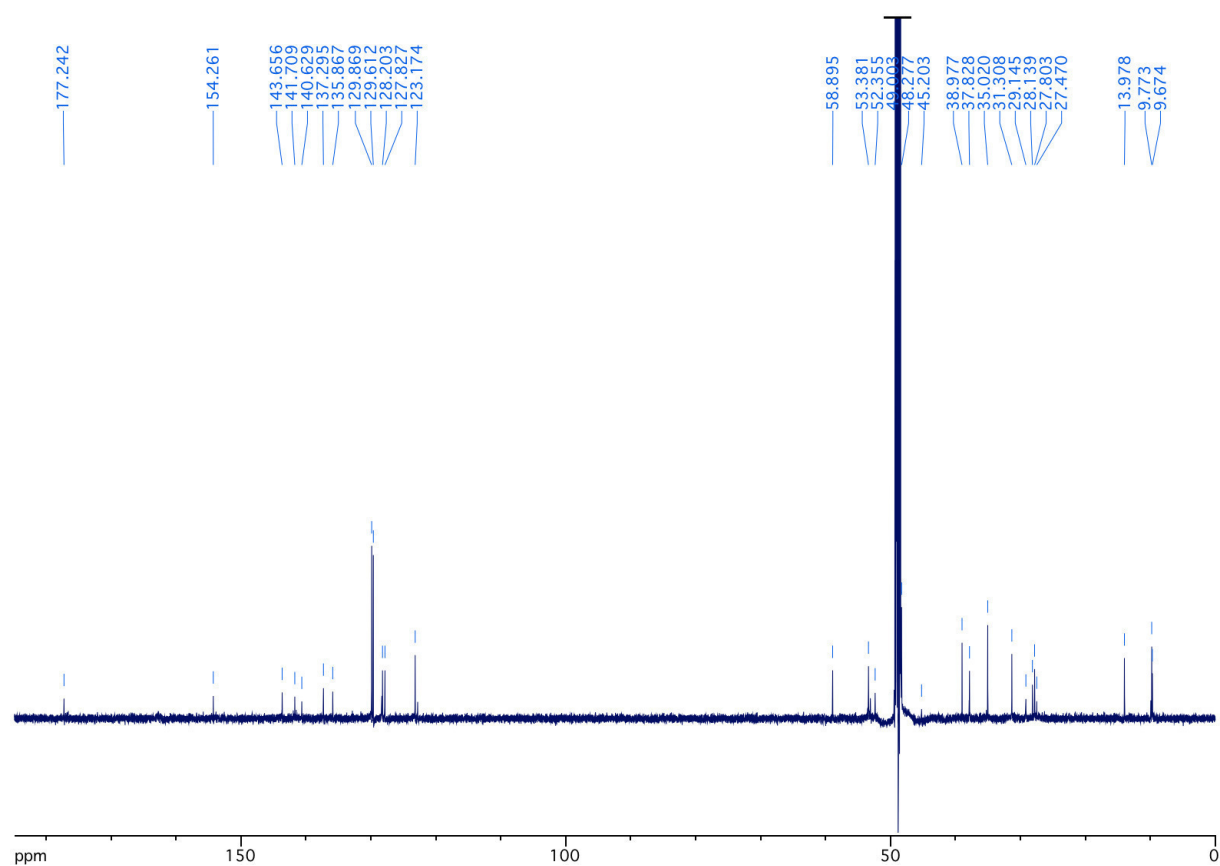
SI-5: NMR-spectra

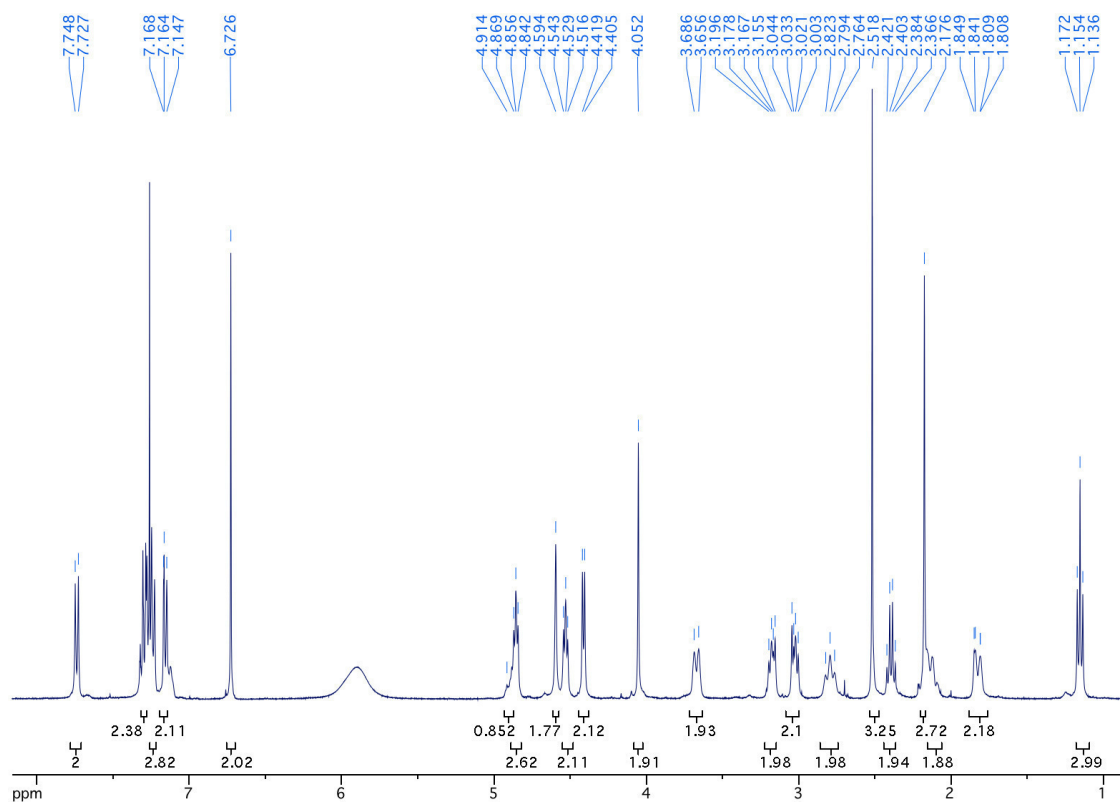
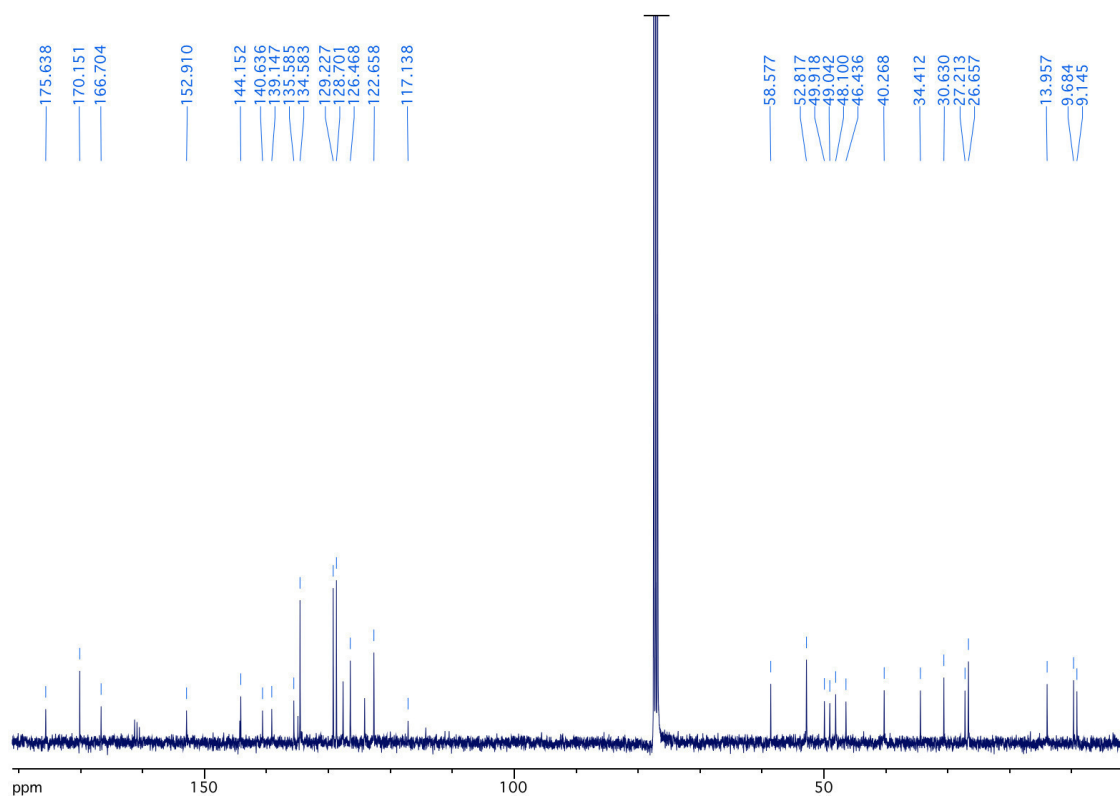
Compound 1

 ^1H -NMR in $\text{D}_6\text{-DMSO}$, 600 MHz ^{13}C -NMR in $\text{D}_6\text{-DMSO}^*$, 151 MHz* ^{13}C signals were detected indirect by HMBC and HSQC

Compound 2

 $^1\text{H-NMR}$ in $\text{D}_6\text{-DMSO}$, 600 MHz $^{13}\text{C-NMR}$ in $\text{D}_6\text{-DMSO}$, 151 MHz

Compound **27** $^1\text{H-NMR}$ in $\text{D}_6\text{-DMSO}$, 600 MHz $^{13}\text{C-NMR}$ in DMSO , 151 MHz

Compound **28** $^1\text{H-NMR}$ in $\text{D}_6\text{-DMSO}$, 400 MHz $^{13}\text{C-NMR}$ in $\text{D}_6\text{-DMSO}$, 101 MHz

SUMMARY

This thesis focuses on the synthesis, photophysical characterization and application of photochromic G-protein receptor ligands.

In **Chapter 1** the incorporation of the well-investigated class of photochromic dithienylethenes (DTEs) and fulgides into known dopamine receptor ligands like 1,4-disubstituted aromatic and hydroxybenzoxazinone piperazines as well as aminoindanes is described. Subtype and functional selective photochromic ligands were obtained and characterized by NMR and UV-VIS spectroscopic measurements. The photophysical properties of the DTE based dopamine ligands revealed a high fatigue resistance for the diarylmaleimides in DMSO, but the ringclosure could not be accomplished in aqueous solutions due to a known twisted intramolecular charge transfer (TICT). Several cyclopentene-DTEs showed high PSS, but a fast degradation by forming an irreversible byproduct. Focusing on the fulgides, high photostationary states and switching in polar solvents were possible. Fulgimides, containing the isopropyl group, showed only isomerization between the open E-form and the closed C-form. At a concentration of 1 nM, an open isomer of a cyclopentene-DTE derivative showed a more than 10-fold higher activation of D_{2S}, a pharmacologically important G protein-coupled receptor, than its photochromic closed congener. Interestingly, a indolyl fulgimide-based pair (open/closed) could be discovered as an alternative photoswitch with inverse activation properties exhibiting four-fold higher activity in the closed state. Further studies on the optimization of GPCR-regulating photoswitches and biological investigations including reversible, light-induced control of photochromic ligands when bound to the receptor have to be done.

Chapter 2 deals with photochromic peptidic NPY Y₄ receptor ligands. The neuropeptide Y (NPY) Y₄ receptor is a G protein coupled receptor, which is targeted by pancreatic polypeptide, a homologue of NPY. Selective Y₄R agonists were suggested as potential therapeutics for the treatment of obesity. Highly potent dimeric peptidic Y₄R agonists, constituted of two pentapeptide moieties connected through an aliphatic linker, represent an interesting class of Y₄R ligands. Based on this compound class, photoresponsive Y₄R ligands, containing an azobenzene, azopyrazole, diethienylethene or a fulgimide chromophore were prepared to explore structural requirements of such Y₄R agonists on Y₄R binding. The synthesized Y₄R ligands, containing a non-aliphatic rigid photochromic linker, switch reversible in aqueous buffer and exhibit high Y₄R affinity throughout. This demonstrated that the replacement of the highly flexible aliphatic linker by a considerably less flexible photochromic linker was well tolerated with respect to Y₄R binding. Differences in Y₄R affinity and activity between the individual photoisomers (varying in spatial orientation and flexibility) were marginal. This suggests that the linking element in the dimeric ligands is less critical for the adaptation of high-affinity binding modes at the receptor. As some compounds proved to be weaker partial

agonists than the model dimeric pentapeptide, this study might support the development of Y₄R antagonists.

The synthesis and biological evaluation of covalent binding photochromic GPCR ligands for single molecule spectroscopy was reported in **chapter 3**. The β_2 -adrenergic receptor (β_2 -AR) and the μ -opioid receptor (μ OR) were chosen for investigations towards covalently bound photochromic ligands. Azopyrazoles, comprising an covalent tether, were embedded in the structures of the highly potent β_2 -AR agonist BI-167107 and into the μ OR-agonist fentanyl to obtain photochromic covalent ligands. The azopyrazole acts as the photochromic functional linker between the pharmacophore and the tethering position. Geometric changes should effect binding or receptor activation when toggling between the two photoisomers. A parallel investigation of different synthetic routes to synthesize the pharmacophoric moiety and the covalent groups, including a disulfide or a maleimide as the tethering group, was done. The crucial step for the β_2 -AR ligands was accomplished in a reductive amination reaction connecting the photoresponsive tether and the pharmacophoric moiety as the final step. The μ OR-ligands were synthesized with a disulfide protection group for the disulfide derivative or via a post functionalization of an azopyrazole-fentanyl azide, installing a maleimide- or a NHS ester-tethering group in a click-reaction. The photochemical characterizations of the photochromic ligands revealed high fatigue resistance and high thermal half-lives for the azopyrazoles. Initial biological investigations showed good binding affinities for both the covalent β_2 -AR and μ OR ligands towards the wild type receptor and much higher affinities for their corresponding mutant receptors. Functional studies on β -arrestin recruitment for the β_2 -AR and G-protein signaling for the μ OR showed high intrinsic activities for the synthesized ligands. Finally, the differences in efficacy and binding between the *E*- and *Z*-isomers were only marginal. As the initial studies did not consider the covalent binding, further investigations would be to study irreversible binding and functional assays, to get more insight into the covalent nature of the ligands.

ZUSAMMENFASSUNG

Diese Dissertation behandelt die Synthese, photophysikalische Charakterisierung und Anwendung von photochromen G-Protein gekoppelten Rezeptor-Liganden.

Kapitel 1 beschreibt die Einbindung der bereits gut untersuchten Klassen der photochromen Dithienylethene und Fulgide in bekannte Dopamin-Rezeptor-Liganden wie 1,4-disubstituierte aromatische und Hydroxybenzoxazinon-Piperazine sowie Aminoindane. Es gelang, subtyp und funktionell selektive photochrome Liganden zu synthetisieren, welche mittels NMR-Spektroskopie und UV/VIS-Absorptionsspektroskopie charakterisiert wurden. Die photophysikalischen Eigenschaften der Dithienylethen Dopamin-Liganden wiesen eine hohe Ermüdungsresistenz in DMSO auf. Diese konnte in wässrigen Lösungen aufgrund des bekannten *Twisted intramolecular charge transfer* (TICT) jedoch nicht bestätigt werden. Einige Cyclopenten-Dithienylethene zeigten hohe photostationäre Zustände. Sie formten jedoch ein irreversibles Nebenprodukt, was den Abbau des Photoschalters zur Folge hatte. Bei Betrachtung der Fulgide konnten hohe photostationäre Zustände und eine Schaltbarkeit in polaren Lösungsmitteln festgestellt werden. Fulgimide mit Isopropyl-Rest wiesen ausschließlich eine Isomerisierung zwischen der offenen E-Form und der geschlossenen C-Form auf. Bei einer Konzentration von 1 nM zeigte ein offenes Isomer eines Cyclopenten-Dithienylethens eine 10-fach höhere Aktivierung des pharmakologisch bedeutenden D_{2S}-Rezeptors als das geschlossene Isomer. Als alternativer Photoschalter wurde ein Indolyl-Fulgimid-Isomerenpaar (offen/geschlossen) entdeckt, dessen inverse Aktivierungseigenschaften im geschlossenen Zustand eine vierfach höhere Aktivität zeigte. Um die GPCR-regulierenden Photoschalter weiter zu optimieren und weitere biologische Erkenntnisse bezüglich des lichtinduzierten Schaltens am Rezeptor *in vivo* zu erhalten, müssen weitere Untersuchungen durchgeführt werden.

Das **Kapitel 2** handelt von peptidischen photochromen Neuropeptid Y₄-Rezeptor (NPY Y₄-Rezeptor) Liganden. Der NPY Y₄-Rezeptor ist ein G-Protein Protein-gekoppelter Rezeptor und bindet als natürlichen Liganden das pankreatischen Polypeptid, ein Homolog des NPY. Selektive Y₄-Rezeptor Agonisten wurden zur Behandlung von Fettleibigkeit vorgeschlagen. Hochpotente dimere peptidische Y₄-Rezeptor (Y₄R)-Agonisten, die aus zwei durch einen aliphatischen Linker verbundenen Pentapeptid-Einheiten bestehen, repräsentieren eine interessante Klasse an Y₄R-Liganden. Basierend auf dieser Ligandenklasse wurden photoempfindliche Y₄R-Liganden mit Azobenzolen, Azopyrazolen, Dithienylethenen und Fulgimiden synthetisiert, um strukturelle Anforderungen solcher Y₄R-Agonisten bezüglich der Y₄R-Bindung zu untersuchen. Die synthetisierten Y₄R-Liganden beinhalten einen starren nicht aliphatischen, photochromen Linker, der ein reversibles Schalten in wässrigem Puffer ermöglicht und durchwegs hohe Y₄R-Affinitäten aufweist. Dies zeigt, dass der Austausch des hochflexiblen aliphatischen Linkers durch einen weniger flexiblen photochromen Linker

bezüglich der Y₄R-Bindung gut toleriert wird. Unterschiede in der Affinität und Aktivierung des Y₄R zwischen den jeweiligen Photoisomeren, welche sich in der räumlichen Orientierung und Flexibilität unterscheiden, waren nur gering. Dies lässt vermuten, dass die verbindende Einheit in dimeren Liganden bezüglich der Adaptierung von hoch affinen Bindungsmodi am Rezeptor eine weniger wichtige Rolle spielt. Da einige der photochromen Peptide einen schwächeren Partialagonismus als das Musterpeptid aufwiesen, könnten die vorliegenden Ergebnisse bei der Entwicklung von Y₄R Antagonisten helfen.

Die Synthese und biologische Untersuchung von kovalent bindenden photochromen GPCR-Liganden für die Einzelmolekülspektroskopie ist in **Kapitel 3** dargestellt. Für Untersuchungen bezüglich kovalent gebundenen Photoschaltern wurden der β_2 -adrenerge Rezeptor (β_2 -AR) sowie der μ -Opioid-Rezeptor (μ OR) betrachtet. Als hoch potente Agonisten für β_2 -AR wurde BI-167107, für μ OR Fentanyl verwendet. In beide Liganden wurden Azopyrazole eingebaut und kovalente Ankergruppen angefügt. Das Azopyrazol stellt die photochrome funktionale Einheit zwischen dem Pharmakophor und der Ankerposition dar. Die Änderung der Geometrie des kovalent gebundenen Liganden sollte die Bindung und Aktivierung beeinflussen. Es wurden verschiedene Synthesewege der pharmakologischen Kopfgruppe und der photochromen Einheit mit einer kovalenten Struktur, wie einem Disulfid oder einem Maleimid, entwickelt. Als entscheidender und letzter Schritt der Synthese der β_2 -AR-Liganden wurde eine reduktive Aminierung durchgeführt, welche den kovalent bindenden Photoschalter mit der pharmakologischen Kopfgruppe verbindet. Die μ OR-Liganden wurden mit einer Disulfid-Schutzgruppe oder durch post-Funktionalisierung eines Azopyrazol-Fentanylazides synthetisiert, wobei eine Maleimid- und *N*-Hydroxysuccinimidester-Funktion mittels Click-Reaktion installiert wurde. Die Untersuchung der photophysikalischen Eigenschaften der photochromen Liganden ergab eine sehr gute Ermüdungsresistenz und große thermische Halbwertszeiten der Azopyrazole. Erste biologische Untersuchungen zeigten hohe Bindungsaffinitäten für beide kovalente β_2 -AR-bzw. μ OR-Liganden am jeweiligen Wildtyp-Rezeptor und deutlich höhere Affinitäten an den verwendeten Mutanten der Rezeptoren. Hohe intrinsische Aktivitäten zeigten die synthetisierten Liganden in Experimenten mit β -Arrestin-Assays (für β_2 -AR) bzw. G-Protein-Aktivierung (für μ OR). Letztendlich waren die Unterschiede in der Wirkung und Bindung zwischen den jeweiligen Photoisomeren nur gering. Da diese ersten Untersuchungen noch nicht die kovalente Bindung der Liganden berücksichtigten, sollten weitere Untersuchungen zur irreversiblen Bindung und der damit verbundenen Auswirkungen auf die Funktionalität durchgeführt werden, um ein besseres Verständnis der kovalenten Natur der Liganden zu bekommen.

4. APPENDIX

1. Abbreviations

| | |
|-------------------|---|
| Abs | absorbance |
| AcCl | acetyl chloride |
| Ac ₂ O | acetic anhydride |
| Asp | Aspartate |
| cAMP | cyclic adenosine monophosphate |
| calcd. | calculated |
| DCC | dicyclohexylcarbodiimide |
| DEPT | distortionless enhancement by polarization transfer |
| CHO | Chinese hamster overay |
| CNS | central nerveous system |
| COSY | correlated spin spectroscopy |
| DAP | disubstituted aromatic piperazines |
| DIPEA | diisopropylethylamin |
| DMSO | dimethylsulfoxide |
| DTE | dithienylethene |
| DMP | Dess Martin Periodinane |
| eq | equivalent |
| ESI | electrospray ionization |
| EtOAc | ethyl acetate |
| EtOH | ethanol |
| Et ₂ O | diethyl ether |
| ee | enantiomeric excess |
| GPCR | G-protein coupled receptor |
| h | hour |
| HBTU | 2-(1 <i>H</i> -benzotriazol-1-yl)-1,1,3,3-tetramethyluroniumhexafluorophosphate |
| HMBC | heteronuclear multiple-bond correlation spectroscopy |
| HOBt | 1-hydroxybenzotriazole |
| HPLC | high performance liquid chromatography |
| HSQC | heteronuclear single-quantum correlation spectroscopy |
| HR | high resolution |
| IR | infrared spectroscopy |
| IP | inositol phosphate |
| J | coupling constant |
| λ | wavelength |
| LDA | lithiumdiisopropylamin |

| | |
|-------------------|---|
| LYS | lysine |
| MD | molecular dynamics |
| min | minute |
| M | mol/L |
| MeCN | acetonitrile |
| MeOH | methanol |
| MSNT | 1-(2-mesitylsulfonyl)-3-nitro-1 <i>H</i> -1,2,5-triazole |
| MS | mass spectrometry |
| MW | molecular weight |
| NEt ₃ | triethylamine |
| NMR | nuclear magnetic resonance |
| NOESY | nuclear Overhauser effect spectroscopy |
| ⁿ BuLi | <i>n</i> -butyl lithium |
| p.A. | pro analysi |
| PE | petroleum ether |
| PhAcBr | phenacyl bromide |
| PKA | protein kinase A |
| ppm | parts per million |
| r.t. | room temperature |
| R _f | retention value |
| s | second |
| SEM | standard error of the mean |
| SMFS | single-molecule fluorescence spectroscopy |
| PSS | photostationary state |
| <i>p</i> -TsOH | <i>p</i> -toluenesulfonic acid |
| ^t BuOH | <i>tert</i> -butanol |
| ^t BuOK | potassium <i>tert</i> -butoxide |
| T | temperature |
| THF | tetrahydrofuran |
| TBTU | 2-(1 <i>H</i> -Benzotriazole-1-yl)-1,1,3,3-tetramethylammonium tetrafluoroborate |
| TBTA | Tris[(1-benzyl-1 <i>H</i> -1,2,3-triazol-4-yl)methyl]amin |
| TICT | twisted intramolecular charge transfer |
| TLC | thin layer chromatography |
| Tyr | tyrosin |
| UV | ultraviolet |
| Vis | visible |

2. Danksagung

Mein besonderer Dank gilt meinem Doktorvater Prof. Dr. Burkhard König für die Betreuung meiner Dissertation mit einer sehr interessanten und vielseitigen Themenstellung. Ich bedanke mich für seine Unterstützung und seiner stets offenen Tür bei Problemen jeglicher Art.

Für die Übernahme des Zweitgutachtens möchte ich Prof. Dr. Joachim Wegener danken. Weiterhin geht mein Dank an Prof. Dr. Frank-Michael Matysik und Prof. Dr. Julia Rehbein, dass sie sich die Zeit genommen haben in meinem Prüfungsausschuss mitzuwirken.

Für die gute Zusammenarbeit im Dopamin-Projekt sowie auch im Projekt kovalente Photoschalter, möchte ich Prof. Dr. Peter Gmeiner und Dr. Harald Hübner besonders danken. Weiterhin möchte ich mich auch bei Dr. Max Keller für die Kooperation und im weiteren Michael Skiba und Adam Konieczny für die Mitwirkung im NPY-Projekt bedanken. Der Graduiertenschule GRK 1910 möchte ich für die finanzielle Unterstützung danken.

Großer Dank gilt meinen Kollegen für die großartige Unterstützung fachlicher und sozialer Natur, Ranit, Karin, Alex, Andi, Matthias, Anna und meinen Laborkollegen Simon und Petzi sowie auch der ersten Generation – Simone u. Thea. Natürlich möchte ich auch allen anderen aktuellen und ehemaligen Kollegen des Lehrstuhl Königs für eine angenehme Arbeitsatmosphäre danken.

Ich danke auch Britta, Simone, Kathi, Viola, Regina, Julia und Ernst für jegliche Hilfe und Unterstützung in technischen, organisatorischen und bürokratischen Angelegenheiten rund um die Arbeit im Labor. Vielen Dank an Rudi für die stets ausgezeichnete Beratung und Hilfe bei chromatographischen Fragestellungen und Problemen.

Ich danke den Mitgliedern der Zentralen Analytik der Universität Regensburg sowie den Feinmechanikern und den Elektronikern für eine stets zügige Bearbeitung von Aufträgen.

Bei meinen Praktikanten und Auszubildenden Theresa Ferstl, Florian Lehni, Lorena Oegl, Anna Wittmann, Julia Kefer, Philipp Bittner und Elisabeth Bauer möchte ich mich für die Mitarbeit bedanken.

Von ganzem Herzen danke ich meine Eltern für die großartige Unterstützung auf jeder Ebene, für einen guten Rückhalt und fürs Zuhören. Meiner Frau Kerstin danke ich für ihre unendliche Geduld und ihre aufbauenden Worte, sowie für die entspannte Zeit meines Zusammenschreibens.

3. Curriculum Vitae

Name: Daniel Lachmann
Date of birth/place: 09.12.1987; Kelheim
Nationality: german

EDUCATION

10/2015 – 02/2019 **Ph.D. Thesis** at the Institute of Organic Chemistry, University of Regensburg, (Supervisor: Prof. Dr. B. König)
“Photochromic G-Protein Receptor Ligands”

10/2013 – 9/2015 **Master of Science** in Chemistry, University of Regensburg,
Master Thesis: *“Photochromic dopamine receptor ligands based on fulgides”* (Supervisor: Prof. Dr. Burkhard König)

10/2010 – 9/2013 **Bachelor of Science** in Chemistry, University of Regensburg,
Bachelor Thesis: *“Synthese von Peptiden als NT-Inhibitoren”*
(Supervisor: Prof. Dr. Burkhard König)

09/2004 – 01/2008 Apprenticeship, **Chemical Laboratory Assistent**, University of Regensburg

11/2008 – 07/2010 FOS/BOS Regensburg, Telekolleg, **Fachabitur**

MEMBERSHIPS

03/2016 – 02/2019 Member of the DFG – Graduate Training Group GRK 1910
“Medicinal chemistry of selective GPCR-ligands”

PRESENTATIONS, CONFERENCES AND PUBLICATIONS

- 2018
Retreat GRK 1910, Amberg
Oral - presentation: "**Covalently bound photochromic GPCR-ligands for single molecule spectroscopy**"

Emil-Fischer-Kolloquium, Research day, Erlangen
Oral - presentation: "**Photochromic GPCR-ligands**"
- 2017
Meeting - selective GPCR-Ligands, Regensburg
Oral - presentation: „**Photochromic GPCR-ligands for dopamine and NPY receptors**"
- 2018
II. International Symposium on Photopharmacology, Vic/Barcelona, Spain, poster presentation: "**Photochromic peptidic NPY Y₄ receptor ligands**"

26. Lecture Conference on Photochemistry, München, poster presentation: "**Photochromic GPCR-ligands**"
- 2017
International Symposium on Photopharmacology, Groningen, Netherlands, poster presentation: "**Photochromic dopamine receptor ligands**"
- 2015
19th European Symposium of Organic Chemistry, Lissabon, Portugal, poster presentation: "**New NTS2 selective NT(8-13) peptide analogues incorporating a C^α-tetrasubstituted amino acid**"
- 2019
"**Fulgimides in biological applications**"; D. Lachmann, B. König, *Eur. J. Org. Chem.* **2019**, *submitted*
- 2019
"**Photochromic peptidic NPY Y₄ receptor ligands**", D. Lachmann, A. Konieczny, M. Keller, B. König, *Org. Biomol. Chem.* **2019**, *submitted*

2017

“Photochromic dopamine receptor ligands based on dithienylethenes and fulgides”; D. Lachmann, C. Studte, B. Männel, H. Harald, P. Gmeiner, B. König, *Chem. Eur. J.* **2017**, 23, 13423

“NTS2-selective neurotensin mimetics with tetrahydrofuran amino acids”; N. A. Simeth, B. Manuel, D. Michael, R. C. Kling, D. Lachmann, H. Harald, P. Gmeiner, B. König, *Bioorganic & Medicinal Chemistry* **2017**, 1, 350